TNF 7 WORKSHOP

Chicago, Illinois • July 22-24, 2004

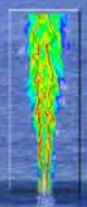

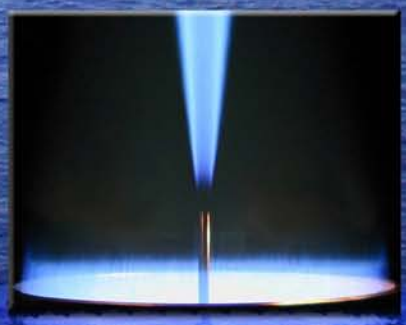

Seventh International Workshop
on Measurement and Computation
of Turbulent Nonpremixed Flames

TNF 7 SPONSORS

Chicago, Illinois • July 22-24, 2004

REACTION
ENGINEERING
INTERNATIONAL

Rolls-Royce

ANSYS

Continuum®

FLUENT

GE

Sponsorship funds are used to reduce the registration fees for students and academic professionals.

SUMMARY

Seventh International Workshop on Measurement and Computation of Turbulent Nonpremixed Flames

22-24 July 2004
Chicago, IL

R. S. Barlow, R. W. Bilger, J.-Y. Chen, A. Dreizler, J. Janicka, A. Kempf, R. P. Lindstedt, A. R. Masri, J. O. Oefelein, H. Pitsch, S. B. Pope, D. Roekaerts

INTRODUCTION

The series of workshops on Measurement and Computation of Turbulent Nonpremixed Flames (TNF) is intended to facilitate collaboration and information exchange among experimental and computational researchers in the field of turbulent combustion. The emphasis is on fundamental issues of turbulence-chemistry interaction in nonpremixed and partially premixed flames, as revealed by comparisons of measured and modeled results for selected flames. Several participating research groups have strong interest in applying this same framework for detailed measurement–model comparisons to the areas of premixed- and stratified premixed combustion. There is also growing interest in the use of detailed simulations to complement experimental benchmarks for model testing and validation. Our goal in these combined efforts is to accelerate the development of advanced combustion models that are soundly based in fundamental science, rigorously tested against experiments, and capable of predicting the behavior of a wide range of turbulent combustion situations.

TNF7 was attended by 80 researchers from 12 countries. Twenty-nine posters were contributed, with abstracts included in the proceedings, and several additional posters were displayed to augment the invited presentations. Discussion sessions addressed several topics, which are listed in order of the agenda:

- Comparison of measured and modeled results on bluff-body-stabilized flames
- Progress on the Sydney swirl flames
- Statistical modeling of extinction and re-ignition
- Update on radiation modeling for TNF target flames
- Measurements and modeling of scalar dissipation
- Progress in LES of Combustion
- Strategies for linking DNS, LES, RANS, and experiments
- Overview of lifted flames
- Status of experimental studies of premixed combustion
- Priorities and planning for future work and TNF8 (Heidelberg, 2006)

For each main topic a session leader (member of the organizing committee or invited speaker) provided an overview, which included the work of others as well as their own, and outlined key issues for discussion and further work. This format has proven effective in maintaining the focus and continuity of the workshop series, while allowing for inclusion of relevant work by people outside the core of active participants in this collaborative process.

This summary briefly outlines highlights from presentations and discussions on these topics. Comments and conclusions given here are based on the perspectives of the authors and do not necessarily represent consensus opinions of the workshop participants. This summary does not attempt to address all topics discussed at the Workshop. Readers are encouraged to also consult summaries from previous TNF Workshops because each workshop builds upon what has been done before.

The complete TNF7 Proceedings are available for download in pdf format from the Internet at www.ca.sandia.gov/TNF. The pdf file includes materials from the proceedings notebook that was distributed to workshop participants in Chicago, as well as additional materials (such as PowerPoint slides) contributed after the workshop.

Several papers relevant to the TNF7 topics and target flames were presented at the 30th Combustion Symposium. Most of these papers may be found in the sections on turbulent combustion within the *Proceedings of the Combustion Institute*, Vol. 30.

ACKNOWLEDGMENTS

Arrangements for the TNF7 Workshop were coordinated by Ms. Judy Neilsen of Sandia. Sponsorship by ANSYS, Continuum Lasers, Fluent, General Electric Aircraft Engines, Reaction Engineering International, Rolls-Royce, and the German SFB-568 research program are gratefully acknowledged. These contributions allowed for reduction of the registration fees for university faculty and students. Support for R. Barlow's work in coordinating TNF Workshop activities is provided by Sandia National Laboratories with funding from the US Department of Energy, Office of Basic Energy Sciences. We especially acknowledge the long-term support of this effort by Bill Kirchhoff, who retired from DOE in 2004.

AN IMPORTANT NOTE OF CAUTION

Results in this and other TNF Workshop proceedings are contributed in the spirit of open scientific collaboration. Some results represent completed work, while others are from work in progress. Readers should keep this in mind when reviewing these materials. It may be inappropriate to quote or reference specific results from these proceedings without first checking with the individual authors for permission and for their latest information on results and references.

HIGHLIGHTS OF PRESENTATIONS AND DISCUSSIONS

PowerPoint slides or other prepared materials for each of the main presentations are included in the TNF7 Proceedings.

Comparisons on the Sydney Bluff-Body Stabilized Jets and Flames

Andreas Kempf coordinated and presented a comparison of model calculations of selected cases of the Sydney University bluff-body flames. This type of comparison of multiple model calculations with each other and with experimental results on velocity and scalar fields is probably the most important function of the TNF Workshop series. Such broad and detailed comparisons are almost never seen in the archival literature, yet they offer important information on the relative success of various modeling approaches and the adequacy of experimental data sets as benchmarks for model validation.

Numerical data for all five hydrogen-methane bluff-body flames (HM1e, HM1, HM2, HM3e, HM3) were contributed and compared. The results originated from Kuan&Lindstedt (Imperial College), Liu&Pope (Cornell), Naud&Roekaerts (Delft, Zaragoza), Pitsch&Raman (Stanford, CTR) and Kempf&Janicka (Darmstadt), using approaches from URANS with flamelet chemistry (Imperial College) via Hybrid PDF methods (Cornell, Delft/Zaragoza) to LES (Stanford/Darmstadt).

For the first time, results for the flames HM2 and HM3 were submitted. Both Kuan&Lindstedt and Liu&Pope achieved excellent predictions, where Kuan&Lindstedt have even managed to accurately predict the mixture fraction downstream of x/D = 1.0.

The low speed case HM1(e) was considered by the groups from Cornell, Delft/Zaragoza, Stanford, and Darmstadt, having achieved some progress for the flow-field and major improvements for the scalar fields. The RANS simulations (Cornell, Delft/Zaragoza) show balanced data now, whereas the LES has both strong features and discerning problems: Darmstadt is struggling with numerical oscillations at the centerline, and Stanford hardly predicts any turbulence for the outer shear layer at all. All four simulations show reasonable predictions of the mixture-fraction close to the bluff body, but only Stanford can match the experimental results downstream from x/D = 1.0. Based on these observations, a discussion evolved on how the outer shear layer affects the mixture fraction field. So far, no final answer can be given.

To conclude, the results presented are major steps forward from TNF6. The methods applied have matured, their understanding has improved, and their cost has dropped, as indicated by the entry of LES and a single groups' ability to simulate four flames (Cornell).

For the future, it is suggested to present the calculations in mixture fraction space as well, given that the computation of the flow-field can be expected to be on a high level at TNF8. This will require the availability of conditional means, which will be compiled by Masri.

Swirl-Stabilized Jets and Flames

A comprehensive data set now exists for a range of swirling jets and flames stabilized on the Sydney burner. Depending on the swirl number and stream velocities, a range of flame shapes are stabilized all of which are documented. Flow precession and instabilities exist for both reacting and non-reacting flows and are driven by different modes; only some of which are understood. Some data are available for the flow precession. The entire data set is now made available on the web. There was extensive discussion about this flow, which is receiving particular interest from various LES groups particularly at Stanford and Darmstadt. The following points are made:

- Conditional means need to be provided for the data available for these flames, both with and without density weightings.

- A path needs to be provided for modelers as to the order of difficulty of the flames, i.e. (i) symmetric flames without precession and far from blow-off, (ii) symmetric flames without precession but close to blow-off, (iii) precessing flames.

- Detailed boundary conditions are needed, including time series for the velocity in the swirling annulus and temperature of the ceramic face.

Statistical Modeling of Extinction and Re-ignition

This session, led by Steve Pope, expanded on the TNF6 comparison of the IEM, MC, and EMST mixing models. Additional comparisons were presented of results using these mixing models within PDF and PaSR calculations of several TNF flames that include extinction and re-ignition. Highlights were also presented from a recent DNS study by Mitarai, Kosaly & Riley of mixing model performance. The presentation also posed the questions: What is the dimensionality of the accessed composition space in flames with extinction, and what are appropriate conditioning variables? The conclusions on mixing models that are outlined in the TNF6 summary are essential background to the following points.

- Understanding of mixing model performance is improving. Resilience to extinction increases in the order IEM < MC < EMST and also increases with increasing C_ϕ. MC produces more scatter than EMST.

- Good performance of EMST and MC has been achieved through tuning of C_ϕ.

- Little progress has been made toward understanding the coupled behavior of mixing models and chemical mechanism. Progress on this point from TNF6 will require general availability of all the mechanisms in use by various groups.

- Mixing models perform better in the DNS study when mixing interactions occur locally within a filtered subvolume (LES context as opposed to RANS context).

- Recent results by Sutherland et al. from a 2D-DNS of a $CO/H_2/N_2$ jet flame with extinction show that CO_2 is much more effective than χ in reducing the realized composition space to a two-dimensional manifold. This serves to illustrate that progress variable approaches provide natural ways to efficiently parameterize extinction.

- The choice of progress variable is crucial, and further insights on these choices are to be gained from DNS with complex chemistry and from analysis of recent multiscalar measurements.

- A Lagrangian Flamelet model (Matarai et al.) and Multiple Mapping Conditioning (Klimenko and Pope) were described as new modeling approaches.

Update on Radiation

TNF target flames typically have a low radiative heat loss. Consequently, the predictions of computational models for flow field, temperature, and chemical composition do not depend strongly on the radiation model and a simple model, the optically-thin model, can be used. To accurately predict features strongly depending on accuracy of temperature, notably NO formation, more sophisticated radiation modelling is useful, at least when flow and combustion models already give good agreement for main species and mean temperature. The answer corresponding to a detailed radiation model should be somewhere between the limits of the adiabatic calculation and the optically thin model, provided turbulence radiation interaction is properly taken into account.

In the contribution at the workshop an outline was given of what is involved in a detailed radiation model. Reference was made to recent works concerning spectral radiative effects, turbulence/radiation interaction and measurements and calculations of spectral radiation intensities.

It is shown that, when using the Planck mean absorption coefficient, one finds little difference between the optically thin approximation and a full solution of the radiative transfer equation using discrete ordinates method (DOM). This is explained by the fact that the emission term is at least one order of magnitude larger than the absorption term in the RTE when the Planck mean absorption coefficient is used. However, the Planck mean absorption coefficient yields a poor estimation of the absorption term. Using a spectral model (SLW) in combination with the DOM, the absorption is found to be higher and the radiative heat loss is in better agreement with the experimental data at least for Flame D. To address other flames of different power or size, the analysis of Li and Modest on scale up is of interest. (See references on slides.)

Because different authors in the literature used a different mix of models and put emphasis on different aspects, the answer on the question which model is recommended for the TNF flames as next step beyond the optically thin model, is not yet fully clear. But the following statements may set the some restrictions on how to proceed:

- It is important to take into account turbulence-radiation interaction, most importantly the effect of temperature fluctuations on the mean emission.

- The effect of correlation between fluctuations in temperature and absorption coefficient is relatively small, but not negligible.

- Spectral effects seem important in the evaluation of absorption term.

- Explicit confirmation that the 'thin eddy approximation' is valid is needed. This could be tested in line calculations.

During the discussion, suggestions were made to construct a simple model extending the optically thin model with a optically thick treatment of the 4.3 μm band of CO_2 (Bilger) and to treat the absorption term using the modified Planck mean absorption coefficient, depending on both local temperature and temperature of the surroundings (Gore).

Scalar Dissipation, Scalar Variance, and Small-Scale Structure

The modeling of scalar dissipation is central to flamelet and CMC approaches, and direct testing of scalar dissipation models by comparison with measurements in TNF target flames is an important priority. The session on scalar dissipation outlined various models for scalar dissipation as well as progress and some remaining challenges on the experimental side. In addition to material presented and discussed at the workshop, there were several papers on scalar dissipation presented and the 30th Symposium. Some highlights from both are listed:

- Significant progress has been made on measurements of scalar dissipation in the piloted flames and turbulent opposed jet flames, as documented in 30th Symposium papers from Sandia and TU Darmstadt.

- Preliminary comparisons of measured and modeled scalar dissipation in piloted flame D revealed wide variation among the modeled results (see plots in the proceedings). The reasons for such large discrepancies are not clear and will require further investigation.

- We are not yet able to accurately quantify the experimental uncertainty in scalar dissipation measurements. This is because experimental errors depend in a complicated way on spatial averaging effects, noise contributions to the measured scalar gradient, and bias inherent in

measurements of a 3D quantity using 1D or 2D diagnostics. Some information on these effects is included in the proceedings.

- New insights on effects of spatial averaging, noise contributions, and 1D–2D bias in measurements of scalar dissipation and scalar variance are also provided in 30th Symposium papers by Barlow, Karpetis, Wang & Clemens, Wang & Tong, and Geyer et al. Work is in progress by these groups to better understand these issues, and it is hoped that we will know enough to assign quantitative uncertainty intervals to the measurements before TNF8 and begin to really discriminate among the various models for scalar dissipation.

- Careful attention needs to be given to comparisons of results on the mean and variance of mixture fraction and temperature, in addition to scalar dissipation. Criteria for consistent comparison of measured and modeled results must also be defined and must account for the issues listed above.

- Issues of spatial resolution and noise were shown to be well under control in the new measurements of scalar variance on piloted flames, such that quantitative comparison with models may be carried out with confidence.

- The 30th Symposium paper by Geyer et al. includes analysis that interprets the effect of experimental noise in scalar dissipation measurements by adding noise to mixture fraction results from LES. This is an important illustration of the potential benefits of close coupling of experiments and detailed simulations. More work along this line is expected and encouraged.

- There is great potential for future comparison of doubly conditioned statistics, where the second conditioning variable might be something other than scalar dissipation.

LES of Combustion

Johannes Janicka was separately invited to lead the TNF7 discussion on LES and present a topical review at the 30th Symposium. This gives us the benefit of access to a fully documented review of the state of combustion LES in addition to the overview slides in the TNF7 Proceedings. Discussion of LES was also prompted by the presentation from Luc Vervisch, and some of those discussion points are included here.

Current practice with respect to LES was discussed at length. The following is suggested as the current state-of-play:

- Almost all LES calculations that are currently made do not perform grid independence studies. Users simply make a judicious choice of the filter width based on what they know about the flames or flows in question and proceed with their calculations.

- How much of the energy containing eddies are resolved during LES depends very much on the choice of the filter width and on the nature of the problem. Users seem to claim that they resolve most of these and use a figure of about 80%.

There was discussion about what constitutes "**good LES**", and the following criteria were proposed and accepted as NECESSARY, except for the third criterion which was thought to be problem specific and hence desirable rather than necessary.

1. Provide relevant estimates of the filter size. A standard method of achieving this is to plot estimates of the integral length scale, L_I, the Kolmogorov length scale, L_K, and the Gibson scale, L_G. The filter width can then be set on this plot. Here reference may be made to Figure 1 of Pitsch and Duchamp de Lageneste (*Proc. Combust. Inst*. 29:2001-2008, 2002) where a regime diagram for LES is presented.

2. Vary the filter size and check if the basic flame properties are preserved. The statistical, time averaged properties of the total signal (resolved plus SGS) should NOT depend on the filter size. The procedure to do this may be explicit or implicit filtering.

3. When there is no sub-grid turbulence, the SGS closure should reproduce the filtered laminar flame solution. This was argued to be possible only for premixed combustion and was thought to be not needed in some flow configurations or indeed not possible in diffusion flames. Hence it was deemed to be only a desirable criterion.

Linking DNS, LES, RANS, and Experiments

The overview presentation on this cross-cutting theme included examples from nonpremixed flames, premixed flames, and regimes in between. A clear message is that detailed simulations (both LES and DNS) are increasingly being used as tools to understand fundamental phenomena in turbulent combustion and also to interpret or augment experiments. Results from various groups were discussed: Sandia, Cambridge, NAL, Darmstadt, University of Washington, INSA-CORIA.

1. Some projections on the future of DNS were made, and it was suggested that turbulent Reynolds number of about 1500 will be a possible target within the next ten years using reduced chemistry.
2. So far, DNS of turbulent flames can be organized into three groups:
    a. DNS of a fully synthetic problem, as a planar flame (premixed, partially-premixed or diffusion) interacting with a freely decaying turbulence.
    b. DNS of a laboratory flame configuration, but after a serious scale-down. Typically, the ratio between premixed characteristic flame thickness and turbulent integral length scale is about ten times smaller in the DNS than it is in the experiment.
    c. DNS of a laboratory flame, but considering only a small portion of the flow, as it is done in the lifted flame simulation by the NAL group (Mizobuchi et al.).

    Various chemistry and transport properties have been used for all those simulations: Single-step, reduced, tabulated or detailed chemistry, combined with fixed or variable Lewis and Schmidt number or even complex transport.

There was a large consensus on the weakness of the estimation of prediction capabilities of SGS closures from DNS. Because of the lack of large scales in DNS, it can only be viewed as a very first step, which cannot be considered as fully conclusive. However, DNS results are very useful as a complement to experiments, to better select the underlying physical assumptions that may be used in SGS modeling. An example of this was given from DNS of flames stabilized on evaporating droplets, where DNS is combined with OH measurements to elucidate complex flame structures that will appear at the SGS level.

Update on Lifted Flames

A brief update was given on recent progress in current understanding of lifted flames stabilized in cold or vitiated co-flows. Submissions were received from the following research groups and presented at the meeting:

- Mastorakos at Cambridge: Experiments in flames auto-igniting in heated air
- Pope at Cornell: PDF calculations of lifted flames in vitiated co-flow
- Chen at Berkeley: PDF calculations of lifted flames in vitiated co-flow
- Mansour at Cairo: Lifted, partially premixed flames, PIV-LIF
- Lyons at North Carolina State: LIF imaging and PIV in lifted flames in cold co-flow

The following observations are made:

- Lifted flames in cold co-flows are receiving little current attention from the modeling community, and there is not yet a comprehensive data set for well-characterized flames where full flow, mixing, and composition field data are available at the stabilization base. The closest to that is the data set provided by Lyons et al.

- Lifted flames in vitiated co-flows are receiving attention with a particular focus on auto-ignition as a stabilization mechanism. The Cabra configuration with a large, hot co-flow seems to have (i) lifted modes where stabilization occurs by premixed flame propagation; and (ii) auto-ignition modes where the flame is dominated by convection and reaction only. Investigations are continuing to further unravel the mysteries of such flames.

- A new and interesting configuration is devised by Mastorakos where pulses of fuel issuing in heated air auto-ignite in a distinct way and with a popping or crackling noise. The noise is qualitatively very similar to the Cabra flame when it is believed to be in auto-ignition mode.

Chemical Mechanisms

Peter Lindstedt pointed out deficiencies in some current mechanisms of methane especially with reference to low temperature combustion relevant to auto-ignition. A near-term priority is to make available a reliable methane mechanism for broad applications including low-temperature combustion and auto-ignition.

Turbulent Premixed Flames

Several groups that are actively involved in the TNF Workshop series are also conducting research on turbulent premixed combustion and are interested in applying the same process of collaborative comparisons of measured and modeled results to selected premixed target flames. Andreas Dreizler presented an overview of the current state of premixed combustion experiments. Key discussion points from this session are:

- Turbulent premixed combustion processes will be addressed in future TNF workshops.

- An emphasis on chemistry and turbulence-chemistry interaction will be maintained.

- Several potential target flames were discussed; advantages and disadvantages of the configurations are not addressed here.
    - Piloted jet flame, data set from Chen et al., Combust. Flame 107 (1996) 223. Data available.
    - Low swirling flame, initial reference Bédat & Cheng, Combust. Flame 100 (1995) 485. Different designs of the burner are circulating. Before deciding for a specific configuration some agreement within the TNF community should be achieved. Collaborative experiments are planned by TU Darmstadt and Lund University (Mark Linne).
    - Strong swirling flame, information on data and design to be published soon (Schneider & Dreizler), data on flow field and turbulence structure available, detailed information on inflow boundary conditions available, scalar field work-in-progress. GT-relevant nozzle configuration.
    - V-flame and bluff-body flame, data available from F. Dinkelacker
    - Confined premixed swirl burner (Sandia), so far no detailed data available.
    - Premixed burner in vitiated co-flow (Sydney). This is in development as a simple extension of the vitiated-coflow burner from Berkeley. High shear rates are generated between jet and coflow.
    - Stratified-premixed burners are also in development by Erlangen and Darmstadt

Challenges of Sharing and Mining Large Experimental and Computational Data Sets

The first several TNF Workshops focused on comparison of single-point statistics of velocity and scalars in relatively simple flame geometries. Such data sets are easy to distribute, and the generation of collective comparison plots can be reasonably managed by one or two people. Collaborative comparisons in the future will have to address new challenges.

- Rigorous comparison of measured and modeled results is becoming increasingly difficult as we move to more complex flames. Complex flow fields must be documented before detailed consideration of finite-rate chemistry can be carried out in composition space. In the future, it may be desirable to develop automated tools for collecting and comparing results. Any interface that is developed must be simple, or it will not be used.

- In a similar context, it would be useful to collect and preserve results from various calculations of TNF flames, particularly once the calculations are published in the archival literature and especially if the results are “good”. In many cases, the details of a calculation are lost when the graduate student finishes. This restricts our ability as a community to really understand whether we are making progress.

- The very large DNS of the lifted H_2 jet flame by Mizobuchi and coworkers confronts the combustion community with a challenge to develop efficient methods to mine and share very large data sets. Large LES calculations of a few million nodes present similar challenges. Even the relatively small data sets from recent multi-scalar line imaging experiments at Sandia are more difficult to share than the simple point statistics that have been the main basis of TNF flame comparisons until now. PLIF and PIV imaging data present their own challenges. Work is clearly needed to find efficient methods for data sharing, so that we can explore increasingly complex science without becoming bogged down in the mechanics for data handling.

ORGANIZATION OF TNF8

Location and Dates: The TNF8 Workshop will be held in or near the Heidelberg, Germany around the time of the 31st Combustion Symposium. The schedule is likely to mimic that of TNF7.

Possible Focus Topics: Focus topics for TNF8 will be defined more specifically during the year before the workshop. However, it seems likely that some the following will receive attention:

- Progress in LES: It is anticipated that rapid advances in combustion LES, including increased resolution as well as advances in combustion submodels, will offer interesting opportunities for comparison with experiments and for extraction of new physical insights.

- Scalar Dissipation: More detailed comparisons on measured and modeled results for scalar dissipation and related quantities in the piloted CH_4/air flames are anticipated. In order to do this well, we will need to compare more than just scalar variance and scalar dissipation. Comparisons should extent to back to aspects of the turbulent velocity and scalar fields, such that the reasons for the wide differences among predicted scalar dissipation profiles seen at TNF7 may be understood. In addition, work must be completed to quantify the combined effect of noise, spatial averaging, and angle bias in the measurements of scalar dissipation, such that realistic uncertainty estimates may be provided.

- Mixing Models: It would be interesting to carry forward work on the performance of mixing models in combination with chemical mechanisms, as advocated at TNF6. This will require general availability of all the chemical mechanisms used by various groups.

- Sydney Bluff-Body and Swirl Flames: Further comparisons on the Sydney bluff-body and swirl flames should address details of turbulence-chemistry interaction by including comparisons in mixture fraction coordinates. This is expected to require conditioning on specific spatial locations, as opposed to inclusion of data from complete radial profiles (as was done for simple and piloted jet flames).

- Premixed Flames: TNF-style comparisons involving premixed combustion are awaiting the availability of at least one appropriate data set that includes measurements of velocity and scalar fields and are based on well defined boundary conditions that are computationally friendly. Premixed combustion activity at TNF8 will depend on the pace experimental progress and the adoption by modelers of one or more target cases.

- Lifted Flames: More activity on lifted flames, including the vitiated co-flow flames, can be expected, and this may expand to address the lifted CH_4 flame cases from Berkeley.

TNF7 Proceedings – Final Web Version

Table of Contents

(Additional or updated material has been included in this final version.)

Seventh International Workshop on Measurement and Computation of Turbulent Nonpremixed Flames

22-24 July 2004, Chicago, Illinois
Editors: R. S. Barlow and J. C. Oefelein

PREFACE:

The TNF Workshop series facilitates collaboration and information exchange among experimental and computational researchers in the field of turbulent nonpremixed and partially premixed combustion, with current emphasis on fundamental issues of turbulence-chemistry interactions in gaseous, non-sooting flames. The 1st TNF Workshop was held in Naples, Italy in July 1996. Its purpose was to select experimental data sets for testing combustion models and establish guidelines for collaborative comparisons of measured and calculated results on these target flames. Subsequent workshops were held in Heppenheim, Germany (1997), Boulder, Colorado (1998), Darmstadt, Germany (1999), Delft, The Netherlands (2000), and Sapporo, Japan (2002). Proceedings are available on the internet at http://www.ca.sandia.gov/TNF.

Our overall objectives are to: 1) provide an effective framework for comparison of different combustion modeling approaches, 2) establish series of benchmark experiments and calculations that cover a progression in geometric and chemical kinetic complexity, 3) identify and correct inconsistencies in the experimental data sets and expand the experimental knowledge base for benchmark flames, and 4) gain a better understanding of the capabilities and limitations of combustion models and experimental methods. We emphasize that this is not a competition, but rather a means of identifying areas for potential improvements in a variety of modeling approaches and experimental techniques. This collaborative process benefits from contributions by participants having complementary areas of expertise, including velocity measurements, scalar measurements, turbulence modeling, chemical kinetics, reduced mechanisms, mixing models, radiation, and combustion theory. The process also benefits from rapid communication over the internet. Data sets, computational submodels, and results of comparisons are being made available on the web to allow convenient access by all interested researchers. In many cases the results presented at this workshop represent work in progress. Accordingly, we strongly recommend that you check with the originator before using or quoting information in these proceedings.

The TNF Workshop format is intended to promote open discussion of fundamental research issues that are relevant to our overall objectives. All participants are encouraged to be active in these discussions, during the scheduled technical sessions and in small groups at other times.

ACKNOWLEDGEMENTS:

Partial support for the organization of the TNF Workshop series is provided by Sandia National Laboratories with funding from the United States Department of Energy, Office of Basic Energy Sciences. Special thanks to Ms. Judy Nielsen of Sandia.

Sponsorship contributions from ANSYS, Continuum, Fluent, GE Aircraft Engines, Reaction Engineering International, Rolls-Royce, and the SFB-586 Program are gratefully acknowledged.

Cover art by Daniel Strong, with flame images from R. Cabra, B. Dally, D. Geyer, P. Kalt, A. Kempf, and H. Pitsch.

TNF7 ORGANIZING COMMITTEE:

R. S. Barlow, R. W. Bilger, J.-Y. Chen, A. Dreizler, J. Janicka, R. P. Lindstedt, A. R. Masri, J. C. Oefelein, H. Pitsch, S. B. Pope, and D. Roekaerts

TNF7 -- Participants

Aggarwal, Prof. Suresh	University of Illinois at Chicago	USA
Anand, Dr. M.S.	Rolls Royce Corp	USA
Bai, Prof. Xue-Song	Lund Institute of Technology	Sweden
Barlow, Dr.Robert	Sandia National Laboratories	USA
Behrendt, Prof. Frank	Berlin University of Technology	Germany
Bilger, Prof. Robert	University of Sydney	Australia
Buchholz, Mr. Bert	University of Rostock	Germany
Cant, Dr. Stewart	Cambridge University	United Kingdom
Cao, Mr. Renfeng	Cornell University	USA
Chandy, Mr Abhilash	Purdue University	USA
Chen, Dr. Jacqueline	Sandia National Laboratories	USA
Chen, Prof. J.-Y.	University of California at Berkeley	USA
Cho, Mr. Eun-Seong	Seoul National University	Korea
Claramunt, Mr. Kilian	Technical University of Catalonia	Spain
Clemens, Prof. Noel	University of Texas at Austin	USA
Consul, Dr. Ricard	Technical University of Catalonia	Spain
Coppola, Mr. Gianfilippo	Yale University	USA
Dally, Dr.Bassam	Adelaide University	Australia
Dibble, Prof. Robert	University of California at Berkeley	USA
Dinkelacker, Dr. Friedrich	Universitdt Erlangen - LTT	Germany
Dreizler, Dr. Andreas	Technical University of Darmstadt, EKT	Germany
Ferreira, Dr. Jorge Carregal	ANSYS Germany GmbH	Germany
Frank, Dr. Jonathan	Sandia National Laboratories	USA
Ganguly, Mr. Ranjan	University of Illinois at Chicago	USA
Geyer, Mr. Dirk	Technical University of Darmstadt, EKT	Germany
Gomez, Prof Alessandro	Yale University	USA
Gordon, Mr. Robert	University of Sydney	Australia
Gore, Dr. Jay	Purdue University	USA
Hawkes, Evatt	Sandia National Laboratories	USA
Hewson, Dr. John	Sandia National Laboratories	USA
Huh, Prof. Kang Y.	Pohang University of Science & Technology	Korea
Ihme, Mr. Matthias	Stanford University	USA
Ikeda, Dr. Yuji	Imagineering. Inc.	Japan
James, Dr. Sunil	Rolls-Royce Corporation	USA
Janicka, Prof. Johannes	Technical University of Darmstadt, EKT	Germany
Jones, Prof. William	Imperial College London	United Kingdom
Kaiser, Mr Sebastian	Yale University	USA
Kalt, Dr. Peter	University of Adelaide	Australia
Kang, Dr. Sungmo	Hanyang University	Korea
Karpetis, Dr. Adonios	Sandia National Laboratories	USA
Kempf, Dr. Andreas	EKT, TU-Darmstadt, Germany	Germany
Kim, Dr. Jong Soo	Korea Institute of Science and Technology	Korea
Kim, Mr. Gunhong	Hanyang University	Korea
Kim, Prof. Yongmo	Hanyang University	Korea
Klimenko, Dr. Alex	The University of Queensland	Australia
Kosaly, Prof. George	University of Washington	USA
Krishnaswami, Dr. Sundar	GE Aircraft Engines	India
Kronenburg, Dr. Andreas	Imperial College London	United Kingdom
Kyritsis, Dr. Dimitrios	University of Illinois at Urbana-Champaign	USA
Lindstedt, Prof. Peter	Imperial College London	United Kingdom
Long, Prof. Marshall	Yale University	USA
Lu, Ms. Liuyan	Cornell University	USA

Masri, Prof. Assaad	The University of Sydney	Australia
Mehravaran, Mr. Kian	Michigan State University	USA
Meier, Dr. Wolfgang	German Aerospace Center DLR	Germany
Merci, Dr. Bart	Ghent University	Belgium
Meyer, Dr. Terrence	Innovative Scientific Solutions, Inc.	USA
Mizobuchi, Dr. Yasuhiro	Japan Aerospace Exporalation Agency	Japan
Nathan, Dr. Graham	The University of Adelaide	Australia
Naud, Dr. Bertrand	LITEC-CSIC	Spain
Oefelein, Dr.Joseph	Sandia National Laboratories	USA
Pfitzner, Prof. Michael	Universität der Bundeswehr Munchen	Germany
Pitsch, Prof. Heinz	Stanford University	USA
Pope, Prof. Stephen	Cornell University	USA
Rahn, Dr. Larry	Sandia National Laboratories	USA
Raman, Dr. Venkatramanan	Center for Turbulence Research	USA
Ren, Mr. Zhuyin	Cornell University	USA
Roekaerts, Prof. Dirk	Delft University of Technology	The Netherlands
Sayre, Mr. Alan	Babcock & Wilcox	USA
Shinjo, Dr. Junji	Japan Aerospace Exporalation Agency	Japan
Sinha, Mr Ashok	University of Illinois at Chicago	USA
Stevens, Dr. Eric	GE Aircraft Engines	USA
Sutherland, James	Sandia National Laboratories	USA
Szego, Mr. George	University of Adelaide	Australia
Takeno, Prof. Tadao	Meijo University	Japan
Tong, Prof. Chenning	Clemson University	USA
Torres, Mr. Jose Salvador Ochoa	Fluid Mechanic Group University of Zaragoza	Spain
Vervisch, Prof. Luc	INSA/Coria/CNRS	France
Wang, Mr. Guanghua	University of Texas at Austin	USA
Williams, Prof. Forman	University of California, San Diego	USA
Zimmer, Dr. Laurent	Japan Aerospace Exporalation Agency	Japan

TNF7 – Agenda

Holiday Inn – Chicago City Center, 22-24 July 2004
(Times may be adjusted to accommodate discussion.)

Thursday July 22, 2004

4:00 – 5:00	Registration and Poster Setup
5:00 – 9:00	Welcoming Remarks, Reception, and Poster Session 30-Second Advertisements by Poster Authors

Friday July 23, 2004

7:30 – 8:00	Continental Breakfast in the Meeting Room
8:00 – 8:15	Overview of the TNF Workshop Process, Introductory Remarks (Rob Barlow)
8:15 – 9:45	Comparison of Measured and Modeled Results on the Sydney Bluff-Body Flames (Andreas Kempf) Discussion of Progress, Problems, and Future Work on the Sydney Bluff-Body and Swirl Flames (Discussion Leader: Assaad Masri)
9:45 – 10:00	Coffee Break
10:00 – 11:00	Statistical Modeling of Extinction and Re-ignition (Coordinator: Steve Pope)
11:00 – 11:20	Update on Radiation (Dirk Roekaerts)
11:20 – 11:30	Short Break
11:30 – 1:00	Modeling and Measurement of Scalar Dissipation and Spatial Structure (Coordinators: Bob Bilger and Rob Barlow)
1:00	Lunch *Afternoon free for small group discussions and other activities.* *Meeting of organizers and presenters to readjust the schedule as needed.*
5:00 – 6:00	Poster Hour (with refreshments)
6:00	Dinner
7:30 – 8:30	LES of Combustion (Coordinator: Johannes Janicka)
8:30 – 9:30	Linking DNS, LES, RANS, and Experiments (Coordinator: Luc Vervisch)

TNF7 – Agenda

Holiday Inn – Chicago City Center, 22-24 July 2004
(Times may be adjusted to accommodate discussion.)

Saturday July 24, 2004

8:00 – 8:30	Continental Breakfast in the Meeting Room
8:30 – 10:00	Continued Discussion on Day-1 Topics (Respective coordinators to lead discussions, timing to be determined.)
10:00 – 10:30	Update on Lifted Flames (Assaad Masri)
10:30 – 11:00	Coffee Break
11:00 – 11:45	Premixed Combustion (Coordinator: Andreas Dreizler)
11:45 – 12:30	Proposals and Priorities for Future TNF Collaborations and Comparisons (Discussion Leader: Bob Bilger)
12:30	Lunch (Working lunch for the Organizing Committee)
1:30 –	Summary Discussion and Planning for the next Workshop (Discussion Leader: Johannes Janicka)
	Free Discussion Time
3:00	Adjourn, Remove Posters

TNF7 Workshop – Contributed Posters

Abstract Title	Authors
Partially Premixed n-Heptane/Air Counter Flow Flames	P. Berta, I.K. Puri, and S.K. Aggarwal
Turbulent Lifted Flame in a Vitiated Coflow Investigated Using Joint PDF Calculations	R. Cao, S. B. Pope, and A. R. Masri
Modeling Turbulent Non-Premixed Jet Flames using FLUENT's PDF Transport Model: Effect of Mixing Model on Flame Extinction	A.J. Chandy, G.M. Goldin, and S.H. Frankel
Laminar Flamelet Modeling of Turbulent Piloted Methane/Air Diffusion Flame	K.Claramunt, D. Carbonell, R. Cònsul, C.D. Pérez-Segarra, and A. Oliva
On the Modelling of Turbulent Jets in a Hot and Diluted CoFlow	B. B. Dally and F. Christo
Numerical Simulation of a Premixed Dump Combustor using LES and a Filtered G-Equation	M. Düsing, A. Sadiki, and J.Janicka
Simulation of Raman Spectra for the Evaluation of Concentration Data in Hydrocarbon-air Flames	D. Geyer and A. Dreizler
Comparison of 1^{st} and 2^{nd} order CMC predictions for Sandia Flames D, E and F	I. Han and K. Y. Huh
Application of a Steady Flamelet/Progress Variable Model to Sandia Flame D	M. Ihme and H. Pitsch
Lifted Flame Studies Under Gas Turbine Combustor Conditions	B. Janus, A. Dreizler, and J.Janicka
Multi-Scalar Imaging in Argon-Diluted Jet Flames	S. A. Kaiser, M. B. Long, and J. H. Frank
Numerical Modeling for Turbulent Lifted Jet Flame with Vitiated Coflow	S. Kang, H. Kim, J. Yu and Y. Kim
LES Of the Darmstadt Opposed Jet Flame: A setup allowing to identify and to work on problems in sub-models	A. Kempf and J. Janicka
Simulation of Turbulent Flame Lift Off by the Method of Flame Hole Dynamics	J. S. Kim and J. Kim
Match Conditional Variance in PDF Modelling	A.Y. Klimenko
Composition PDF Calculations of Turbulent Lifted Flames of H_2/N_2 Issuing into a Vitiated Co-Flow	L. Lu, R. Cao, S.B. Pope, and G.M. Goldin

Abstract Title	Authors
Experimental Data Base from Swirl Flames in a Gas Turbine Model Combustor	W. Meier, P. Weigand, X.R. Duan, R. Giezendanner, U. Meier, B. Lehmann, and M. Aigner
Investigation of the Effect and Behaviour of Different Turbulent Mixing Models on Transported Scalar PDF Simulation Results for Delft Flame III	B. Merci, B. Naud, D. Roekaerts, and N. Beishuizen
Studies of Micro-Vortex/Flame Interactions and Implications for Flamelet Modeling Theory	T.R. Meyer, V.R. Katta, J.R. Gord, and W.M. Roquemore
An Attempt to Understand the Vigorously Turbulent Flames in a Hydrogen Jet Lifted Flame	Y. Mizobuchi, J. Shinjo, S. Ogawa, and T. Takeno
PDFD: A hybrid code for solving the joint velocity-composition PDF equation. Application to the modeling of a bluff-body stabilized flame	B. Naud, N.A. Beishuizen, and D. Roekaerts
A Web Portal for Multi-scale Chemical Science Data and Applications	L. Rahn, T.C. Allison, S. Bittner, B. Didier, M. Frenklach, W.H. Green, Jr., D. Hale, MF. Hategan-Marandiuc, C. Lansing, G.von Laszewski, D. Leahy, J.D. Myer, M. Minkoff, D. Montoya, L. Oluwole, C. Pancerella, R. Pinzon, W. Pitz, J, Riese, B. Ruscic, K. Schuchardt, A.F. Wagner, T. Windus, C Yang, and G. Young
LES-Transported FDF Simulations of a Bluff-Body Stabilized Flame	V. Raman, H. Pitsch, and R. Fox
Turbulence Structure of Premixed Combusting and Isothermal Swirling Flows	C. Schneider, A. Dreizler, and J. Janicka
Control of Confined Nonpremixed Flames Using a Microjet	A. Sinha, R. Ganguly, and I.K. Puri
Reignition Scenarios in a Simulated Diffusion Flame	P. Sripakagorn and G. Kosaly
Experimental Study of Subgrid-scale Mixing for Improving Large Eddy Simulation of Turbulent Combustion	C. Tong
Effects of Imaging System Blur on Measurements of Flow Scalars and Scalar-Gradients	G. Wang and N. T. Clemens
Mean Spectral Radiation Data of Flame D	Y. Zheng, J. P. Gore, and R.S. Barlow

Partially Premixed n-Heptane/Air Counterflow Flames

P. Berta, I. K. Puri*, and S. K. Aggarwal

Department of Mechanical and Industrial Engineering
University of Illinois at Chicago, Chicago IL 60607 – USA

Abstract

Liquid fuels are an important energy source, since they are used in numerous propulsion and energy conversion applications. The characteristics of liquid fuel combustion are very complex. The fuel is introduced into the combustion chamber in the form of a spray that consists of droplets with a wide size and velocity distribution, resulting in disparate vaporization rates. In order to avoid the complexities associated with the droplet/vapor transport and nonuniform evaporation processes, a fundamental investigation of liquid fuel combustion in idealized configurations is very useful. Such an investigation can also facilitate the validation of fundamental theoretical/computational models through measurements in flames. Although most practical liquid fuels are blends of several components, n-heptane has been examined for its role as a surrogate liquid fuel for sake of simplicity. It is also a reference fuel in the definition of the octane number, and its oxidation chemistry has been extensively investigated.

Partially premixed flames contain a rich premixed fuel–air mixture in a pocket or stream, and, for complete combustion to occur, they require the transport of oxidizer from an appropriately oxidizer–rich (or fuel–lean) mixture that is present in another pocket or stream. Partial oxidation reactions occur in fuel–rich portions of the mixture and any remaining unburned fuel and/or intermediate species are consumed in the oxidizer–rich portions. Partially premixed flames are important in numerous applications. They are relevant to turbulent nonpremixed combustion, which can contain regions where local extinction occurs, followed by partial premixing and re-ignition. Partially premixed combustion plays a fundamental role in the stabilization of lifted nonpremixed flames in which propagating premixed reaction zones anchor a nonpremixed reaction zone. In addition, droplet-containing group flames contain regions of partially premixed combustion. These flames are also important in most liquid-fueled combustion devices including gas turbine, diesel, and rocket engine combustors.

A detailed schematic diagram of the experimental setup is presented in Figure 1. The separation distance between the nozzles of the counterflow burner is 15 mm and their diameter is 27.38 mm. The fuel is introduced from the bottom nozzle. A nitrogen curtain is established through an annular duct surrounding the fuel jet in order to isolate the flame from ambient disturbances. The nitrogen and burned gases are exhausted and cooled through another annular duct around the oxidizer nozzle. The velocities of the two streams are chosen to conform to the global strain rate,

$$a_g = \frac{2|V_O|}{L}\left(1+\frac{|V_F|}{|V_O|}\sqrt{\frac{\rho_F}{\rho_O}}\right),$$

and to satisfy the momentum balance, $\rho_O V_O{}^2 = \rho_F V_F{}^2$.

* Corresponding author: ikpuri@uic.edu

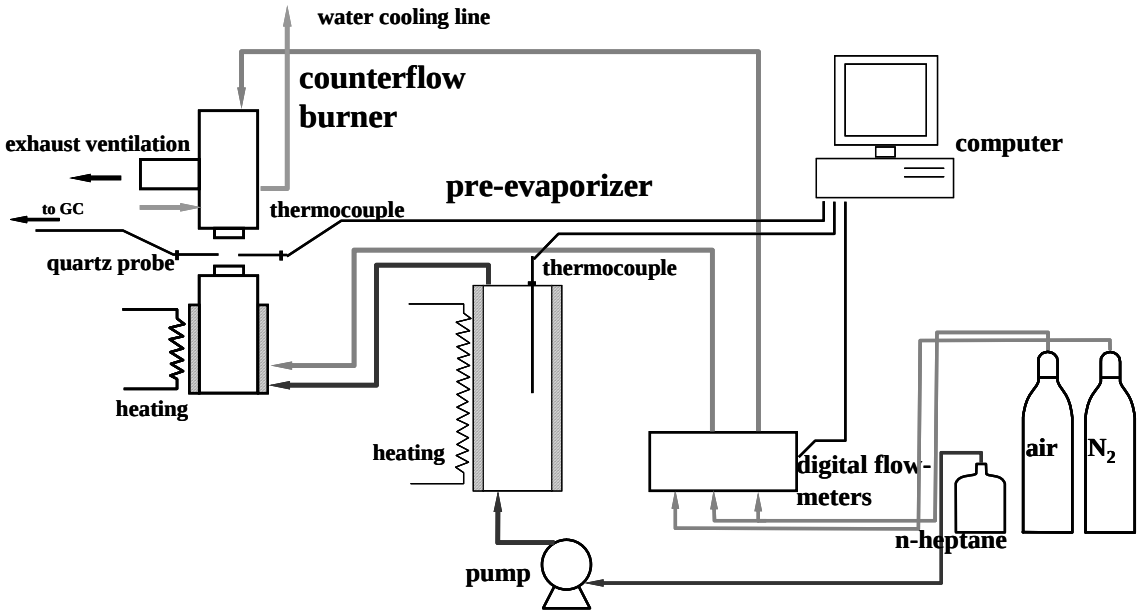

Figure 1. Experimental Apparatus

The oxidizer is air at room temperature while the fuel stream consists of mixtures of air and prevaporized n-heptane. The fuel nozzle is heated and the temperature is controlled to maintain the fuel-containing stream at a 400 K temperature at the burner exit. The air/n-heptane is mixed in a prevaporizer, which consists of a stainless steel chamber electrically heated. The desired mass flowrate of n-heptane into the prevaporizer is maintained by a liquid pump, while gaseous nitrogen is introduced through the bottom of the chamber.

A complete set of temperature and species concentration measurements has been obtained for several partially premixed configurations (Figure 2). These experimental results are extremely valuable for the development of a theoretical model capable of improving fundamental understanding of combustion processes of liquid fuels. A properly characterized reaction mechanism can accurately describe the combustion inside a piston/cylinder assembly, inside a gas turbine, i.e., wherever complex turbulent flames are involved.

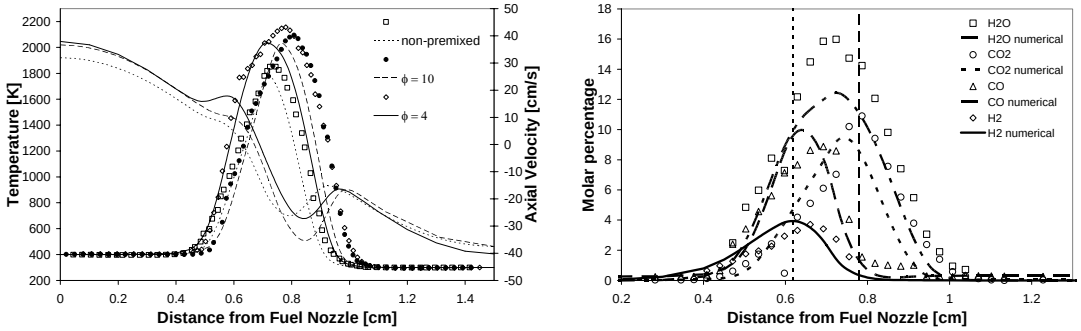

Figure 2. Temperature and velocity profiles for nonpremixed and partially premixed flames (left) and main species concentration profiles for $\phi = 4$ (right). The experimental results (dots) are compared with numerical simulations (lines).

TURBULENT LIFTED FLAME IN A VITIATED COFLOW INVESTIGATED USING JOINT PDF CALCULATIONS

Renfeng Cao[1], Stephen B. Pope[1], and Assaad R. Masri[2]
[1] *Cornell University, USA;* [2] *University of Sydney, Australia*
rc239@cornell.edu

The joint velocity-turbulence frequency-composition PDF method is applied to a lifted turbulent jet flame with H_2/N_2 fuel issuing into a wide co-flow of lean combustion products, which are at a temperature of about 1045 K. This burner geometry developed by Cabra et al. [1] provides a platform for studying complex lifted flames which may be undergoing auto-ignition. Previous calculations have revealed high sensitivity to the chemical mechanism [2] while experiments have shown that the stabilisation height is very sensitive to the coflow temperature [3].

Model calculations with detailed chemistry are performed using three existing mixing models (IEM, MC and EMST) and two chemistry mechanisms (the Mueller and Li mechanisms), which are implemented using ISAT [4]. Numerically accurate results are obtained and compared with the experimental data. A new parallel algorithm involving domain partitioning of particles, has been implemented to facilitate these computations [5].

The velocity fields are compared with the measurements of Kent [6]. The effects of various boundary conditions are investigated and some of them are compared with the available measurements performed by Wu and coworkers [3]. The scalar fields are compared with the measurements of Cabra et al. [7].

One of the most important characteristics of this flame is that the stabilization height of this lifted flame is very sensitive to the coflow temperature [3]. One percent (i.e., 10K) change in the coflow temperature (which is well within the experimental uncertainty) can double the lift-off height. Other parameters such as fuel jet temperature, the coflow velocity and the jet velocity have little effect on flame lift-off.

This work presents detailed calculations of flame structure at various co-flow temperatures and compares the lift-off heights with measurements. It also investigates the effects of mixing models and chemical kinetic mechanisms on the calculation of lift-off height as well as other flame parameters such as temperature and species concentrations. It is shown in Fig. 1 that all calculations reproduce the measured lift-off heights reasonably well. The three mixing models give relatively similar results implying that the cases studied here are mainly controlled by chemical kinetics. The Li mechanism results in earlier ignition than the Mueller mechanism and hence gives shorter lift-off height over the whole test range. It is also found that different values of the mixing model constant C_f (C_f =1.5, 2.0, and 2.5) has little effect on the lift-off. There is no strong evidence to show that one specific mixing model is superior to others for this flame.

The joint PDF calculations generally give better agreement with the measurements than previous composition PDF calculations [2]. The composition PDF method over-predicts the spreading of the velocity and mixture fraction because of the use of the k-e model with standard coefficients (which is well known to yield excessive spreading of round jets). Figure 2 shows the Favre mean and rms mixture fraction obtained using the joint PDF and composition PDF calculations.

Generally, the velocity field and mixture fraction profiles are not very sensitivity to the boundary conditions, mixing models and chemistry mechanisms. But other variables such as temperature and reactive species are very sensitive to the coflow temperature. In order to compare with the measurements for those variables sensitive to the coflow temperature, the comparison is made at fixed lift-off height H/D. This corresponds to a 1% reduction in the coflow temperature in the calculations, which is well within the 3% experimental uncertainty. Good agreement with measurements is shown for the velocity, mixture fraction, temperature and species. More details can be found in [8].

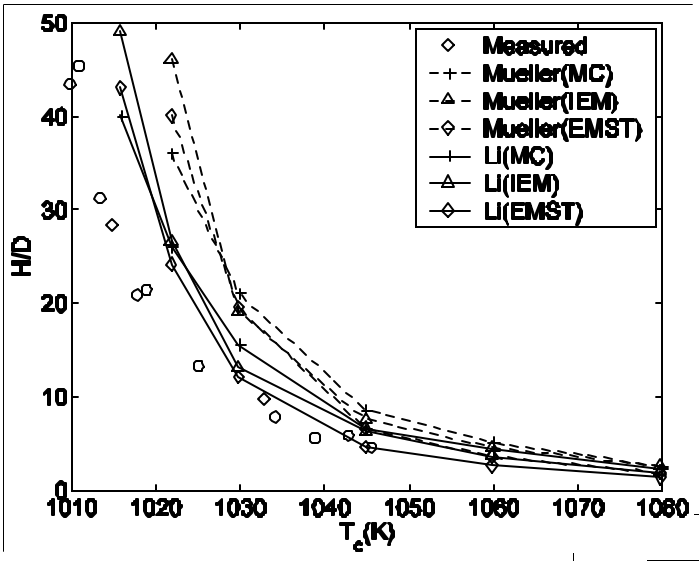

Figure 1

Lift-off height against coflow temperature. Circles: measurement [3]; Lines: joint PDF calculations using Mueller mechanism (solid line) and Li mechanism (dashed line) with different mixing models. MC, line with cross; IEM, line with diamond; EMST: line with triangle.

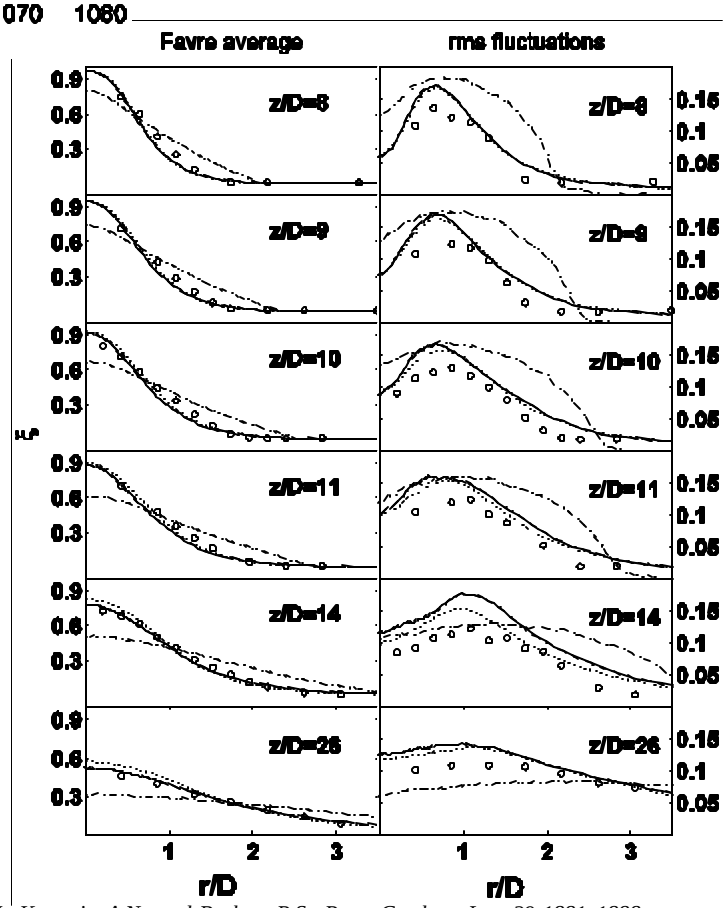

Figure 2

Radial profiles of Favre mean (left plots) and rms (right plots) mixture fraction. Circles, measurements [7]; dashed line: composition PDF calculations (MC, Mueller mechanism, T_c=1045 K); dotted line: joint PDF calculations with the same settings as those of composition PDF calculations (MC, Mueller mechanism, T_c=1045 K); solid line: joint PDF calculations using EMST mixing model, the Mueller mechanism, and coflow temperature T_c=1033 K. All the inlet velocity profiles of joint PDF calculations are taken from the composition PDF calculation.

References:

[1] *Cabra, R., Myrvold, T., Chen, J.Y., Dibble, R.W., Karpetis, A.N., and Barlow, R.S., Proc. Combust. Inst. 29:1881-1888, 2002*

[2] *Masri, A..R.., Cao, R.., Pope, S.B., and Goldin, G.M,, Combust. Theory Model. 8:1-22, 2004*

[3] *Wu, Z., Starner, S.H., and Bilger, R.W., 'Lift-off heights of turbulent H_2/N_2 jet flames in a vitiated coflow', Proceedings of The 2003 Australian Symposium on Combustion and The Eighth Australian Flame Days, Honnery,D.R. (Ed.) (ISBN 0-7326-2251-4), The Combustion Institute, 2003*

[4] *Pope,S.B., Combust. Theory and Model., 1, 41-63, 1997*

[5] *Cao, R., D.A. Caughey and S.B. Pope, Fall Technical Meeting of the Eastern States Section of the Combustion Institute, Penn State University, University Park, PA, October 26-29, 2003.*

[6] *Kent, J.E., "Gas velocity measurements of a lifted H_2/N_2 jet flame in a vitiated co-flow", BE Thesis, the University of Sydney, 2003.*

[7] *Cabra R, and Dibble R.W., http://www.me.berkeley.edu/cal/VCB/, 2002*

[8] *Cao, R, Pope, S.B., and Masri, A.R,. "Turbulent lifted flame in a vitiated coflow investigated using joint PDF calculations", Combust. Flame (submitted)*

Modeling Turbulent Non-premixed Jet Flames using FLUENT's PDF Transport Model: Effect of Mixing Model on Flame Extinction

A. J. Chandy[1], G. M. Goldin[2], S. H. Frankel.[1]
[1]School of Mechanical Engineering, Purdue University, West Lafayette, IN, USA
[2]FLUENT Inc, Lebanon, NH, USA

Introduction

The accurate modeling of turbulent reacting flows is crucial for the prediction of emissions, efficiency and other characteristics of combustion equipment. Non-premixed jet flames are of practical importance in diesel engines and they are of the type that involves separate entry of fuel and oxidizer into a combustion chamber where they mix and burn. Strong effects of turbulent fluctuations on chemical reactions can cause local extinction in non-premixed turbulent flames when the reactions are slow with respect to the turbulent time scale. Successful modeling of local extinction phenomena therefore requires a rigorous means of representing such intense interaction between turbulence and finite-rate chemistry. Probability Density Function (PDF) methods are currently one of the most popular approaches for predicting extinction dynamics since they overcome the most important closure problems. The measurements of piloted-jet methane flames made recently by Barlow and Frank [1] provide a library of comprehensive data which is ideal for testing combustion models. These flames, with different main jet velocities, exhibit different amounts of local extinction and are accordingly labeled D, E and F in order of increasing jet velocity. Starting from flame D, local extinction becomes visible, while flame F has substantial local extinction.

Methodology

In the modeling of turbulent reactive flows based on PDF methods, the change in fluid composition due to reaction is treated exactly, while the molecular mixing has to be modeled. In spite of the success of PDF methods in predicting phenomena such as extinction [2], studies [3] have demonstrated the sensitivity of extinction results to the choice of the mixing model and constants. The objective of this study is to apply the Lagrangian based PDF methodology available in the commercial finite volume code FLUENT to flames D and E and to study the effect of three mixing models namely the interaction by exchange with the mean (IEM) mixing model, the modified Curl (MC) mixing model and the Euclidean Minimum Spanning Tree (EMST) mixing model on local flame extinction. The ingredients of the PDF model consist of a joint composition PDF model; the mixing model; and the computer assisted reduced mechanism (CARM) of methane oxidation [4] which is computed by the in situ adaptive tabulation (ISAT) algorithm [5]. The standard k-e turbulence model, modified for axisymmetric jets, was used to close the Reynolds Averaged Navier-Stokes (RANS) equations.

Results

Predictions of radial profiles of mean and r.m.s of key flow variables from PDF calculations are compared with experimental data to analyze the effect of the mixing models on flame extinction. Typical comparisons of flame D are presented in Fig.1. In general, the agreement between computations and experiments is good, the largest discrepancies being for the predictions of radicals. Between the three mixing models, the

IEM and EMST models show the best agreement with experiments, with the latter exhibiting slightly better behavior for particular scalar profiles. Contour plots of temperature indicate the reduction of reaction zone thickness due to finite rate chemistry effects. Scatter plots of flames D and E for the different mixing models indicate the capability of the EMST mixing model to predict extinction better than the others (IEM and MC). This is because the EMST model is local in composition space, i.e. the change in composition due to mixing is influenced by the neighborhood in composition space.

Future Work

While the PDF model in FLUENT does a reasonable job in predicting statistics of flames D and E, it should be appreciated that the accuracy of the present calculations is limited by the accuracy of the velocity model (in this case the k-e turbulence model). Work is underway to combine the PDF methodology along with Large Eddy Simulation to calculate the same set of flames. Future work would also include simulations of flame F, which has a significant local extinction.

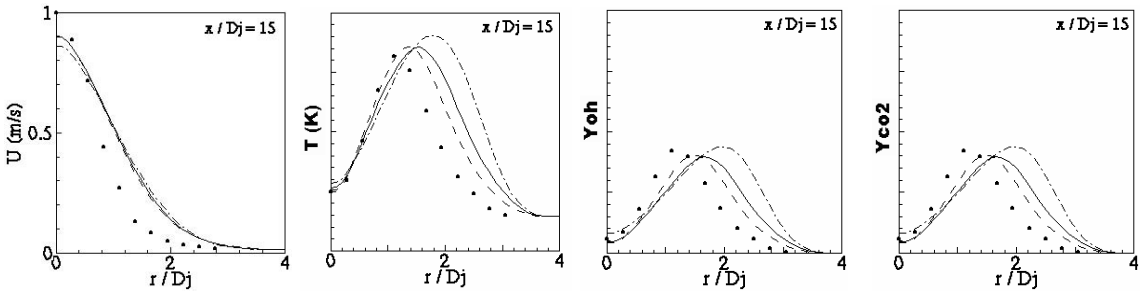

Fig. 1. Radial profiles of mean quantities of flame D at x/D_j = 15 (D_j, Fuel Jet diameter = 7.2 mm). Symbols, experiment; lines: PDF calculations with IEM (solid), EMST (dashed) and MC (dash-dotted)

References

[1] Barlow, R. S., and Frank, J.H., 1998, "Effect of turbulence on species mass fractions in methane/air jet flames," *Proceedings of Combustion Institute,* **27**, pp. 1087.

[2] Norris, A.T., and Pope S.B., 1995, "Modeling of extinction in turbulent diffusion flames by the velocity-dissipation-composition PDF method," *Combust. and Flame,* **100**, pp. 211-220.

[3] Xu, J., and Pope, S. B., 2000, "PDF Calculations of Turbulent Nonpremixed Flames with Local Extinction," *Combust. and Flame,* **123**, pp. 281-307.

[4] Mallampalli, H. P., Fletcher, T. H., and Chen, J.Y., *Fall Meeting of the Western States Section of the Combustion Institute,* 1996, paper: 96F-098. http://www2.et.byu.edu/:8080/~tom/Papers/Hemant-SS96/WSS.html

[5] Pope, S.B., 1997, "Computationally Efficient Implementation of Combustion Chemistry using In Situ Adaptive Tabulation," *Combust. Theory and Modeling,* **1**, 41-63.

Laminar Flamelet Modeling of Turbulent Piloted Methane/Air Diffusion Flame.

K. Claramunt, D. Carbonell, R. Cònsul, C.D. Pérez-Segarra, A. Oliva

Centre Tecnològic de Transferència de Calor (CTTC)
Universitat Politècnica de Catalunya (UPC). c/Colom 11
E-08222, Terrassa, Barcelona, Spain

e-mail labtie@labtie.mmt.upc.es

The turbulent piloted methane/air diffusion flame (Flame-D), which has been experimentally investigated by Barlow and Frank [1], has been simulated numerically using an unsteady flamelet model. RANS model is used solving the Favre-averaged equations of continuity, momentum, energy, species, mixture fraction and its variance. An Eddy-viscosity Two-equation model ($k-\epsilon$) is used [2] with the common modification of the constant $C\epsilon_2 = 1.8$. The flamelet equations including differential diffusion can be expressed as [3]:

$$\rho\frac{\partial T}{\partial \tau} = \frac{\rho\chi}{2}\frac{\partial^2 T}{\partial Z^2} + \frac{\rho\chi}{2c_p}\frac{\partial c_p}{\partial Z}\frac{\partial T}{\partial Z} - \frac{1}{c_p}\sum_{i=1}^{N} h_i\dot{w}_i + \frac{\partial T}{\partial Z}\frac{\rho\chi}{2c_p}\sum_{i=1}^{N} c_{p_i}\frac{1}{Le_i}\frac{\partial Y_i}{\partial Z} \tag{1}$$

$$\rho\frac{\partial Y_i}{\partial \tau} = \frac{\rho\chi}{2Le_i}\frac{\partial^2 Y_i}{\partial Z^2} + \dot{w}_i + \frac{1}{4}\left(\frac{1}{Le_i}-1\right)\frac{\partial Y_i}{\partial Z}\left[\frac{\partial \rho\chi}{\partial Z} + \rho\chi\frac{c_p}{\lambda}\frac{\partial}{\partial Z}\left(\frac{\lambda}{c_p}\right)\right] \tag{2}$$

where T is temperature; c_{p_i} specific heat of ith species; h_i enthalpy of ith species; $\dot{w}_i$ net rate of production of ith species; Y_i mass fraction of ith species; Le_i Lewis number of ith species defined as $Le_i = \lambda/(c_p\rho D_{im})$ with D_{im} the effective diffusivity of the ith species; τ the flamelet time; Z the mixture fraction and χ the scalar dissipation rate.

Flamelet equations are converted into discretized equations using the finite volume technique. They are discretized in mixture fraction space concentrating the mesh around the stoichiometric value Z_{st}. The operator-splitting technique has been used (when it is necessary) to find an appropriate initial solution. Damped-Newton method is employed to reach the final solution. When unsteady simulations are carried out, the radiative source term is included using the Optically Thin approximation with the RADCAL absorption coefficients. The calculations has been performed with the GRI3.0 Mech and assuming unity-Lewis numbers.

For the CFD solution, finite volume technique over orthogonal staggered grids is applied with a fully implicit temporal differentiation. Central differences are employed for the evaluation of the diffusion terms, while Upwind scheme is used for the evaluation of convective ones. A segregated SIMPLE-like algorithm is considered in order to couple the velocity and pressure fields. A parallel multiblock algorithm based on domain decomposition techniques running with loosely coupled computers has been used [4].

A postprocessing procedure, based on the generalised Richardson extrapolation for h-refinement studies and on the GCI proposed by Roache, was used to establish a criterion on the sensitivity of the simulations to the computational model parameters that account for the discretization: the mesh spacing and the order of accuracy. This tool estimates the order of accuracy of the numerical solution (observed order of accuracy p), and the error band where the grid independent solution is expected to be contained (uncertainty due to discretization GCI), also providing criteria on the credibility of these estimations [4][5].

The coupling between the CFD code and the unsteady flamelet model is solved with an interactive procedure [6]. For each height the flamelet velocity propagation and all the profile of χ are evaluated and used in the flamelet calcultion, instead of assuming a functional dependence of χ ($f(Z)$). The axial flamelet velocity propagation used to evaluate the flamelet time τ can be defined as the stoichiometric velocity V_{zst} or as the averaged radial velocity V_{av}.

In Fig1.(a) the $\widetilde{Z}$ and the $\widetilde{T}$ are compared with the experimental data [1]. Slight discrepancies are found in $\widetilde{Z}$ that might be attributed to the turbulent model. These differences can be improved by the

Pope modification. $\widetilde{T}$ in function of $\widetilde{Z}$ is presented in the Fig1.(b) with good agreement, which means that the combustion model works well. When radiation is included, the unsteady calculation is necessary and the results are clearly improved. The centrelines mass fractions are enhanced by the unsteady radiative calculations, specially the species presented in this work, CO, H_2 and NO. Anyhow these species are overpredicted. CO and H_2 mass fractions are predicted reasonably accurate, and the NO profile is in the same order of magnitude. The responsible of the discrepancies might be the reaction mechanism and the turbulence model.

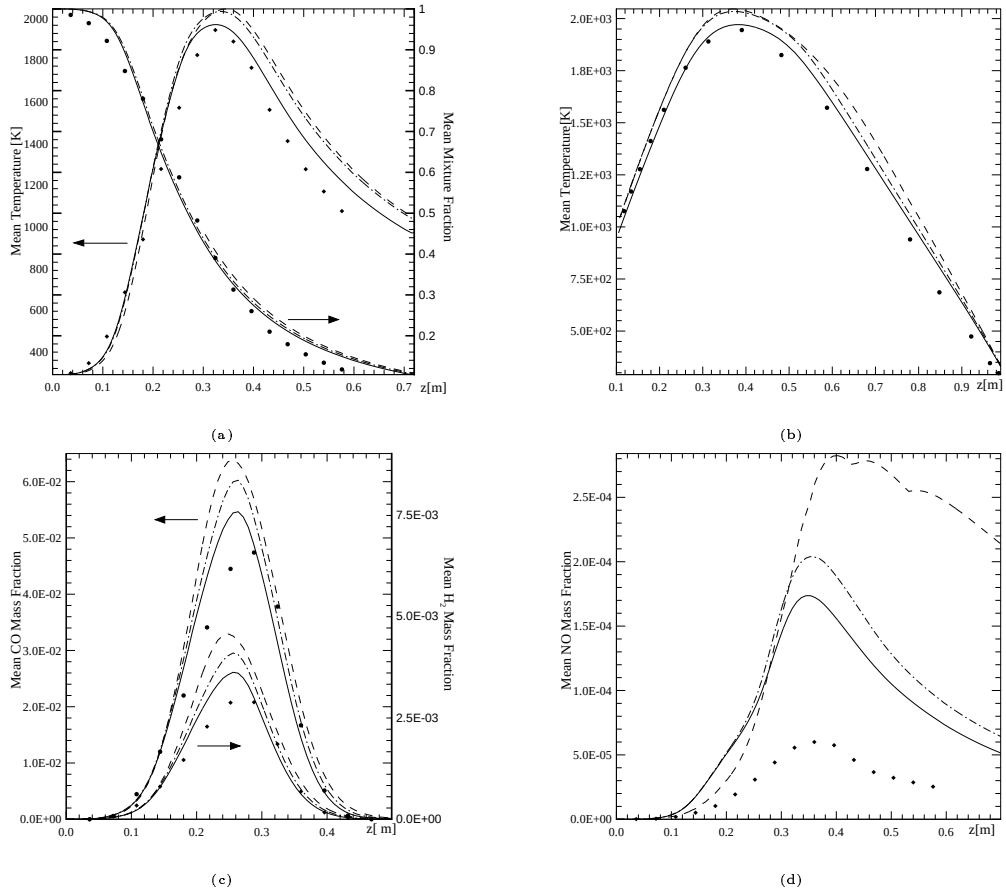

Figure 1: Numerical results compared with experimental data (symbols) obtained by using Unsteady Flamlets including radiation (solid lines), Unsteady Flamelets neglecting radiation (dot-dashed lines) and Steady Flamelets neglecting radiation (dashed lines).

References

[1] R.S. Barlow and J.H. Frank. In *Twenty-Seventh Symposium (International) on Combustion*, pages 1087–1095. The Combustion Institute, Pittsburgh, 1998.

[2] B.E. Launder and B.I. Sharma. *Letters in Heat Transfer*, 1:131–138, 1974.

[3] H. Pitsch and N. Peters. *Combustion and Flame*, 114:26–40, 1998.

[4] R. Còsul, C.D. Pérez-Segarra, K. Claramunt, J. Cadafalch, and A. Oliva. *Combustion Theory and Modelling*, 7(3):525–544, August 2003.

[5] K. Claramunt, R. Còsul, C.D. Pérez-Segarra, and A. Oliva. *Combustion and Flame*, 137:444–457, 2004.

[6] H. Pitsch, M. Chen, and N. Peters. In *Twenty-Seventh Symposium (International) on Combustion*, pages 1057–1064. The Combustion Institute, Pittsburgh, 1998.

ON THE MODELLING OF TURBULENT JETS IN A HOT AND DILUTED COFLOW

Bassam Dally and Farid Christo*
School of Mechanical Engineering
Adelaide University, SA 5005, Australia

* Defence Science and Technology Organisation
Weapons Systems Division
Edinburgh, South Australia, 5111, AUSTRALIA
bassam.dally@adelaide.edu.au

In many practical applications fuel jets are injected into hot and diluted surroundings. Such configuration is most prominent in MILD combustion where exhaust gases and heat recirculation plays an important role in establishing this combustion regime. Dally et al [1] reported detailed experiments on a laboratory scale burner which consisted of an insulated fuel jet, 4mm in diameter, issuing into hot combustion products from 80mm annulus. They reported measurements of temperature, mixture fraction and concentration of major and minor species using the single-point Raman-Rayleigh-LIF techniques. Table 1 shows the flow conditions for the three flames investigated in that study. The temperature of the coflow was maintained at ~1300K while the oxygen concentration was varied by replacing excess air with nitrogen.

Table 1Flow conditions for the flames investigated in this study

Fuel Jet (CH_4/H_2)			**Oxidant Coflow**				
Case	**Re#**	**T(K)**	**T(K)**	**YO_2 %**	**YN_2 %**	**YH_2O %**	**YCO_2 %**
HM1	**9482**	**305**	**1300**	**3**	**85**	**6.5**	**5.5**
HM2	**9482**	**305**	**1300**	**6**	**82**	**6.5**	**5.5**
HM3	**9482**	**305**	**1300**	**9**	**79**	**6.5**	**5.5**

In this abstract we present modelling results for HM3 flame only. The main aim of this work is to examine the capability of a commercially available CFD package for modelling MILD combustion. Results (not shown) using conserved scalar based models (i.e. mixture fraction/PDF and flamelet models), were found inadequate. Therefore volumetric reactions based models were used; an eddy-dissipation model (EDM) with finite-rate global chemistry (7 species, 3 reactions), and an eddy-dissipation concept (EDC) approach with multi-step chemistry. In the EDC model, calculations were performed using methane skeletal kinetics (Smooke: 16 species, 33 reactions), and detailed mechanism (modified GRI3: 33 species, 233 reactions). The effect of differential diffusion on the accuracy of prediction was also examined.

Figure 1 illustrates the effect of differential diffusion on prediction accuracy. Excluding differential diffusion from the model yields a peak temperature that is 10% higher than the experimental value. Significant improvement in accuracy (of 0.3% relative error) however, was achieved when differential diffusion is included in the model. The effect of diffusion can be attributed to the laminarization of the flow due to the relatively high temperature of the coflow and the small increase of temperature in the reaction zone, which can also lead to lower density

gradients and reduced scalar fluctuations. It is clear therefore that differential diffusion plays an important role and should not be ignored.

Figure 2 shows calculated and experimental radial profiles of mass fraction of CO, CO_2 and OH (plotted in mixture fraction space), 30mm downstream from the jet exit. The EDM model shows the least agreement with the experiment, while the EDC model provides closer agreement with the experiment.

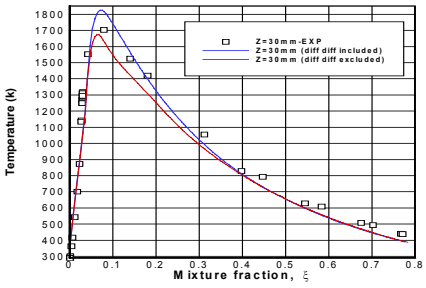

Figure 1: Effect of differential diffusion (diff diff) on model accuracy (EDC combustion model with Smooke mechanism).

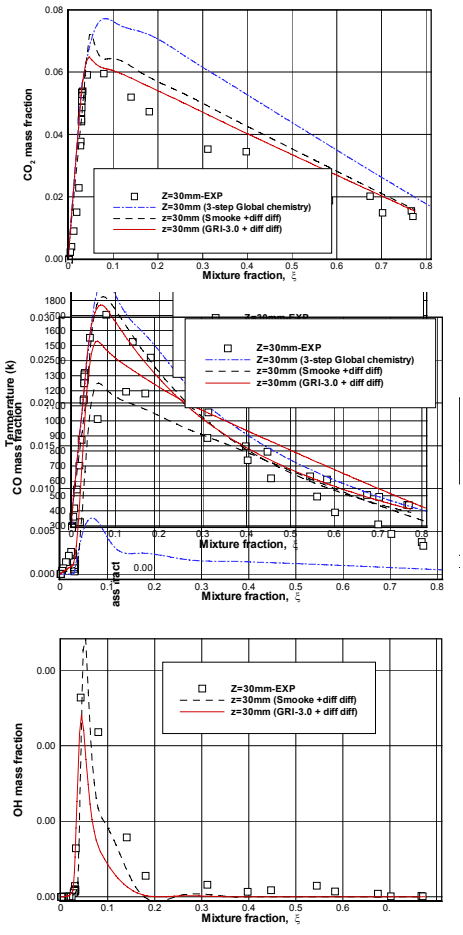

Figure 2: Effect of kinetics mechanism on model accuracy using EDM model with 3-step global chemistry, and EDC with Smooke and GRI-3.0 mechanisms (differential diffusion included in all models).

In summary, it is clear that detailed chemical kinetics is required to accurately capture the structure of MILD flames. Full details on this work are presented in Christo and Dally [2].

References:

1. B.B. Dally, A.N. Karpetis, R.S. Barlow, 'Structure of Turbulent Nonpremixed Jet Flames in a Diluted Hot Coflow', *Proceedings of the Combustion Institute*, 29 (2002), 1147-1154
2. F.C. Christo and B.B. Dally, 'On the modelling of turbulent jets in a hot and diluted coflow', submitted to Combustion and Flame, June 2004.

Numerical Simulation of a Premixed Dump Combustor using LES and a Filtered G-Equation

M. Düsing, A. Sadiki, J. Janicka
Institute for Energy and Powerplant Technology, TU Darmstadt, Germany
duesi@hrzpub.tu-darmstadt.de, sadiki@ekt.tu-darmstadt.de,
janicka@ekt.tu-darmstadt.de

Large-Eddy Simulation (LES) in three dimensions with a filtered G-equation was used for the simulation of a turbulent premixed flame with equilibrium chemistry. This strategy is supported by the instationary character of the flame and the fact that the spatial resolution Δx and the filterwidth Δ are large against the flame thickness l_f. Special care was taken to treat the filtered flamefront as a thin surface. The ORACLES-burner (case C_1), which was investigated here with LES, consists of a premixed C_3H_8-air flame behind a sudden symmetrical, double expansion. It can be considered as a highly simplified LPP system [1].
For filtering of the G-equation, we follow the analysis of Oberlack et al. [2], who introduced a PDF-averaged G-equation and Pitsch [3], who introduced a conditional-filtered G-equation as shown in (1).

$$\frac{\partial G}{\partial t} = (\mathbf{u}_u + s_l\,\mathbf{n}_f)\cdot\nabla G \quad \overset{Filtering}{\Rightarrow} \quad \frac{\partial \widehat{G}}{\partial t} = \widehat{\mathbf{u}_u\cdot\nabla G} + \widehat{s_l\,\mathbf{n}_f\cdot\nabla G}$$
$$\overset{Modeling}{\Rightarrow} \quad \frac{\partial \widehat{G}}{\partial t} = \left(\widetilde{\mathbf{u}}_u + s_t\,\mathbf{n}_{\hat{f}}\right)\cdot\nabla G \tag{1}$$

Thereby $G(\mathbf{x},t) = G_0$, $G(\mathbf{x},t) < G_0$, and $G(\mathbf{x},t) > G_0$ correspond to the flamefront, the unburnt, and burnt side respectively. The flame normal vector, the laminar and turbulent flame velocities and the velocity on the unburnt side of the flame are denoted by $\mathbf{n}_f = -\nabla G/|\nabla G|$, s_l, s_t, and $\mathbf{u}_u$. The superskripts $\widehat{\cdot}$, and $\widetilde{\cdot}$ denote for flame conditioned and Favre filtering. The filtered G-equation exhibits all symmetries introduced in [2]. Since a level-set method is used, there is need to keep $|\nabla\widehat{G}|$ bounded. Therefore a signed distance function is applied ($|\nabla\widehat{G}| = 1$). Using a newly developed modification of the reinizialisation scheme by Russo [4] to assure this condition the introduced errors are minimised [5].
Within the numerical simulations the extension velocity $F_{Ext} = \widetilde{\mathbf{u}}_u\cdot\mathbf{n}_f + s_t|_{\widehat{G}=G_0}$ is calculated first at the flamefront only. Using jump conditions the filtered velocity on the unburnt side of the flame $\widetilde{\mathbf{u}}_u$ is therefore reconstructed. Afterwards a 3d-version of the F_{Ext}-method [6] for time integration of $\widehat{G}$ is used. Thus the spatial initial value problem $\nabla\widehat{G}\cdot\nabla F_{Ext} = 0$ with $F_{Ext}|_{\widehat{G}=G_0}$ as initial values and $\partial\widehat{G}/\partial t = F_{Ext}$ is solved within the whole domain. This method conserves the signed distance function. The reinizialisation is used only to avoid numerical inaccuracies to accumulate. It is furthermore needed when topology changes have occured.
For discretization of the filtered incompressible Navier-Stokes equation a Smagorinsky model ($C_S = 0.2$) and a 2nd order central scheme is used. Since $l_f \ll \Delta x$ is valid, we distinguish between the unburnt and burnt sides of the flame for the fluxes of momentum. Therefore, the filtered flamefront and the momentum on both sides are reconstructed. In this way the thin character of the filtered flamefront is considered throughout the simulation. For time integration a three-step low-storage Runge-Kutta scheme was used. Adiabatic boundary conditions were used [6]. Since the Gibson-length is almost resolved $s_t = s_l$ was chosen as a first guess. The laminar flamespeed was calculated as $s_l = s_l^0(1 - \mathcal{L}\,\kappa_{\hat{f}})$. Thereby the undisturbed flame speed $s_l^0 = 0.3\,\mathrm{m\,s^{-1}}$, the curvature of the filtered flame $\kappa_{\hat{f}}$ and the Markstein-length $\mathcal{L} = 1.1\cdot10^{-3}$m were used.
In order to verify the numerical procedure the numerical scheme was applied to several test cases. In the following results made for the ORACLES-burner are presented and discussed. The numerical setup consists of a cartesian grid ($717.6 \times 20 \times 130.6\mathrm{mm}^3$, # control volumes ≈ 165000, $\Delta x \approx \Delta \approx 2.55$ mm $\Rightarrow \Delta/l_f \approx 14$) [6]. The simulation was carried out on a single Pentium 4 prozessor (2.5 GHz). Thereby, $\approx 150\,000$ timesteps and a real time of ≈ 1.5s have been calculated.

Figure 1 shows a snapshot of the filtered G-field. Moving downstream the corrugation of the flame front increases. At the tip of the flame topology changes occur frequently. These events are handled naturally by the level-set approach.
Comparison of mean velocities and variances between numerical and experimental data are presented on the right hand sides of Fig. 2. Thereby the value $U_B = 11\,\mathrm{m\,s^{-1}}$ corresponds to the bulk velocity within the channel. Furthermore values of the mean progress variable $\langle c \rangle = \left\langle \mathcal{H}(\widehat{G} - G_0) \right\rangle$, and the probability of finding the flamefront within a cell $\mathcal{P}_{\widehat{f}}$ are displayed on the left hand sides of Fig. 2. Thereby $\langle \cdot \rangle$ denotes for Reynolds-averaging of the samples and $\mathcal{H}(\cdot)$ is the Heaviside-function. Up to $x_1/H = 4$ the numerical results are in good agreement with the experiments. At $x_1/H = 8$ the mean velocities, and the fluctuations are overestimated within the simulatons. This behaviour results from the delicate interplay between fluctuations and heat release of the flame. Thereby velocity fluctuations amplify the wrinkling of the flamefront. Thus the flame surface increases, which further amplifies the heat-relase and thus the velocity and its fluctuations.

Bibliography:

[1] P. Bruel, P.D. Nguyen, AIAA paper 03-0958, 2003.
[2] M. Oberlack, H. Wenzel, N. Peters, Combust. Theory Model., 5:363-383, 2001.
[3] H. Pitsch, Ann. Res. Briefs, CTR, 3-14, 2002.
[4] G. Russo, P. Smereka, J. Comp. Phys., 163:2-22, 2000.
[5] M. Düsing, Large-Eddy Simulation turbulenter Vormischflammen, PhD-thesis, TU Darmstadt, 2003.
[6] D. Adalsteinsson, J.A. Sethian, J. Comp. Phys., 148:2-22, 1999.

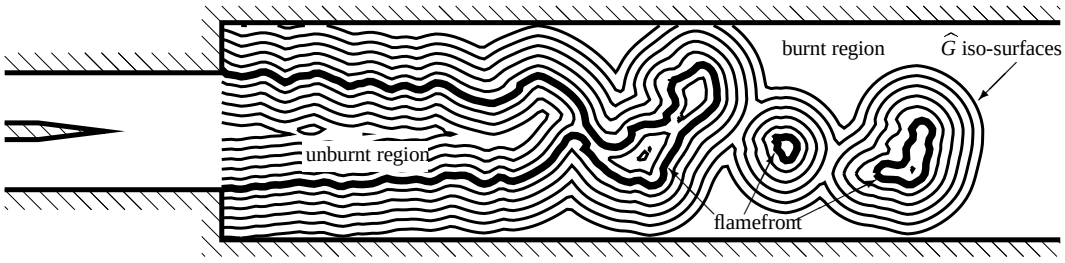

Figure 1: Snapshot of the $\widehat{G}$-field. The thick line corresponds to the filtered flamefront $\widehat{G} = G_0$, while thin lines correspond to iso-surfaces of $\widehat{G}$ apart of the flame.

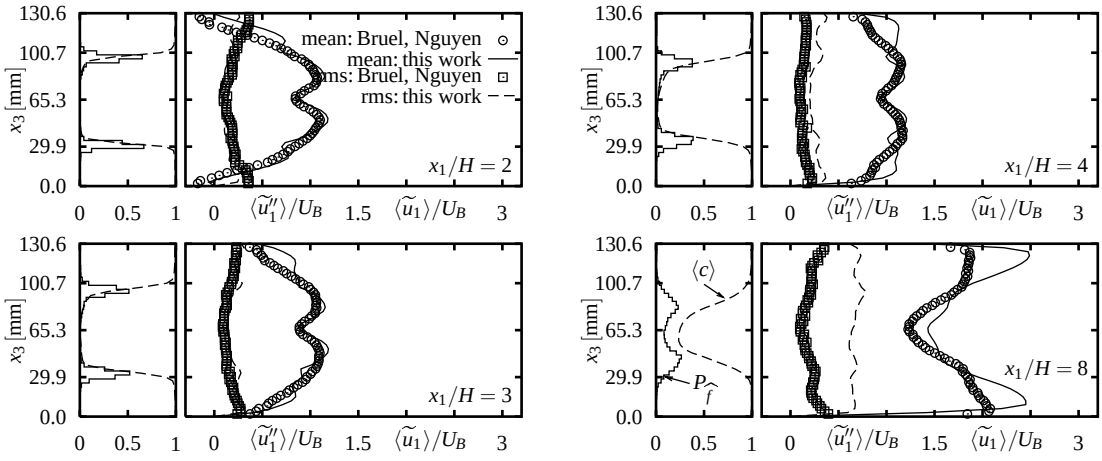

Figure 2: Mean progress variable $\langle c \rangle$, probability of finding flame surface within a cell $\mathcal{P}_{\widehat{f}}$ (left) and comparison with experiments of mean streamwise velocity (right).

Simulation of Raman spectra for the evaluation of concentration data in hydrocarbon-air flames

D. Geyer and A. Dreizler

geyer@ekt.tu-darmstadt.de, dreizler@ekt.tu-darmstadt.de
FG Energie- und Kraftwerkstechnik, TU Darmstadt,
Petersenstrasse 30, D – 64287 Darmstadt, Germany

1. Introduction

The application of Raman scattering in turbulent hydrocarbon flames is based on rotational-vibrational Raman transitions of the Stokes side. Evaluation of Raman spectra is either based on a matrix inversion method or on a full spectral fit [1]. The advantage of the latter method is due to its capability to correct inherently the crosstalk of Raman scattering originating from different molecules and of interferences from laser-induced fluorescence (LIF), as long as spectral libraries for these interferences are available. Furthermore, wavelength dependent background radiation and noise are visible in the corresponding spectra and can be treated in a spectral fit directly.

Although Raman spectroscopy is a widely used technique in combustion diagnostics the simulation of Raman spectra covering a wide range of temperatures for both di- and triatomic molecules so far is not available. In this contribution the generation of temperature dependent spectra libraries for H_2, O_2, N_2, CO in a range from 300 to 2500 K is described, including 2nd order effects in a perturbative approach. For CO_2 an approach is presented taking into account perturbations like Fermi- and Coriolis interactions or *l*-type doubling up to sixth order. A much simpler model is used for H_2O, due to the lack of more detailed spectroscopic information. Lastly, for CH_4 a pure experimental spectra library is employed.

2. Simulation of Raman spectra

To build up a temperature dependent Raman spectra library, the number of collected photons for each allowed transition is calculated. In the frame of Placzek's polarizability theory, the transition moment in the laboratory frame is dependent on the derivatives of the molecules isotropic and anisotropic polarizabilities as well as from factors arising from the integration of the polarizability over the molecules wavefunctions and from factors resulting from the transformation of polarizability in a molecule fixed coordinate system to the laboratory system.

For diatomic molecules in a singlet electronic ground state like H_2, N_2 or CO this transformation is contained in the Placzek-Teller coefficients [2], the Raman spectrum exhibits only O-, S-, and Q -branches. In contrast, the triplett state involved with O_2 leads to a transition of angular momentum coupling from Hund's case A to Hund's case B at low rotational quantum numbers, yielding additional weak R- and P-branches. Rotation-vibrational interaction and anharmonicities (2nd order effects) on the transition moments are taken into account by a perturbative approach based for instance on Herman-Wallis factors.

In case of CO_2 a strong Fermi coupling occurs between the Raman active vibrational v_1 symmetric stretching mode and the also Raman active overtone $2v_2$ of the molecules bending mode. Transition moments have to be calculated for unperturbed transitions for each of this modes separately and the perturbations, which includes nine different types like Fermi- and Coriolis interaction, are considered by mixing coefficients applied to the unperturbed moments. These mixing coefficients are the eigenfunctions of CO_2, originating from the solution of the secular equation for the effective block diagonal Hamiltonian [3]. Since a large number of vibrational levels contribute to the mixing at higher quantum numbers, the perturbations become even more important at higher temperatures. Thus, a large number of transitions in the O-, P-, Q-, R-, and S- branches, more than 100 millions in the current approach, have to be taken into account for flame diagnostics. Beside the mixing coefficients, also the energy levels employed to compute the transition wavenumbers of CO_2 are obtained as the eigenvalues by solving the secular equation.

For the simulation of ν_1 H_2O Raman spectra much less information on the molecule is available since description of the energy surface within the frame of a perturbation approach fails already at low quantum numbers. For that reason, an energy level database [4] is used and only the isotropic part of the polarizability tensor is accounted for by computing the transition moments in this preliminary approach. However, since Raman scattering of H_2O is highly isotropic these simplifications, combined with the use of the energy level database, provides more than $3x10^4$ transitions and are considered giving reliable cross-sections up to 2000 K [5].

To achieve the actual appearance of rotational-vibrational Raman bands observed in corresponding experiments, each transition has to be convoluted with the detection-unit transfer-function. The transfer-function is determined experimentally by Rayleigh scattering from helium for each molecule separately. As an example the following figure shows CO_2 Fermi-coupled $\nu_1+2\nu_2$ Raman bands for different temperatures.

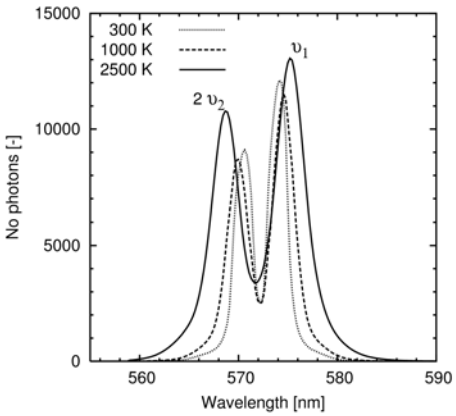

Simulated Raman bands of CO_2 for different temperatures. The shapes result from convolution of each single rotational-vibrational Raman transition with the detection-unit transfer-function. In this specific case the detection-unit consists of an achromatic corrected custom-designed lens system (LINOS), a 270 mm imaging spectrometer (Spex) and an intensified CCD camera (Roper scientific).

3. References

[1] R. S. Barlow, C. D. Carter, and R. W. Pitz, "Multi-species diagnostics in turbulent flames," in *Applied Combustion Diagnostics*, K. Kohse-Höinghaus and J. B. Jeffries, eds. (Taylor & Francis, New York, 2002).

[2] D. A. Long, *The Raman Effect: A Unified Treatment of the Theory of Raman Scattering by Molecules* (Wiley, 2002).

[3] S. A. Tashkun, V. I. Perevalov, J.-L. Teffo, A. D. Bykov, and N. N. Lavrentieva, "CDSD-1000, the high-temperature carbon dioxide spectroscopic databank," Journal of Quantitative Spectroscopy and Radiative Transfer **82**(1-4), 165-196 (2003).

[4] J. Tennyson, private communication (2002).

[5] D. Geyer, A. Dreizler, and J. Janicka, "Simulation of Raman Spectra of molecules relevant for methane flames. Part 2: triatomic molecules," In preparation.

Comparison of 1st and 2nd order CMC predictions for Sandia Flames D, E and F

Insuk Han, Kang Y. Huh
Pohang University of Science and Technology, Korea

The 1st order CMC has successfully been applied to a wide range of turbulent flames, in which all scalar quantities are primarily correlated with the instantaneous mixture state, i. e., mixture fraction. There have been concerns about accuracy of the 1st order conditional closure of the reaction rate for fluctuating flame structures far from the equilibrium state. Conditional fluctuations tend to increase at a lower Damkohler number near extinction or ignition limits as shown in the scatter plots of Flames D, E and F. The 2nd order CMC scheme is developed to make corrections for a few critical rate limiting steps, while 1st order closure is employed for all the other faster elementary steps. Here comparison is made between 1st and 2nd CMC predictions for Flames D, E and F for measured major and minor species involving NO. Results show significant improvement for Flame D especially near the jet exit where some local extinction occurs. Differences between measurement and calculation tends to decrease downstream, as the flame structure gets closer the equilibrium state. Although the 2nd order CMC shows some improvement over the 1st order CMC for Flame E and F, NO is significantly overpredicted. Although not represented in the figures in this abstract, second order correction is also made to the slow Zeldovich steps for thermal NO as well as the three rate limiting steps of hydrocarbon combustion [1]. Further improvement in NO prediction is expected by this additional 2nd order correction procedure. Downstream deviation of NO tends to increase since it is an accumulated effect from the jet exit. The k-e turbulence model must also be partly responsible for downstream deviation, since the turbulence model determines the pdf in terms of mixture fraction, which determines again the scalar dissipation rate according to the pdf transport equation. It is obvious that the 2nd order correction as suggested in Ref. [1] is not enough for Flame F with the most severe local extinction.

[1] Kim, S. H. and Huh, K. Y., “Second-Order Conditional Moment Closure Modeling of Turbulent Piloted Jet Diffusion Flames”, Combustion and Flame (in press).

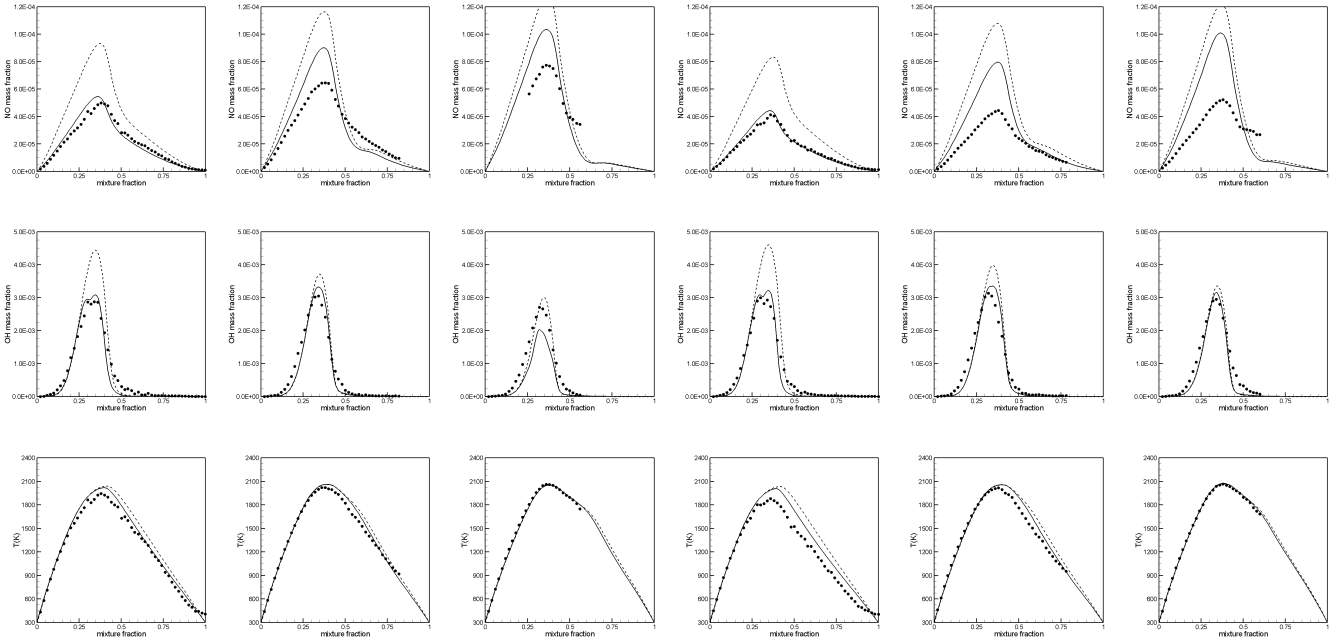

x/D=15 x/D=30 x/D=45 x/D=15 x/D=30 x/D=45

Flame D Flame E

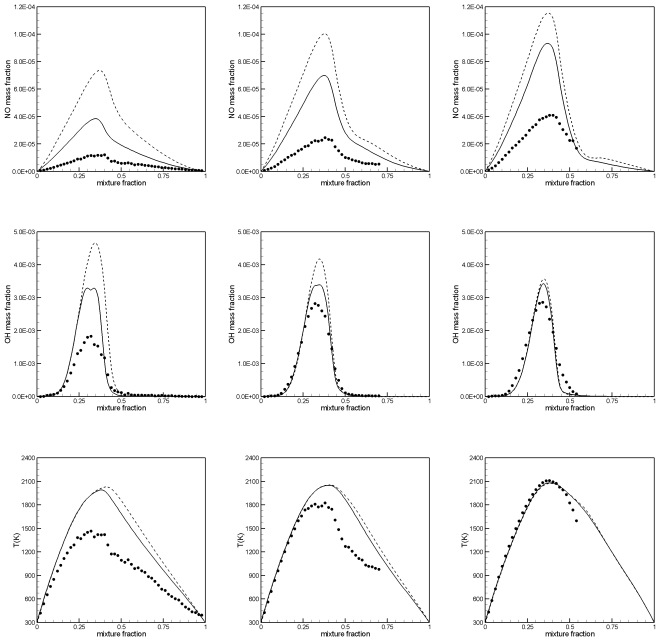

x/D=15 x/D=30 x/D=45

Flame F

Application of a Steady Flamelet/Progress Variable Model to Sandia Flame D

M. Ihme and H. Pitsch
Flow Physics and Computation
Department of Mechanical Engineering
Stanford University
Stanford, CA 94305

Large eddy simulation (LES) appears to be a promising approach for the numerical modeling of non-premixed, turbulent combustion processes. In this approach the energy-containing, large-scale motion is sufficiently resolved so that only the action of the numerically unresolved scales requires modeling [1]. Even though molecular mixing and chemical reaction as rate-limiting mechanisms occur on these scales, an adequate modeling seams to be more feasible compared to the Reynolds-averaged Navier-Stokes (RANS) approach.

In the present work a steady flamelet/progress variable (FPV) approach [2] is employed for the numerical simulation of the Sandia flame D experiment. In this model all chemical species are expressed in terms of the mixture fraction Z and a reactive scalar, the flamelet parameter λ. By using the flamelet parameter rather than the scalar dissipation rate χ, this model is, in principle, able to account for transitional effect, which occur when a flamelet extinguishes or re-ignites. The flamelet parameter is chosen in such a way that it is statistically independent from the mixture fraction which simplifies the modeling of the joint presumed probability density function (PDF) of Z and λ. Assuming statistical independence between Z and λ, the presumed joint PDF is modeled by a beta distribution for Z and delta function for λ. The flamelet parameter λ can be expressed in terms of a reaction progress variable C. Then, only one additional transport equation for the mean progress variable $\widetilde{C}$ in addition to the equation for $\widetilde{Z}$ needs to be solved to describe all chemical species.

The governing equations for mass, momentum, mixture fraction, and progress variable are solved in a cylindrical coordinate system employing a low Mach-number, finite volume code, which has been developed by Pierce & Moin [3]. The computational mesh contains 256 cells in axial direction, 152 in radial direction, and 64 grid points in circumferential direction on a computational domain $80 \times 25\ D$ in axial and radial direction, respectively. The subgrid-scalar fluxes are computed by the dynamic Smagorinsky model and the residual scalar variance $\widetilde{Z''^2}$ is computed by employing a gradient transport assumption with a dynamic modeling approach following Pierce & Moin [4].

The mean and root mean square value of the axial velocity along the centerline are in reasonable agreement with the experimental data and the mean mixture fraction along the centerline is slightly over-predicted in the lean part approximately for $x/D \geq 45$, resulting in elevated mean temperature and mass fraction for CO and CO_2.

A comparison of the time-averaged mean quantities of the chemical species conditioned on the mixture fraction with the experimental data for different axial stations, $x/D = 15$, 30 and 45, is shown in Fig. 1. The conditional mean temperature obtained from the simulation is in good agreement with the experimental data. The fuel and oxidizer consumption in the rich part is slightly over-predicted, leading to an over-prediction of water, molecular hydrogen, and carbon monoxide, respectively. Even though CO and H_2O are over-predicted, carbon dioxide, as stable reaction product from the water-gas shift reaction, is in excellent agreement with the experimental data.

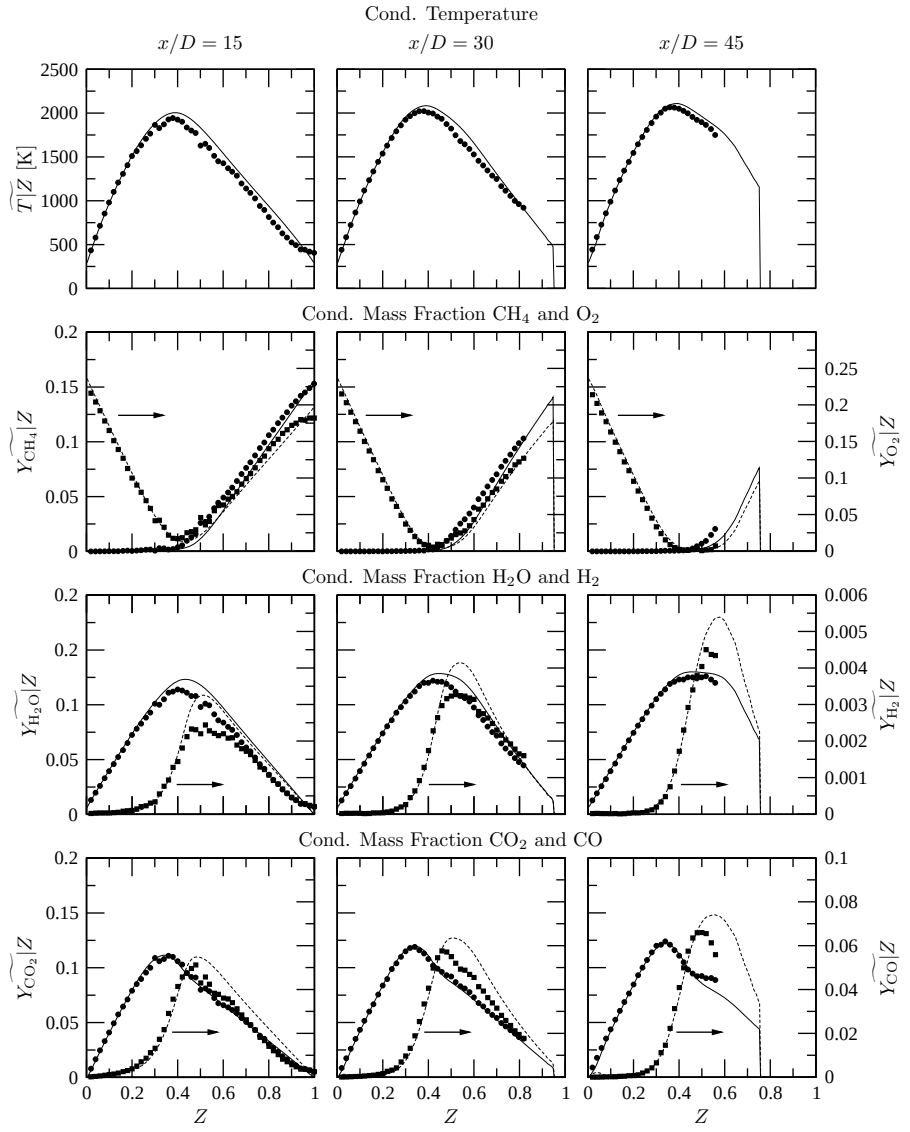

Figure 1: Comparison of mean temperature and mean product mass fractions conditioned on mixture fraction obtained from the simulation (lines) with experimental data (symbols).

References

[1] S.B. Pope, *New J. Phys.* 6, 35: 1-24, 2004.

[2] C.D. Pierce, P. Moin, *J. Fluid Mech.* 504: 72-97, 2004.

[3] C.D. Pierce, P. Moin, *Progress-variable approach for large-eddy simulation of turbulent combustion*, Report No. TF-80, Stanford University, 2001.

[4] C.D. Pierce, P. Moin, *Phys. Fluids* 10 (12): 3041-3044, 1998.

Lifted flame studies under gas turbine combustor conditions

B. Janus, A. Dreizler*, J. Janicka
*Corresponding author: dreizler@ekt.tu-darmstadt.de
FG Energie- und Kraftwerkstechnik, TU Darmstadt,
Petersenstrasse 30, D – 64287 Darmstadt, Germany

1. Introduction

This study reports on measurements in a generic non-premixed gas turbine combustor segment. Flow and scalar field were characterized using various laser diagnostic methods. The optically accessible burning chamber allowed for measurement of inflow conditions close-by the nozzle important for comparisons with numerical simulations. The generic nozzle design is sufficiently simplified to be precisely reproduced by block structured computational grids but shows typical features of gas turbine applications. To expose the influence of heat release on the flow field properties, both isothermal and combusting conditions were investigated. Striking features of the present configuration are a detached flame, multiple recirculation zones, and complex coherent flow structures.

2. Nozzle and operation conditions

The nozzle consists of a round gaseous fuel jet surrounded by a single swirled, heated combustion air flow. The swirl is generated by tangential vanes as can be seen from Fig. 1 (distorted). The air flow rate at the given parameter set corresponded to a $\Delta p/p$=3% pressure drop across the nozzle, typical for gas turbine applications. For the reacting case natural gas was used as fuel. Since the flow field of the reacting as well as the isothermal case is of fundamental importance, natural gas was substituted by an appropriate mixture of helium and air in order to get the same density and hence keep up the Reynolds similarity for both cases. Conditions of the operating point are specified in Table 1.

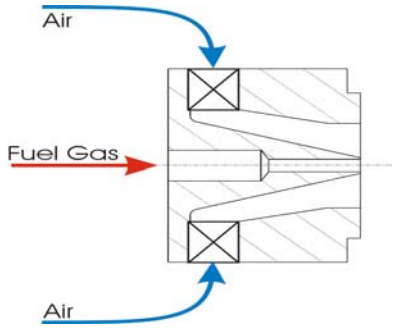

Fig. 1
Nozzle cross-section

Combustor pressure p	2bar
Combustion air temperature T	623K
Combustion air mass flow rate $\dot{m}$	30g/s
Equivalence ratio ϕ	0.8
Re_{air}	46000
Re_{fuel}	40800

Table 1
Operating point

The nozzle was operated in a modular high pressure combustion rig capable of providing gas turbine combustor inlet conditions corresponding to pressures up to p=10bar and temperatures up to T=773K with an max. primary air flow of $\dot{m}$=150g/s. Air from a compressor was split into combustion air and cooling air with a mass flow ratio of $m_{combustion}/m_{cooling}$=1/3. The combustion air was electrically heated, while the cooling air remained unheated. Compressed natural gas was supplied by a piston compressor.

3. Results

Flow and scalar fields have been investigated using LDV, planar OH and acetone tracer PLIF [1]. OH distributions served to determine lift-off height, flame spreading angle and flame brush, whereas acetone tracer PLIF was used to investigate turbulent mixing.

At least two recirculation zones (RZ1, RZ2) and a stagnation point (SP) appear (see Fig. 2). RZ1 is typical for highly swirling flows and results from a positive axial pressure gradient that is associated with the vortex breakdown phenomenon. RZ2 is located close to the nozzle in the shear layer between the fuel jet and the air inflow. It penetrates into the nozzle causing negative axial velocity components at the nozzle exit. The stagnation point is located on the centre line. It is caused by the impact of the fuel jet and the reverse flow region.

As shown in connection with mean axial and radial velocity components, Fig. 3 presents the mean OH distribution in a longitudinal section. The mean lift-off height is ~20 mm and corresponds well with the stagnation point observed from LDV data. Moreover, at this location mixture fraction studies as highlighted in Fig. 4 and 5 show that in mean at 20 mm stoichiometric conditions are met. The spreading angle of the OH distribution is 73°.

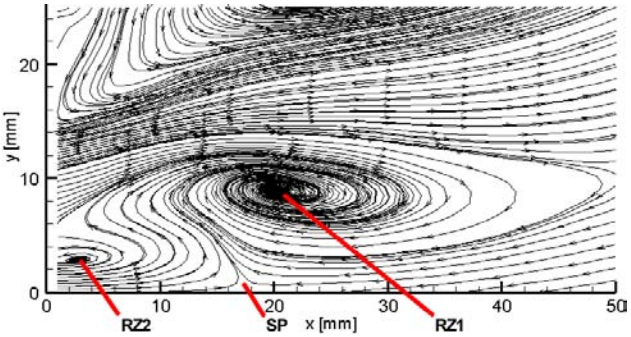

Fig. 2
Half section of streamline plot for isothermal flow constructed from radial and axial velocity profiles recorded by LDV

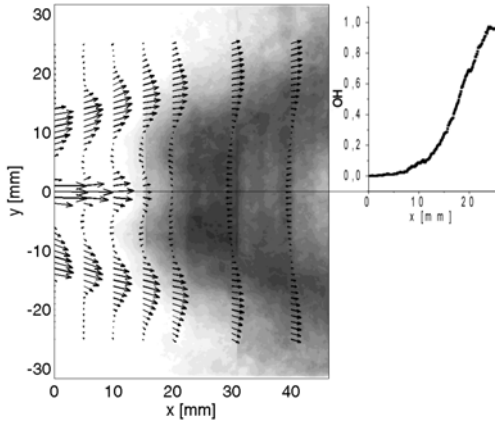

Fig. 3
2D velocity plot with mean OH distribution along centerline

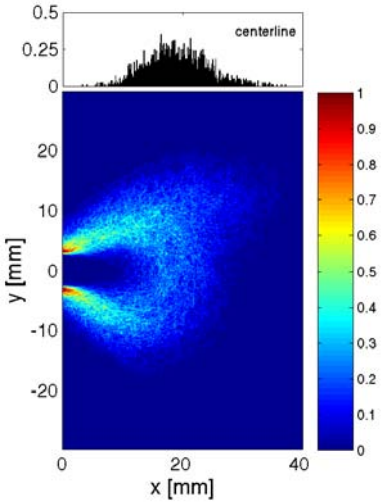

Fig. 4
2D histogram of stoichiometric mixture fraction with centreline plot

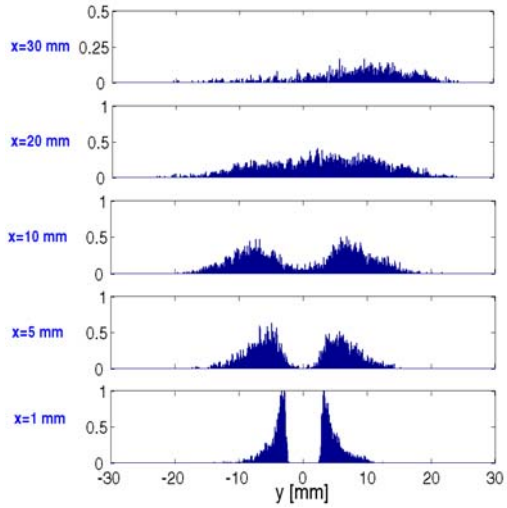

Fig. 5
Radial profiles of stoichiometric contours

4. References

[1] B. Janus, A. Dreizler, J. Janicka, Flow field and structure of swirl stabilized non-premixed natural gas flames at elevated pressure; Proceedings of ASME TURBO EXPO 2004, June 14-17, Vienna.

Multi-Scalar Imaging in Argon-Diluted Jet Flames

Sebastian A. Kaiser[†], Marshall B. Long[†], Jonathan H. Frank*
[†]*Department of Mechanical Engineering, Yale University, New Haven, CT*
**Combustion Research Facility, Sandia National Laboratories, Livermore, CA*
Contact: jhfrank@ca.sandia.gov

Recent work on multi-scalar imaging in partially premixed turbulent methane-air flames on the Sandia piloted jet burner will be presented. This work is a continuation of previous planar single-shot measurements presented in [1, 2]. From the measured scalars it is possible to extract two-dimensional images of temperature, mixture fraction, and forward reaction rate of the reaction CO + OH = CO_2 + H. The flames investigated here were similar to the TNF Sandia flames D – F. For the present work, however, the fuel was diluted by a mixture of argon and oxygen, rather than air to optimize the flame for the diagnostics utilized. Two different diluent compositions were considered: dilution by a mixture of argon/oxygen 3.75/1 (by volume), and 8/1. The first corresponds to "argon-air", that is, the ratio argon/oxygen is the same as that of nitrogen/oxygen in air. This results in a stoichiometric mixture fraction of 0.41, compared to 0.35 for air dilution. To match the air-dilution value for the case of argon/oxygen, a ratio of 13/1 would be required. However, flames with this diluent could not be stabilized, and so 8/1 was chosen since it gives stability and general appearance similar to that of the standard air-diluted flames. The stoichiometric mixture fraction then is 0.37. The composition and flow rates of the lean premixed pilot flame were appropriately modified to reflect the change of the main jet.

A schematic of the experimental arrangement is shown below. Four scalars were simultaneously imaged on a single-shot basis. Rayleigh scattering of the light from two frequency-doubled Nd:YAG lasers (532 nm, 1.9 J/pulse combined) was imaged onto an unintensified interline-transfer camera. From the opposite side of the burner the depolarized component of the Rayleigh scattering was isolated by a sheet polarizer and an interference filter and imaged onto an ICCD camera. A Nd:YAG-pumped dye laser was used to excite OH fluorescence at 285 nm, and fluorescence from the A-X(0,0) and (1,1) bands of the was detected. A dichroic mirror on the

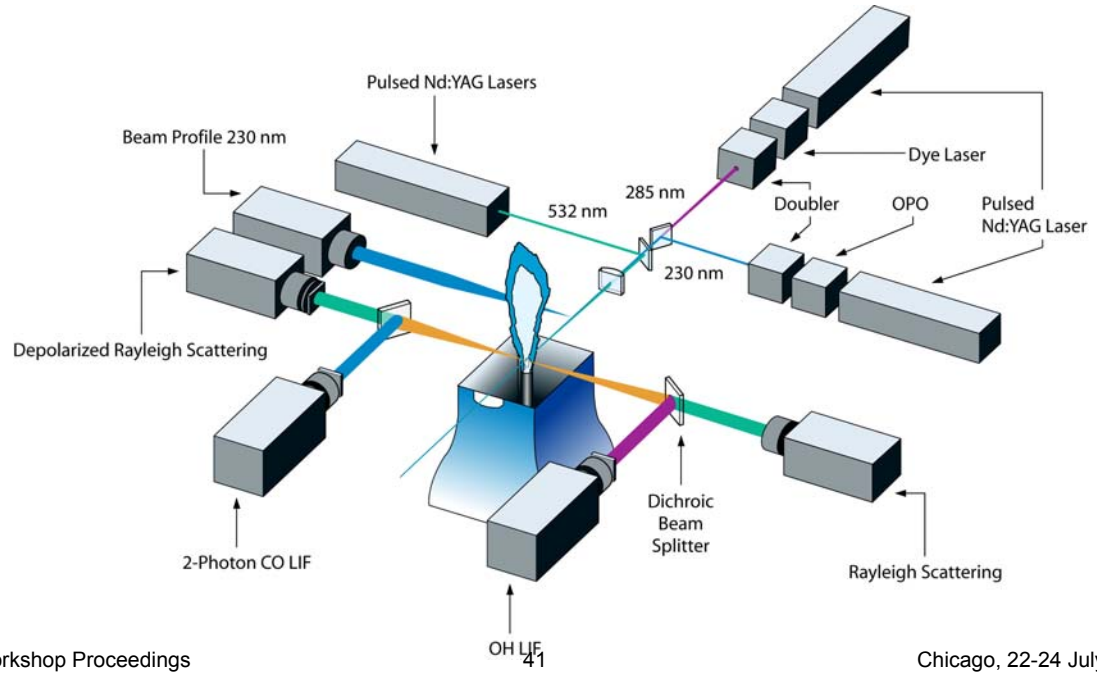

side of the Rayleigh-camera was used to transmit the Rayleigh scattering and reflect the OH fluorescence, which was imaged on an ICCD. Two-photon fluorescence of CO was excited at 230 nm with two Nd:YAG-pumped OPO's (40 mJ combined). CO fluorescence was detected at 484 nm, separated from the depolarized Rayleigh scattering by another dichroic mirror and imaged onto an ICCD. As a non-linear process, the CO fluorescence is very sensitive to variations in laser energy. To correct for shot-to-shot fluctuations, Rayleigh scattering of the 230 nm beam from the air of the jet coflow was imaged in the vicinity of the measurement plane onto an ICCD, yielding the laser-sheet intensity profile through horizontal integration.

Previous work [3-5] has shown that through judicious choice of the excitation/detection schemes for CO and OH fluorescence the pixel-by-pixel product of the two images can be made proportional to the forward rate of the reaction CO + OH = CO_2 + H over the temperature range of interest. In addition, the knowledge of the local mixture fraction and temperature allows for the quenching corrections necessary to obtain relative CO and OH concentrations. In methane flames of moderate local strain rate, mixture fraction and temperature can be determined by measuring the polarized and the depolarized component of Rayleigh scattering. As an isotropic molecule, methane has no measurable depolarized signal, while Rayleigh scattering from typical diatomics, such as oxygen and nitrogen, is depolarized to by ~1 %. A suitable linear combination of the normalized polarized and depolarized scattering components can be shown to be monotonic in mixture fraction. Strained laminar flame calculations yield the necessary auxiliary relations. Argon, like all noble gases, also has zero depolarization ratio and its use as a diluent increases the contrast between the coflow air and the fuel mixture. Especially for increased strain rates, the precision of the mixture-fraction calculation can be increased by measuring additional scalars, and in the current measurements both CO and OH fluorescence are available for this purpose.

Since resolving small-scale structures is of fundamental importance in turbulence research, special care was taken to quantify the resolution of these measurements. The spatial overlap of the laser sheets as well as the thickness of each sheet was monitored by inserting a sampling wedge into the combined beams after the sheet-forming lens. After appropriate attenuation, the sheet profiles were recorded on a CCD camera. The maximum thickness of the combined sheets was xxx in the center of the field of view, and yyy at the edges. The projected pixel areas were 58 x 58 μm for the Rayleigh, depolarized Rayleigh, and CO camera, and 78 x 78 μm for the OH camera. The actual lateral resolution is reduced by lens aberrations and the inherent limitations of intensified cameras. Resolution estimates from standard targets will be presented.

References:

1. Frank, J.H., Kaiser, S.A., and Long, M.B., *Proc. Comb. Inst.*, 29, 2687-2694 (2002).
2. Fielding, J., Frank, J.H., Kaiser, S.A., Smooke, M.D., and Long, M.B., *Proc. Comb. Inst.*, 29, 2703-2709 (2002).
3. Frank, J. H., and Najm, H. N., Joint Meeting of the U.S. Sections of the Combustion Institute, Oakland, CA, 2001.
4. Rehm, J. E., and Paul, P. H., *Proc. Combust. Inst*. 28:1775-1782 (2000).
5. Paul, P. H., and Najm, H. N., *Proc. Combust. Inst*. 27:43-50 (1998).

Numerical Modeling for Turbulent Lifted Jet Flame with Vitiated Coflow

Sungmo Kang, Hoojoong Kim, Jonghyuk Yu and Yongmo Kim
Department of Mechanical Engineering, Hanyang University, Seoul 133-791, Korea
e-mail : ymkim@hanyang.ac.kr

The flame liftoff characteristics considerably influences the flame stabilization and pollutant formation in practical combustion devices and largely depends on flow configurations, fuel type, heat losses and mixing conditions etc. The lifted non-premixed turbulent jet flames involve many fundamental mechanisms which involve ignition, local extinction, re-ignition, and flame propagation. Since these physical phenomena are strongly coupled and highly nonlinear, explanations of the stabilization mechanism have been quite controversal.

This study is mainly motivated to numerically analyze the detailed flame structure and stabilization mechanism in a lifted turbulent H_2/N_2 jet flame in a coflow of lean H_2/air hot-combustion gases. Cabra *et al*.[1,2] experimentally and numerically investigated a lifted turbulent H_2/N_2 jet flame in a coflow of lean H_2/air hot-combustion gases. This vitiated coflow burner has the advantage of representing both liftoff and auto-ignition in a rather simple flow configuration and nearly stationary flame field. In this study, to realistically represent the turbulent partially premixed nature in the flow region between nozzle exit and flame base, the level-set based flamelet approach has been applied. The chemical kinetics of hydrogen is based on Mueller mechanism[3] and GRI21 mechanism.

Figure 1 shows the predicted and measured contours of OH mass fraction in the lifted turbulent H_2/N_2 jet flame by utilizing the Mueller mechanism. The predicted flame pattern is in a good conformity with the measured one. In terms of the lift-off height, the agreement between prediction (x/d=10.35) and experiment (x/d=10) is quite good. The predicted lift-off height is noticeably influenced by the hydrogen reaction mechanism employed in the present study. When GRI21-H2 mechanism is used, the liftoff height is slightly underestimated(x/d=9.4). Figures 2 shows the radial profiles of mixture fraction, temperature, OH and H_2 mass fraction. Even if there are the noticeable deviations from measurement, in the overall flame structure, the predicted profiles reasonably well agree with the experimental data. Numerical results indicate that the present approach realistically simulates the essential features of the lifted turbulent H_2/N_2 jet flame with a vitiated coflow.

References:

1. Cabra, R., Myrvold, T., Chen, J.Y., Dibble, R.W., Karpetis, A.N., and Barlow, R.S., *Proc. Combst. Inst*., vol. 29, pp. 1881-1888, 2002.
2. Cabra, R., http://www.me.berkeley.edu/cal/VCB/
3. Mueller, M.A., Kim, T.J., Yetter, R.A., and Dryer, F.L., "Flow Reactor Studies and Kinetic Modeling of the H_2/O_2 Reaction", *International Journal of Chemical Kinetics*, vol. 31, pp. 113-125, 1999.

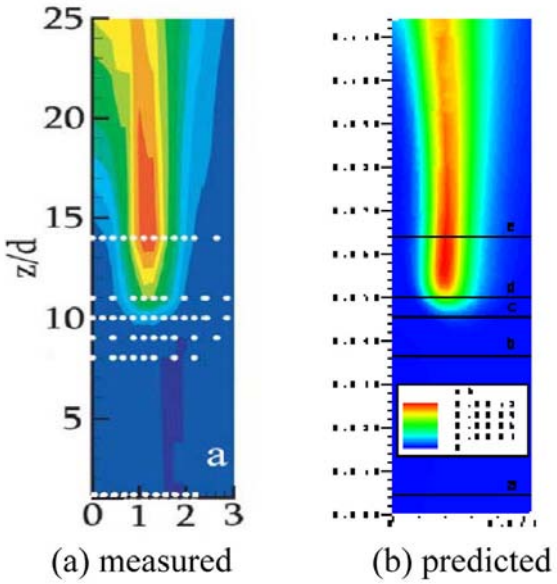

Fig. 1 Predicted and measured contours of OH mass fraction in a lifted turbulent H_2/N_2 jet flame (d=4.57 mm).

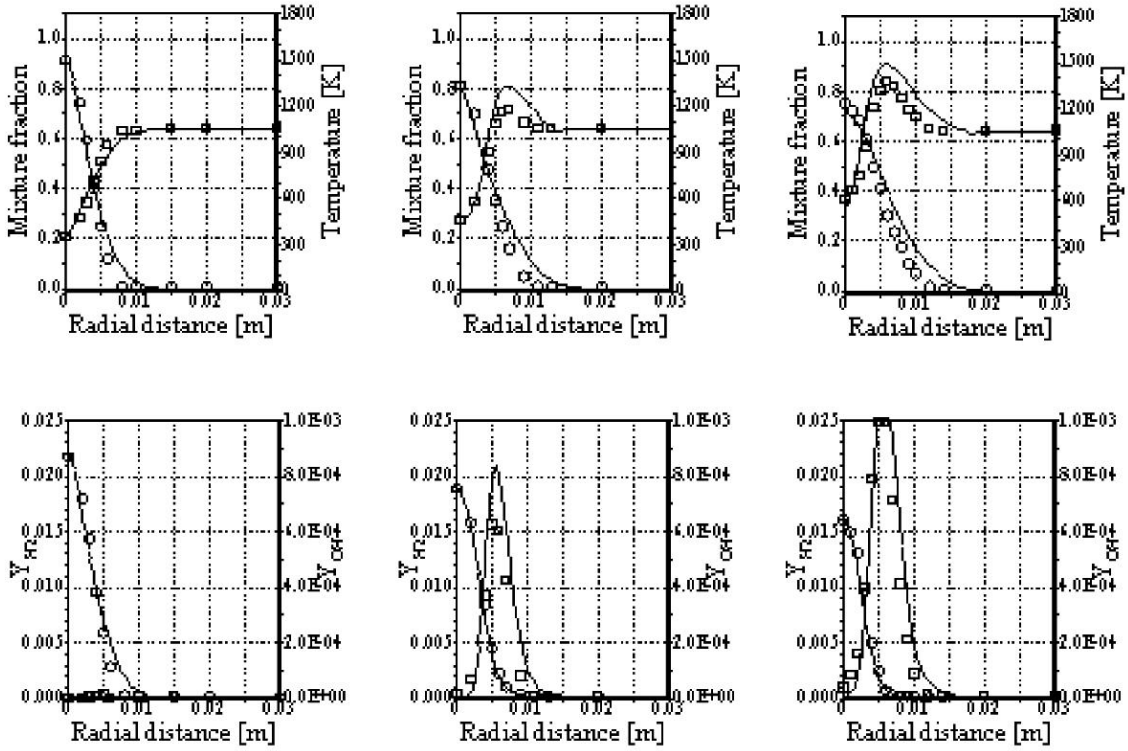

Fig. 2 Radial profiles of mean mixture fraction, temperature, H_2 and OH mass fractions.

LES of the Darmstadt opposed jet flame: A setup allowing to identify and to work on problems in sub-models

A. Kempf, J. Janicka
Institute for Energy- and Powerplant Technology
Petersenstr. 30
64287 Darmstadt, Germany
www.tu-darmstadt.de/fb/mb/ekt
akempf@gmx.net – janicka@ekt.tu-darmstadt.de

Large Eddy Simulation has shown [1, 2] to provide accurate predictions of turbulent reactive flows. However, some underlying models must be improved further, which requires a test-case that allows for the well-resolved LES and DNS of a highly turbulent reactive flow, such as the Turbulent Opposed Jet.

This contribution shows the Darmstadt Opposed Jet Burner, compares numerical and experimental results, considers the influence of the inflow-data and mentions some aspects that may be considered to improve the LES.

This work relies on an incompressible formulation, where momentum flux is discretized by an energy conserving second order central scheme. Scalar fluxes are described by a total variation diminishing (TVD) scheme to avoid artificial oscillation. The sub-grid fluctuations are modeled according to Smagorinsky with a dynamically (Germano-procedure) determined model-constant. The chemical state is determined from a steady flamelet model based on the mixture fraction formulation. To account for sub-grid fluctuations in mixture-fraction, a beta-distribution has been assumed. The sub-grid variance is modeled by the variance resolved by the local test-cell. An elaborate description of this approach is available in [3].

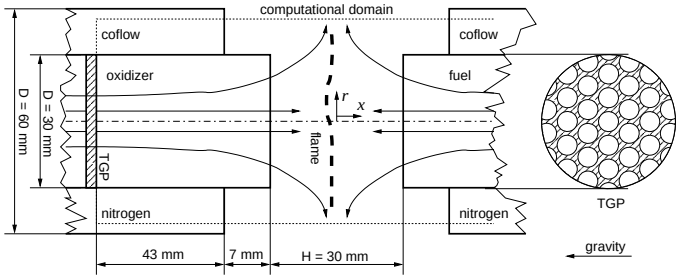

The Opposed Jet Burner consists of two coaxial nozzles (diameter 30 mm) opposed to each other (separated by 30 mm) spending fuel (methane/air mixture, 25/75 vol.) and oxidizer (air) respectively. The oxidizer streams at a bulk-rate of 3.4 m/s ($Re = 6,650$), which is close to the experimentally determined extinction limit of 3.7 m/s. The rate of fuel-flow was set to balance momentum, so that the stagnation plane is located at half the nozzle distance. At a position 50 mm upstream of each nozzle, turbulence generating plates (TGP) were inserted to create a (statistically) reproducible turbulent state. Surrounding the nozzles, an inert co-flow of 60 mm in diameter provides some shielding and inhibits un-burnt fuel from igniting in the flue.

The entire setup has been modeled by a cylindrical domain of 130 mm in length and 25 mm in radius. It was first resolved by a grid with $517 \times 87 \times 64$ ($\approx 2.9 \cdot 10^6$) cells in axial, tangential and radial direction. The feeding-pipes, the nozzles and the co-flow were described by immersed boundary conditions. The flow through the turbulence generators was resolved by adapting the inflow-velocity-profiles. This leads to an instantaneous velocity fields as shown in the following figure (axial velocity, [m/s]).

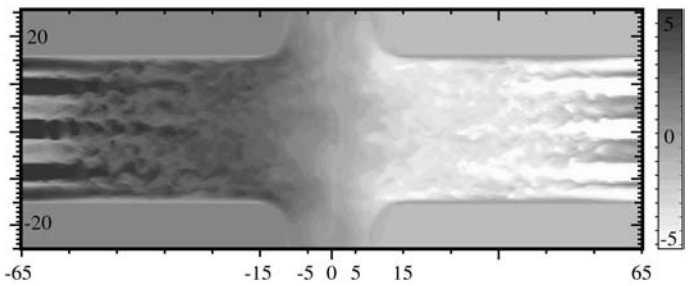

The small jets that impinge from the TGP develop instabilities that interact and result in turbulence. This process of turbulence production is hard to model with non-transient methods and results in young turbulence that, again, poses a challenge to classical models. The plot shows the development of the axial mean velocity and of the fluctuation (rms) along the center line, in-between the nozzle. The LES shows the decrease of the center line velocity within the nozzle, which is due to the spreading of the jets. As well, it shows how turbulence is generated and dissipated in-between the TGP and the nozzle-exit. The agreement between LES- and experimental data portends that the process of turbulence production and dissipation is reasonably predicted by the LES.

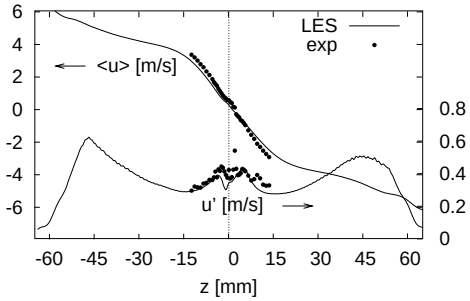

The present simulation resolves 0.254 mm in axial direction, which is twice the experimentally determined Kolomogorov length $\eta \approx 0.13$ mm at the nozzle exit. This means that a DNS of this flow is as possible as Large Eddy Simulations on different grid levels. This allows to test single sub-models as well as entire simulations. Furthermore, the configuration provides access to derived quantities like scalar dissipation, which is very important for the description of mixing. It is in such (secondary) quantities where the LES has serious need for improvements. For example, there are systematic deviations between numerical and experimental data for the scalar rate of dissipation conditioned on the mixture fraction: The figure shows the scalar dissipation rate versus the mixture fraction. Both experimental and numerical data were processed by the same algorithms and code. Filled symbols represent the experimental data, continuous line shows the LES results. For comparison, some steady flamelet solutions are shown as well (broken lines), whereas the open symbols provide the experimental results for the non-reactive case.

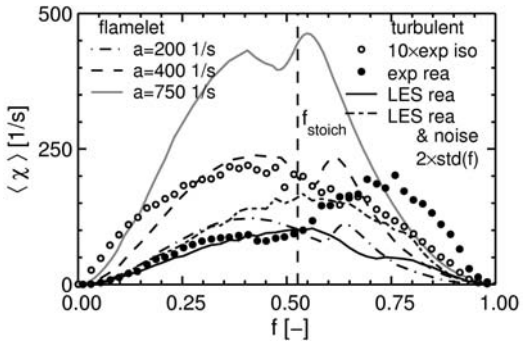

Obviously, there is a need to improve some underlying models to obtain reasonable predictions of (secondary) quantities such as the conditioned scalar rate of dissipation. The opposed jet configuration allows to vary the grid-resolutions, so that the model contributions change over a wide range. This allows for an efficient testing, development and improvement of the models.

References

[1] H. Steiner, H. Pitsch, *Large-Eddy Simulation of a Turbulent Piloted Methane/Air Diffusion Flame (Sandia Flame D)*, Phys. Fluids. 12 (2000)

[2] D. Geyer, A. Kempf, A. Dreizler, J. Janicka, *Scalar Dissiparion Rates in Isothermal and Reactive Turbulent Opposed-Jets: 1D-Raman/Rayleigh Experiments Supported by LES*, accepted for Proc. Combust. Inst. 30 (2004)

[3] A. Kempf, *Large-Eddy Simulation of Non-Premixed Turbulent Flames*, Doctoral Thesis, TU-Darmstadt, Fortschritt-Berichte VDI, Reihe 6, Nr. 513, ISBN 3-18-351306-4, Darmstadt, 2004,

[4] A. Kempf, H. Forkel, J.-Y. Chen, A. Sadiki, J. Janicka, *Large Eddy Simulation of a Counterflow Configuration with and without Combustion*, Proc. Combust. Inst. 28: 28-34 (2000)

Simulation of Turbulent Flame Lift Off by the Method of Flame Hole Dynamics

Jong Soo Kim[1] (kimjs@kist.re.kr) and Junhong Kim[2] (toad75@snu.ac.kr)

1. Air Resources Research Center, Korea Institute of Science and Technology

39-1 Hawolgok, Songbuk, Seoul, 136-791 KOREA

2. Dept. Mechanical Engineering, Seoul National University

San 56-1 Shinlim, Gwanak, Seoul, 151-742 KOREA

The lift off phenomenon in turbulent nonpremixed flames is investigated by the method of flame hole dynamics. Since the turbulent flame lift off can be viewed as a process of a gradual increase in the partial burning probability, the problem of modelling turbulent flame lift off comes down to modelling partial burning turbulent flame. The method of flame hole dynamics is based on the theory of flame edge, that is a boundary of flame hole initially formed by strong turbulence. Then, the flame edges propagate forward or backward, depending on the flow condition imposed on the edge structure, so as to expand or contract the flame holes. By balancing the randomly moving flame-hole area under stationary turbulence, the statistics of local partial quenching event could be obtained.

Two different models of flame hole dynamics are tested in this study. In the first flame hole dynamics model, the flame holes are assumed to be controlled by the extinction scalar dissipation rate (SDR), at which the holes are formed, the ignition SDR, at which the holes are destroyed, and the crossover SDR, at which the holes stop expanding or contracting because of zero edge propagation speed at the condition. Once these three SDRs are assigned, the holes are allowed to contract (expand) if the local scalar dissipation rate is smaller (greater) than the crossover scalar dissipation rate. Under this flame hole dynamics, the flame edge is implicitly assumed to respond to the local mixing condition infinitely fast. However, the flame dynamics model based on three characteristic SDRs possesses two crucial shortcomings. First, flame edges do not respond to the local flow and secondly, flame edge response is not infinitely fast particularly near the crossover condition. In order to remedy such shortcomings, the second flame hole dynamics model incorporates the level set method in order to describe the detailed edge propagation under turbulent flow condition with the edge propagation speed given as a function of the scalar dissipation rate. In this study, these two flame hole dynamics models are tested numerically by carrying out the direct numerical simulations for partially quenched turbulent nonpremixed flames established in a turbulent channel mixing layer for the fuel and oxidizer streams.

The numerical simulation is carried out in two stages as outlined in Fig. 1. First, the turbulent flow and mixing fields are directly solved for the channel mixing layer and a time

sequence of 2-D SDR is extracted at the virtual reaction surface, flatly extended from the split plate of the mixing layer. Then, the flame hole dynamics models are projected to the SDR time sequence to simulate the random walk of the binary reacting state (i.e. on or off of the reaction) for each flame surface grid.

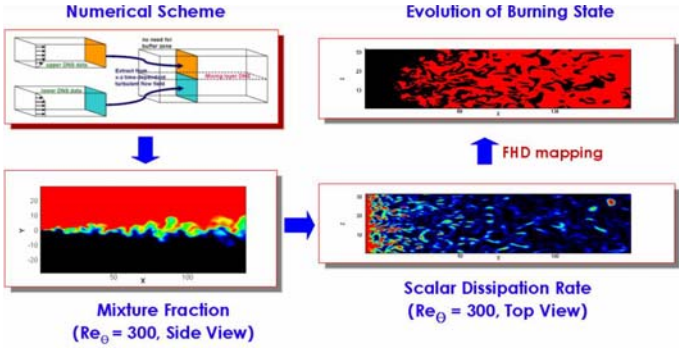

Fig. 1 Schematics of the FHD Simulations

Shown in Fig. 2 are the numerical results of the partial burning probabilities conditioned with the scalar dissipation rate for the both FHD models. The FHD model with three critical SDRs exhibits two distinct characteristics. First, the conditioned probability shows a stiff transition across the crossover SDR, thereby implying that the crossover SDR, but not the extinction SDR, is the main parameter controlling local quenching. Also the conditioned probability becomes almost invariant at sufficient downstream distances, so that the overall burning probability varies mainly because of the change in the overall SDR. In addition, the FHD with the level set method exhibits also two distinctions. The region of higher conditioned probability is pushed downstream because the edge propagation speed in the region of crossover condition is slower compared to downstream velocity. The transition across the crossover SDR also becomes much smoother by the finiteness of the edge response time.

In the future, the flame hole dynamics will be further improved by incorporating the full 3-D nature of the reaction surface convolution as well as the detailed edge propagation data obtained from realistic flamelet calculations.

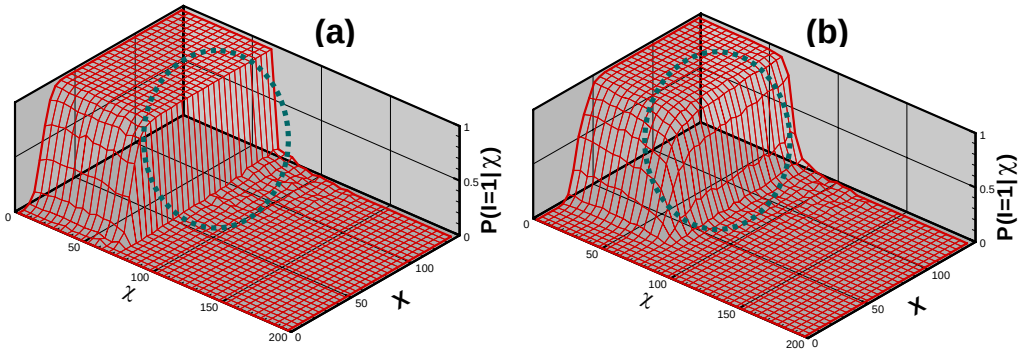

Fig. 2 Conditioned partial burning probabilities; (a) FHD with 3 critical SDRs, and (b) FHD with level set description

(This research is supported by the CDRS Frontier Research Center.)

Matching Conditional Variance in PDF modelling

A.Y.Klimenko
Mech. Eng. Division, The University of Queensland
Qld 4072, Australia
Email: klimenko@mech.uq.edu.au

In nonpremixed flames, the initial concentrations are, typically, deterministic functions of the mixture fraction. Hence, the initial volume accessed in the species composition space represents a line parameterised by the mixture fraction. In a reacting flow, the space accessed by concentrations evolves into a volume of much larger dimension due to superimposed influence of the reactions and mixing [1]. Mixing increases the accessed volume by filling its cavities. If a scalar Y is not a linear function of the mixture fraction Z, the deviations from the linear function are determined by local values of the scalar dissipation. Due to fluctuating nature of the scalar dissipation in a turbulent flow, the scalar Y begins to scatter around Q=<Y|Z> which is the average value of Y conditioned on Z. Dimensional analysis gives the following value for the conditional generation term

$$G = t_0 < N \mid Z >^2 \left(\frac{\partial^2 Q}{\partial Z^2} \right)^2 , \qquad N = D(\nabla Z)^2 \tag{1}$$

increasing the value of the conditional variance V=<(Y')^2|Z> that determines scattering and Y around Q and is expressed in terms of Y'=Y-Q. Here t_0 is a certain characteristic time determined by the properties of turbulence and N is the scalar dissipation. Arguments based on the theory of the inertial interval of turbulence indicate that t_0 is linked to Lagrangian correlation time of the scalar dissipation [2].

The transport equations for Q and V are specifically studied in Conditional Moment Closure (CMC) [3] but, for any PDF model, it is also most desirable to match the physical value of G. In the present work, we analyse the generation of the conditional fluctuations term G in several models: both traditional models -- Curl's and IEM (Interaction by Exchange with the Mean) [4,5] -- and different versions of the recently suggested Multiple Mapping Conditioning (MMC) model [6,7,8,9]. For IEM model, mixing does not generate any conditional fluctuations and G=0 (the conditional fluctuations can also be generated by spatial inhomogeneities but this process in not considered in the present work). Curl's mixing does generate conditional fluctuations and G is similar to equation (1), although G appears to be dependent on the shape of the PDF due to non-local character of the Curl's model. In MMC, matching the physical value of the conditional generation term is one of the criteria for selection of the model parameters [8,9]. A brief discussion of the MMC methodology and specific MMC models examined in the present work is given below.

The MMC approach [6] to turbulent non-premixed combustion is characterised by dividing all fluctuations of the reactive species into major and minor. The major fluctuations are treated with assistance of the stochastic reference variables while the minor fluctuations are either neglected (conditional MMC) or treated by conventional mixing models (probabilistic MMC) [6,7]. In its treatment of the major fluctuations, the MMC approach is compliant with all mixing criteria (such as linearity, independence, localness, boundness, etc). The major fluctuations are restricted to a certain manifold whose dimension is determined by the dimension of the reference space [1]. Generally, the concept of MMC can be characterised as a combination of CMC and PDF methodology. The MMC reference variables may represent turbulent fluctuations of different physical nature. In simplified versions of MMC, the reference variables simulate the mixture-fraction-type fluctuations (although it should be noted that the reference variables are not identical to the actual variables that represent the simulated mixture fractions). The two-stream mixing problem that is considered in the present work has a single mixture fraction and a single mixture-fraction-like reference variable. (MMC can also simulate multi-stream mixing [6].) Neglecting the minor fluctuations (that is in line with the conditional methods) generate models that are similar to the first order CMC but MMC models provide additional consistent modelling of the PDFs of

the conditioning variables. In probabilistic MMC, a conventional mixing model is used to treat minor fluctuations.

The probabilistic models examined in the preset work are MMC-IEM and MMC-Curl's that are distinguished by the conventional mixing model that is used to treat the minor fluctuations. The analysis of G in MMC-IEM is technically complicated [8] but it proves that a non-zero value for G that matches equation (1). The MMC-Curl's also has a similar value of G but with a constant multiplier that is different from MMC-IEM. In both models matching the magnitude of G (or that of the conditional variance) should be used a criterion for selecting the characteristic dissipation time for the minor fluctuation (the "minor dissipation time").

Another class of MMC models involve additional reference variables that are used to simulate fluctuations of the scalar dissipation. We will denote these models as MMC-N. The scalar dissipation has been previously used as an additional conditioning variable [10]. Here, we may have a set of the reference dissipation-like variables that simulate the whole temporal evolution of N that is presumed to be log-normal. It can be shown [8] that a proper criterion for selecting parameters of the model that simulated process of N should have the same correlation function as the Lagrangian correlation function of the scalar dissipation and this would ensure that adequate simulation of G in (1) by the model. In fact, this criterion implies that the simulated process should match as closely as possible the Lagrangian stochastic properties of the scalar dissipation N(t). Practically, the stochastic reference variables should be selected so that each variable is Gaussian and represents a certain scale in turbulent cascade with, probably, equidistant distribution of the logarithms of the scales. In a more simple models with a single N-like reference variable, its time scale should simply match the Lagrangian correlation time of the scalar dissipation.

The present work outlines an important criterion for performance of the PDF models: matching the physical value of the mixing term that generates scattering around the conditional means (the conditional generation term). This scattering is induced by fluctuations of the scalar dissipation is the one that is ultimately responsible for local extinction. When combustion is far from its extinction, the reactions are strong enough to compensate for any inadequate simulation of the conditional scattering, the situation changes when extinction is approached: the balance between reactions and conditional scattering becomes much more sensitive. It seems that accurate modeling of this balance should involve simulation of the Lagrangian properties of the scalar dissipation as it is shown in [8].

1. S.B. Pope. Accessed compositions in turbulent reactive flows. Fete Antonia. The University of Newcastle, 2003.
2. A.Y.Klimenko, "Conditional moment closure and fluctuations of scalar dissipation", *Fluid Dynamics*, 28, 630-637, (1993).
3. A.Y. Klimenko and R.W. Bilger. Conditional moment closure for turbulent combustion. Prog. Energy Combust. Sci, 25:595--687, 1999.
4. S.B. Pope. Pdf methods for turbulent reactive flows. Prog. Energy Combust. Sci., 11:119--192, 1985.
5. C.Dopazo. Recent developments in PDF methods. In P.A. Libby and F.A. Williams, editors, Turbulent Reacting Flows, pages 375--474. Academic Press, 1994.
6. A.Y. Klimenko and S.B. Pope.A model for turbulent reactive flows based on multiple mapping conditioning. Physics of Fluids, 15:1907--1925, 2003.
7. A.Y. Klimenko. Modern modelling of turbulent non-premixed combustion and reduction of pollution emission. Proc. Clean Air VII, Lisbon (on CD-ROM), volume 14 paper 4, 2003.
8. A.Y.Klimenko, "MMC modeling and fluctuations of the scalar dissipation", Aust Comb. Symp. Monash University, paper PO20, 2003
9. A.Y. Klimenko. On matching the conditional variance in pdf turbulent combustion modeling. Phys. Fluids, submitted 2003.
10. C.M. Cha, G. Kosaly, and H. Pitsch. Modelling extinction and reignition in turbulent nonpremixed combustion using a doubly-conditioned moment closure approach. Phys. Fluids, 13: 3824--3834, 2001.

COMPOSITION PDF CALCULATIONS OF TURBULENT LIFTED FLAMES OF H_2/N_2 ISSUING INTO A VITIATED CO-FLOW

L. Lu [1*], R. Cao [1], S.B. Pope [1], G. M. Goldin [2]
[1] *Sibley School of Mechanical and Aerospace Engineering, Cornell University, USA;* [2] *Fluent Inc, USA*
ll267@cornell.edu

In application to turbulent reactive flows, probability density function (PDF) methods are particularly attractive because nonlinear chemical reactions appear in closed form in the PDF equations. In this work, we employ a composition PDF approach coupled to the commercial CFD software, FLUENT, to perform comprehensive numerical simulations of a simple jet of hydrogen-nitrogen mixture issuing into a vitiated co-flow stream [1]. In-Situ-Adaptive Tabulation (ISAT) is used to implement detailed chemical mechanisms. Parallel processing makes it feasible to investigate the effects of different turbulence models, mixing models, chemical mechanisms and boundary conditions.

In this study, three different turbulence models, namely, the k-ε models, the LRR-IP model and Rotta's model are used and the sensitivity to the model coefficients is investigated. Three different mixing models, the Modified Curl (MC), the interaction by exchange with the mean (IEM) and the Euclidean minimum spanning tree (EMST) models are employed and compared, and the sensitivity to the mixing model coefficient is investigated. Based on a previous numerical accuracy study [2], numerically accurate solutions are obtained for two different H_2 mechanisms (the Mueller mechanism and the Li mechanism), each consisting of ten species. The sensitivity of the flame to the boundary conditions, especially the co-flow temperature, is also rigorously addressed.

Calculations show the flame is extremely sensitive both to the co-flow temperature and the chemical mechanism. One percent (about 10K) decrease in the co-flow temperature can make the lift-off height double. Compared with the experimental data, all the numerical calculations using different turbulence models, mixing models and mechanisms capture the right tendency with the change of co-flow temperature, i.e., higher co-flow temperature results in a shorter lift-off height. The Li mechanism has a shorter ignition delay and therefore yields a shorter lift-off height compared with the Mueller mechanism. Calculations show that the MC model predicts a larger lift-off height compared with the IEM model and the EMST model over all the tested co-flow temperatures.

In spite of extreme sensitivity of the flame to the co-flow temperature, the conserved quantities, mixture fraction and its variance, are insensitive to the co-flow temperature. So it is sound to compare the numerical results of the mixture fraction and its variance with the experiment data under the "same" co-flow temperature.

Figure 1 shows the radial profiles of mean mixture fraction and r.m.s of mixture fractions for different turbulence models at different axial locations: one in the upstream, two in the flame region and the last downstream. All the cases use the MC model and the Mueller mechanism. As may be seen from Figure 1, for the k-ε models, better agreement with the experimental data is achieved by adjusting the standard model coefficients, i.e., changing the model coefficients to get an accurate spreading rate of the jet. The results from joint velocity-turbulence frequency-composition PDF method (+ sign in the figure) performed by Cao et. al [3] are also shown in the figure. Compared with the composition PDF, the joint PDF generally makes better predictions, especially for the behaviour at the edge of jet.

References:

[1] Cabra, R., Myrvold, T., Chen, J.Y., Dibble, R.W., Karpetis, A.N., and Barlow, R.S., Proc. Combust. Inst. 29:1881-1888 (2002).
[2] Masri, A.R., Cao, R., Pope, S.B., and Goldin, G.M,, Combust. Theory Model. 8:1-22 (2004).
[3] Cao, R, Pope, S.B., and Masri, A.R. TNF workshop (2004)

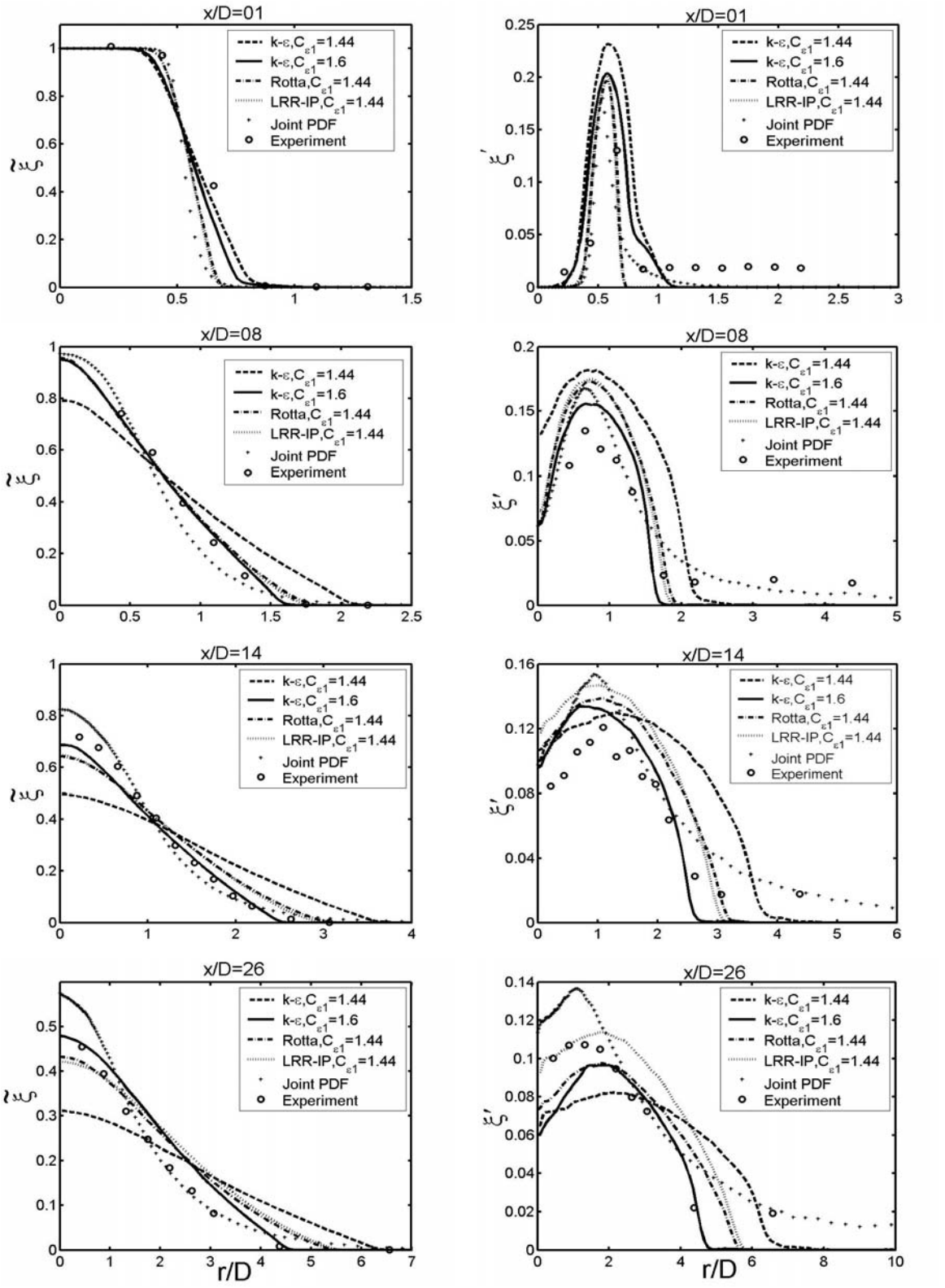

Figure 1 Radial profiles of mean mixture fraction and r.m.s of mixture fraction for different turbulence models at different axial locations.

Experimental Data Base from Swirl Flames in a Gas Turbine Model Combustor

W. Meier, P. Weigand, X.R. Duan, R. Giezendanner, U. Meier, B. Lehmann, M. Aigner

DLR-Institut für Verbrennungstechnik, Pfaffenwaldring 38, 70569 Stuttgart, Germany
E-mail: wolfgang.meier@dlr.de

The German Aerospace Center (DLR) has established a gas turbine model combustor for confined swirling, partially premixed CH_4/air flames, displayed in Fig.1. Co-swirling air is supplied to the burner through a central nozzle (diameter 15 mm) and an annular nozzle (i.d. 17 mm, o.d. 25 mm contoured to an o.d. of 40 mm) and CH_4 is fed through 72 channels (0.5 mm x 0.5 mm) forming a ring between the air nozzles. This configuration is a modified version of a gas turbine combustor with an air blast nozzle for kerosene. The squared combustion chamber has an inner diameter of 85 mm, a height of 114 mm, and is equipped with 4 quartz windows for almost unrestricted optical access. Three atmospheric pressure flames have been investigated in detail using various laser measuring techniques. The 3 velocity components were measured by laser Doppler velocimetry, the flame structures were visualized by planar laser-induced fluorescence of CH and OH, and the joint probability density functions of the major species concentrations, temperature, and mixture fraction were determined by laser Raman scattering. The 3 flames studied showed a different behavior with respect to combustion instabilities: Flame A was operated at an overall equivalence ratio of Φ=0.65, a thermal power of P=35 kW, and a Reynolds number of Re=58000. This flame burned very stable. Flame B, operated at Φ=0.75, P=10 kW, and Re=10000, exhibited self-excited thermoacoustic oscillations at a frequency of 290 Hz, and flame C (Φ=0.55, P=7.6 kW, Re=10000), which was run near the lean extinction limit, and was subject to unstable ignition. The main goals of the investigations were a detailed experimental analysis of phenomena of gas turbine combustion and the establishment of a comprehensive data base for the validation of numerical combustion models.

In brief, the main characteristics of the flames, as revealed by the measurements, can be summarized as follows. The flames were cone-shaped and exhibited a pronounced inner recirculation zone with hot combustion products and a weaker outer recirculation zone. All 3 flames were not attached to the fuel nozzle and were, thus, partially premixed before ignition. The CH layers were generally thin (0.3-0.4 mm) and strongly corrugated. The flames were short (< 50 mm) and dominated by fast mixing of fuel, air, and combustion products and by pronounced effects of turbulence-chemistry interaction in the form of local flame extinction and ignition delay. While flames A and C exhibited a similar shape, the oscillating flame B was flatter and showed pronounced periodic variations of all measured quantities during an oscillation cycle which could be revealed by phase-resolved measurements.

The poster will present a comparison of the 3 flames and discuss the prominent features of their combustion behaviors. Due to the complex burner design and flow fields, these flames certainly belong to the more complicated systems within the TNF Workshop, close to real gas turbine

combustion. Although this is a difficult field for combustion models the authors would like to encourage the modelers to try these flames and use the data sets which are available on request.

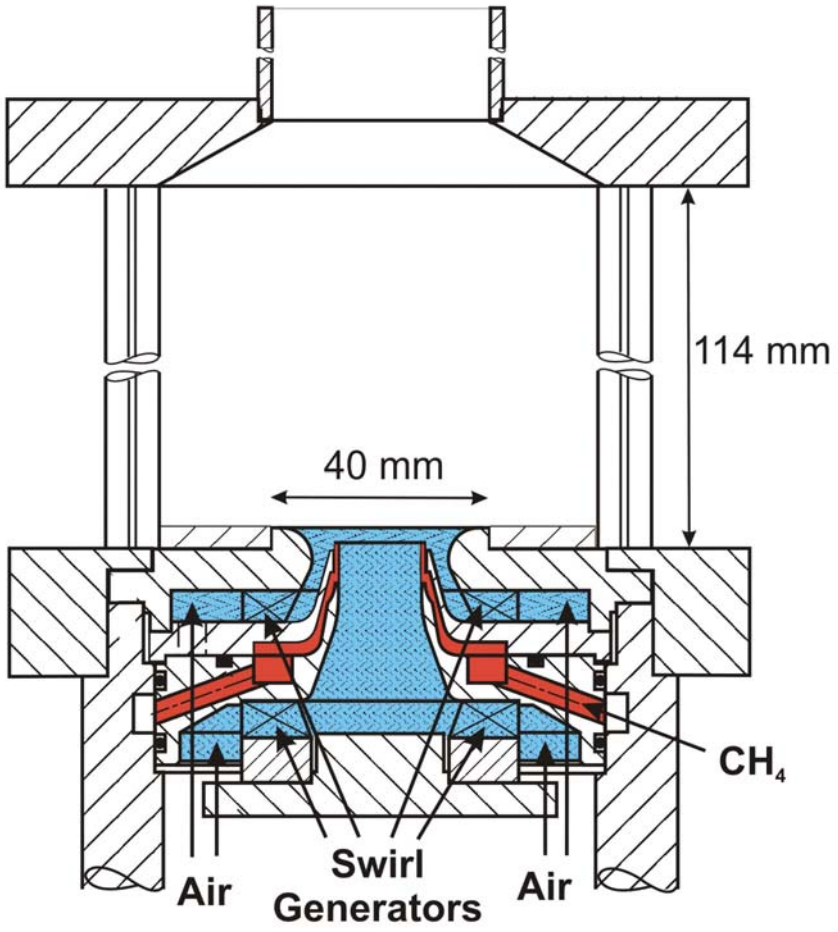

Fig.1: Schematic drawing of the gas turbine model combustor used at DLR Stuttgart. Gaseous fuel (here CH_4) is injected between two concentric air nozzles with swirl generators.

Investigation of the effect and behaviour of different turbulent mixing models on transported scalar PDF simulation results for Delft Flame III

Bart Merci[1,2], Bertrand Naud[3], Dirk Roekaerts[4,5] and Nijso Beishuizen[4]

[1]Ghent University, Dept. of Flow, Heat and Combustion Mechanics (Belgium)
[2]Postdoctoral Researcher of the Fund of Scientific Research – Flanders (Belgium)(FWO-Vlaanderen)
[3]LITEC-CSIC, Zaragoza (Spain)
[4]Delft University of Technology, Faculty of Applied Sciences (The Netherlands)
[5]Shell Global Solutions, Amsterdam (The Netherlands)
E-mail: Bart.Merci@UGent.be

Introduction

Results are presented for Delft Flame III[1,2], a flame with relatively strong turbulence- chemistry interaction. The transported scalar PDF approach is followed, i.e. no velocity components are used as independent PDF density variables. Three different mixing models are compared: the IEM model, the modified Curl's (MC) method and the EMST model. For all models, $c_\phi = 2$.

Models and Numerical Aspects

Turbulence is modeled with a non-linear k-ε model in low-Reynolds formulation, with an original transport equation for ε[3-6]. As chemistry model, the simple C_1 skeletal scheme of [7] is used, containing 16 species and 41 reactions. To that purpose, the fuel is modeled as 85.3% CH_4 – 14.7% N_2 (by volume). The number of particles per cell is 100. Averaging is done over the latest 50 iterations in order to reduce statistical error[8]. The error tolerance for the ISAT[9] tabulation is set to 10^{-6}. The computational mesh, 300D x 60D, contains 100 x 60 cells. All results are grid independent. The equations are solved with the commercial CFD-package FLUENT.
The construction of the inlet conditions is another issue: the fuel jet emerges from a pipe with a constriction upstream of the nozzle exit, while the primary air emerges from an annulus with a conical shape. As a consequence, the flow is not fully developed at the nozzle exit. The problem has been circumvented through separate calculations: the flow inside the nozzle head (central pipe and primary annulus) has been computed on a very fine mesh and the flow field quantities at the nozzle exit are used as inlet boundary conditions for the flame simulations. However, in the end, the detail of the inlet boundary conditions turns out not to be crucial for the quality of the simulation results. This makes the test case appealing for modelers, since a source of uncertainty is eliminated (or at least reduced).
Another issue is the modeling of the pilot flames. Experimentally, the pilot flames emerge from 12 separate holes. Here, steady simulations are performed in the assumption of axisymmetry. The pilot flames are necessary in order to prevent flame lift-off (both in the experiment and in the numerical simulations). Here, they are modeled by a source term in the transport equation for the mean static enthalpy: a source term of 1.5 $10^8 W/m^3$ is added in the region $0 < x < 20mm$, $3.5mm < r < 6mm$, corresponding to the thermal power of the pilot flames.

Results and Discussion

The results of different calculations are presented on the poster. First, pre-assumed β-PDF simulations have been performed, under the assumption of chemical equilibrium. No pilot flames are required: the flame ignites anyway. The flow field, in terms of mean velocity and turbulent kinetic energy, is very well reproduced with the applied turbulence model and construction of inlet boundary condition. Also the radial profiles of mean mixture at different axial positions are in very good agreement with the

experimental data. Because mixture fraction variance is over-predicted, the values of the mean temperature are in good agreement with the experiments, too.
Next, the transported PDF simulations have been done for the three mixing models. A first major observation was the importance of the pilot flames: they are definitely required to ignite the flame and keep it burning (numerically). Moreover, the details of the modeling are important to maintain the quality of the flow field predictions (and as such the mixing of oxidizer and fuel): when the density is too low near the rim between the central fuel jet and the primary air annulus, which happens when no reaction takes place (i.e. when no energy from the pilot flames is added), the turbulent viscosity and turbulence production become too high in that region. This is felt downstream on the axis as a sudden increase in the turbulent shear stress, slowing down the central jet far too quickly. This is then reflected in worse flow field (and thus mixing) results. This explains why the modeling of the pilot flames is so important here.
Looking at scatter plots at different axial positions, it is clear that the three mixing models have a completely different behaviour: the IEM model predicts global extinction, while EMST hardly predicts any local extinction at all. The latter may partly be due to an excessive amount of energy, supplied to model the pilot flames: in [10], it is stated that the EMST model is the most resistant to global extinction, so that it can be expected that, when too much energy is supplied, the amount of local extinction is the lowest (and in casu too low) for that mixing model. At the moment of writing, this is not completely clear yet. The modified Curl's method predicts local extinction in qualitative agreement with the experiments, but predicts flame lift-off (in contrast to the experiments) unless the pilot flame power is artificially increased.
Due to the global extinction with the IEM model, the mean temperature becomes too low and the density too high. This effect is noticed in the flow field predictions. The differences between MC and EMST, clearly visible in scatter plots, are less pronounced in the flow field (and mixture fraction) profiles, when the artificially increased pilot flame power is applied. Otherwise, the flame lifts off and the differences are large. The mentioned small differences are probably due to the fact that the conditional means do not differ very much: in combination with profiles of mean mixture fraction being almost equal, this leads to a very similar mean density and flow field. This indicates that, as long as the turbulence – chemistry interaction is reasonably well reproduced (i.e. the flame does not extinguish or lift off), the influence from the turbulence model on the flow field is larger than the influence from the mixing model for the flame under study. The effect of the chemistry model is still to be investigated.

Acknowledgements

Part of this research was funded by FWO-Vlaanderen project G.0070.03. This work is also done as contribution to INTAS project 2000-353. The last author is supported by Technology Foundation STW, The Netherlands.

References

[1] Nooren, P.A., Wouters, H.A., Peeters, T.W.J., Roekaerts, D., Maas, U. and Schmidt, D., *Comb. Theory Modelling*, Vol. 1, pp. 79-96 (1997).
[2] van Veen, E. and Roekaerts, D., *Comb. Science Technol.*, Vol. 175, pp. 1893-1914 (2003).
[3] B. Merci, D. Roekaerts, T.W.J. Peeters, E. Dick and J. Vierendeels, *Comb. Flame*, Vol. 126 (1-2), pp. 1533-1556 (2001).
[4]B. Merci, E. Dick and C. De Langhe, *Comb. Flame*, Vol. 131, No. 4, pp. 465-468 (2002).
[5] B. Merci and E. Dick, *Int. J. Heat Mass Transfer*, Vol. 46 (3), pp. 469-480 (2003).
[6] B. Merci, C. De Langhe, K. Lodefier and E. Dick, *J. Thermophys. Heat Transfer*, Vol. 18(1), pp. 100-107 (2004).
[7] Correa, S.M., *Comb. Flame*, Vol. 93 (1-2), pp. 41-60 (1993).
[8] Muradoglu, M., Pope, S.B. and Caughey, D.A., *J. Comp. Phys.*, Vol. 172, pp. 841-878 (2001).
[9] Pope, S.B., *Comb. Theory Modelling*, Vol. 1, pp. 41-63 (1997).
[10] Ren, Z. and Pope, S.B., *Comb. Flame*, Vol. 136 (1-2), pp. 208-216 (2004).

Studies of Micro-Vortex/Flame Interactions and Implications for Flamelet Modeling Theory

T. R. Meyer and V.R. Katta
Innovative Scientific Solutions, Inc.
2766 Indian Ripple Road
Dayton, OH 45440
trmeyer@innssi.com

J. R. Gord and W. M. Roquemore
Air Force Research Laboratory
Propulsion Directorate
Wright-Patterson Air Force Base, OH 45433

Introduction

According to flamelet theory [1], the local instantaneous composition and temperature of the mixture in a nonpremixed system can be modeled as being the same as those in a stretched laminar diffusion flame. The mixture fraction and scalar dissipation rate are then used in linking the turbulent flame structure to that of the laminar flames. At a critical value of scalar dissipation rate, the laminar diffusion flame extinguishes due to large mixture fraction gradients. The reaction zone in physical space becomes so narrow that diffusive heat loss will lead to quenching. This scalar-dissipation-rate analogy has been used in flamelet theories in modeling extinction and ignition phenomena in turbulent flames. The unsteady effects in the reaction zone are usually considered by incorporating the unsteady diffusion of reactants and heat conduction [2]. Flamelet theories have been successfully applied to the modeling of various nonpremixed flame systems [3]. A numerical and experimental investigation is performed in the present study to aid the understanding of the unsteady fluid-flame interaction process associated with small-scale laminar flamelets and, thereby, verify the applicability of the laminar flamelet theory. Micro-vortex/flame interactions, which can be considered to be the building blocks of statistical theories of turbulence, are utilized for establishing unsteady highly strained flamelets with varying vortex size, velocity, and fuel composition.

Numerical Model

An experimentally verified CFDC model [4, 5] was used for understanding the flame structure near extinction and for testing the validity of flamelet theories. Time-dependent, axisymmetric Navier-Stokes equations written in the cylindrical-coordinate (z-r) system are solved along with species- and energy-conservation equations [4]. A detailed-chemical-kinetics model with 13 species and 74 reactions is used to describe the hydrogen-air combustion process; the rate constants for this H_2-O_2-N_2 reaction system were obtained from Ref. [6]. To examine the effects of fuel composition, numerical studies are also performed for methane-air flames. A detailed-chemical-kinetics model is used with 31 species and the GRI 1.2 chemistry model to simulate methane-air combustion.

Experimental Setup

The opposing-jet-flame burner used for these studies was designed by Rolon [7]. The burner assembly consists of 25-mm-diameter nozzles (d_o), 40-mm-diameter outer nozzles (D_o), and syringe tubes of 0.2-mm to 5-mm diameter (d_i). A flat flame is formed between the fuel and air jets having velocities of 0.69 and 0.5 m/s, respectively. An annular nitrogen flow of 0.1 m/s is used from both the fuel and air side nozzles. The hydrogen-to-nitrogen ratio employed for the fuel jet is 0.38. Only the region between the lower and upper nozzle exits was modeled in the present study. Measurements using hydroxyl radical planar laser induced fluorescence and particle image velocimetry are performed for validation purposes. A comparison between experimental and numerical data for these conditions is available in the literature [8].

Results

Hydrogen-air flames indicate that large-scale vortex/flame interactions exhibit characteristics that are consistent with flamelet theory. Micro-scale vortex-flame interactions, on the other hand display behavior that deviates significantly from flamelet theory. For comparison, the temperatures and heat release rates at different instants are shown in Figs. 1 and 2, respectively, for the large- and micro-scale vortex/flame interaction cases. The temperature profiles for the large-scale vortex at different instants in Fig. 1 represent those of a stretched flame. Thickness and peak temperature decreased as the flame was stretched and translated (i.e., wrinkled). On the other hand, during most of the micro-vortex/flame-interaction process the flame temperature upstream of the vortex head was not

perturbed. When the micro-vortex exits the flame zone, it carries hot products with it. These temperature profiles suggest that flame is not being stretched by the vortex.

The heat-release-rate profiles for the large-scale vortex of Fig. 2 (left) represent that of a stretched laminar flame. The peak heat release rate increased as the flame was stretched by the large-size vortex. Interestingly, the heat release rate near the head of the micro-vortex shown in Fig. 2 (right) increased significantly [at 64 and 80 μs in Fig. 2] even though it was not perturbed in the upstream locations. The peak values are clipped in Fig. 2 for clarity. At 64 μs the heat release rate for the micro-vortex increased to 3130 J/cm^3/s while at 80 μs it increased to 11,600 J/cm^3/s. By comparison, the peak heat release rate only increased to 290 J/cm^3/s in the case of a large-vortex/flame interaction. The super-high reactivity (40 times greater) in the micron-size vortex/flame interaction results from the mixing of products and air--not from flame stretch.

The micron-size vortex used in this study reached 0.3 mm in diameter when it was passing through the flame zone. This is much larger than the Kolmogorov length scale of 0.03 mm obtained based on the turbulence Reynolds number and length-scales of 500 and 3 mm, respectively. This implies that a significant portion of the length scales in a turbulent reacting flow promote mixing in the reaction zone rather than wrinkling the reaction layer. In other words, a significant part of the turbulence-chemistry interaction may not follow laminar flamelet theory. Computations for methane-air flames are currently underway and will be compared with hydrogen air flames.

References

1. N. Peters, *Proc. Combust. Inst.* 21 (1986) 1231-1256.
2. B. Cuenot, F. N. Egolfopoulos, and T. Poinsot, *Combust. Theory Modeling* 4 (2000) 77-97.
3. S. K. Liew, K. N. C. Bray, J. B. Moss, *Comb. Flame*, 56 (1984) 199-213.
4. V. R. Katta, L. P. Goss, W. M. Roquemore, *AIAA J.* 32 (1994) 84.
5. W. M. Roquemore and V. R. Katta, *J. Visualization* 2 (2000) 257.
6. M. Frenklach, H. Wang, M. Goldenberg, G. P. Smith, D. M. Golden, C. T. Bowman, R. K. Hanson, W. C. Gardiner, V. Lissianski, Gas Research Institute Technical Report No. GRI-95/0058 (Gas Research Institute, Chicago), November 1, 1995.
7. J. C. Rolon, F. Aguerre, S. Candel, *Combust. Flame* 100 (1995) 422.
8. V. R. Katta, T. R. Meyer, J. R. Gord, and W. M. Roquemore, *Combust. Flame* 132 (2003) 639.

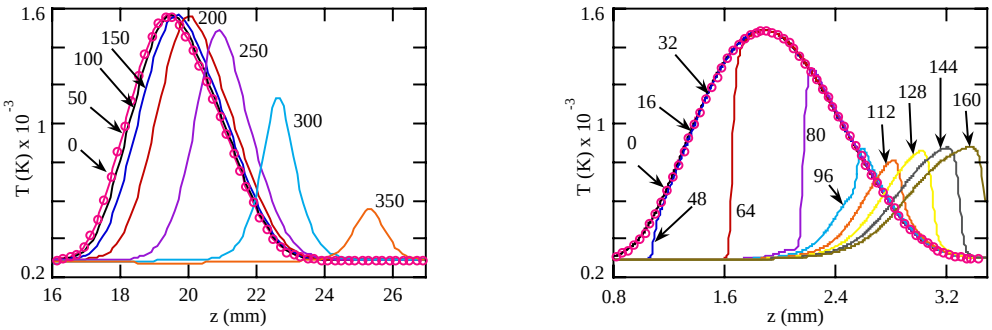

Fig. 1. Temperatures for large (left) and small (right) vortices. Numbers are flame interaction times in μs.

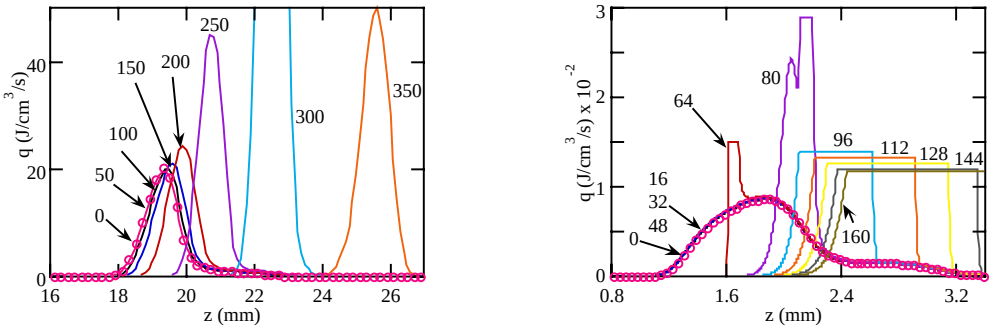

Fig. 2. Heat release rates for large (left) and small (right) vortices. Numbers are flame interaction times in μs.

An attempt to understand the vigorously turbulent flames in a hydrogen jet lifted flame

Yasuhiro Mizobuchi[1*], Junji Shinjo[1], Satoru Ogawa[1] and Tadao Takeno[2]
[1]Japan Aerospace Exploration Agency
[2]Meijo University
[*]Email: mizo@chofu.jaxa.jp

The development of computer hardware and parallel computing technique has realized Tera Flops computing and some non-reacting flow simulations have been done with more than one billion grid points. As for the combustion, simulations with detailed chemistry and rigorous transport properties can be made with tens or hundreds million grid points for methane or hydrogen flames. Then simulations of laboratory-size flames are possible, even though the fuels, size and configurations are restricted. The hugely massive flame simulations produce huge amount of data that contain strongly three-dimensional and unsteady phenomena, and have the potential to describe the flames to which the laminar flame theory, which has been the basis of the flame analysis, cannot be applied. Implementation of this kind of simulation raises new problem with respect to the post-processing, both on the software (analytical concept and method…) and hardware (storage system, cpu, graphics, network…).

The authors have been simulating a hydrogen jet lifted flame by DNS (Direct Numerical Simulation) approach[1]. The nozzle diameter is 2mm and the hydrogen jet velocity is 680m/sec. See Ref.[2] for the details of the flame configurations. The analysis in terms of flame index[3] clearly illustrated the global structure of the lifted flame as shown in Fig. 1, and showed that it is not a single flame but consists of three flame elements, the leading edge flame, the inner turbulent rich premixed flame, the outer diffusion flame islands.

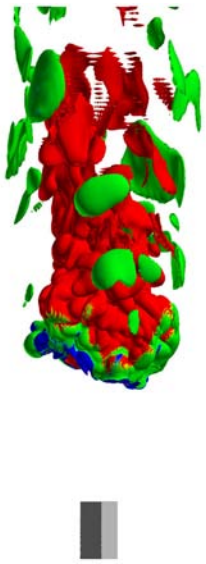

Figure 1: Global structure of a hydrogen jet lifted flame. Iso-surfaces of H_2 consumption rate at 10^4mol/m^3/sec are shown, where the surface color is the combustion mode, red: rich premixed, blue: lean premixed, green: diffusive.

Among the three flame elements, the inner rich flame is the most affected by turbulence. As shown in Fig.2, the heat release layer is largely deviated from the hydrogen consumption layer and disrupted. The black line in Fig.2a) is the iso-line of mixture fraction at 0.09, which corresponds to about 4.0 in equivalence ratio. The deviation seems to be remarkable in the very rich region. The scales of turbulence and combustion are numerically estimated at the point 16mm down stream from the nozzle and 2.8mm from the jet centerline in radial direction, where the deviation starts to get large. The velocity fluctuation v' is 34m/sec. The two-point correlation is calculated to estimate the length scales. The turbulence is not homogeneous at all, but the

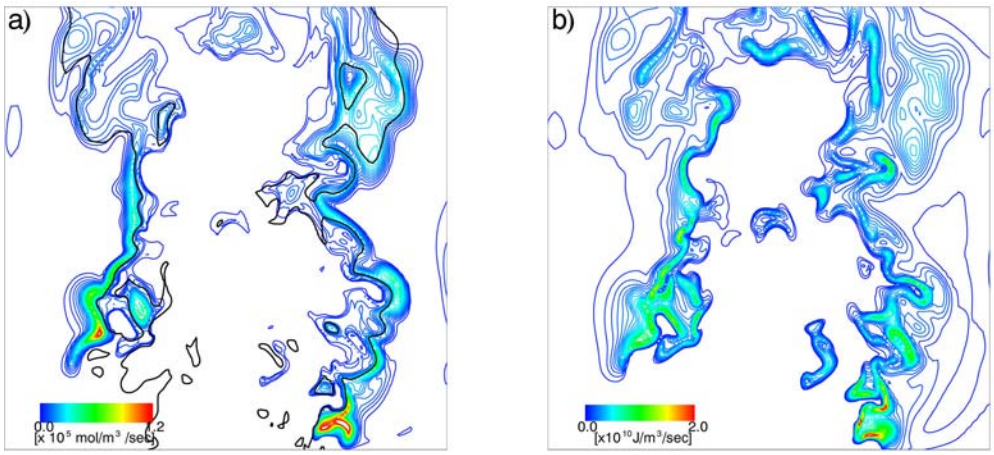

Figure 2: Deviation of heat release layer from H_2 consumption layer, a): H_2 consumption rate distribution, b): heat release rate distribution. The black lines in a) are iso-lines of mixture fraction at 0.09.

averaged integral length l is roughly estimated to be 1.4mm and the Kolmogorov scale about 0.03mm. The flame thickness l_F (defined by the heat release layer thickness) of the 1-D normal H_2/air premixed flame at equivalence ratio 4.0 are calculated, by PREMIX[4], to be about 1.5mm, as seen in fig.3. From the comparison of these scales, it is easily understood that the internal structure of the flame can be strongly disturbed by turbulence.

Kinetics of hydrogen flame is simple and it is advantageous for the numerical simulation. But the structure of the hydrogen flame is different from the structure assumed by the laminar flame theory, in which the fuel consumption takes place in a very thin reaction layer balancing with the molecular diffusion, and a rather thick preheat zone exists ahead of the reaction layer where convection and molecular diffusion balance. As reported by Dixon-Lewis[5], H diffuses very rapidly to the unburnt side and then the clear structures of the thin reaction layer and the preheated zone do not exist as shown in Fig.3. The balances hold around the burnt side edge of the reaction layer and unburnt side edge of the flame only. With this recognition, nevertheless, we started the analysis from the viewpoint of the laminar flamelet concept, because the laminar flame theory is the only deterministic basis of flame analysis.

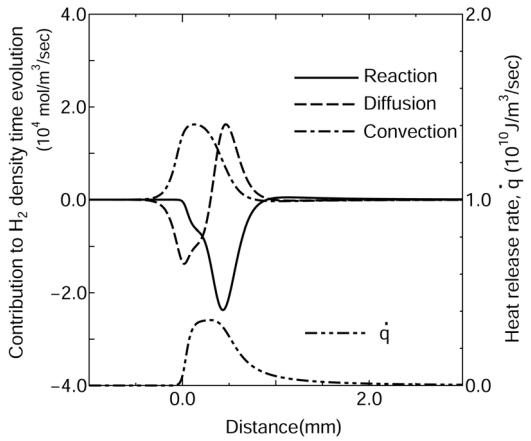

Figure 3: Fractional contributions of respective terms to H_2 density time evolution in a 1-D normal H_2/air premixed flame at equivalence ratio 4.0, with heat release rate distribution.

The time evolution of hydrogen density is decomposed into five terms, namely, convection and molecular diffusion in flame-normal and -tangential directions and chemical reaction as,

$$\partial \rho_{H_2} / \partial t = c^N + c^T + d^N + d^T + \dot{\omega} \qquad (1)$$

where, c, d and $\dot{\omega}$ represent the contributions of the convection, the molecular diffusion and the chemical reaction, respectively and the subscripts N and T denote flame normal and tangential directions. If the laminar flame like structure exists, $\dot{\omega}$ and d^N should be in balance in the burnt side of the reaction layer for premixed flame, and in the oxidizer side for diffusion flame (from the results of 1-D counterflow diffusion flame computation). Figure 4 shows the balance between $\dot{\omega}$ and d^N on the iso-surface of $\dot{\omega}$ at 10^4mol/sec/m^3. The surface color is the degree of balance defined as $\alpha = 1 - |d^N - \dot{\omega}| / \max(|d^N|, |\dot{\omega}|)$, and $\alpha = 1$ when the two terms completely balance. In most part of the outer diffusion flame islands and the outer side of the leading edge flame, the balance nearly holds. On the other hand, in the inner rich premixed flame, the degree of balance is small in most part of the surface.

The previous analysis tells us that the inner rich premixed flame does not have the usual flame structure, although it is stabilized in a quasi-steady state. An attempt is now being made to understand which term controls the fuel consumption. The following equation is solved about a flame element by using the information on the neighboring 4 flame elements to obtain the coefficients a_1-a_4.

$$\Delta\dot{\omega} = a_1 \Delta c^N + a_2 \Delta c^T + a_3 \Delta d^N + a_4 \Delta d^T \qquad (2)$$

If the flame is in the laminar flamelet regime, the molecular diffusion controls the fuel consumption, and then a_3=-1 and other coefficients are zero. So far, the orderly results have not been yet obtained about the inner rich premixed flame, while $a_3 \approx$-1 for the diffusion flame islands. This analysis is just at the early stage. To tackle this complex phenomenon, analytical methods based on new concepts of analysis will be needed.

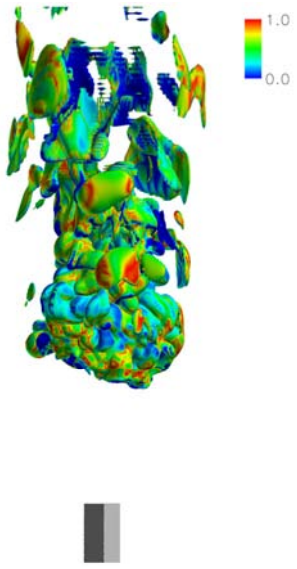

Figure 4: Balance between H_2 consumption and H_2 supply by molecular diffusion.

References

[1] Y. Mizobuchi et al., *Proc. Combust. Inst.* (2002), 29:2009-2015.
[2] H. Yamashita et al., *Proc.Combust. Inst.* (1996), 26:27-34.
[3] T. S. Cheng et al., *Combust. Flame* (1992), 91:323-345.
[4] R. J. Kee et al., Sandia report sand 85-8240, Sandia National Laboratory(1985).
[5] Dixon-Lewis, *Philos. Trans. R. Soc. Lond* (1979), *A* 292:45-99.

PDFD: A hybrid code for solving the joint velocity-composition PDF equation. Application to the modelling of a bluff-body stabilised flame

B. Naud[1], N.A. Beishuizen[2] and D. Roekaerts[2]
[1]*LITEC, Consejo Superior de Investigaciones Científicas, Zaragoza, Spain*
[2]*Thermal and Fluids Sciences, Delft University of Technology, The Netherlands*
Contact: dirkr@ws.tn.tudelft.nl

Introduction

Modelling of turbulent non-premixed flames has been a topic of research for many years at Delft University of Technology. In particular, transported velocity-composition PDF approaches have been used, following the work of S.B. Pope [1]. In the context of RANS modelling, several PhD projects [2, 3, 4, 5] have lead to the 2D computer program 'PDFD', based on a hybrid Finite-Volume / particle method. The hybrid method includes the correction algorithms presented in [6, 7] and the local time-stepping algorithm presented in [8].

The poster presents the details of the chosen hybrid method with its own specificities and new features. Results of a bluff-body stabilised flame simulation similar to that presented in [9] are shown as an application. Focus is on the consistency of the method and on the numerical aspects, rather than on a detailed modelling of turbulence-chemistry interactions.

Specificity of the method

Details on the numerical implementation are presented in the poster: space discretisation and time integration schemes, choice of coordinate systems, interpolations and splines, particle number control, ...

The main specificity of the hybrid method implemented in 'PDFD' is that Reynolds stresses are solved in the Finite-Volume (FV) submodel. Evolution of particle velocity fluctuation is given by a generalised Langevin model, consistent at the level of pressure strain correlation modelling with the chosen Reynolds-stress model [10]. Fig. 1 compares the FV and particle Reynolds-stresses obtained in the bluff-body flame

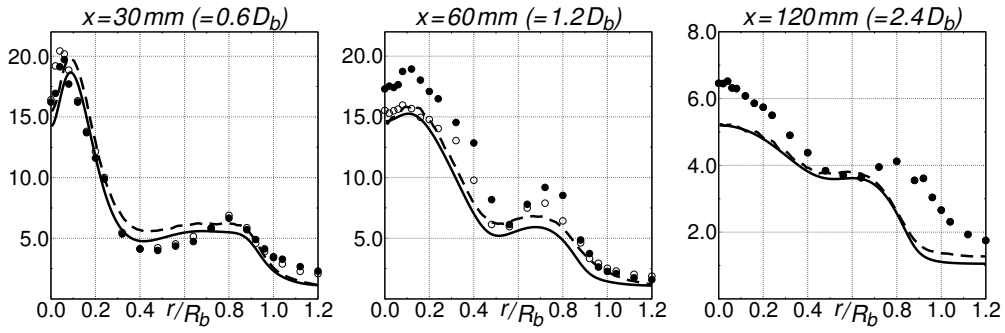

Figure 1: Radial profiles of rms fluctuations of axial velocity $\sqrt{\widetilde{u''u''}}$. Symbols correspond to the measured values (two different datasets), the continuous lines correspond to the FV fields and the dashed lines to the particle fields.

calculation. The slight difference may be attributed to a small inconsistency in the modelling of triple correlations [5]. A standard equation for dissipation ϵ is solved: particle turbulence frequency is obtained as ϵ/k interpolated at particle position.

The FV part of the code is based on the PISO pressure-correction algorithm in order to solve the Reynolds-averaged Navier-Stokes (RANS) equations. Using a low Mach number approximation, particle mean density can directly be used as a state equation. In order to reduce statistical fluctuations, a smooth relaxation based on the energy correction presented in [6] imposes the particle mean density to be used in

the RANS equations. Fig. 2 shows the convergence of the inverse of mean density at twelve monitor points.

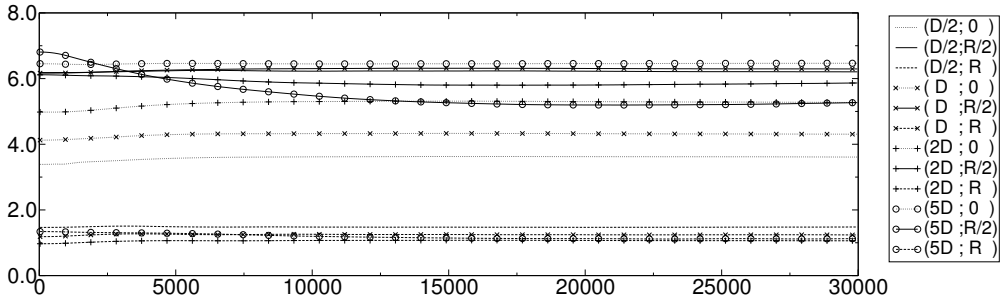

Figure 2: Convergence history of the inverse of density $\widetilde{v}^{FV}$ at twelve monitor points.

In the present approach, the FV part plays a leading role since it provides the mean velocity, mean velocity gradient, mean pressure gradient, Reynolds stresses, gradient of Reynolds stresses and dissipation to be used in particle property evolution. A low bias error is therefore expected. The only sources of bias may come from the density coupling or from the mixing model (where a particle mean composition is used to evolve particle composition).

New features

A slightly modified version of the velocity correction algorithm presented in [7] is proposed. A new way of computing iteration averages is detailed, allowing to control the memory of the average while keeping a fixed weight for the contribution of the last iteration.

References

[1] S.B. Pope, *Prog. Energy Combust. Sci.* 11 (1985) 119–192.

[2] T.W.J. Peeters. *Numerical modeling of turbulent natural-gas diffusion flames*. PhD thesis, Delft University of Technology, 1995.

[3] H.A. Wouters. *Lagrangian models for turbulent reacting flows*. PhD thesis, Delft University of Technology, 1998.

[4] P.A. Nooren. *Stochastic modeling of turbulent natural-gas flames*. PhD thesis, Delft University of Technology, 1998.

[5] B. Naud. *PDF modeling of turbulent sprays and flames using a particle stochastic approach*. PhD thesis, Delft University of Technology, 2003.

[6] M. Muradoğlu, S.B. Pope, and D.A. Caughey. The hybrid method for the PDF equations of turbulent reactive flows: consistency conditions and correction algorithm. *Journal of Computational Physics*, 172:841–878, 2001.

[7] P. Jenny, S.B. Pope, M. Muradoğlu, and D.A. Caughey. A hybrid algorithm for the joint PDF equation of turbulent reactive flows. *Journal of Computational Physics*, 166:218–252, 2001.

[8] M. Muradoğlu and S.B. Pope. A local time-stepping algorithm for solving the Probability Density Function turbulence model equations. *AIAA Journal*, 40:1755–1763, 2002.

[9] M. Muradoğlu, K. Liu, and S.B. Pope. PDF modeling of a bluff-body stabilized turbulent flame. *Combustion and Flame*, 132:115–137, 2003.

[10] H.A. Wouters, T.W.J. Peeters, and D. Roekaerts. On the existence of a Generalized Langevin model representation for second-moment closures. *Physics of Fluids*, 8(7):1702–1704, 1996.

A Web Portal for Multi-scale Chemical Science Data and Applications

Larry Rahn,[1] Thomas C. Allison,[6] Sandra Bittner,[3] Brett Didier,[2] Michael Frenklach,[8] William H. Green, Jr.,[7] Darrian Hale,[1] Mihael F. Hategan-Marandiuc,[3] Carina Lansing,[3] Gregor von Laszewski,[3] David Leahy,[1] James D. Myers,[2] Michael Minkoff,[3] David Montoya,[5] Luwi Oluwole,[7] Carmen Pancerella,[1] Reinhardt Pinzon,[3] William Pitz,[4] Jane Riese,[5] Branko Ruscic,[3] Karen Schuchardt,[2] Albert F. Wagner,[3] Theresa Windus,[2] Christine Yang,[1] and Ginger Young[5]

[1]Sandia National Laboratories, Livermore, CA
[2]Pacific Northwest National Laboratory, Richland, WA
[3]Argonne National Laboratory, Argonne, IL
[4]Lawrence Livermore National Laboratory, Livermore, CA
[5]Los Alamos National Laboratory, Los Alamos, NM
[6]NIST, Gaithersburg, MD
[7]Massachusetts Institute of Technology, Cambridge, MA
[8]University of California, Berkeley, CA
rahn@sandia.gov

The Collaboratory for Multi-scale Chemical Science (CMCS) project is working to integrate key combustion community data and application resources and make them available to collaborative teams and the broader research community through a grid-capable portal framework. CMCS provides sophisticated portal-based interactive views of combustion data including, for example, molecular structures and XY-graphs, from a variety of widely-used file formats. Overall, the CMCS production server currently provides access to data spanning 5 chemistry disciplines and 10 orders of magnitude in length scale. 25 metadata extractors, 40 translations/views, and several web services simplify data movement and analysis.

A number of national and international scientific expert groups have been attracted by CMCS' vision and unique capabilities and are working as pilot users and collaborators. A 13 member IUPAC (International Union of Pure and Applied Chemistry) Task Group is working to critically evaluate existing data and recommend improved thermochemical values of important radicals. This task group is using the CMCS infrastructure to coordinate and will be using the Active Thermo-chemical Tables (ATcT) chemical network analysis tool to statistically combine large amounts of data managed in CMCS to pro-duce new reference values for radical thermochemistry. The PrIMe (Process Informatics Model) group is a research team of about 40 international scientists that is forming for a similar purpose — to assemble curated kinetics data and to develop optimal reaction models. A High Quality Electronic Structure pilot group consisting of BES SciDAC researchers has formed to develop community standard benchmarks for assessing the accuracy of computational methods for predicting molecular properties for large and open shell systems. A multi-university consortium, formed to address the challenges in the development of Homogenous Charge Compression Ignition Engines, is working with CMCS to deal with complex chemical kinetic mechanisms and their translation and/or reduction for modeling applications. The NIST Real Fuels Initiative is working with PrIMe and the combustion modeling community through CMCS to address problems in combustion chemistry and to make validated data available to industry. A DNS Simulations of Turbulent Combustion group, involving two more BES SciDAC projects working with the Scientific Data Management

SciDAC center, is advancing a combustion feature analysis capability for large reacting flow simulations data sets.

Together, these interacting pilot groups rep-resent a significant fraction of leading combustion research efforts and they are poised to have a revolutionary impact on the field. CMCS continues to extend capabilities, and is working to expand provenance to include sensitivity and error information and to develop community peer review mechanisms. The team will continue to address issues related to knowledge grid research while developing an operational, scalable, and sustainable community research resource.

LES-Transported FDF Simulations of a Bluff-Body Stabilized Flame

Venkatramanan Raman, Heinz Pitsch
Center for Turbulence Research, Stanford University, CA-94305
&
Rodney Fox
Dept. of Chemical Engineering, Iowa State University, Ames, IA-50014
Email : vraman@stanford.edu

The objective of the current work is to establish the hybrid LES-Transported filtered-density function (FDF) simulation technique as a viable method for studying turbulent reactive flows. Recently, Colucci *etal* [1] have introduced the Monte-Carlo based FDF approach that directly evolves the sub-filter PDF using a particle-scheme. Several test configurations have shown that the LES-FDF scheme provides a alternate way of handling reactions [2]. However, extension to variable density flows poses several numerical challenges in addition to the large computational expense of particle based schemes. Here, a LES-FDF scheme is formulated for flows with large density gradients and used for the simulation of the Sydney bluff-body stabilized burner [3]. To verify consistency with the Eulerian computations of the same flow, a simple laminar flamelet model is used to describe chemistry.

The hybrid consists of a conventional LES solver and a particle-based Monte-Carlo scheme. A variable-density low-mach number LES solver is formulated in cylindrical coordinates with state-of-the-art sub-filter models for the sub-filter flux terms [4]. The Monte-Carlo solver is coupled in a time-accurate sense such that the every LES time-step is followed by a FDF time-step. The FDF scheme uses the velocity fields as input to advance the particles in physical space. Since the LES solver is cast in the cylindrical reference frame, the particle scheme needs to use the same coordinate system. The particle velocities are formulated in the Cartesian frame and then transformed back to the cylindrical coordinates. Transport in composition space is through mixing and reaction. Here, a simple IEM mixing model is used. For the configuration considered, only the FDF of the mixture-fraction is evolved and thus the reaction source term is identically zero. To maintain consistency between the particle and Eulerian density fields, novel particle-correction algorithms have been implemented. The poster will contain a comprehensive discussion of the consistency conditions and the numerical algorithms used. The new LES-FDF scheme has been tested in the context of simpler flows and the accuracy established elsewhere [5].

The Sydney flame [3] is simulated using both the LES-FDF scheme as well as a completely Eulerian scheme using filtered mixture-fraction. The geometry used extends 100D $\times$ 40D where D is the jet diameter of 3.6 mm. To ensure that the velocity gradients are adequately resolved a grid of 320 $\times$ 120 $\times$ 64 points is used. The inlet flow profiles for the fuel jet is obtained using a separate periodic pipe flow simulation. Several thousand planes of well-developed pipe flow velocity data is stored and used in the simulation. The coflow is assumed to have a flat profile though any change in the profile did not have significant effect on the stationary solution. A laminar flamelet model is used with the GRI-2.11 chemistry to obtain a flamelet table using a single strain rate of 100 s^{-1}. The LES sand FDF solvers are parallelized using domain decomposition based schemes. Typically the simulations are carried out on 32-48 processors with total walltime exceeding several hundred hours.

Figure 1. shows time-averaged stream traces obtained from the LES-FDF calculation. It is observed that the velocity components are predicted quite accurately. In addition, RMS of the velocity components show very good agreement with experimental data. More detailed comparisons will be provided in the poster. In addition, instantaneous FDF will be compared to the beta-function used for defining the sub-filter FDF in the Eulerian calculations. Preliminary results show that the beta-function approximation is consistent

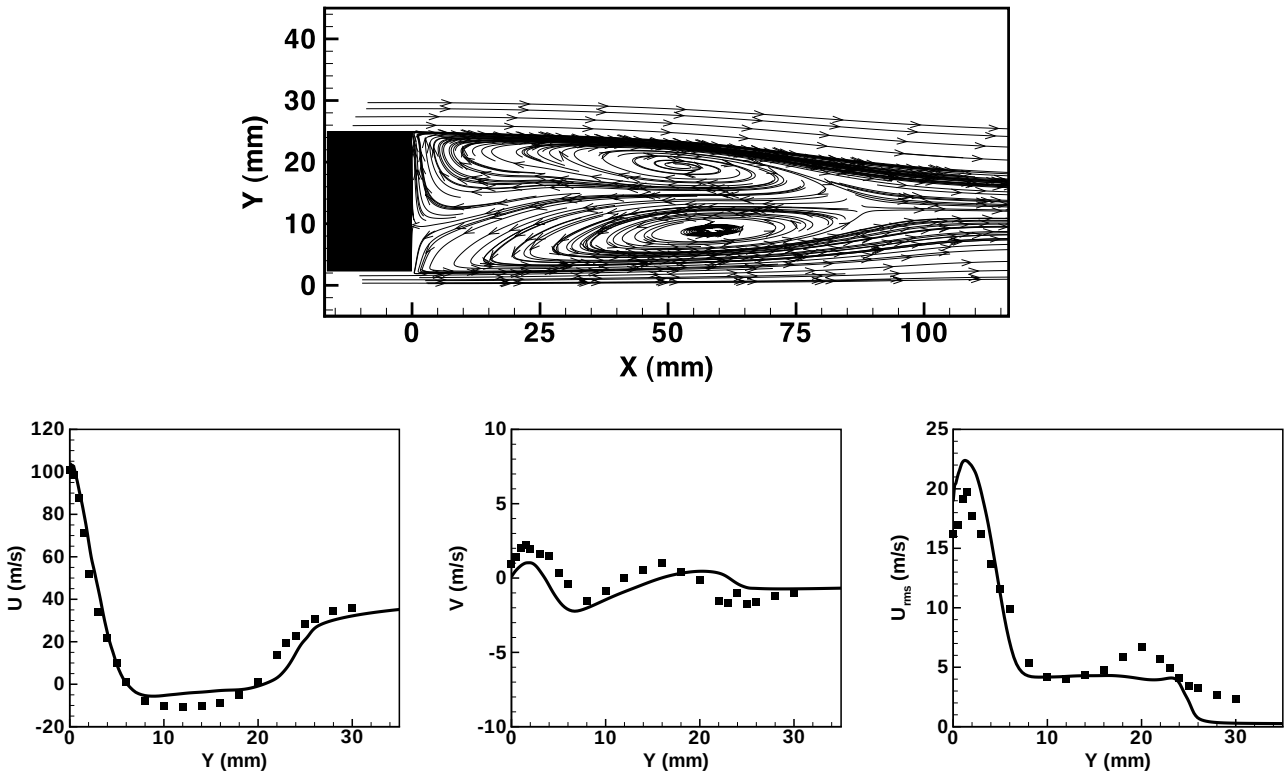

Figure 1: (Top) Streamlines from LES-FDF simulation in the recirculation zone. (Bottom) Time-averaged velocity profiles at axial position X=30 mm.

with the FDF computed from the Lagrangian scheme. However, regions of large variance show significant deviations.

References

[1] P. J. Colucci, F. A. Jaberi, P. Givi, Filtered density function for large eddy simulation of turbulent reacting flows, Physics of Fluids 10 (2) (1998) 499–515.

[2] F. A. Jaberi, P. J. Colucci, S. James, P. Givi, S. B. Pope, Filtered mass density function for large-eddy simulation of turbulent reacting flows, Journal of Fluid Mechanics 401 (1999) 85–121.

[3] B. B. Dally, A. R. Masri, R. S. Barlow, G. J. Fietchner, Instantaneous and mean compositional structure of bluff-body stabilized nonpremixed flames, Combustion and Flame 114 (1998) 119–148.

[4] C. D. Pierce, Progress-variable approach for large-eddy simulation of turbulence combustion, Ph.D. thesis, Stanford University (2001).

[5] V. Raman, H. Pitsch, R. O. Fox, Quadrature moments method for the simulation of turbulent reactive flows, in: CTR Annual Research Briefs, Center For Turbulence Research, 2003, pp. 261–275.

Turbulence structure of premixed combusting and isothermal swirling flows

C. Schneider, A. Dreizler*, J. Janicka
**Corresponding author: dreizler@ekt.tu-darmstadt.de*
FG Energie- und Kraftwerkstechnik, TU Darmstadt,
Petersenstrasse 30, D – 64287 Darmstadt, Germany

1. Introduction

A series of unconfined swirling premixed natural gas/air flames was investigated. Reynolds-numbers spanned from ~10,000 to 42,000. Respective isothermal flows were studied additionally to gain insight into changes of fluid dynamical features caused by combustion. Statistical moments, Reynolds-stresses, temporal time scales, spatial length scales, and power spectral densities (PSD) were deduced from one- and two-point laser Doppler velocimetry (LDV) data. Properties of the turbulent flows and dependencies on Reynolds-number, swirl number, and chemical reactions are discussed. Most distinct differences between combusting and isothermal case were precessing vortex cores (PVC) occurring only for the latter cases.

The study is aimed to serve as a data base of a generic flame geometry featuring important characteristics of industrial applications for validation of numerical simulations. Therefore, nozzle exit profiles as important inlet conditions to numerical simulations are thoroughly documented.

2. Nozzle design and test cases

A schematic of the unconfined premixed swirl burner is shown in figure 1. Different cases investigated are listed in table 1.

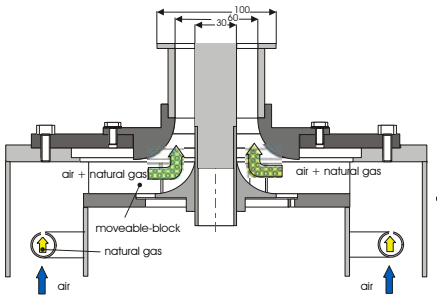

Fig. 1
Cross-section of the nozzle design

		PSF30	*PSF90*	*PSF150*
$S_{0,th}$	[-]	0.75	0.75	0.75
	[kW]	30	90	150
λ	[-]	1.2	1.2	1.0
Q_{gas}	[m_n^3/h]	3.02	9.06	15.1
Q_{air}	[m_n^3/h]	34.91	104.33	145.45
$Re_{tot.}$	[-]	10000	29900	42300

Table 1
Flow configurations investigated

The burner consisted of a 30 mm wide annular slit surrounding a central bluff body with d=30 mm. Upstream of the nozzle, swirl was generated by a moveable block geometry. Theoretical swirl numbers $S_{0,th}$ could be adjusted in the range from 0 to 2.0 and was set to 0.75. Values of $S_{0,th}$ exceeding 0.8 resulted in flash back. 70 mm upstream of the moveable block, natural gas was injected into the combustion-air flow at 300K using a perforated ring line. To achieve defined boundary conditions, the burner was placed into a co-axial air flow, emanating from an annular orifice with D=220 mm in diameter. The mean velocity of this co-flowing air was set to 0.5 m/s.

3. Results

For reacting and isothermal conditions radial profiles spanning from x=1 to 120 mm of all velocity components, two Reynold-stresses, PSDs, integral time and length scales have been determined. The most important characteristics are briefly summarized here:

- From the nozzle exit an annular swirling jet emanates which is characterised by an inner and an outer shear layer. Downstream, axial velocity is maintained while tangential momentum is passed over to radial momentum.
- By vortex breakdown an internal recirculation zone (IRZ) is formed responsible for well known flame stabilisation. In case of isothermal conditions a precession of the IRZ is observed leading to distinct frequencies in the PSD. Frequencies span from ~40 to 200 Hz and are dependent on Re-number. The energy content of these coherent structures is dependent on the location within the flow and most pronounced in shear layers. It reaches up to 40% of the overall fluctuation level. Figure 2 exemplary shows PSDs measured at different locations within isothermal flow fields. As obvious from figure 3, these coherent structures do not appear in the combusting case. Here, the slope of the inertial subrange depends strongly on the location. Relatively close-by the nozzle a slope of ~-5/3 is observed as shown in figure 3 for axial heights of 10 mm. Further downstream at 90 mm the slope is much steeper indicating stronger viscous forces due to higher temperatures.

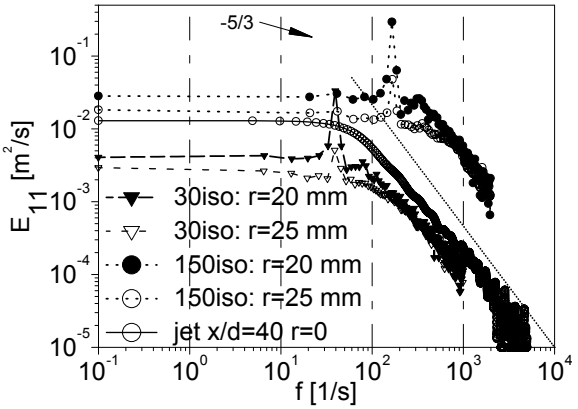

Fig. 2
PSDs for isothermal conditions at different Re-numbers and locations. Frequencies are independent on location but energy content varies significantly and is highest in the vicinity of the inner shear layer.

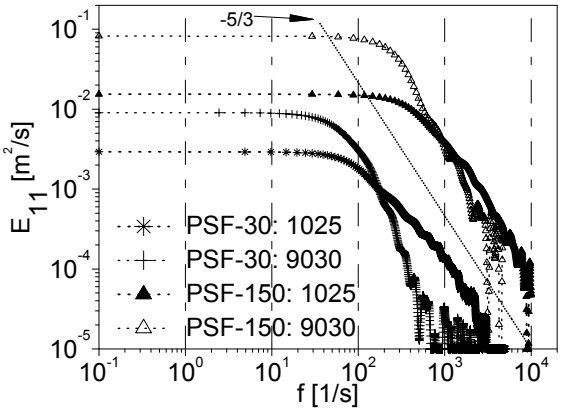

Fig. 3
PSD for 30 and 150 *kW* cases measured at x=10 mm, r=25 mm (stars, solid triangles) and x=90 mm, r=30 mm (crosses, open triangles)

- Statistical moments indicate Reynolds-similarity for the PSF-90 and PSF-150 combusting cases only, whereas the Strouhal-number analysis for isothermal flows indicates similarity for all cases from PSF-30iso to PSF-150iso. A constant Strouhal-number equals ~0.25.
- In axial direction time and length scale increase downstream while the ratio of longitudinal to transversal length scales decreases. In general, homogeneous isotropic turbulence conditions are not fulfilled for the present configuration.

Control of Confined Nonpremixed Flames Using a Microjet

A. Sinha, R. Ganguly, and I.K. Puri

Department of Mechanical and Industrial Engineering
University of Illinois at Chicago
Chicago, Illinois, 60607

Industrial burners, such as those used in materials processing furnaces, require precise control over the flame length, shape and other physical flame attributes. The mechanism used to control the flame topology should be relatively simple, safe, and devoid of an emissions penalty.

We have explored the feasibility of hydrodynamic control of confined nonpremixed flames by injecting air through a high-momentum central microjet. An innovative strategy for the control of flame shape and luminosity is demonstrated based on a high-momentum coaxial microjet injected along the center of a confined nonpremixed flame burning in a coflowing oxidizer stream. The near field geometry of the flow field is modified by the entrainment of ambient oxidizer caused by the high momentum microjet. Other work to effect near field flow was done by Lawton and Weinberg [1] applied an external electric field while Hertzberg [2] used acoustic forcing to modify a nonpremixed flame.

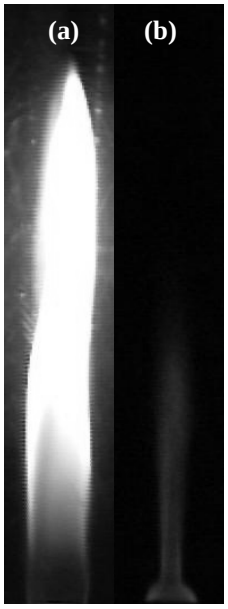

Fig. 1: The (a) regular, and(b) microjet-assisted Nonpremixed flames

The introduction of the microjet shortens a nonpremixed flame as shown in Figure 1. Also the application of microjet reduces the amplitude of the buoyancy-induced flickering. The change in hydrodynamic profile is evident from the Schlieren images of Figure 2, which qualitatively shows the streamlines of the hot gases in the flame and the cold air from the surrounding. The only difference in Figure 2 (a) and (b) being the absence presence of the microjet respectively. The flame transits from a buoyancy dominated regime to a momentum dominated regime, thereby reducing the effect of gravity. Similar work done by Ban et al. [3] showed that it is possible to almost eliminate the effect of gravity and produce a nearly spherical nonpremixed flame when the dimensionless Peclet number Pe (= ud/D, where D denotes the pertinent mass diffusivity) has a value smaller than five.

Visually, the microjet controlled flame appears to be much leaner in soot. Without any complex tooling for premixing, a classical yellowish nonpremixed flame is observed to be transformed to a nonsooting bright blue flame. It has been found that a microjet-assisted flame length follows a second degree relation with the fuel flow rate, making it more sensitive to the fuel flowrate than laminar or turbulent nonpremixed flames. At fixed microjet and coflow velocities, this provides greater flexibility for the dynamic control of flame lengths. The introduction of a microjet does not produce significant cooling that would be detrimental to overall heat transfer.

Measurements of NO_x and CO emissions show that the method is robust. Effective flame control without an emissions penalty (refer to Fig. 3) is possible over a large range of microjet velocities that significantly alter the flame shape. Since the influence of the microjet is primarily of a hydrodynamic nature, inert microjet fluids can be used. In previous work done by Ganguly

and Puri[4], it has been shown that a similar near-field hydrodynamic effect can be obtained by the use of nitrogen as the microjet fluid.

The primarily hydrodynamic nature of the microjet permits the use of inert microjet fluids such as high temperature recirculated exhaust gas in practical devices utilizing sequential combustors.

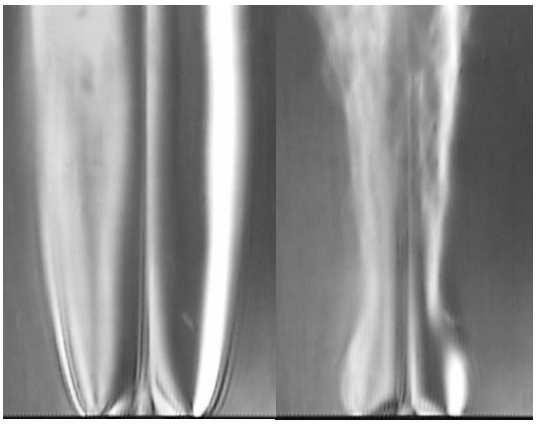

(a) **(b)**

Figure 2: Rainbow Schlieren images of (a) a nonpremixed and (b) a microjet-assisted flames giving qualitative idea of the streamlines of hot and cold gases

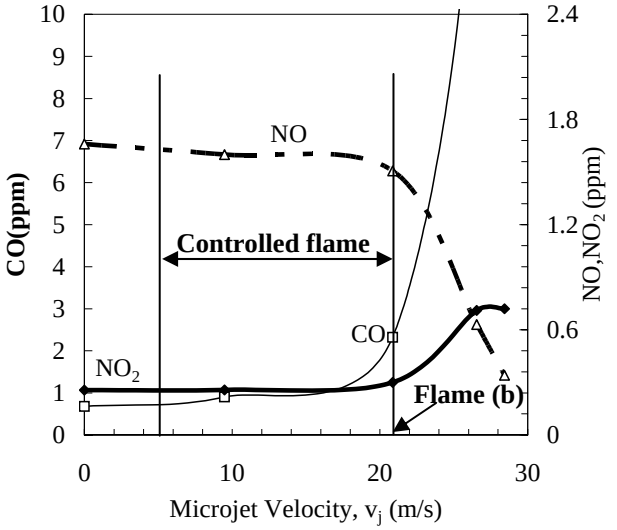

Figure 3: CO, NO and NO_2 emission data shows the working range of microjet flames without a significant emission penalty

Corresponding author:
Ishwar K Puri
University of Illinois at Chicago
2039 ERF, 842 W. Taylor Street
Chicago IL 60607-7022 USA

Fax: 312-413-0447
Tel: 312-355-3317
ikpuri@uic.edu

References

[1] Lawton, J., Weinberg, F.J., 1969. Electrical Aspects of Combustion. Clarendon Press, Oxford.
[2] Hertzberg, J. R., 1977. Conditions for a split diffusion flame. Combust. Flame, 109, 314-322.
[3] Ban, H; Venkatesh, S; Saito, K., 1994. Convection-diffusion controlled laminar micro flames. ASME J. Heat Tr. 116, 954-959.
[4] Ganguly, R., Puri, I.K., 2004, Experiments in Fluids, 36, 635-641.

Reignition Scenarios in a Simulated Diffusion Flame

Paiboon Sripakagorn* and George Kosa'ly
Department of Mechanical Engineering, University of Washington, Seattle, WA 98195-2600

DNS of initially nonpremixed reactants with simple chemistry under homogeneous decaying velocity field has been used to study local extinction and reignition. In addition, this work investigates the time history of individual points ("flame elements") along the stoichiometric surface.

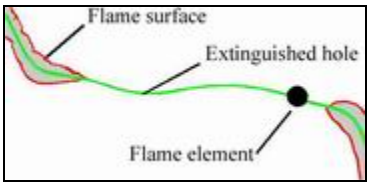

(a)

Features on the stoichiometric surface : flame surface (red), extinguished hole (green), tracked flame element (black dot).

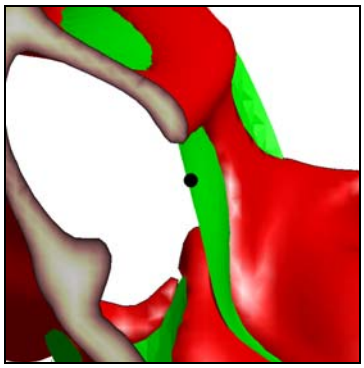

(b)

This study identifies three major scenarios of reignition: independent flamelet, propagating edge flame, and engulfment by a hot neighborhood.

To distinguish between different scenarios the local, instantaneous behavior of the following quantities are monitored:

$$\text{Normalized flame index, } G_s = \frac{\nabla Y_F \cdot \nabla Y_O}{|\nabla Y_F||\nabla Y_O|}$$

$$\text{Lateral diffusion term, } i_p = D\left(\frac{\partial^2\theta}{\partial x_1^2}+\frac{\partial^2\theta}{\partial x_2^2}\right) \quad , \quad \text{Normal diffusion term, } i_n = D\frac{\partial^2\theta}{\partial x_3^2}$$

In a burning or frozen diffusion flame, G_s = -1, while in partially premixed combustion G_s >-1. The terms i_p and i_n characterize the heat conduction per unit time in the $x_1 - x_2$ plane (locally tangent to the stoichiometric surface) and in the x_3 direction (perpendicular to the stoichiometric surface), respectively. In a burning flame element, i_p is zero and i_n is negative. Positive i_p and i_n indicates heat conduction toward a flame element along and perpendicular to the stoichiometric surface respectively.

Among the three scenarios, the independent flamelet scenario is the case where the flamelet formulation provides a good approximation to both the extinction and reignition processes. This poster focuses on the last two scenarios where the flamelet formulation fails.

Next, spatial snapshots of the reignition of two flame elements (black circle) are shown together with the time evolution of the reaction rate, G_s and i_p (or i_n) from the tracking procedure.

* Paiboon.S@chula.ac.th

Support by NSF (Grant #CTS-0133925) is acknowledged.

Reignition via edge (triple) flame propagation

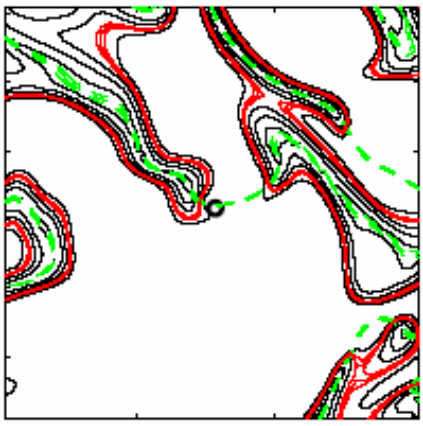

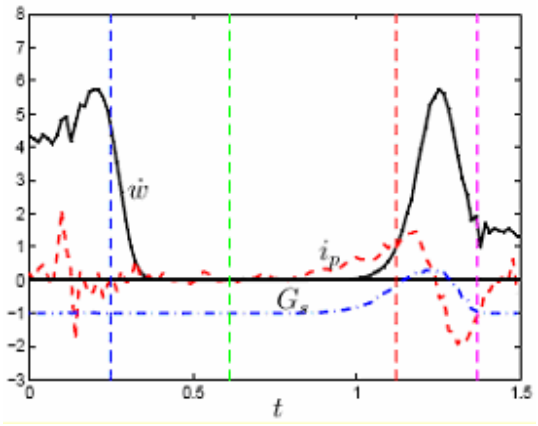

The encroachment of an edge (triple) flame can be clearly seen. The index G_s indicates the presence of a premixed flame at the time of the increase of the reaction rate $\dot{w}$ (reignition). The increase of i_p demonstrates that the heat flux causing the reignition is directed laterally along the stoichiometric surface.

Reignition via engulfment

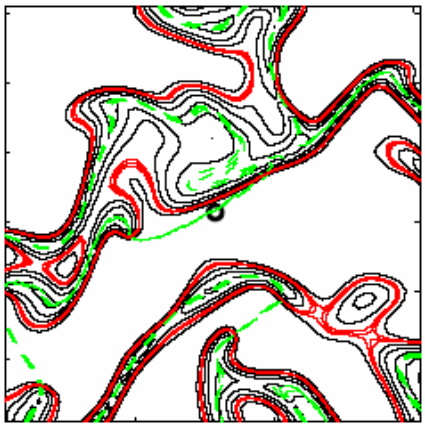

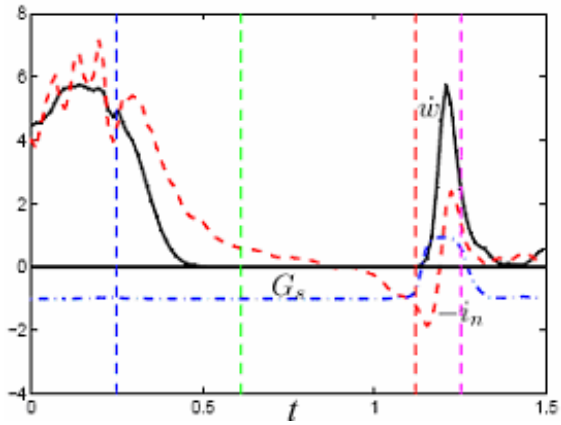

The flame element has been engulfed from the north by a hot neighborhood. The index G_s indicates the existence of premixed edge flame while i_n indicates the engulfment (the heat flux causing the reignition is primarily perpendicular to the stoichiometric surface).

Relative importance of reignition scenarios

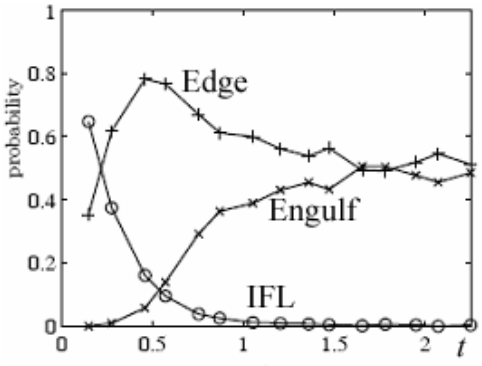

The independent flamelet scenario is of minor importance. The edge flame scenario dominates early and remains important throughout. After an initial period, engulfment scenario reaches the same level as of the edge flame scenario.

References

P. Sripakagorn, et.al. 2002 “Extinction and reignition in a diffusion flame (A direct numerical simulation study),” J. Fluid Mech. (submitted for publication)

Experimental study of subgrid-scale mixing for improving large eddy simulation of turbulent combustion

Chenning Tong
Department of Mechanical Engineering, Clemson University, Clemson, SC 29634-0921
ctong@ces.clemson.edu

Introduction

Large-eddy simulation (LES) is gaining increasing importance as an approach for computing turbulent combustion. One of the advantages of LES over the Reynolds averaged approaches is that in LES the highly flow-dependent large-scale velocity and scalar, which control the overall flow dynamics and mixing, are explicitly computed rather than modeled. Another advantage, which has become clear in our recent studies, is that both the statistical and spatial structures of the subgrid-scale mixture fraction, which have a strong impact of the flame structure, are closely related to the inertial-range dynamics, therefore can potentially be predicted accurately in LES. Therefore, in LES the effects of turbulent mixing, which is essential to modeling turbulent combustion, can potentially be modeled more accurately.

Our research focuses on SGS mixing issues met in modeling mixing in LES of turbulent non-premixed combustion. In such LES the filtered density functions (FDF) of scalars (i.e., distributions of scalar values in each grid volume), which depend strongly on the mixing of the subgrid-scale (SGS) scalars and turbulence-chemistry interaction, is generally needed to predict chemical reaction rates. An important modeling method uses the transport equation of the filtered density function scalars, in which the reaction source term is in closed form. Our research examines issues in using this approach by investigating the SGS mixing of conserved scalars, which often play a crucial role in LES of nonpremixed combustion.

We focus on the understanding of the physics of SGS mixing, which will provide an essential basis to improving mixing models. Issues include the FDF, its dynamics, and its connection to the inertial range dynamics. Statistical *a priori* tests, which compare statistics of modeled variables to measurements, are being performed. Implication for modeling SGS mixing and combustion regimes will be examined.

Measurements of LES variables

To obtain the FDF and other LES variables, spatial filtering is need. In our study two-dimensional (streamwise and radial directions) was employed. The streamwise filtering was performed by invoking Taylor's hypothesis and the cross-stream filtering was realized with three sensors aligned in the cross-stream direction. The spacing between adjacent sensors can be varied to give a filter width from $\Delta/\eta = 63$ to 250. Box filters were used because the resulting FDFs are analogous to a PDF.

Measurements were made in a heated turbulent jet with a Reynolds number of 40,000 ($R_\lambda \approx 230$). Passive temperature fluctuations were used as a conserved scalar. Data were collected at $x/D_j = 80$, well into the self-similar (fully developed) region. The mean axial velocity on the jet centerline U_c at this down stream location was 3.07 m/s and the Kolmogorov scale $\eta = (\nu^3/\epsilon)^{1/4}$ was 0.16 mm. The scalar dissipation scale $\eta_\phi = (\gamma^3/\epsilon)^{1/4}$ was 0.22 mm. Here γ, and ϵ are the thermal diffusivity and the energy dissipation rate respectively.

Analyses of SGS mixing

We analyze the FDF and other variables using conditional averages. Unlike a PDF, a FDF is not a statistic but a random precess, therefore requires statistical descriptions. We use the first two moments of the scalar FDF, the resolvable-scale scalar and the SGS scalar variance, and the filtered scalar dissipation rate as conditioning variables. The latter two are important variables for the dynamics of the inertial-range scalar; therefore such conditioning link the FDF to the inertial-

range dynamics. It is interesting to note that the beta model parameterizes this conditional FDF conditional on the resolvable-scale scalar and the SGS scalar variance, therefore has some physical basis.

In general, the results show that depending on the *instantaneous* SGS conditions the SGS mixing generally has two regimes: the spectral equilibrium (production equal to or less than dissipation) and nonequilibrium regimes, in which the SGS scalar and velocity have qualitatively different characteristics. The equilibrium SGS scalar is generally close to Gaussian and well mixed. The scalar dissipation depends weakly on the SGS scalar. The nonequilibrium SGS scalar, on the other hand, is bimodal and highly nonpremixed. The scalar dissipation has a strong bell-shaped dependence on the SGS scalar. This mixing regime is similar to the early stages of initially binary mixing. Furthermore, the SGS scalar contains diffusion-layer structures, which are similar to the scalar structure in the counter-flow model for laminar flamelets. The equilibrium SGS velocity is also close to Gaussian whereas the nonequilibrium SGS velocity has an approximately uniform distribution and is under local rapid distortion. When both the SGS velocity and scalar are in nonequilibrium there is strong dependence of scalar dissipation on the SGS velocity. We find that the degree of nonequilibrium can be quantified using the SGS variance and the filtered dissipation rate, which can be modeled in LES.

The nonuniversal FDFs appear to contradict expectations based on Kolmogorov's refined hypotheses that conditional statistics of inertial-range turbulence are universal. They also suggest that nonequilibrium inertia-range turbulence have distributions that depend on the degree of nonequilibrium. Therefore, the degree of nonequilibrium of the SGS velocity scalar can potentially be used to model the FDF and other variables.

Implication for combustion regimes

The different conditional scalar FDF shapes and the different structures of the SGS scalar under equilibrium and nonequilibrium conditions can have a strong influence on the flame structure. A key for LES accuracy is its ability to identify (explicitly or implicitly) and to model different combustion regimes. At high Damköhler numbers, turbulent nonpremixed combustion is generally considered to be in the laminar flamelet regime if the integral-scale mixture fraction fluctuations are large compared to the reaction zone width in the mixture fraction space. Otherwise distributed reaction zones prevail. On the other hand, Bilger uses the rms dissipation-scale scalar fluctuations and the reaction zone width in the mixture fraction space to delineate the two regimes.

In LES the filter size is generally in the inertial range and is much larger than the scalar dissipation scale. Thus, for large SGS mixture fraction fluctuations laminar flamelets are generally expected whereas for small SGS mixture fraction fluctuations distributed reaction zones are expected. (The widths of distributed reaction zones can be larger than the filter scale whereas that of a flamelet must be smaller.) However, these criteria for delineating the combustion regimes do not take into account the structure of the SGS mixture fraction, which can also have a strong impact on the flame structure. The bimodal SGS scalar (under spectral nonequilibrium conditions) contains diffusion layers, over which there is a large jump in mixture fraction, independent of Reynolds number, therefore are highly conducive to flamelets. On the other hand, quasi-equilibrium, near Gaussian SGS mixture fraction fields largely follow the Kolmogorov's cascade picture and there are generally no large mixture fraction jumps present over the dissipation scales. Therefore, such SGS fields are more likely to result in distributed reaction zones. This suggests a modification to the current criteria for delineating combustion regimes. The structure of the SGS mixture fraction can be characterized by the SGS variance and the filtered scalar dissipation rate. Therefore, LES has the potential to correctly identify and model the SGS flame structure.

Effects of Imaging System Blur on Measurements of Flow Scalars and Scalar-Gradients

Guanghua Wang and Noel T. Clemens*
Department of Aerospace Engineering and Engineering Mechanics
The University of Texas at Austin
Austin, Texas 78712-1085

There is substantial current interest in developing techniques to image the mixture fraction field in turbulent nonpremixed flames to infer the scalar dissipation rate field. In some cases, however, the scalar structures that are imaged may be corrupted by blur induced by the imaging system. The modulation transfer function (MTF) is the accepted means of quantifying resolution in the optics community (Smith, 2000), but relatively few flow imaging studies have explicitly used the MTF to quantify the resolution (Clemens, 2002). In many studies the resolution of the optical system is characterized by the area that a pixel maps to in the object plane as obtained by geometrical optics; however, when low *f/#* optics or image intensifiers are used this may not adequately describe the resolution. In this work we develop a simple analytical model of the effect of imaging system blur on simplified scalar structures to assess resolution requirements on the measurement of scalar length scales and scalar gradients. The objective is to give the experimentalist a methodology for quantitatively assessing the impact of imaging system blur on the accuracy of scalar measurements.

The analysis, which is discussed in Wang and Clemens (2004), is based on 1-D models of the imaging system blur and the scalar distributions. As shown by Buch and Dahm (1996), the scalar profiles at the dissipation scale can be modeled as an error function, $\xi(x) = \left(1 - erf\left(x/\lambda\right)\right)/2$, where ξ is the scalar concentration, x is the spatial coordinate and λ is the characteristic diffusion (or dissipation) length scale. The model profile as well as the corresponding gradient and dissipation rate profiles are shown in Fig. 1. The imaging system resolution is cast in terms of the line-spread function (LSF), which is modeled as Gaussian $LSF(x) = e^{-(x/\sigma)^2/2} \Big/ \left(\sigma\sqrt{2\pi}\right)$, where σ is the standard deviation of the profile. The MTF is the Fourier transform of the LSF. An accepted means of obtaining the LSF (or MTF) of an optical system is to infer its value from the step-response function (SRF), which can be obtained by the scanning knife-edge technique (Chazallet and Glasser, 1985). Figure 2 shows a measured SRF for a Kodak MegaPlus ES1.0 CCD camera, fitted with a Nikon 105mm lens (*f/2.8*) and operated at a magnification of unity, and the corresponding $MTF(s) = e^{-(\sigma s)^2/2}$ is shown in Fig 3. We define a normalized scalar dissipation structure thickness, $\lambda^*_{20\%} = \lambda_{20\%}/\sigma$, which is the layer thickness of the dissipation structure at 20% of the maximum dissipation normalized by the standard deviation of the Gaussian LSF. The analysis shows that the relative error in the: (*i*) dissipation structure thickness is $\sqrt{1+6.44/(\lambda^*_{20\%})^2} - 1$, (*ii*) peak gradient is $1 - 1\Big/\sqrt{1+6.44/(\lambda^*_{20\%})^2}$ and (*iii*) peak dissipation is $6.44\Big/\left(6.44 + (\lambda^*_{20\%})^2\right)$. Figure 4 shows the relative errors for the above quantities. As expected, the errors in all quantities are large for substantial blurring (i.e., small values of $\lambda^*_{20\%}$) and decrease to zero for large $\lambda^*_{20\%}$. It can be shown that if $\lambda^*_{20\%} \geq 7.5$, then the relative errors in all quantities will be smaller than 10%, which gives us a criterion for accurately resolving different scalar quantities. This suggests that the minimum true dissipation structure thickness must be at least 7.5σ and the measured (blurred) thickness must be at least 7.9σ. This implies that the requirement for limiting the errors induced by optical system blur is rather stringent, and may be difficult to meet in imaging experiments that require fast (low *f/#*) optics.

Simulations were also made to assess the effects of having clustered, or closely spaced, dissipation structures, such as occur in high Schmidt number turbulent flows. The analysis was conducted for two and three interacting scalar structures and the blurring effects were qualitatively similar but quantitatively different for the two cases. Interestingly, these results show that the relative error in the scalar-structure thicknesses is sometimes smaller

* clemens@mail.utexas.edu

for the clustered-structures than for the single-structures, but the error is much larger for the peak gradient and peak dissipation rate.

REFERENCES

Buch KA, Dahm WJA (1996), "Experimental study of the fine-scale structure of conserved scalar mixing in turbulent shear flows. Part 1. Sc>>1", *J. Fluid Mech.* 317:21–71

Chazallet F and Glasser J (1985), "Theoretical bases and measurement of the MTF of integrated image sensors". In: Granger EM and Baker LR (eds) *Image Quality: an Overview*, Proc. SPIE 549: 131–144

Clemens NT (2002), "Flow imaging", In: Hornak JP (ed) *Encyclopedia of Imaging Science and Technology*, John Wiley and Sons, New York, pp 390-419

Smith WJ (2000), "Modern Optical Engineering: The Design of Optical Systems", 3rd Ed., McGraw-Hill, New York

Wang GH and Clemens NT (2004), "Effects of Imaging System Blur on Measurements of Flow Scalars and Scalar-Gradients", *Exp. Fluids*, to be published

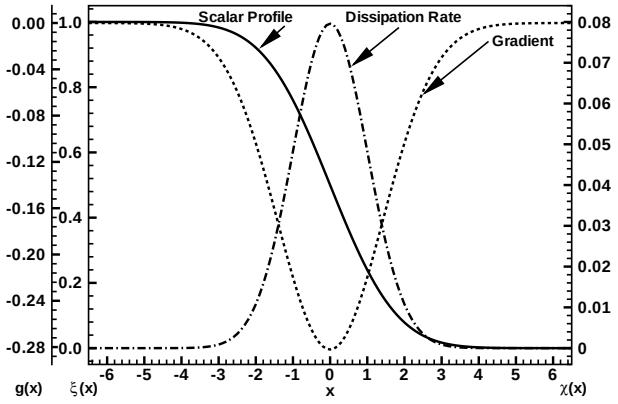

Fig. 1. Scalar profile (error-function) $\xi(x)$, gradient $g(x)$ and dissipation rate $\chi(x)$ for $\lambda = 2$.

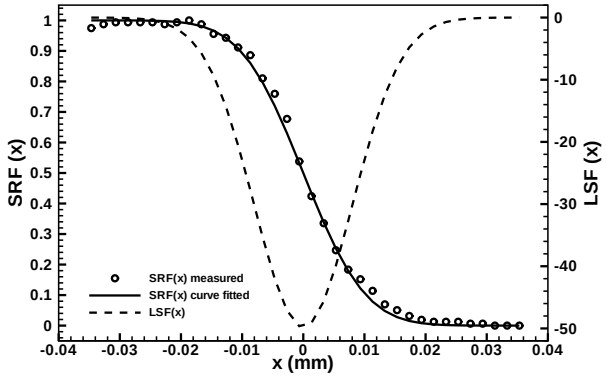

Fig. 2. Measured SRF, curve-fitted SRF and calculated LSF (σ=8.0μm). The imaging was conducted using a Kodak MegaPlus ES1.0 CCD camera, fitted with a Nikon 105mm lens f/2.8 and at a magnification of unity.

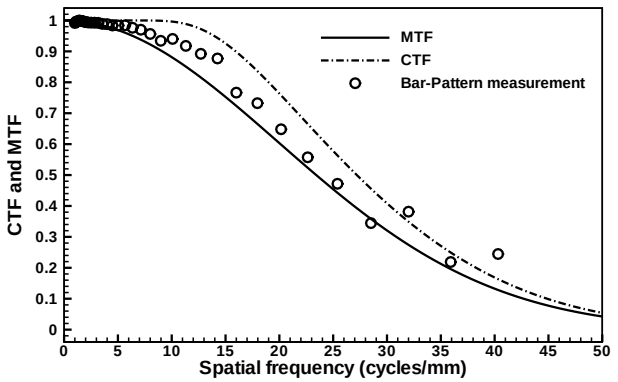

Fig. 3. Comparison of the MTF from Figure 2, the derived CTF and the CTF measured using a standard bar-pattern target (USAF-1951). The imaging system was the same as for Fig. 2.

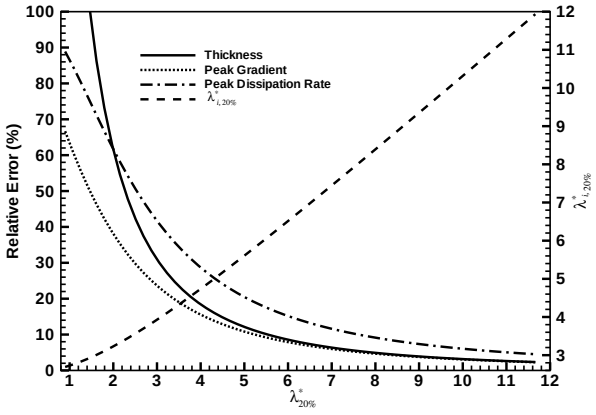

Fig. 4. Relative errors in structure thickness, peak gradient and peak dissipation rate. The scalar profile is modeled as an error-function.

Mean Spectral Radiation Data of Flame D

Yuan Zheng[1*], Jay P. Gore[1] and R. S. Barlow[2]
[1]Purdue University, West Lafayette, IN47907-2014
[2]Sandia National Laboratories, Livermore, CA94551-0969
[*]zhengy@ecn.purdue.edu

For the accurate prediction of nitric oxide formation in turbulent reacting flows, it is very important to model turbulent flame radiation appropriately [1]. Flame D is one of the piloted flames of TNF workshop [2] and has attracted a lot of attention in CFD simulations. Mean line-of-sight (LOS) spectra radiation intensity (I_λ) data are very useful for the validation of radiation models for the CFD simulations of this flame [3]. Small portions of the data have been reported in the literature [4,5]. The complete set of mean I_λ data is reported here.

The radiation measurements were conducted at the Turbulent Combustion Laboratory at Sandia. At three normalized down stream locations (x/D = 30, 45, 60) of Flame D, I_λ for various paralleling horizontal radiation paths from the axis to edge were measured by a fast infrared array spectrometer (FIAS). The temporal, spatial and spectral resolutions of the FIAS were 0.3 ms, 2 mm and 44 nm respectively. The experimental uncertainty of present I_λ measurements was 10%. Details of flow facility, operation conditions, experimental setup and instrumentations have been discussed elsewhere [2,4].

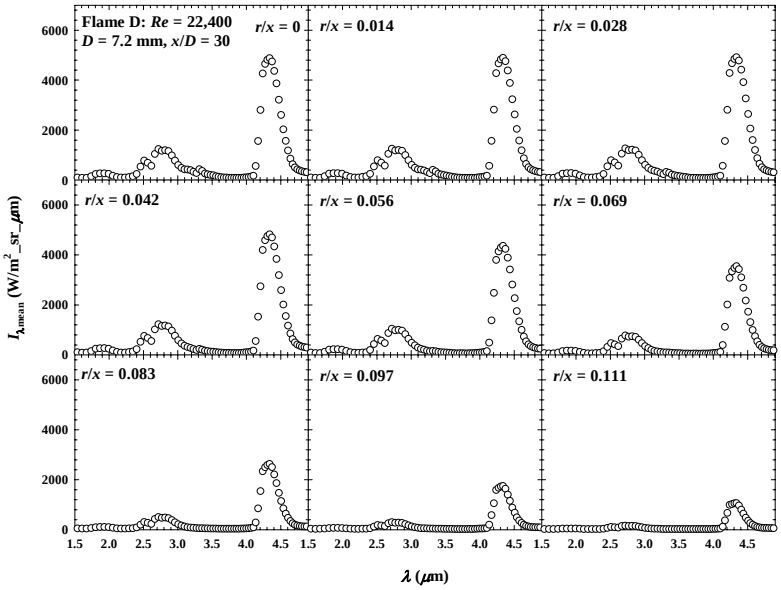

Fig. 1: LOS mean I_λ of Flame D at x/D = 30.

Figure 1 illustrates mean I_λ for nine radiation paths at various radial positions (r) at x/D = 30, where the mean flame front indicated by maximum mean temperature is around r/x = 0.045 [2]. Radiation from H_2O and CO_2 dominates the spectra and results in peaks at 1.86 μm (H_2O), 2.5 μm (H_2O), 2.7 μm (H_2O and CO_2) and 4.3 μm (H_2O and CO_2). Radiation peaks for hydrogen carbon (CH_4) can also be observed at 3.3 μm for paths at r/x = 0, 0.014 and 0.028, which went through fuel rich region. The mean I_λ increase slightly with radial distance until r/x = 0.028, and than decrease with r. Figure 2 illustrates mean I_λ for nine radiation paths at various radial positions at x/D = 45, where the mean flame front is very close to the axis [2]. The mean I_λ decrease with radial distance from the axis to the edge. The mean I_λ for near axis paths are higher than those at x/D = 30. Figure 3 illustrates mean I_λ for nine radiation paths at various radial positions at x/D = 60, where the maximum mean temperature occurs at the axis but is lower than the mean flame front temperature [2]. The mean I_λ also decrease with radial distance from the axis to the edge. The radiation level, however, is lower than that at x/D = 45 as expected. The effects of turbulence-radiation interactions (TRI) could be very strong for radiation paths far away from the axis in Flame D [4]. For these paths, radiation peaks may not be captured in simulations unless TRI are treated properly.

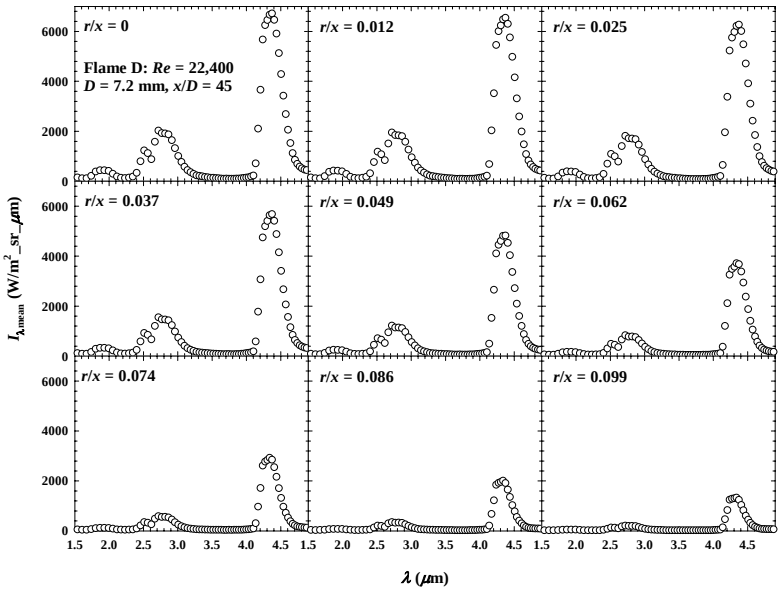

Fig. 2: LOS mean I_λ of Flame D at x/D = 45.

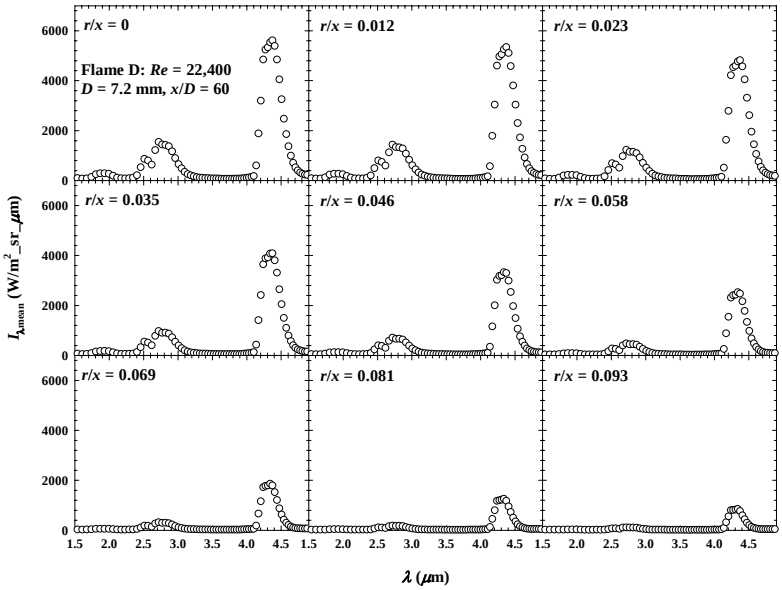

Fig. 3: LOS mean I_λ of Flame D at x/D = 60.

References:
[1] J.H. Frank, R.S. Barlow, C. Lundquist, *Proc. Combust. Inst.* 28 (2000) 447-454.
[2] *International Workshop on Measurement and Computation of Turbulent Non-premixed Flames*, Sandia National Laboratories, www.ca.sandia.gov/TNF, 2004.
[3] P.J. Coelho, O.J. Teerling, D. Roekaerts, *Combust. Flame* 133 (2003) 75-91.
[4] Y. Zheng, R.S. Barlow, J.P. Gore, *ASME J. Heat Transf.* 125 (2003) 678-686.
[5] Y. Zheng, R.S. Barlow, J.P. Gore, *ASME J. Heat Transf.* 125 (2003) 1065-1073.

Contributed Notes and Vugraphs on TNF7 Focus Topics

(included in the order of the agenda)

Bluff-Body Stabilised Flames

Comparison prepared by:
Andreas Kempf, Fachgebiet Energie- und Kraftwerkstechnik, TU-Darmstadt, Germany, akempf@gmx.net
This document is based on the overview by Peter Kalt and Assaad Masri from the TNF-6 proceedings [1].

Introduction

The Bluff-body burner has been presented as a target case at previous TNF Workshops. Some new simulations by Naud and Roekaerts, Raman and Pitsch, Kempf and Janicka and Liu and Pope are presented for validation against the experimental velocity and compositional data. As before, the experimental data is available on the internet [2].

Bluff-Body Burner

The burner was investigated experimentally for different test-cases labeled HM1e, HM1, HM2, HM3, HM3e. A bluff-body burner is located in a coflowing air stream. A central pipe in the bluff-body ejects fuel into the recirculation zone. The diameter of the bluff-body is 50 mm and the central fuel jet diameter is 3.6 mm. The coflow and fuel jet velocity vary with the cases. In general, cases labelled with higher numbers (e.g. HM3 opposed to HM1) feature larger flow rates.

For the cases labelled "e" (HM1e, HM3e), Laser Doppler Velocimetry data is available that has been measured at Sydney University Heat Laboratory. In these cases, the flow-rates were slightly lower than in the non-"e" cases and the fuel consisted of a mixture of Compressed Natural Gas and hydrogen. In these cases, the wind tunnel dimensions were 130mm x 130mm, the free stream turbulence of the air coflow was around 2%.

For the cases HM1, HM2 and HM3, compositional data was measured at the Turbulent Diffusion Flame Laboratory at Sandia's Combustion Research Facilities. In these cases, a methane hydrogen mixture was considered, the wind tunnel dimensions were 305mm x 305mm.

Further information on the set-up and the experimental results are available from [2].

Contributions

The contributions to the previous TNF Workshops are available in these proceedings [1]. For the Seventh TNF Workshop, contributions made for the cases HM1e, HM1, HM2, HM3, HM3e were made by the following contributors:

case	u_{jet}	u_{coflow}	fuel (vol.)	B. Naud, D. Roekaerts	V. Raman H. Pitsch	K. Liu S. Pope	T. Kuan P. Lindstedt	A. Kempf J. Janicka
HM1e	108 m/s	35 m/s	1:1 CNG/H_2	x	x	x		x
HM1	118 m/s	40 m/s	1:1 CH_4/H_2	x*	x	x		x*
HM2	178 m/s	40 m/s	1:1 CH_4/H_2			x	x	
HM3	214 m/s	40 m/s	1:1 CH_4/H_2			x	x	
HM3e	195 m/s	35 m/s	1:1 CNG/H_2					x

* Scalar data from the simulation of case HM1e is plotted against the experimental HM1 data.

[1] Proceedings of the TNF Workshop series: www.ca.sandia.gov/TNF
[2] Website of the Sydney Group: www.mech.eng.usyd.edu.au/thermofluids

Venkatramanan Raman, Heinz Pitsch — HM1e, HM1

Venktramanan Raman, Stanford University, US, vraman@stanford.edu
Heinz Pitsch, Stanford University, US, H.Pitsch@stanford.edu

Method
- LES
- Laminar Flamelet Chemistry

Grid size
320 x 160 x 64

Chemistry
- GRI-2.11 based laminar flamelet table.
- Uses Z, Z_{var}, \chi to determine density and other fields

LES specs
- Finite-Volume energy conserving momentum formulation.
- Dynamic models for diffusivity, viscosity and sub-bilter variance
- Domain decomposition base parallelization

Notes
- Results time-averaged over two-different time-windows to ensure stationarity.
- A recursively-refined LES grid used to minimize effect of sub-filter variance model

Kai Liu, Stephen Pope — HM1e, HM1, HM2, HM3

Kai Liu, Cornell University, US, kl47@cornell.edu
Stephen Pope, Cornell University, US, pope@mae.cornell.edu

Joint Velocity-Turbulence Frequency-Composition Probability Density Function (PDF) simulation

Models
Joint PDF method associated with models:
- Velocity: Simplified Langevin Model (SLM)
- Turbulence frequency: Jayesh-Pope Model (JPM)
- Mixing: Interaction by Exchange with the Mean (IEM) (for HM1E) and Euclidean Minimum Spanning Tres(EMST) (for HM1,2,3)
- Chemistry: simple flamelet model (for HM1E) and ARM2 (implemented by ISAT) (for HM1,2,3).

Numerics
- Finite Volume/Monte Carlo particle hybrid method
- Static simulation

Computational domain
- 7.2 D_{BB} axial direction
- $3D_{BB}$ radial direction.

Number of particles per cell and Grids
- 25 particles per cell and 129X97 for HM1E
- 100 particles per cell and 97X73 for HM1,2,3

Reference
- Kai Liu, Ph.D. Thesis, Cornell University, Jan. 2004
- K. Liu, S. B. Pope, and D. A. Caughey, "Calculations of Bluff-Body Stabilized Flames Using a Joint PDF Model with Detailed Chemistry." To be submitted to Combustion and Flames

Tek Kuan, Peter Lindstedt — HM2, HM3

Tek Kuan, Imperial College London, UK, t.kuan@imperial.ac.uk
Peter Lindstedt, Imperial College London, UK, p.lindstedt@imperial.ac.uk

Approach
- Second Moment Closures

Constants
- c_{nu}=0.09
- $c_{epsilon1}$=1.44
- $c_{epsilon2}$=1.80

PDF
- beta

Grid Size
- 124 by 109 (HM2)
- 189 by 138 (HM3)

Domain
- xmin= 0 mm
- xmax= 150 mm (HM2)
- xma= 160 mm (HM3)
- ymin= 0 mm
- ymax= 100 mm

Chemistry
- fast chemistry

Misc
- Results are profiles averaged over a time window of 50 ms

Bertrand Naud, Dirk Roekaerts — HM1e, (HM1)

Bertrand Naud, LITEC CSIC, Zaragoza, Spain, bertrand@litec.csic.es
Dirk Roekaerts, TU Delft, Netherlands, dirkr@ws.tn.tudelft.nl

Chemistry
- single flamelet with strain rate 100 s-1
- calculation in the opposed-flow diffusion flame geometry using GRI-MECH 3.0 reaction mechanism

PDF
- transported joint PDF of velocity fluctuation and mixture fraction
- Hybrid Finite-volume / particle method:
  - the Finite-Volume part solves the mean flow
  - particles represent the joint PDF

Turbulence modelling
- Launder, Reece and Rodi isotropisation of production model (LRR-IPM) used as Reynolds stress model (consistent generalised Langevin model used for evolution of particle velocity fluctuations)
  Standard constants: $C_1 = 1.8$ / $C_2 = 0.6$
  Daly-Harlow constant: $C_s = 0.22$
- Standard equation for dissipation (epsilon) with constants:
  $C_{eps1} = 1.6$ (instead of 1.44)
  $C_{eps2} = 1.92$ (standard)
  Daly-Harlow constant: $C_s = 0.18$

Micro-mixing model
- IEM with $C_{phi}=2$

Particles
- 50 particles per cell required
- Local time step

Grid
- 2D grid, 6 D_{bb} long / 3 D_{bb} wide
- 160 cells in axial direction
  (stretched from smallest size: 0.9 mm)
- 128 cells in radial direction:
  - 8 cells above fuel pipe
    (uniform = 1.8/8 = 0.225 mm)
  - 80 cells above bluff body
    (stretched from 0.225 mm to = 0.45 mm)
  - 40 cells in coflow (stretched from 0.45 mm)

Calculation
- 10000 outer iterations consisting of: 10 FV iterations / 3 particle time step
- (--> 30000 particle time steps)

Numerics
- 2nd order upwind discretisation in Finite-Volume part of the code
- Bilinear splines used to extract mean fields from particle ensemble
- New iteration averaging procedure to obtain particle mean fields (averages over 1000 iterations)

Andreas Kempf, Johnannes Janicka — HM1e, (HM1), HM3e

Andreas Kempf, TU-Darmstadt, Germany, akempf@gmx.net
Johannes Janicka, TU-Darmstadt, Germany, janicka@ekt.tu-darmstadt.de

Method
- LES
- Mixture Fraction Approach
- Steady Flamelet Chemistry

Chemistry
- Flamelet Tables by Peter Lindstedt
- 97 species, 629 reactions
- strain-rates from 25 s-1 to 1200 s-1
- beta-pdf

Numerics
- Incompressible
- Cylindrical grid
- Finite volumes
- Projection method

Grid Size
- 400x60x64 (ax. rad. circ.) for HM1(e)
- 600x32x60 (ax. rad. circ.) for HM3e

Domain Size
- 4 D_{BB} (ax.), 4.4 D_{BB} (rad.) for HM1(e)
- 6 D_{BB} (ax.), 4.4 D_{BB} (rad.) for HM3e

LES
- Eddy viscosity approach
- Smagorinsky model for turb. viscosity
- Dynamic procedure for turb. viscosity

Transport
- momentum: 2nd order energy conserving
- scalars: total variation diminuishing

Evaluation
- 0.05 s for HM1(e)
- 0.025 s for HM3e

CPU time
- 2 months for HM1(e)
- 1 month for HM3e

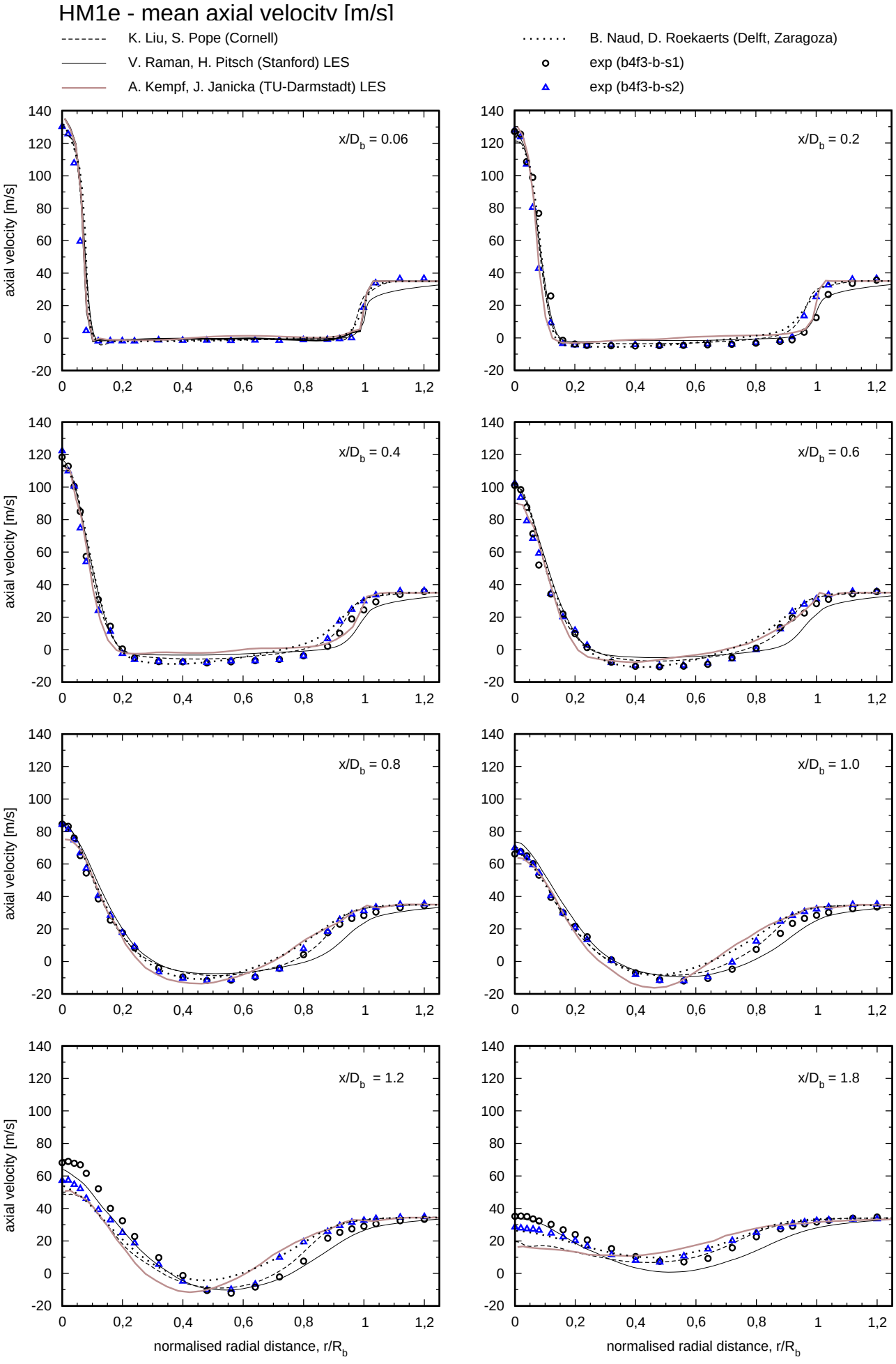
HM1e - mean axial velocity [m/s]
K. Liu, S. Pope (Cornell)
V. Raman, H. Pitsch (Stanford) LES
A. Kempf, J. Janicka (TU-Darmstadt) LES
B. Naud, D. Roekaerts (Delft, Zaragoza)
exp (b4f3-b-s1)
exp (b4f3-b-s2)
x/D_b = 0.06
x/D_b = 0.2
x/D_b = 0.4
x/D_b = 0.6
x/D_b = 0.8
x/D_b = 1.0
x/D_b = 1.2
x/D_b = 1.8
axial velocity [m/s]
normalised radial distance, r/R_b

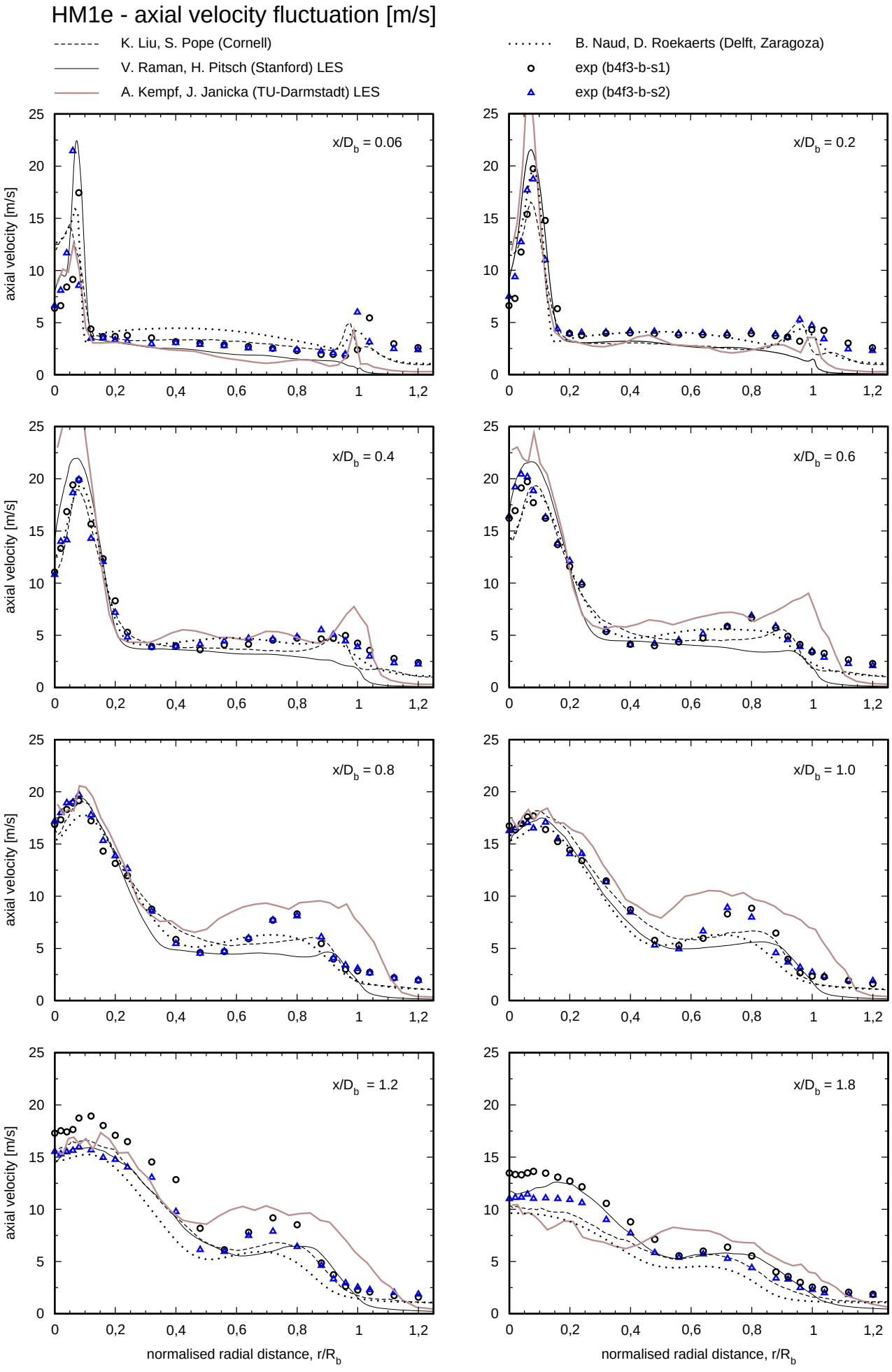
HM1e - axial velocity fluctuation [m/s]
K. Liu, S. Pope (Cornell)
V. Raman, H. Pitsch (Stanford) LES
A. Kempf, J. Janicka (TU-Darmstadt) LES
B. Naud, D. Roekaerts (Delft, Zaragoza)
exp (b4f3-b-s1)
exp (b4f3-b-s2)
x/D_b = 0.06
x/D_b = 0.2
x/D_b = 0.4
x/D_b = 0.6
x/D_b = 0.8
x/D_b = 1.0
x/D_b = 1.2
x/D_b = 1.8
axial velocity [m/s]
normalised radial distance, r/R_b
0
5
10
15
20
25
0,2
0,4
0,6
0,8
1
1,2

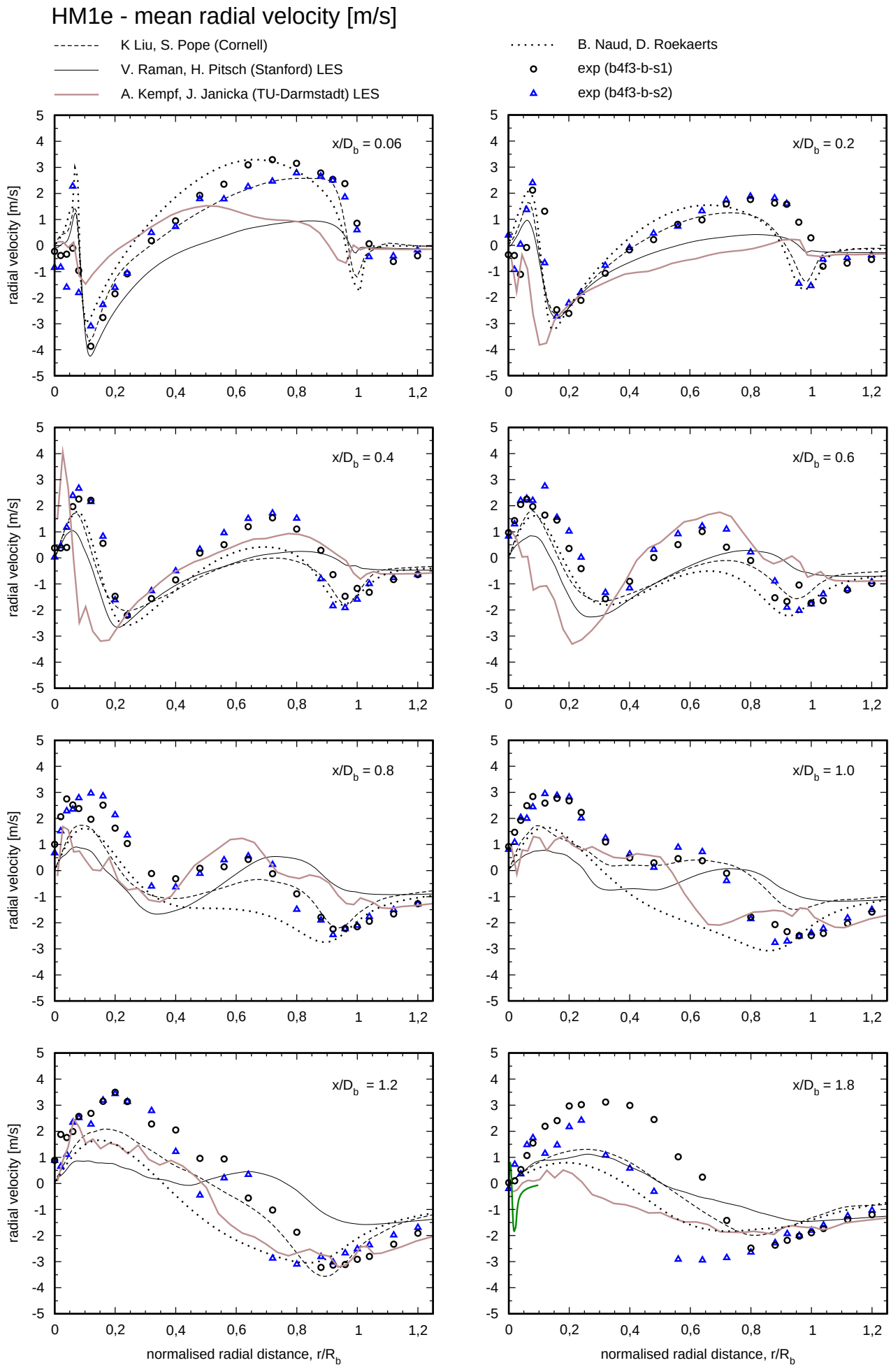
HM1e - mean radial velocity [m/s]
K Liu, S. Pope (Cornell)
V. Raman, H. Pitsch (Stanford) LES
A. Kempf, J. Janicka (TU-Darmstadt) LES
B. Naud, D. Roekaerts
exp (b4f3-b-s1)
exp (b4f3-b-s2)
x/D_b = 0.06
x/D_b = 0.2
x/D_b = 0.4
x/D_b = 0.6
x/D_b = 0.8
x/D_b = 1.0
x/D_b = 1.2
x/D_b = 1.8
radial velocity [m/s]
normalised radial distance, r/R_b

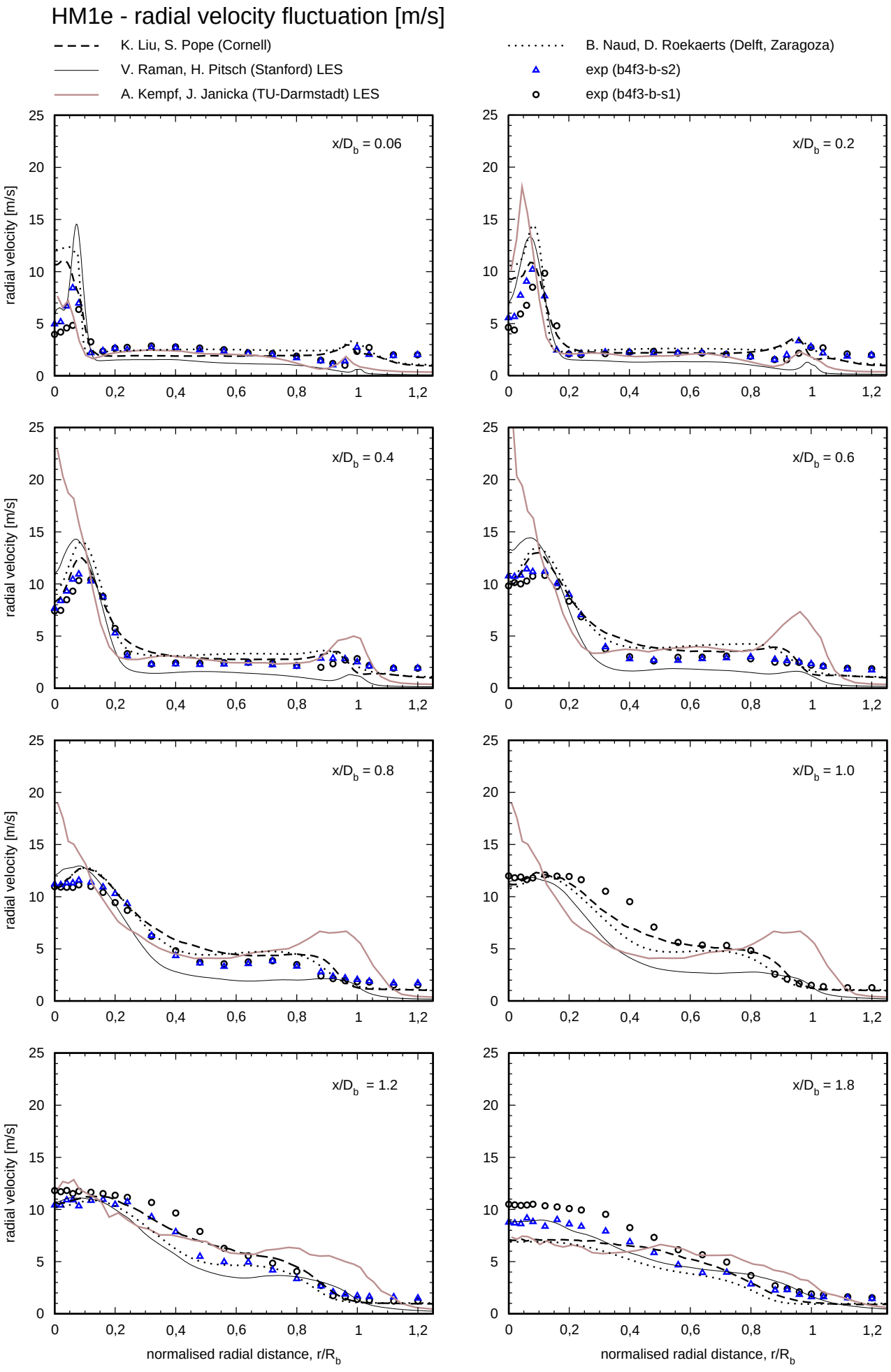
HM1e - radial velocity fluctuation [m/s]
K. Liu, S. Pope (Cornell)
V. Raman, H. Pitsch (Stanford) LES
A. Kempf, J. Janicka (TU-Darmstadt) LES
B. Naud, D. Roekaerts (Delft, Zaragoza)
exp (b4f3-b-s2)
exp (b4f3-b-s1)
x/D_b = 0.06
x/D_b = 0.2
x/D_b = 0.4
x/D_b = 0.6
x/D_b = 0.8
x/D_b = 1.0
x/D_b = 1.2
x/D_b = 1.8
radial velocity [m/s]
normalised radial distance, r/R_b
0
5
10
15
20
25
0,2
0,4
0,6
0,8
1
1,2

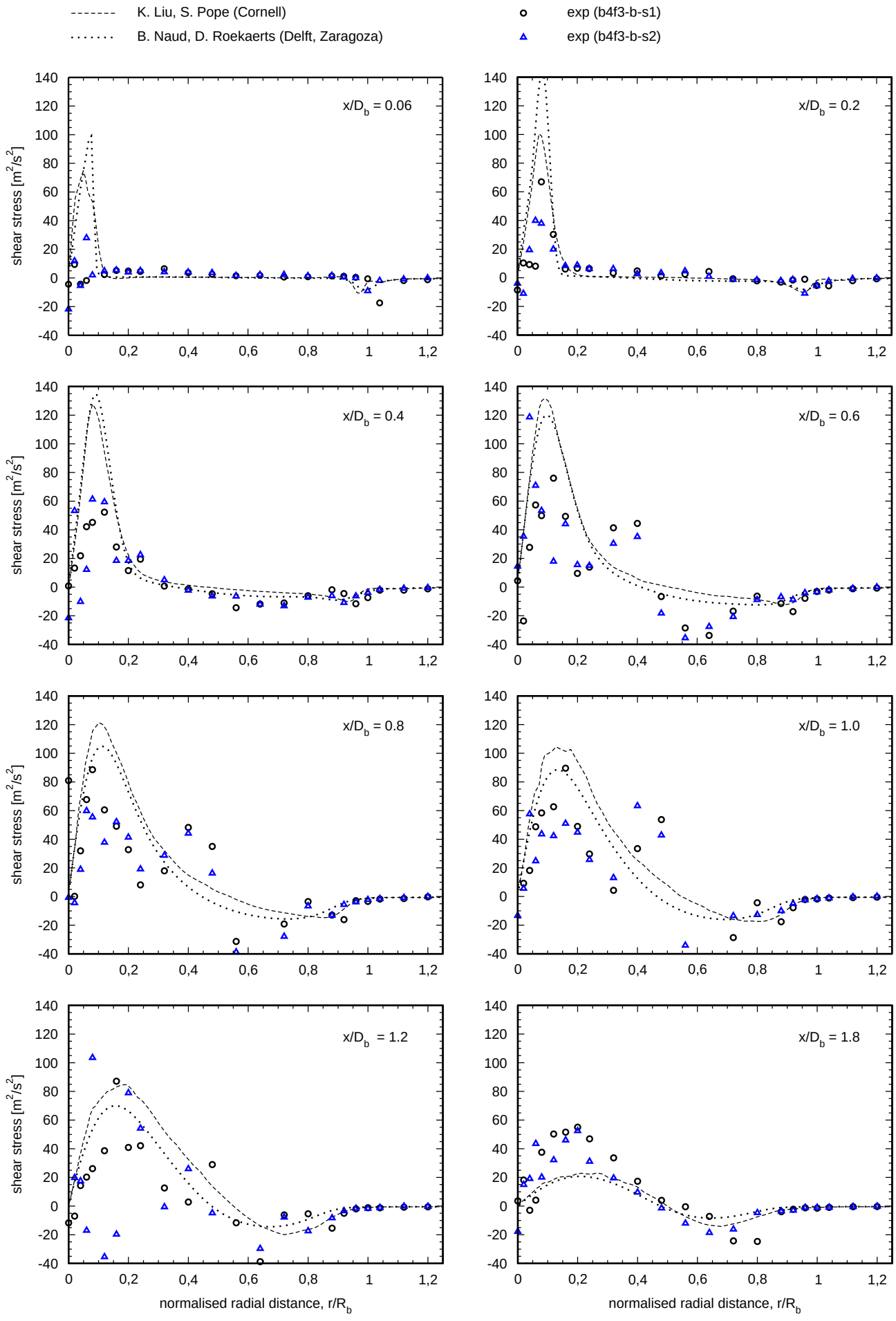
HM1e - shear stress (axial/radial) [m2/s2]
K. Liu, S. Pope (Cornell)
B. Naud, D. Roekaerts (Delft, Zaragoza)
exp (b4f3-b-s1)
exp (b4f3-b-s2)
x/Db = 0.06
x/Db = 0.2
x/Db = 0.4
x/Db = 0.6
x/Db = 0.8
x/Db = 1.0
x/Db = 1.2
x/Db = 1.8
shear stress [m2/s2]
normalised radial distance, r/Rb

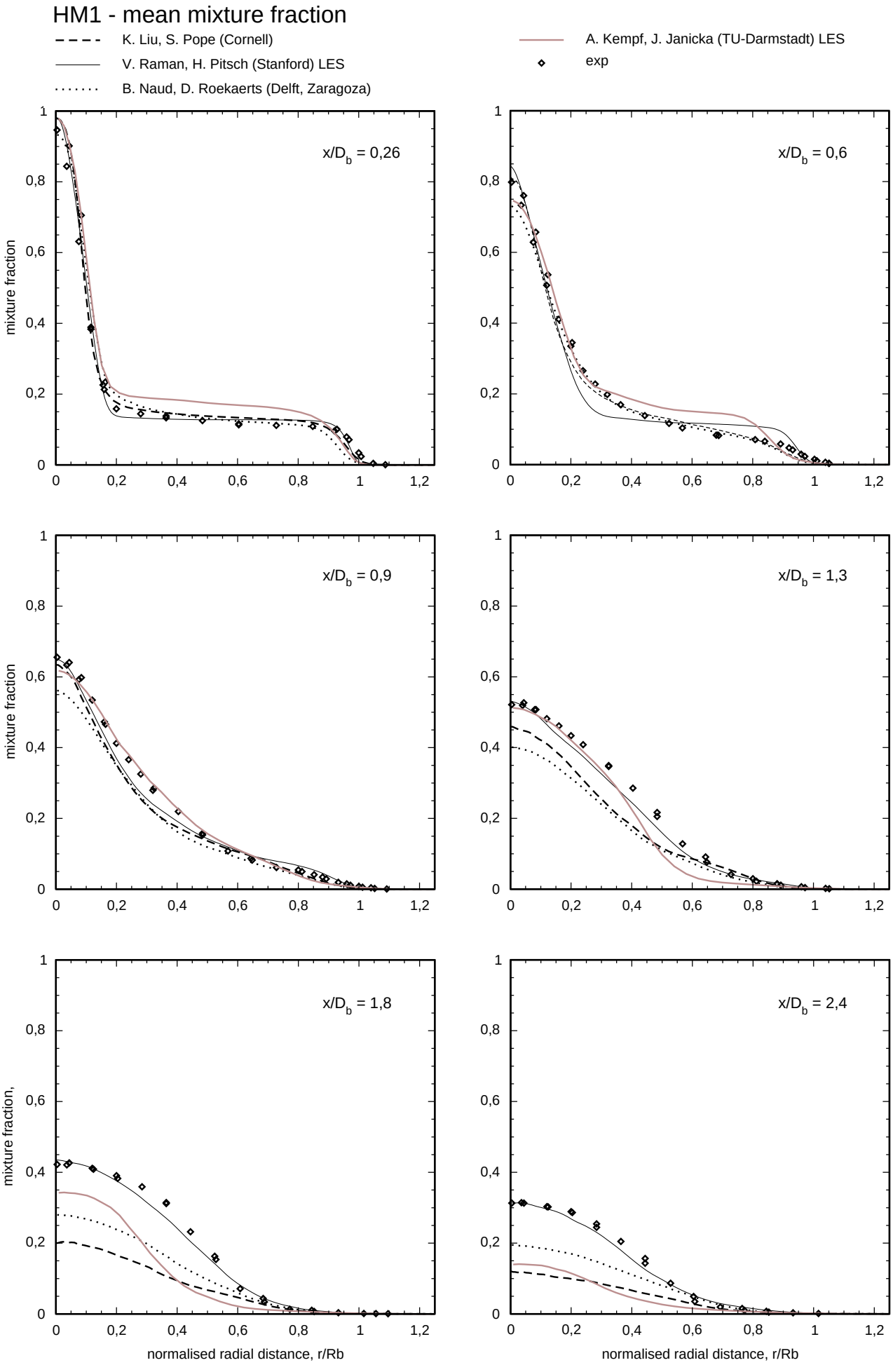
HM1 - mean mixture fraction
K. Liu, S. Pope (Cornell)
V. Raman, H. Pitsch (Stanford) LES
B. Naud, D. Roekaerts (Delft, Zaragoza)
A. Kempf, J. Janicka (TU-Darmstadt) LES
exp
x/D_b = 0,26
x/D_b = 0,6
x/D_b = 0,9
x/D_b = 1,3
x/D_b = 1,8
x/D_b = 2,4
mixture fraction
mixture fraction,
normalised radial distance, r/Rb
0
0,2
0,4
0,6
0,8
1
1,2

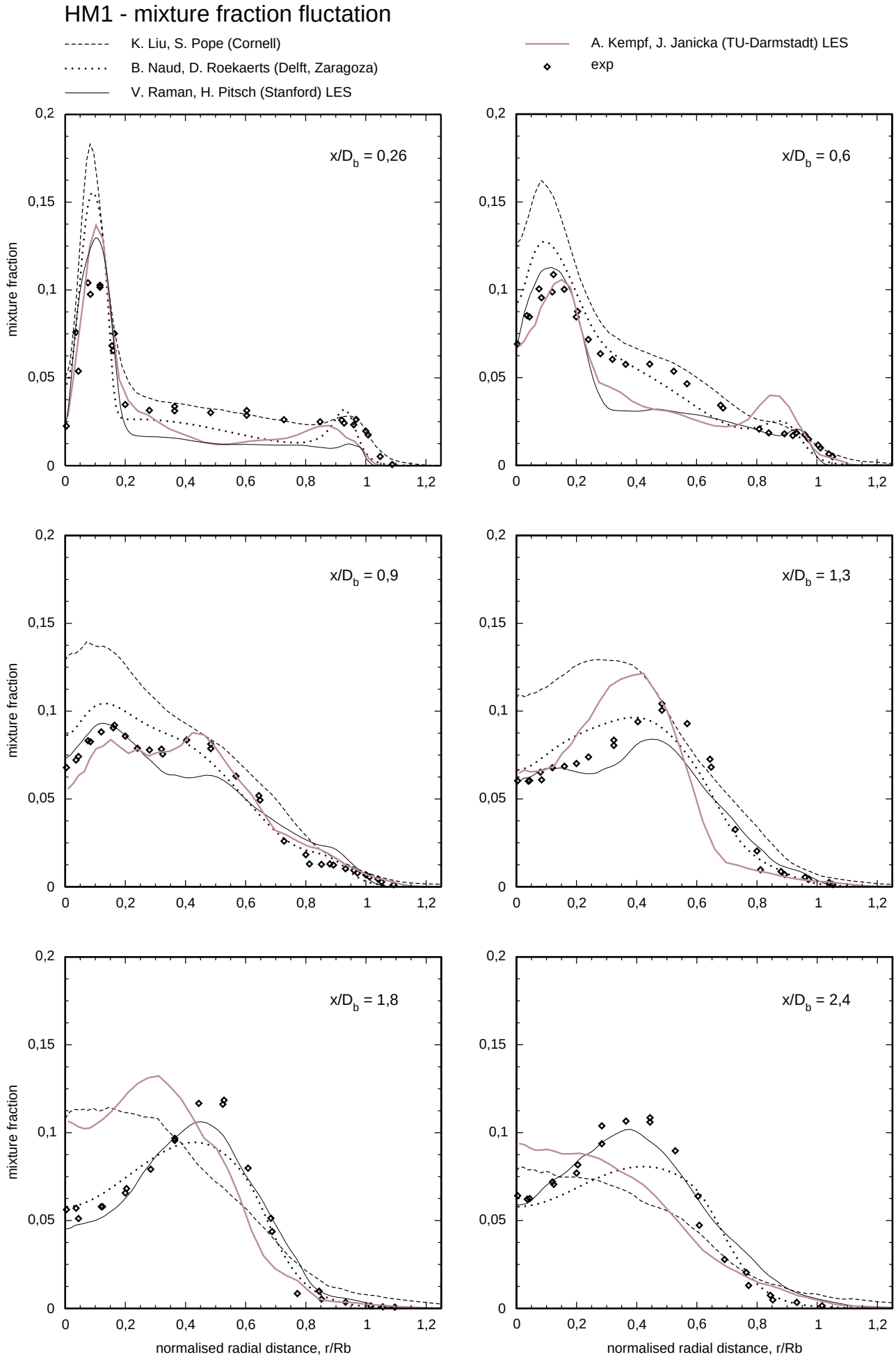
HM1 - mixture fraction fluctation
K. Liu, S. Pope (Cornell)
B. Naud, D. Roekaerts (Delft, Zaragoza)
V. Raman, H. Pitsch (Stanford) LES
A. Kempf, J. Janicka (TU-Darmstadt) LES
exp
x/D_b = 0,26
x/D_b = 0,6
x/D_b = 0,9
x/D_b = 1,3
x/D_b = 1,8
x/D_b = 2,4
mixture fraction
normalised radial distance, r/Rb
0
0,05
0,1
0,15
0,2
0,2
0,4
0,6
0,8
1
1,2

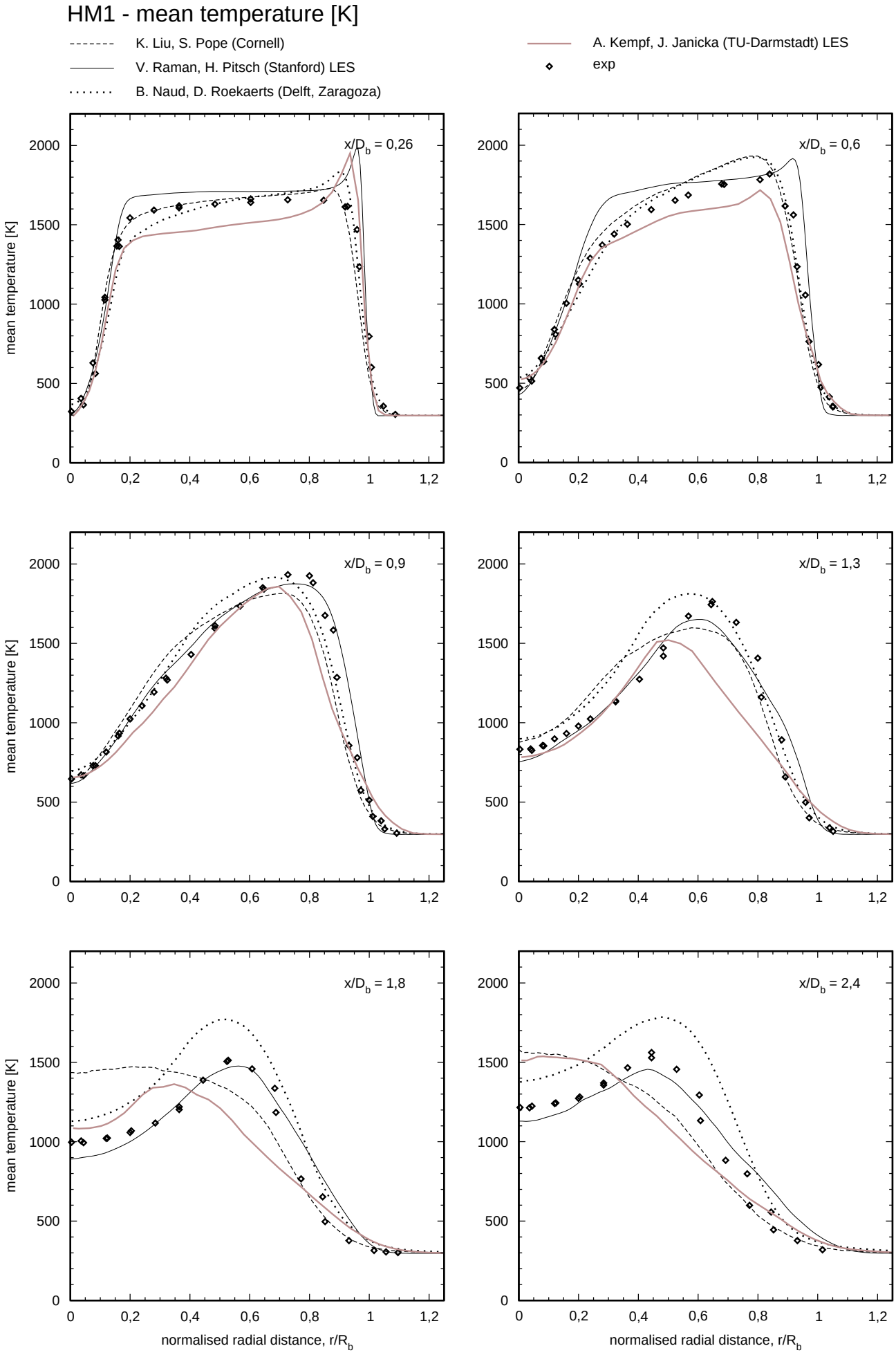
HM1 - mean temperature [K]
K. Liu, S. Pope (Cornell)
V. Raman, H. Pitsch (Stanford) LES
B. Naud, D. Roekaerts (Delft, Zaragoza)
A. Kempf, J. Janicka (TU-Darmstadt) LES
exp
x/D_b = 0,26
x/D_b = 0,6
x/D_b = 0,9
x/D_b = 1,3
x/D_b = 1,8
x/D_b = 2,4
mean temperature [K]
normalised radial distance, r/R_b
0
500
1000
1500
2000
0,2
0,4
0,6
0,8
1
1,2

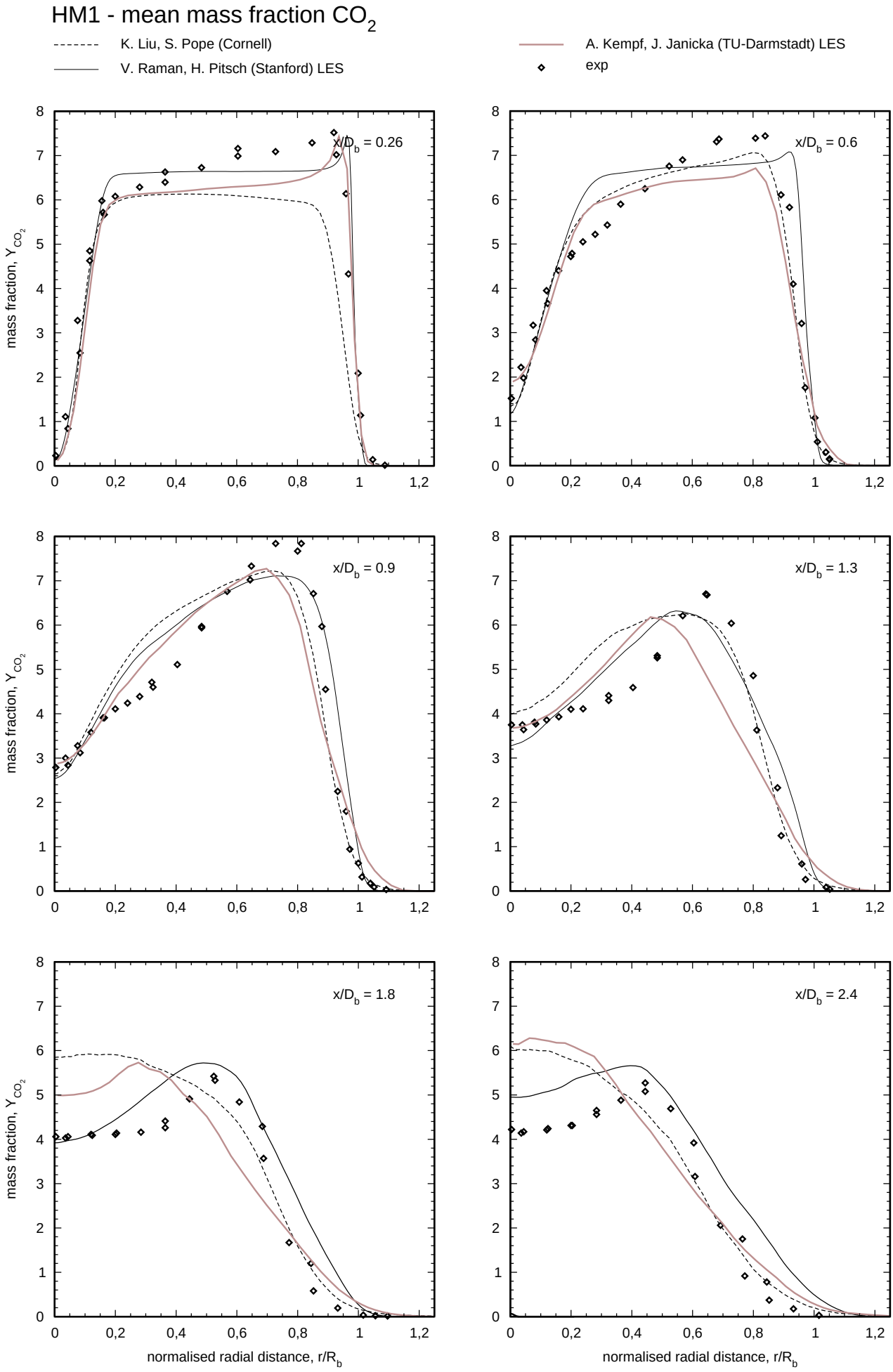
HM1 - mean mass fraction CO_2
K. Liu, S. Pope (Cornell)
V. Raman, H. Pitsch (Stanford) LES
A. Kempf, J. Janicka (TU-Darmstadt) LES
exp
x/D_b = 0.26
x/D_b = 0.6
x/D_b = 0.9
x/D_b = 1.3
x/D_b = 1.8
x/D_b = 2.4
mass fraction, Y_{CO_2}
normalised radial distance, r/R_b

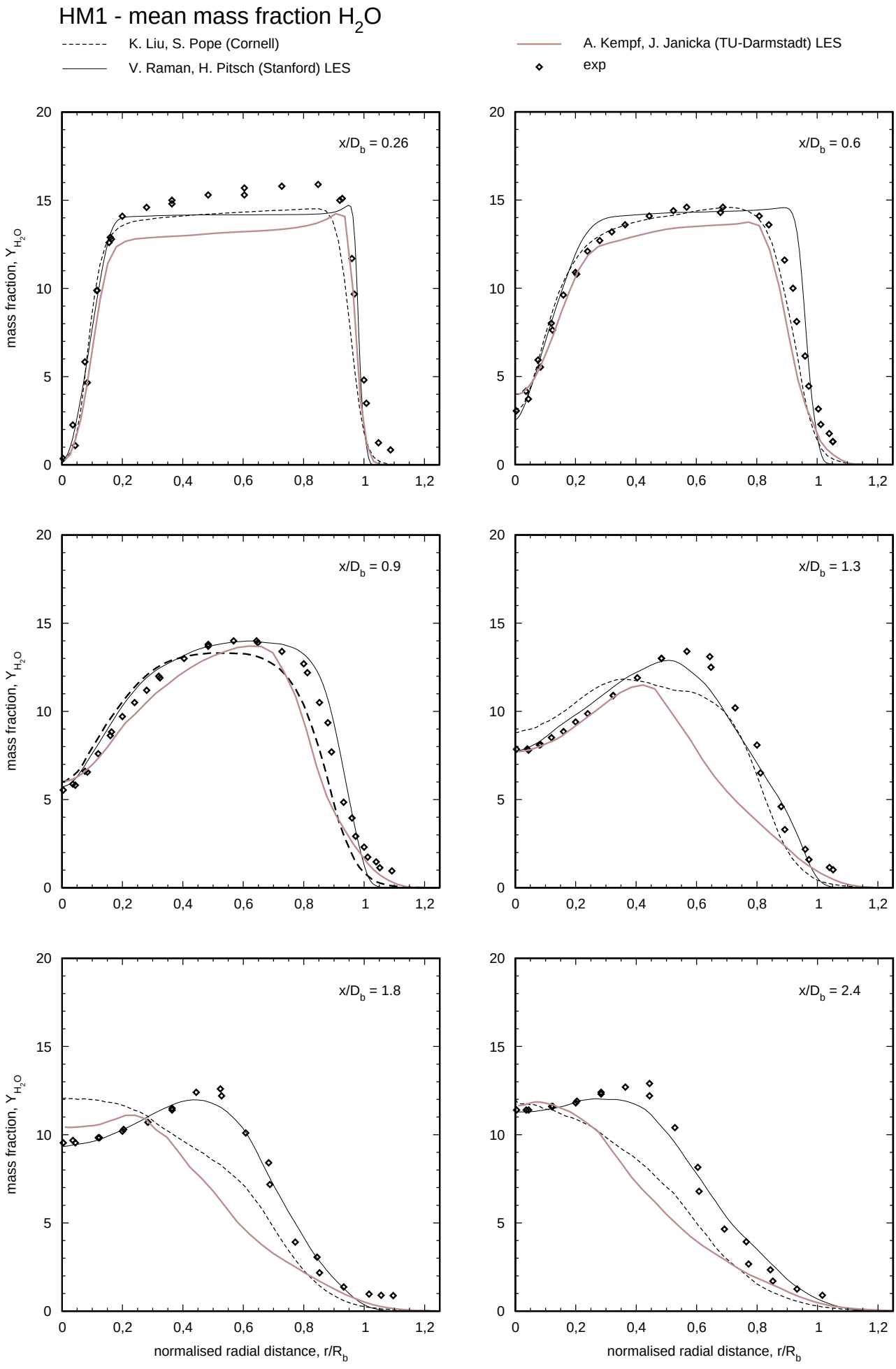
HM1 - mean mass fraction H_2O
K. Liu, S. Pope (Cornell)
V. Raman, H. Pitsch (Stanford) LES
A. Kempf, J. Janicka (TU-Darmstadt) LES
exp
x/D_b = 0.26
x/D_b = 0.6
x/D_b = 0.9
x/D_b = 1.3
x/D_b = 1.8
x/D_b = 2.4
mass fraction, Y_H2O
normalised radial distance, r/R_b

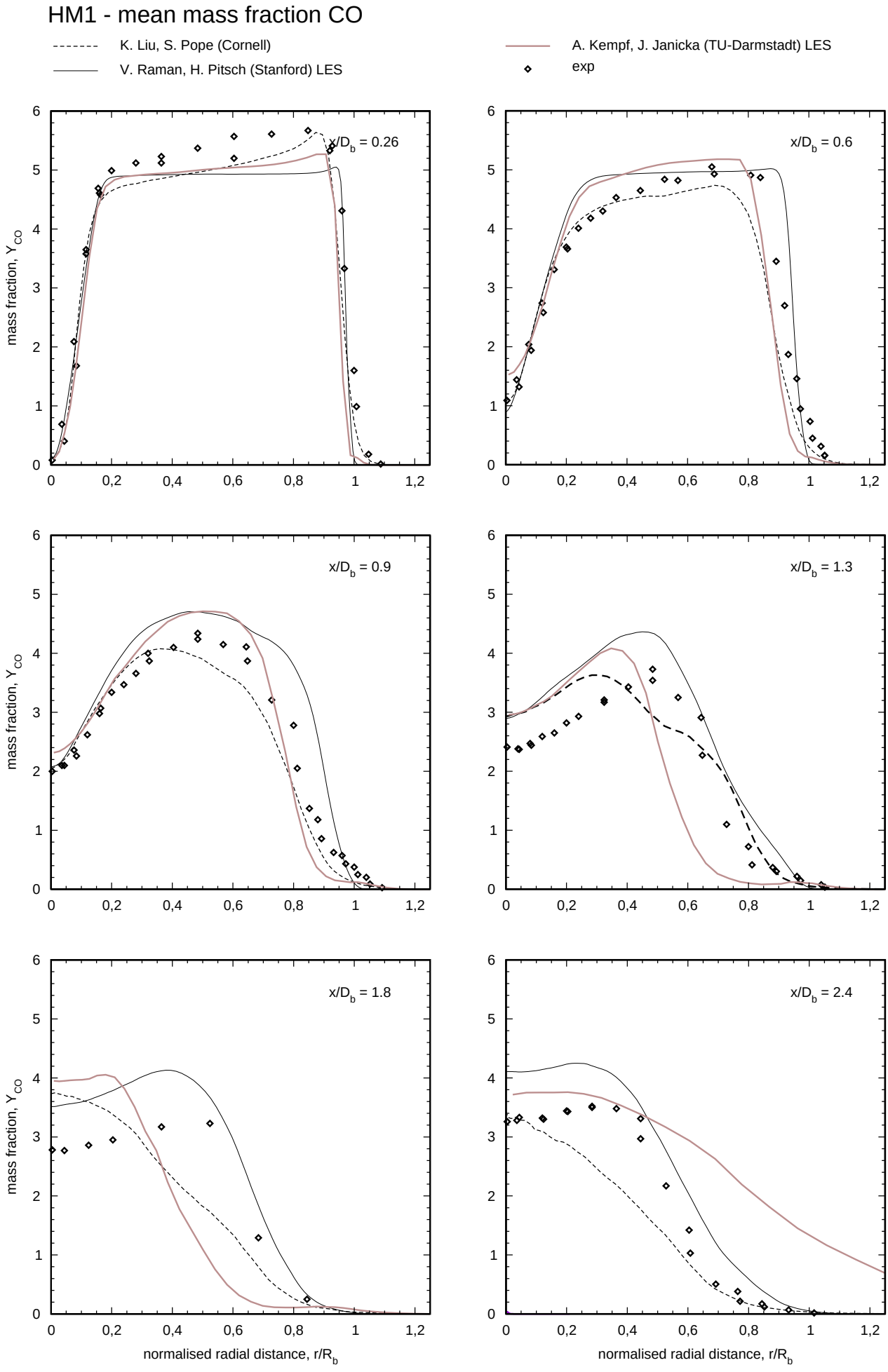
HM1 - mean mass fraction CO
K. Liu, S. Pope (Cornell)
V. Raman, H. Pitsch (Stanford) LES
A. Kempf, J. Janicka (TU-Darmstadt) LES
exp
x/D_b = 0.26
x/D_b = 0.6
x/D_b = 0.9
x/D_b = 1.3
x/D_b = 1.8
x/D_b = 2.4
mass fraction, Y_CO
normalised radial distance, r/R_b

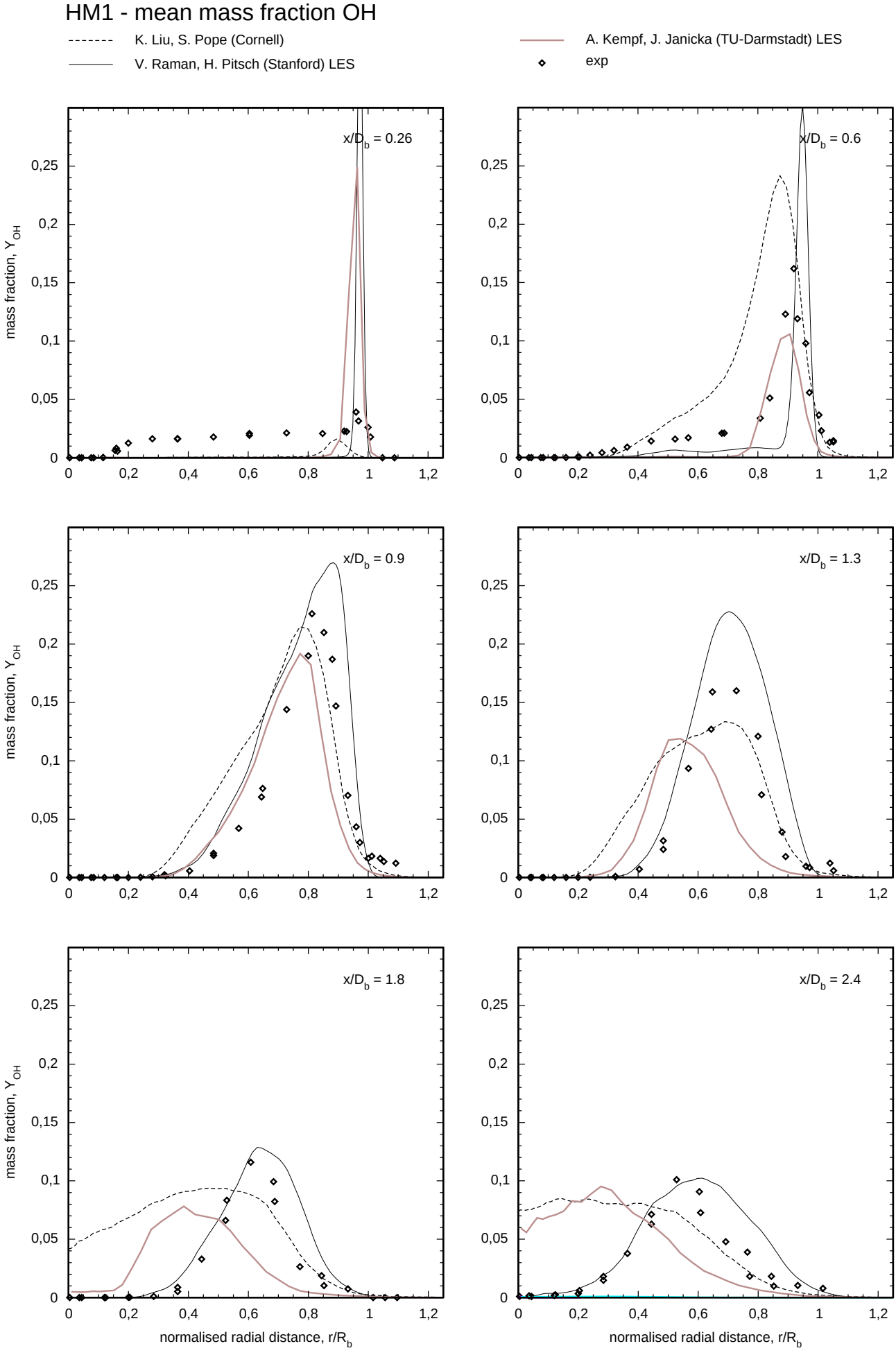
HM1 - mean mass fraction OH
K. Liu, S. Pope (Cornell)
V. Raman, H. Pitsch (Stanford) LES
A. Kempf, J. Janicka (TU-Darmstadt) LES
exp
x/D_b = 0.26
x/D_b = 0.6
x/D_b = 0.9
x/D_b = 1.3
x/D_b = 1.8
x/D_b = 2.4
mass fraction, Y_OH
normalised radial distance, r/R_b
0
0,05
0,1
0,15
0,2
0,25
0,2
0,4
0,6
0,8
1
1,2

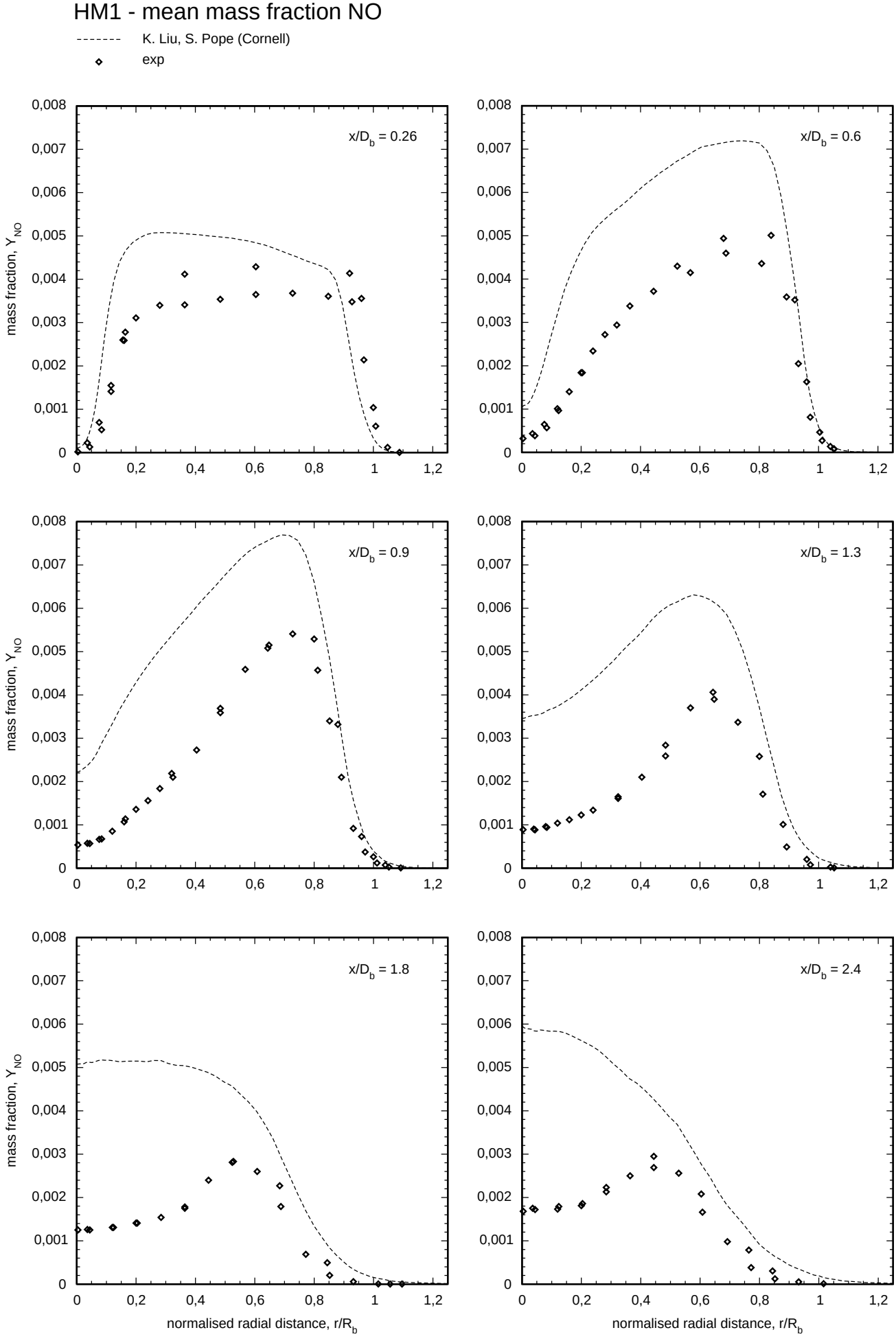
HM1 - mean mass fraction NO
K. Liu, S. Pope (Cornell)
exp
x/D_b = 0.26
x/D_b = 0.6
x/D_b = 0.9
x/D_b = 1.3
x/D_b = 1.8
x/D_b = 2.4
mass fraction, Y_NO
normalised radial distance, r/R_b
0
0,001
0,002
0,003
0,004
0,005
0,006
0,007
0,008
0,2
0,4
0,6
0,8
1
1,2

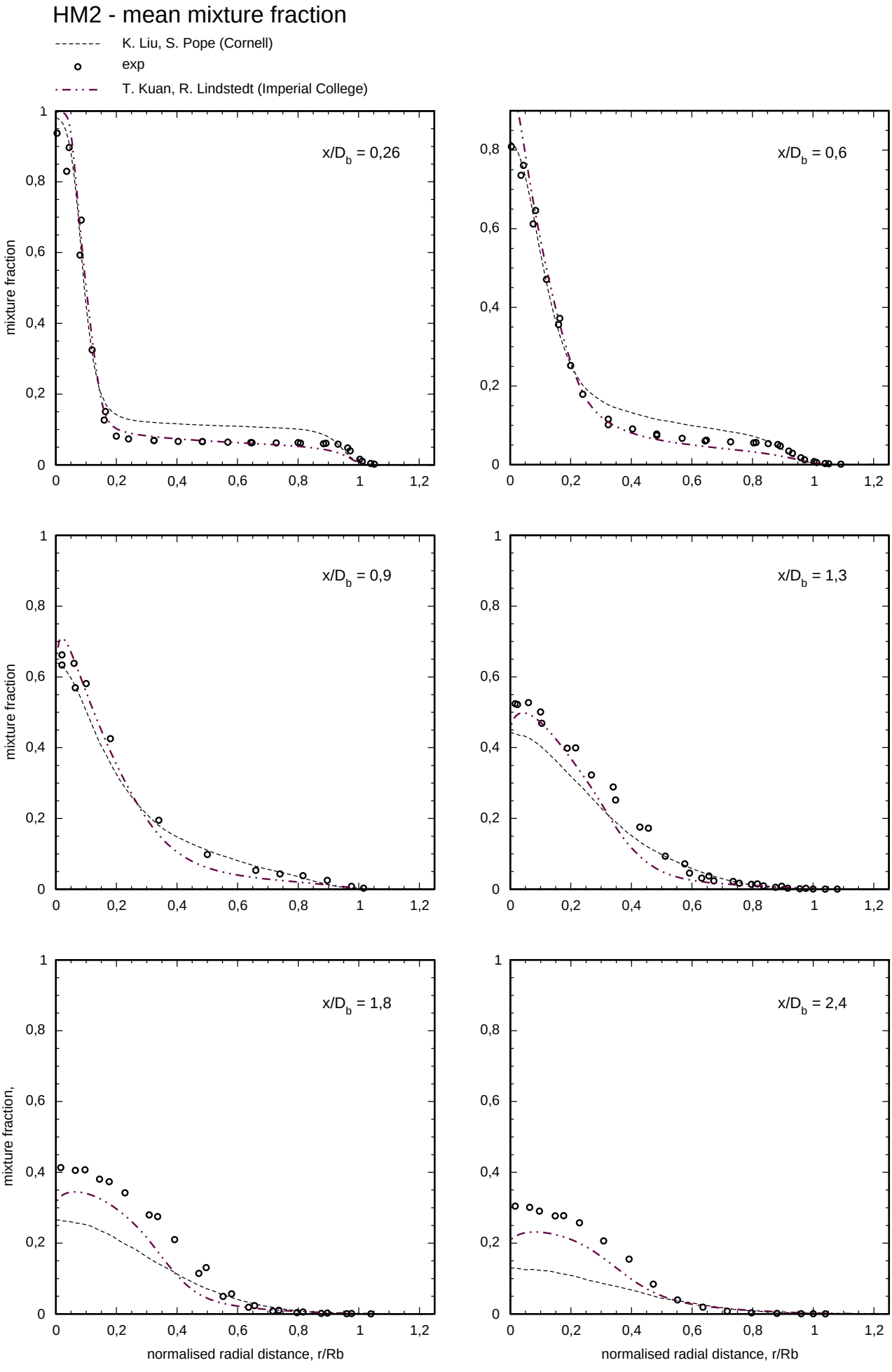
HM2 - mean mixture fraction
K. Liu, S. Pope (Cornell)
exp
T. Kuan, R. Lindstedt (Imperial College)
x/D_b = 0,26
x/D_b = 0,6
x/D_b = 0,9
x/D_b = 1,3
x/D_b = 1,8
x/D_b = 2,4
mixture fraction
mixture fraction,
normalised radial distance, r/Rb

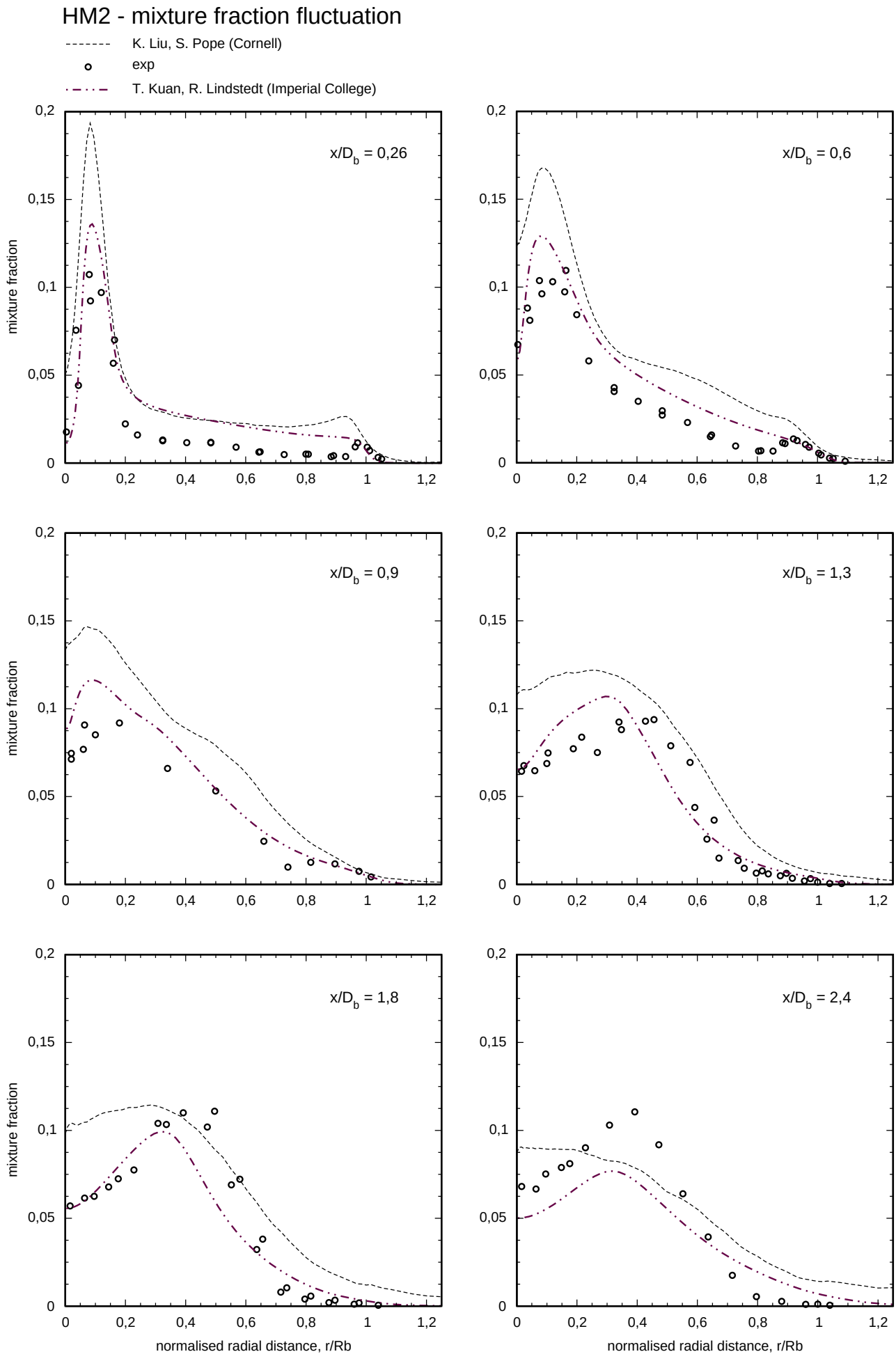
HM2 - mixture fraction fluctuation
K. Liu, S. Pope (Cornell)
exp
T. Kuan, R. Lindstedt (Imperial College)
x/D_b = 0,26
x/D_b = 0,6
x/D_b = 0,9
x/D_b = 1,3
x/D_b = 1,8
x/D_b = 2,4
mixture fraction
normalised radial distance, r/Rb
0
0,05
0,1
0,15
0,2
0,2
0,4
0,6
0,8
1
1,2

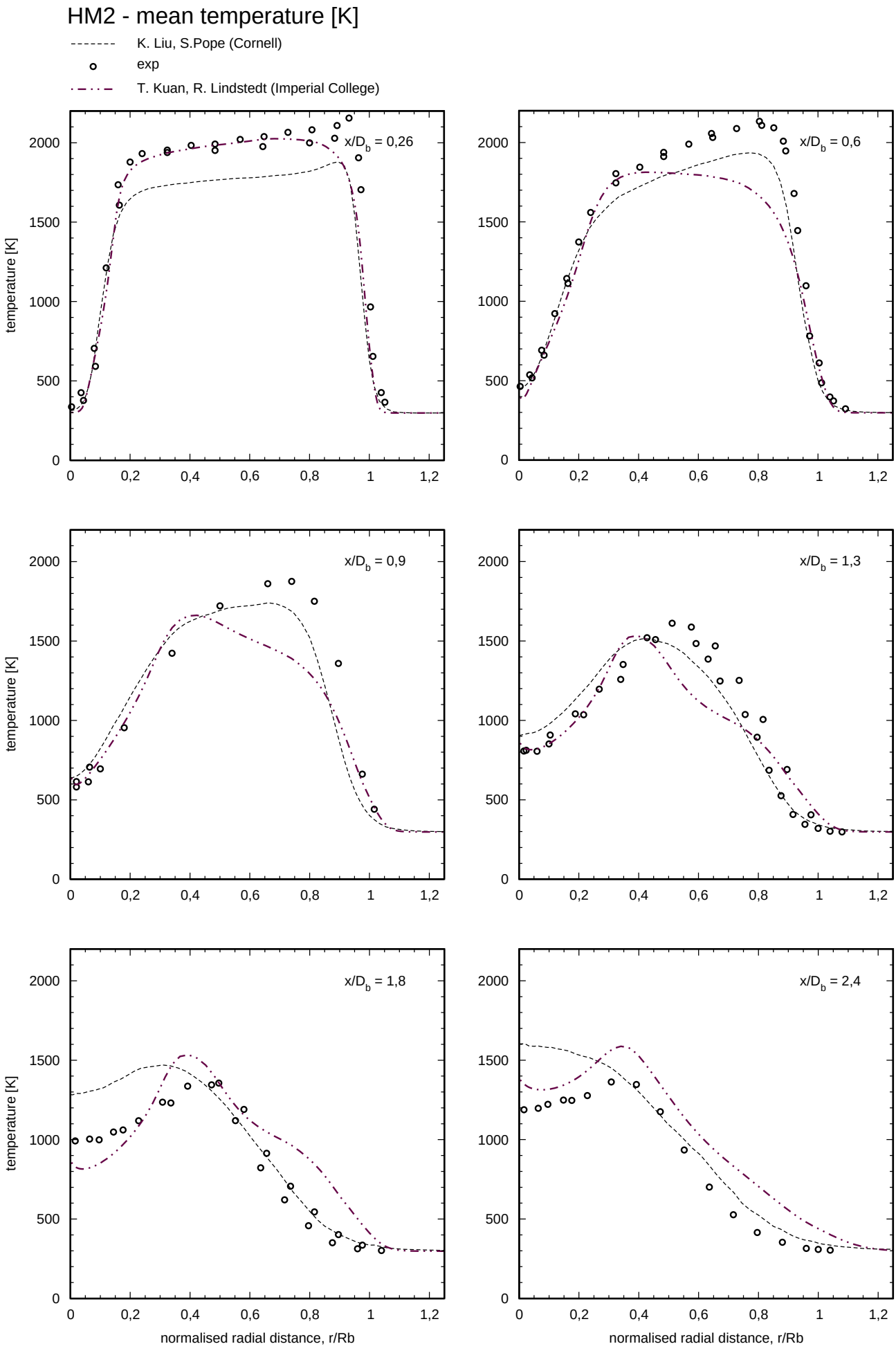
HM2 - mean temperature [K]
K. Liu, S.Pope (Cornell)
exp
T. Kuan, R. Lindstedt (Imperial College)
x/D_b = 0,26
x/D_b = 0,6
x/D_b = 0,9
x/D_b = 1,3
x/D_b = 1,8
x/D_b = 2,4
temperature [K]
normalised radial distance, r/Rb
0
500
1000
1500
2000
0,2
0,4
0,6
0,8
1
1,2

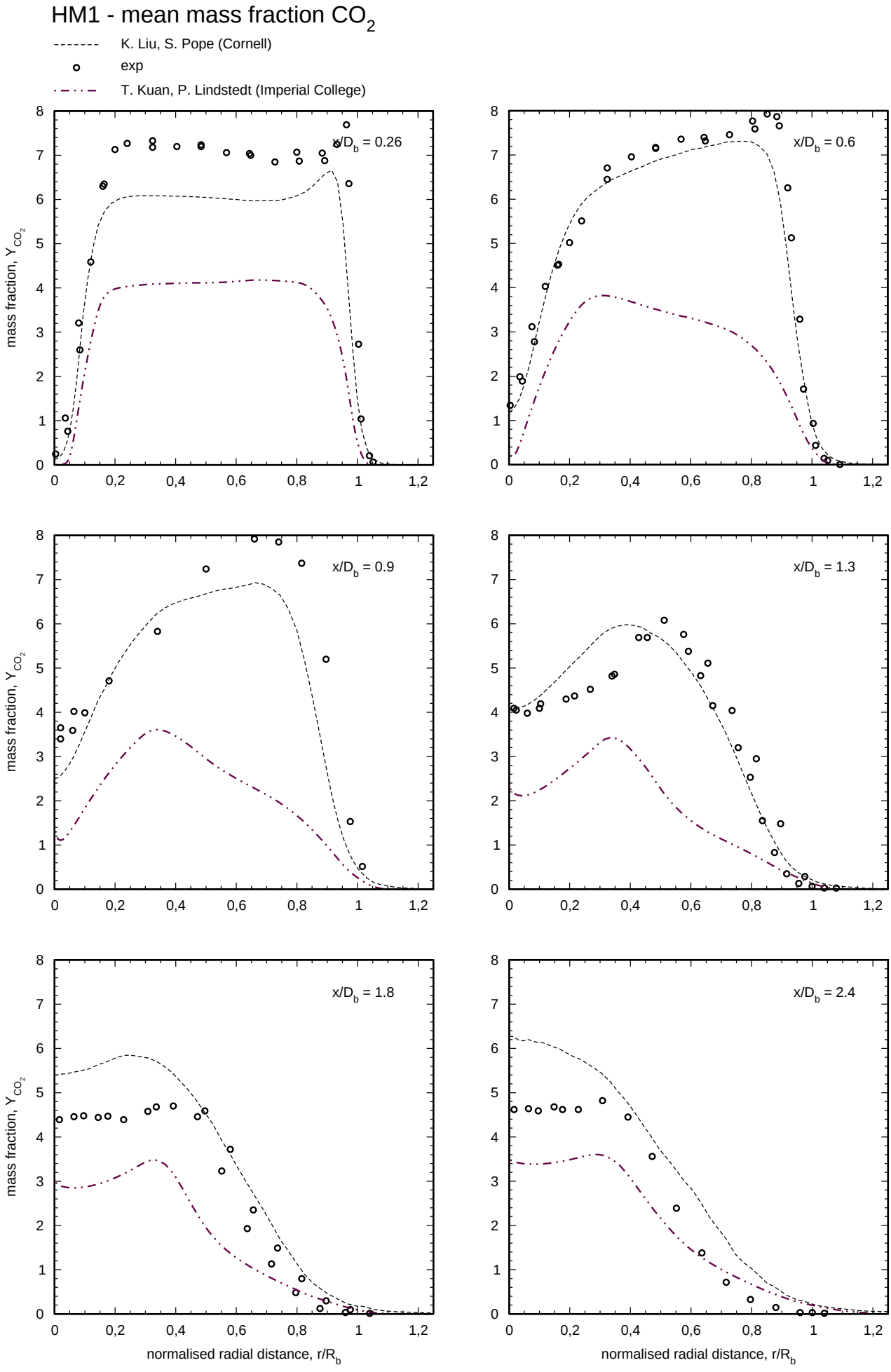
HM1 - mean mass fraction CO_2
K. Liu, S. Pope (Cornell)
exp
T. Kuan, P. Lindstedt (Imperial College)
x/D_b = 0.26
x/D_b = 0.6
x/D_b = 0.9
x/D_b = 1.3
x/D_b = 1.8
x/D_b = 2.4
mass fraction, Y_CO2
normalised radial distance, r/R_b

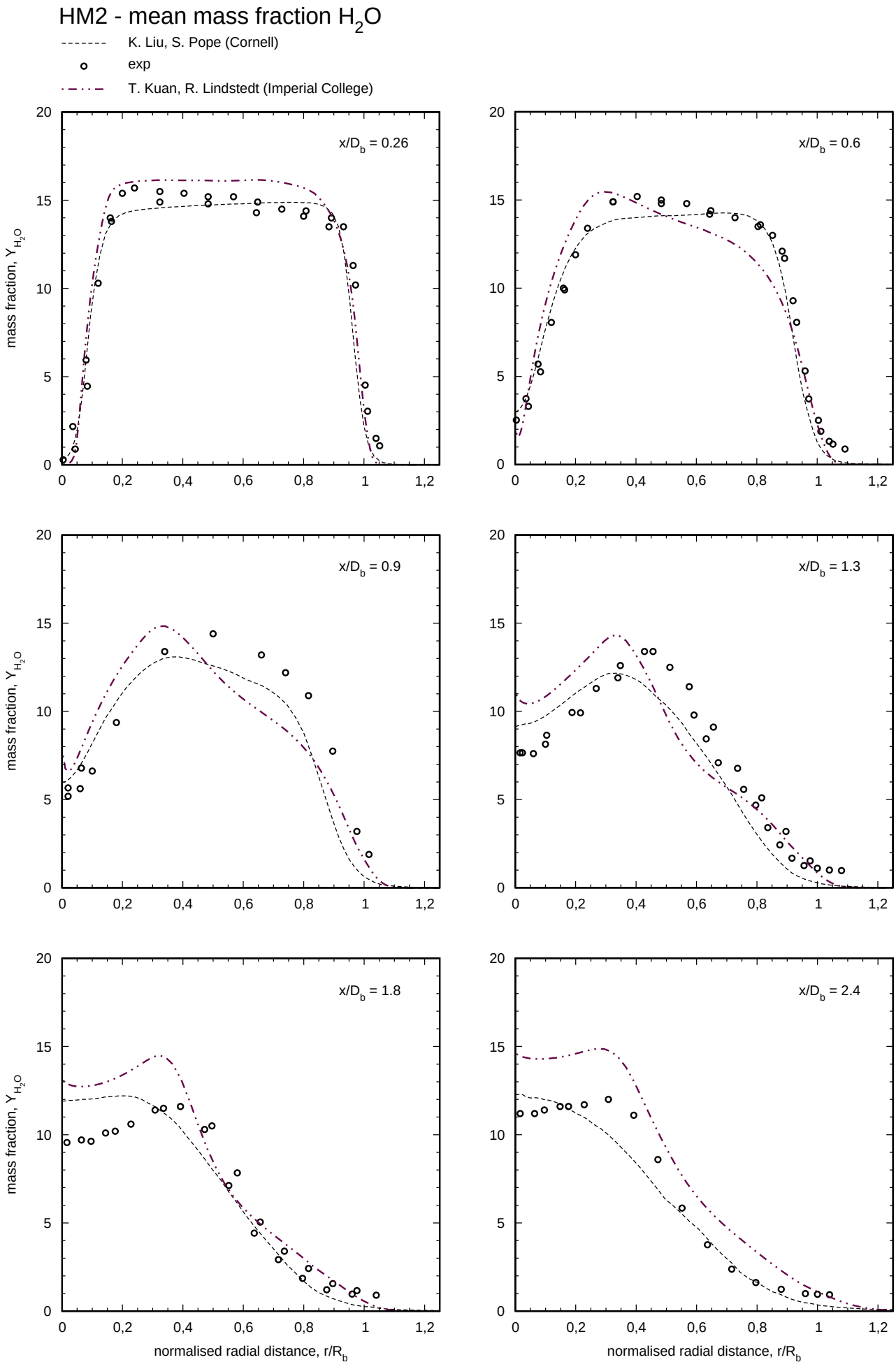
HM2 - mean mass fraction H_2O
K. Liu, S. Pope (Cornell)
exp
T. Kuan, R. Lindstedt (Imperial College)
x/D_b = 0.26
x/D_b = 0.6
x/D_b = 0.9
x/D_b = 1.3
x/D_b = 1.8
x/D_b = 2.4
mass fraction, Y_H2O
normalised radial distance, r/R_b

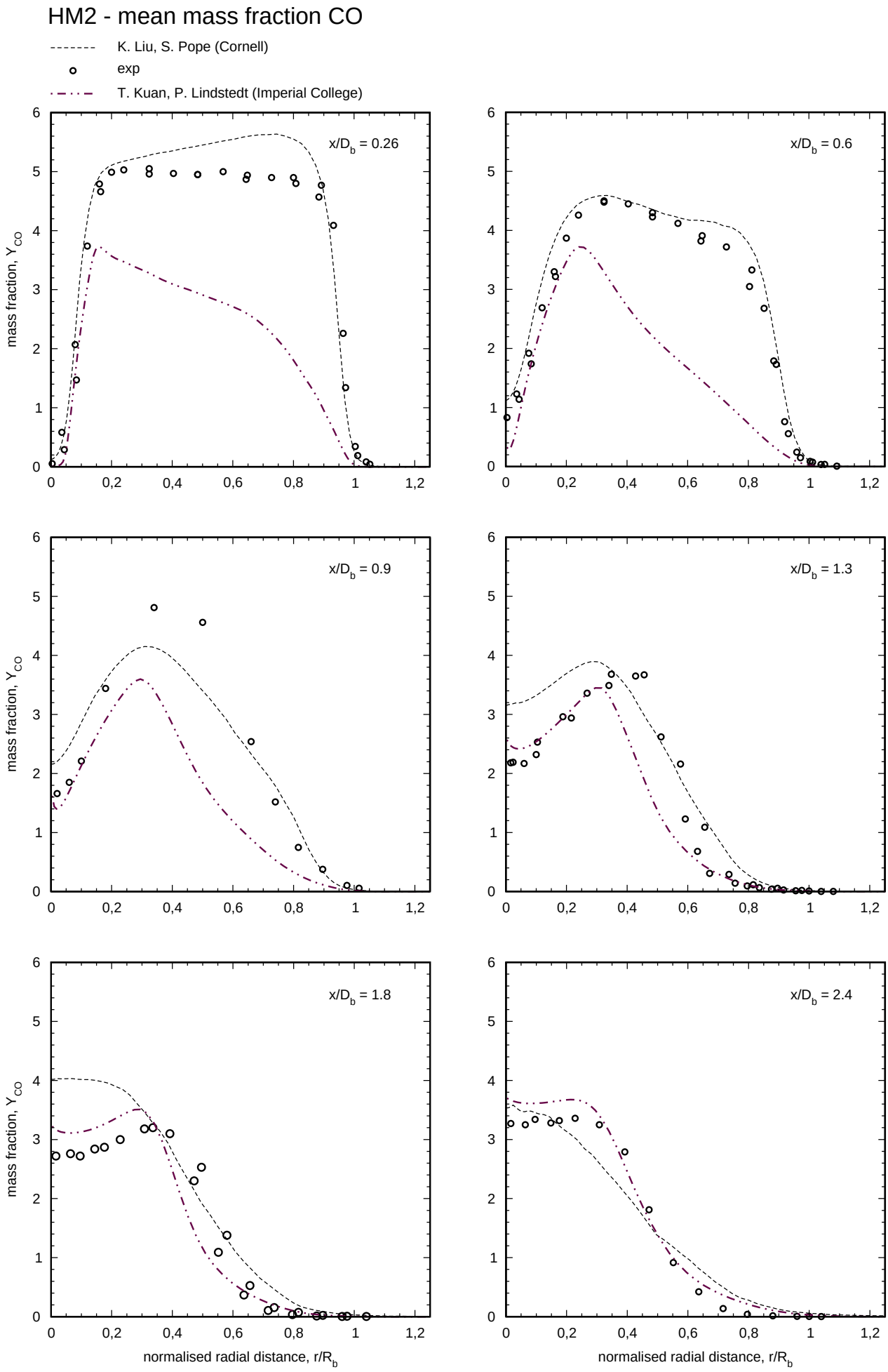
HM2 - mean mass fraction CO
K. Liu, S. Pope (Cornell)
exp
T. Kuan, P. Lindstedt (Imperial College)
x/D_b = 0.26
x/D_b = 0.6
x/D_b = 0.9
x/D_b = 1.3
x/D_b = 1.8
x/D_b = 2.4
mass fraction, Y_CO
normalised radial distance, r/R_b

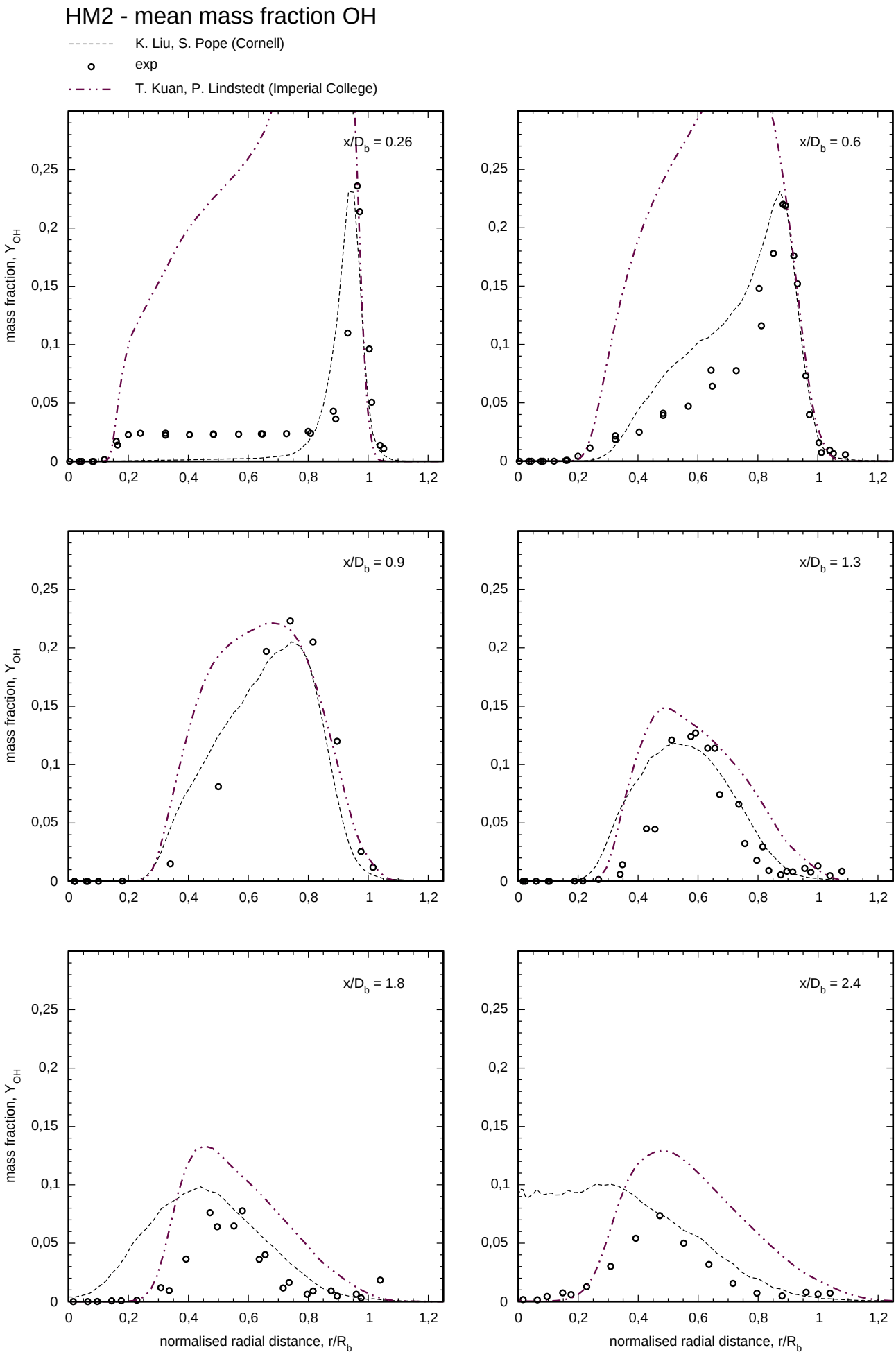
HM2 - mean mass fraction OH
K. Liu, S. Pope (Cornell)
exp
T. Kuan, P. Lindstedt (Imperial College)
x/D_b = 0.26
x/D_b = 0.6
x/D_b = 0.9
x/D_b = 1.3
x/D_b = 1.8
x/D_b = 2.4
mass fraction, Y_OH
normalised radial distance, r/R_b
0
0,05
0,1
0,15
0,2
0,25
0,2
0,4
0,6
0,8
1
1,2

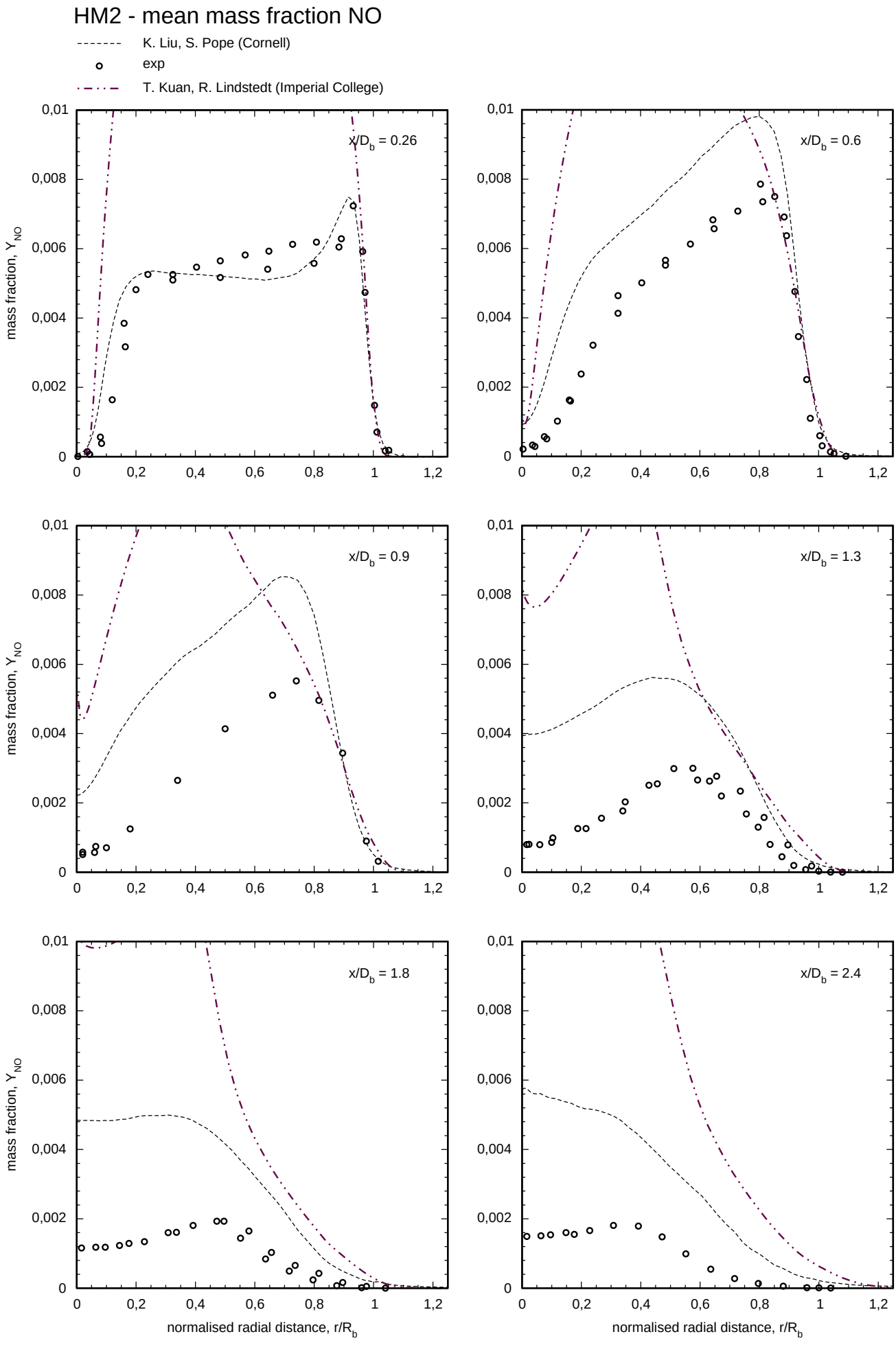
HM2 - mean mass fraction NO
K. Liu, S. Pope (Cornell)
exp
T. Kuan, R. Lindstedt (Imperial College)
x/D_b = 0.26
x/D_b = 0.6
x/D_b = 0.9
x/D_b = 1.3
x/D_b = 1.8
x/D_b = 2.4
mass fraction, Y_NO
normalised radial distance, r/R_b
0,01
0,008
0,006
0,004
0,002
0
0,2
0,4
0,6
0,8
1
1,2

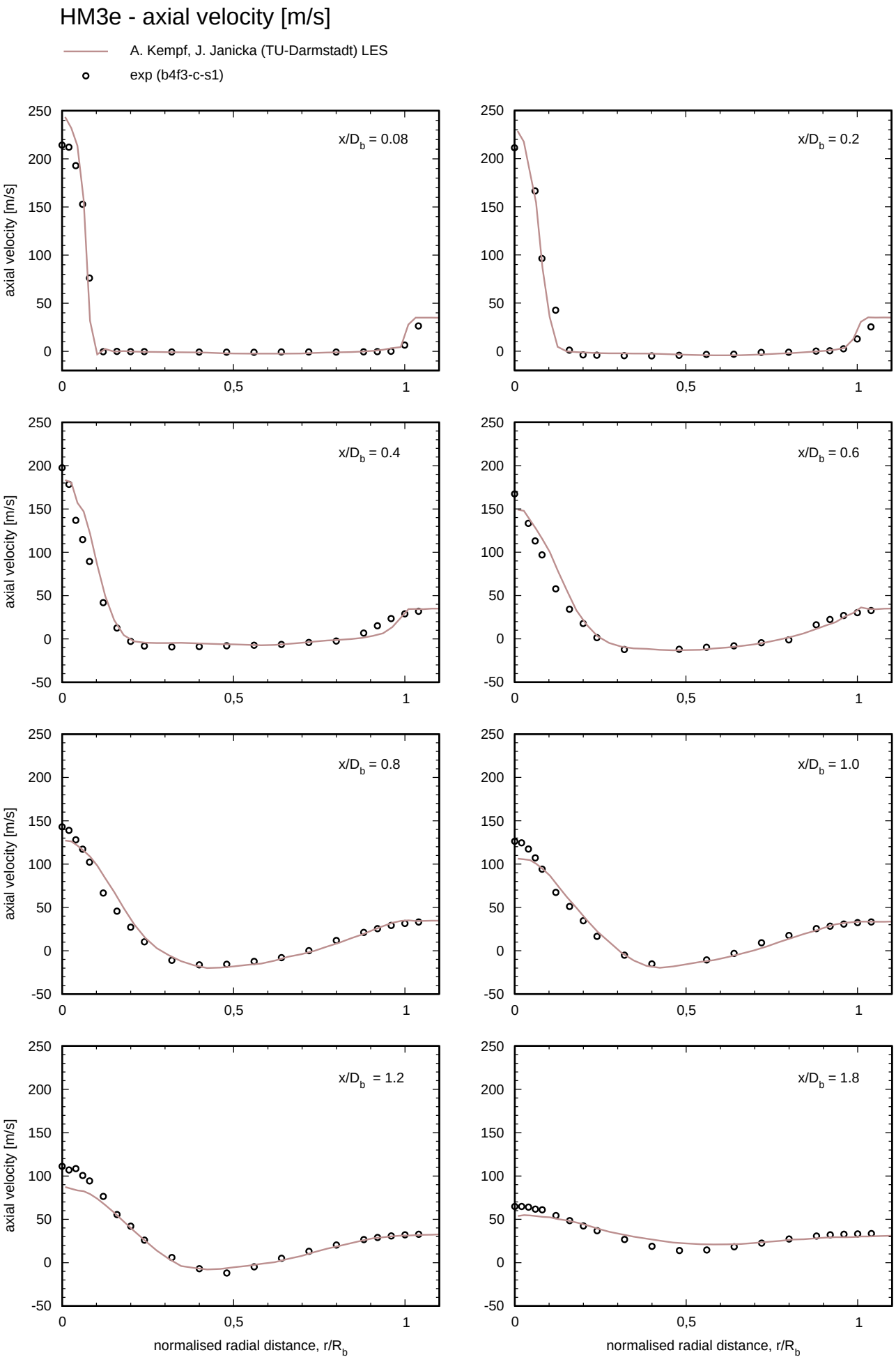
HM3e - axial velocity [m/s]
A. Kempf, J. Janicka (TU-Darmstadt) LES
exp (b4f3-c-s1)
x/D_b = 0.08
x/D_b = 0.2
x/D_b = 0.4
x/D_b = 0.6
x/D_b = 0.8
x/D_b = 1.0
x/D_b = 1.2
x/D_b = 1.8
axial velocity [m/s]
normalised radial distance, r/R_b

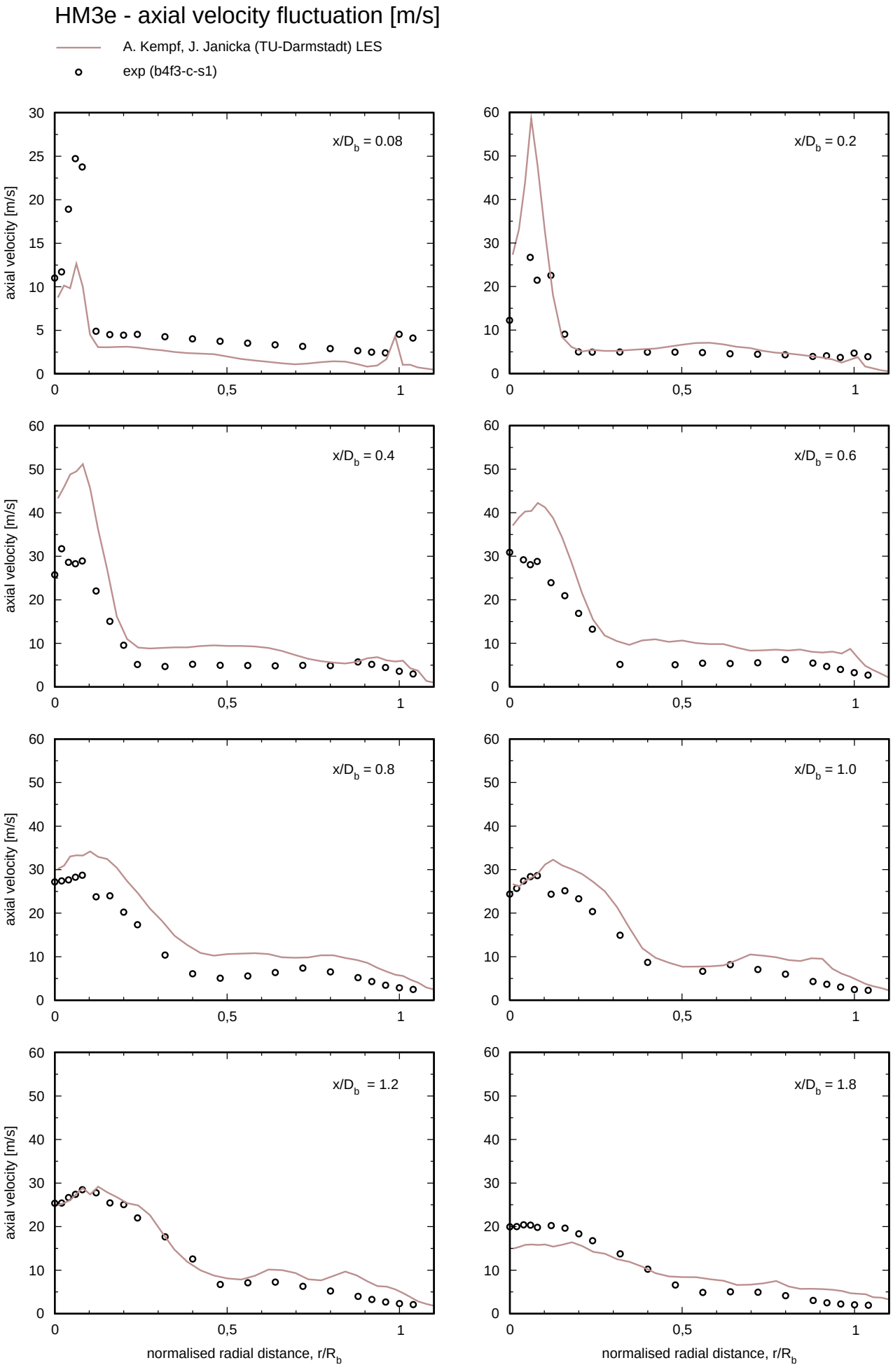
HM3e - axial velocity fluctuation [m/s]
A. Kempf, J. Janicka (TU-Darmstadt) LES
exp (b4f3-c-s1)
x/D_b = 0.08
x/D_b = 0.2
x/D_b = 0.4
x/D_b = 0.6
x/D_b = 0.8
x/D_b = 1.0
x/D_b = 1.2
x/D_b = 1.8
axial velocity [m/s]
normalised radial distance, r/R_b

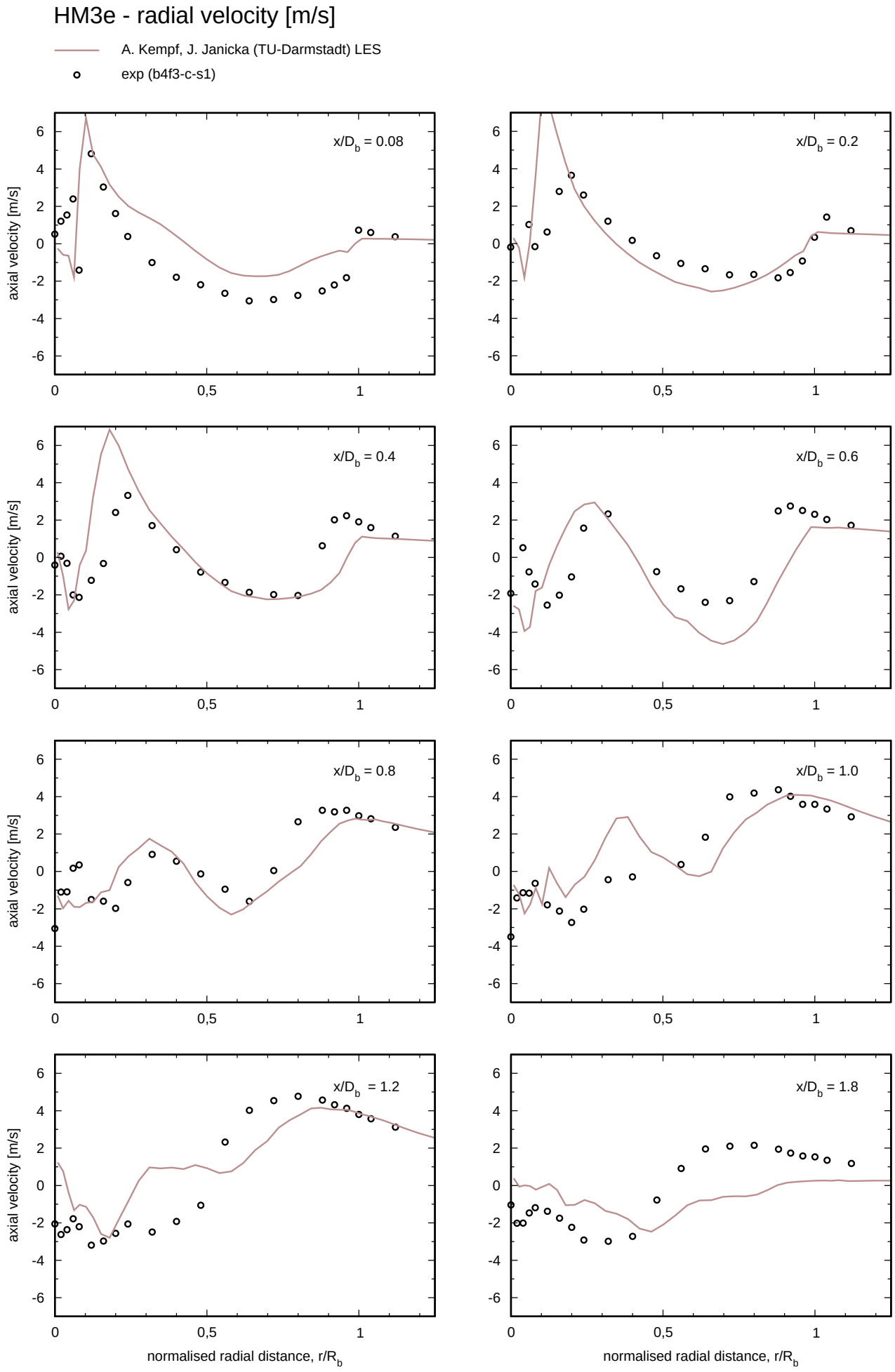
HM3e - radial velocity [m/s]
A. Kempf, J. Janicka (TU-Darmstadt) LES
exp (b4f3-c-s1)
x/D_b = 0.08
x/D_b = 0.2
x/D_b = 0.4
x/D_b = 0.6
x/D_b = 0.8
x/D_b = 1.0
x/D_b = 1.2
x/D_b = 1.8
axial velocity [m/s]
normalised radial distance, r/R_b

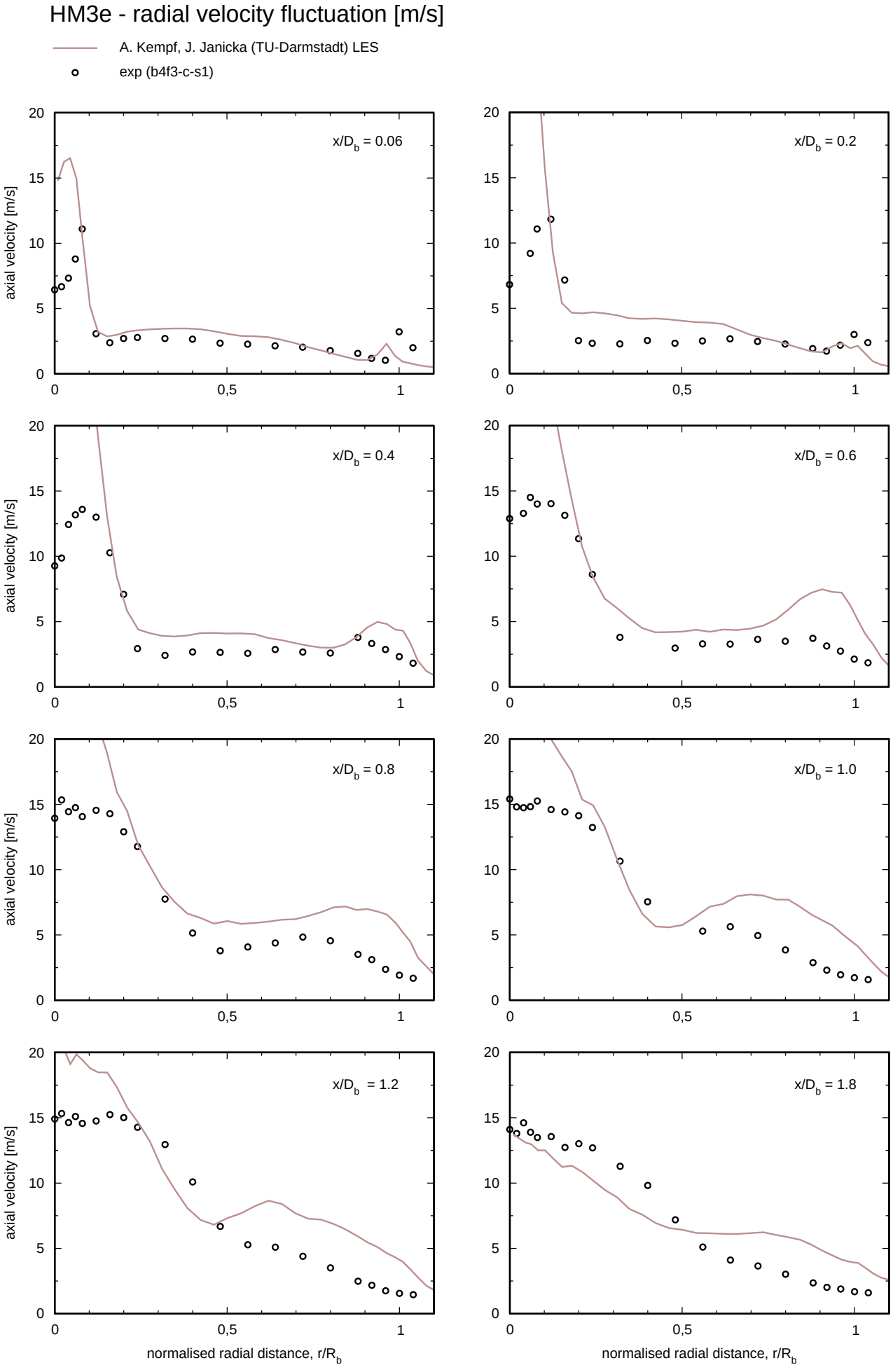
HM3e - radial velocity fluctuation [m/s]
A. Kempf, J. Janicka (TU-Darmstadt) LES
exp (b4f3-c-s1)
x/D_b = 0.06
x/D_b = 0.2
x/D_b = 0.4
x/D_b = 0.6
x/D_b = 0.8
x/D_b = 1.0
x/D_b = 1.2
x/D_b = 1.8
axial velocity [m/s]
normalised radial distance, r/R_b
0
5
10
15
20
0,5
1

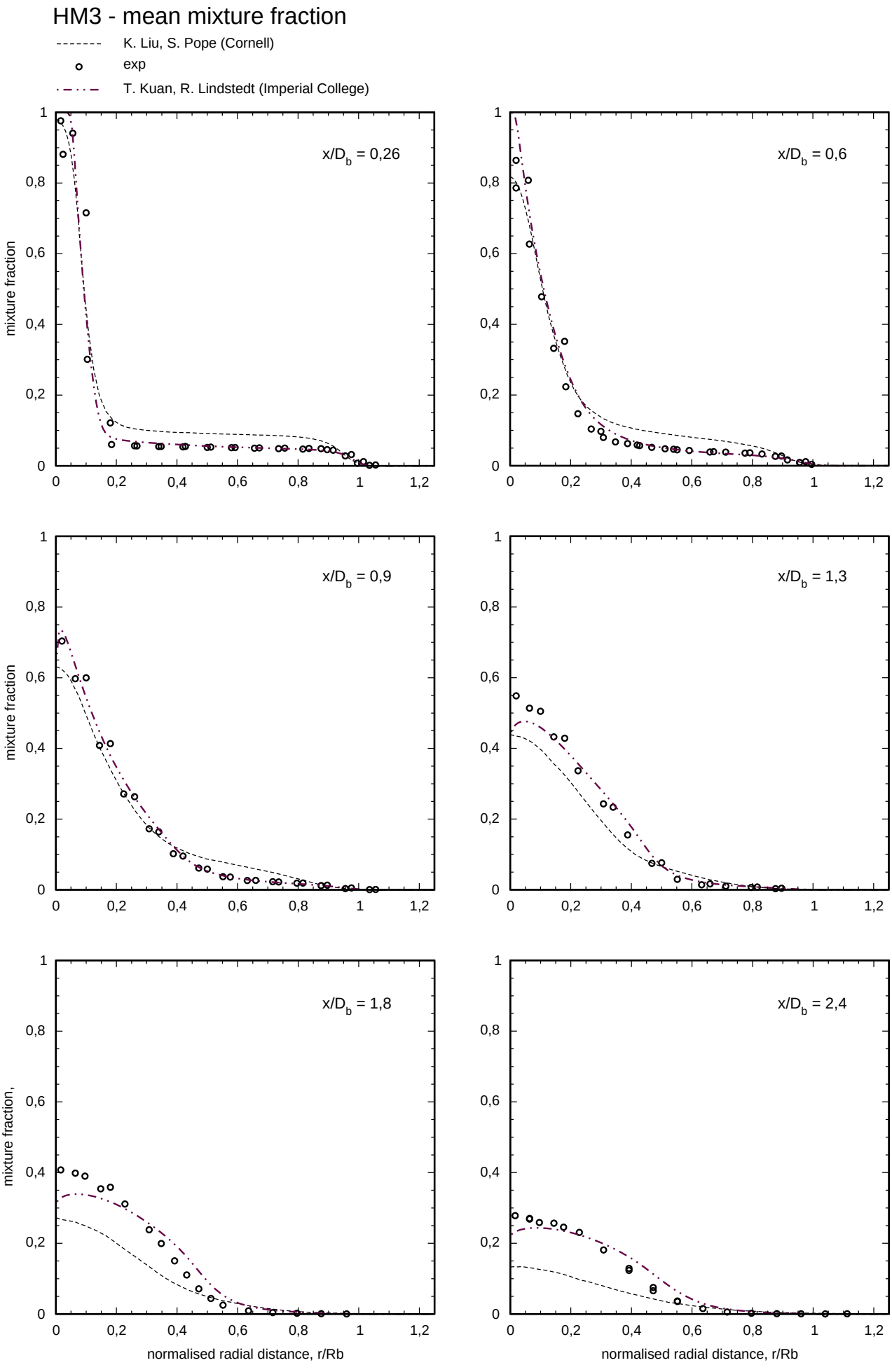
HM3 - mean mixture fraction
K. Liu, S. Pope (Cornell)
exp
T. Kuan, R. Lindstedt (Imperial College)
x/D_b = 0,26
x/D_b = 0,6
x/D_b = 0,9
x/D_b = 1,3
x/D_b = 1,8
x/D_b = 2,4
mixture fraction
mixture fraction,
normalised radial distance, r/Rb
0
0,2
0,4
0,6
0,8
1
1,2

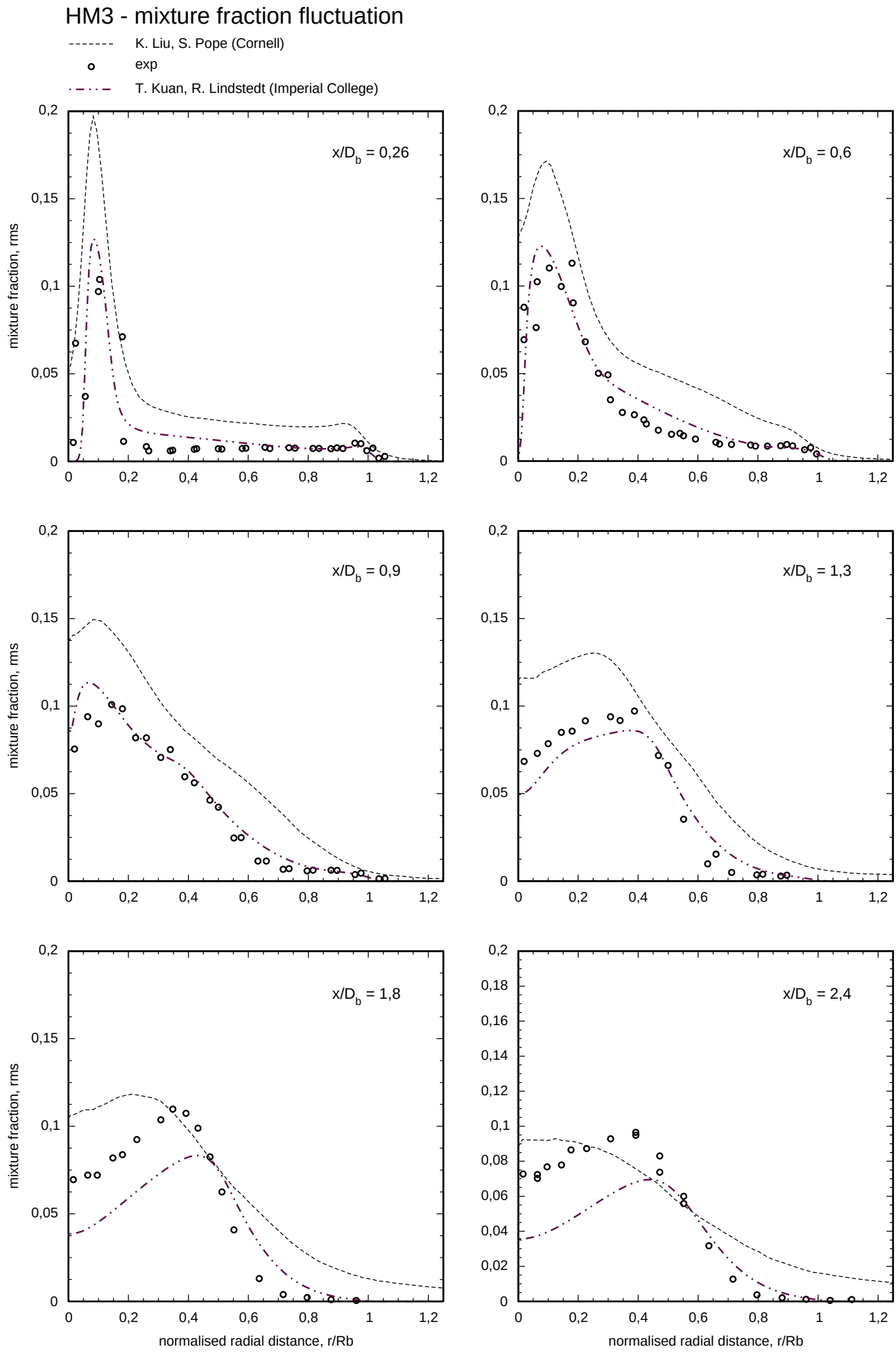
HM3 - mixture fraction fluctuation
K. Liu, S. Pope (Cornell)
exp
T. Kuan, R. Lindstedt (Imperial College)
x/D_b = 0,26
x/D_b = 0,6
x/D_b = 0,9
x/D_b = 1,3
x/D_b = 1,8
x/D_b = 2,4
mixture fraction, rms
normalised radial distance, r/Rb

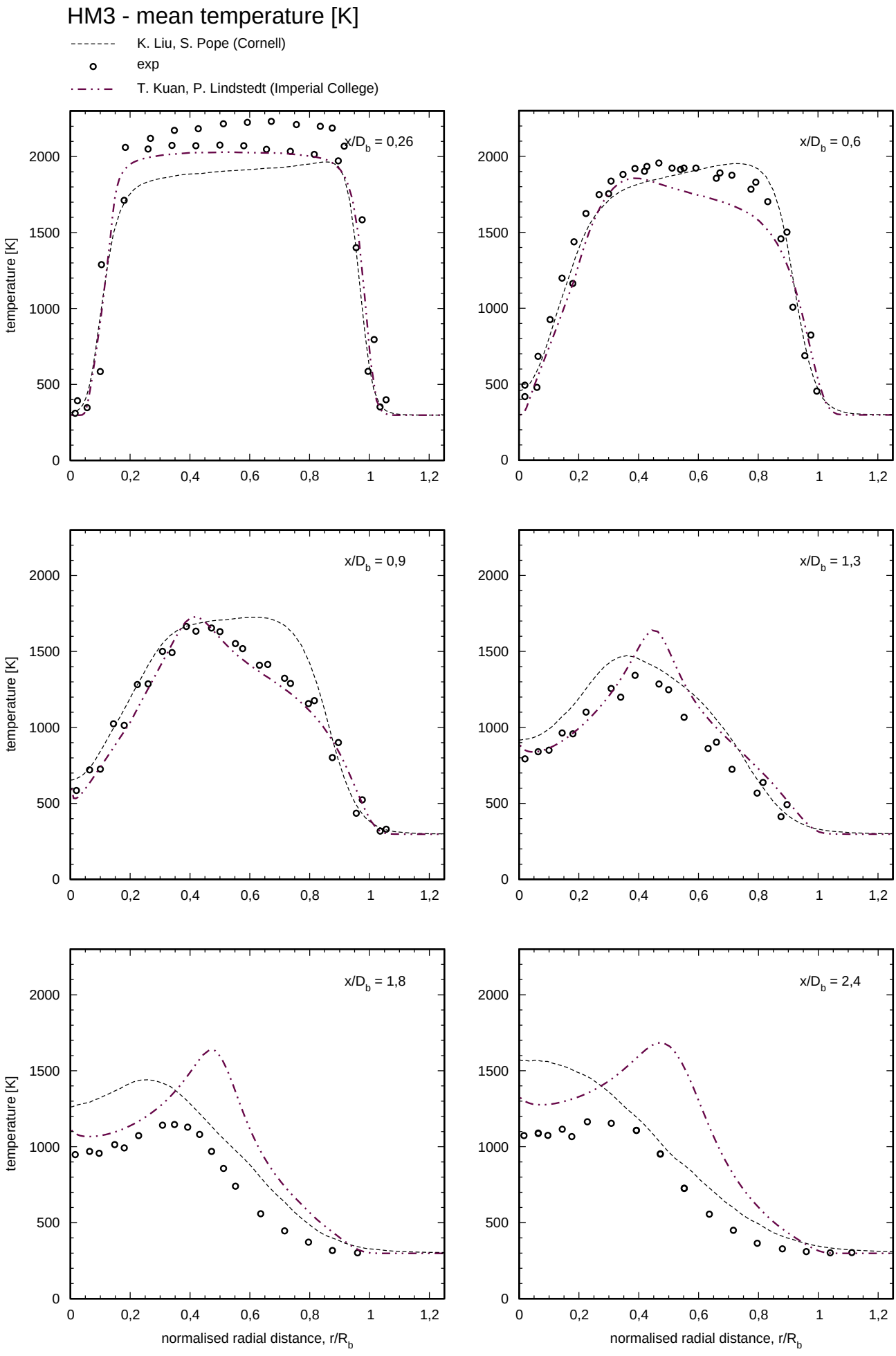
HM3 - mean temperature [K]
K. Liu, S. Pope (Cornell)
exp
T. Kuan, P. Lindstedt (Imperial College)
x/D_b = 0,26
x/D_b = 0,6
x/D_b = 0,9
x/D_b = 1,3
x/D_b = 1,8
x/D_b = 2,4
temperature [K]
normalised radial distance, r/R_b
0
500
1000
1500
2000
0,2
0,4
0,6
0,8
1
1,2

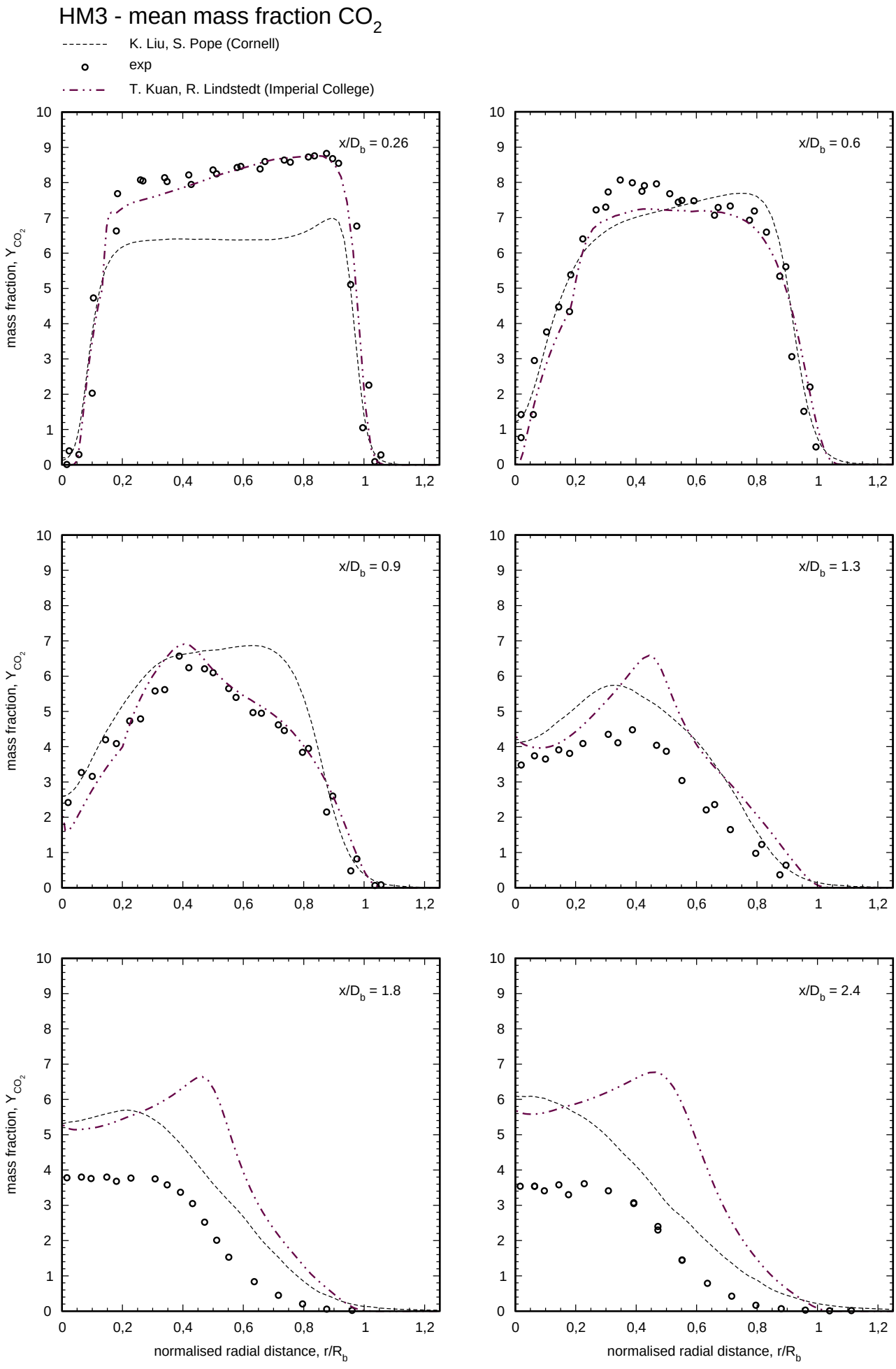
HM3 - mean mass fraction CO_2
K. Liu, S. Pope (Cornell)
exp
T. Kuan, R. Lindstedt (Imperial College)
x/D_b = 0.26
x/D_b = 0.6
x/D_b = 0.9
x/D_b = 1.3
x/D_b = 1.8
x/D_b = 2.4
mass fraction, Y_CO2
normalised radial distance, r/R_b

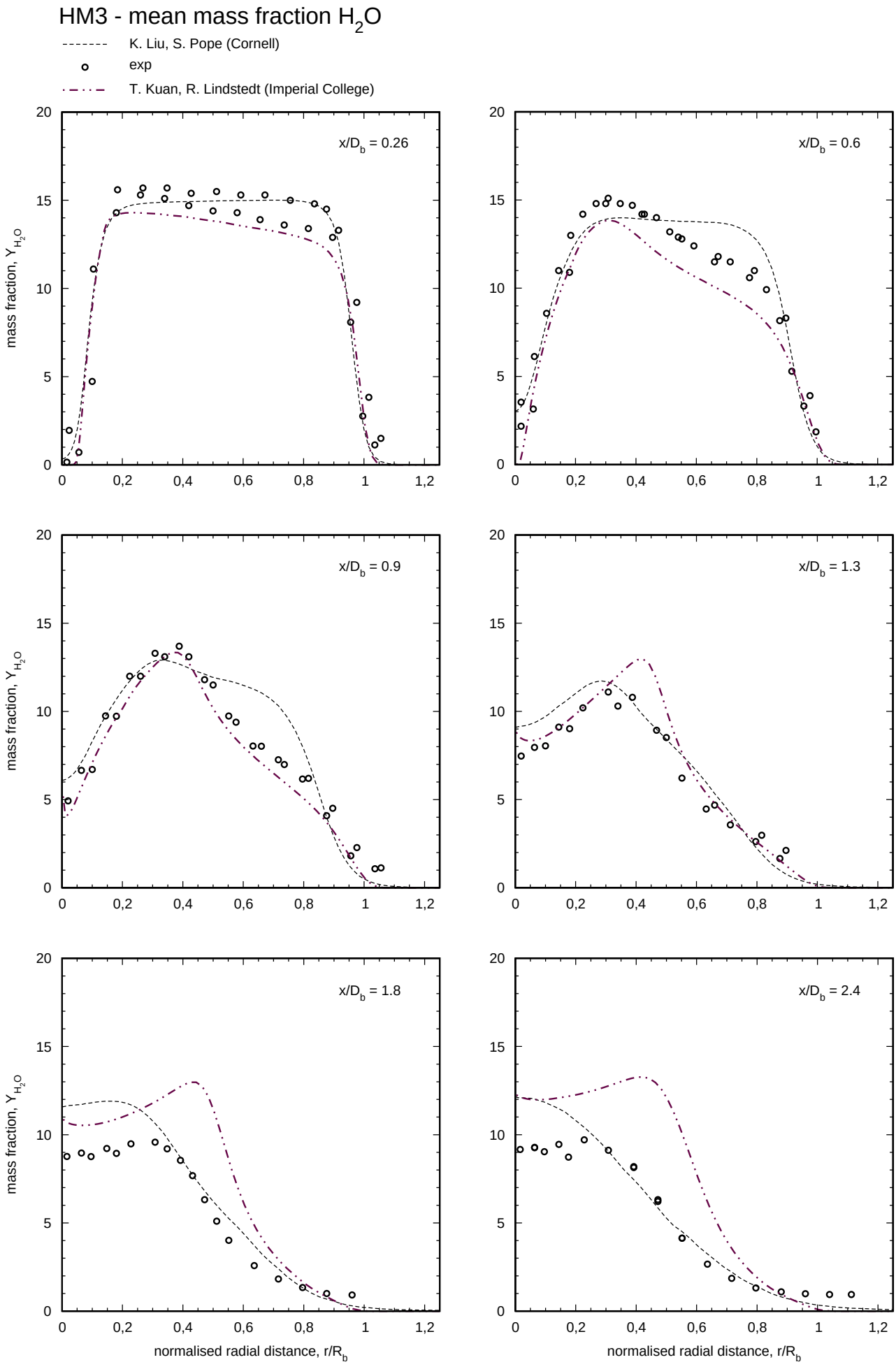
HM3 - mean mass fraction H_2O
K. Liu, S. Pope (Cornell)
exp
T. Kuan, R. Lindstedt (Imperial College)
x/D_b = 0.26
x/D_b = 0.6
x/D_b = 0.9
x/D_b = 1.3
x/D_b = 1.8
x/D_b = 2.4
mass fraction, Y_H2O
normalised radial distance, r/R_b

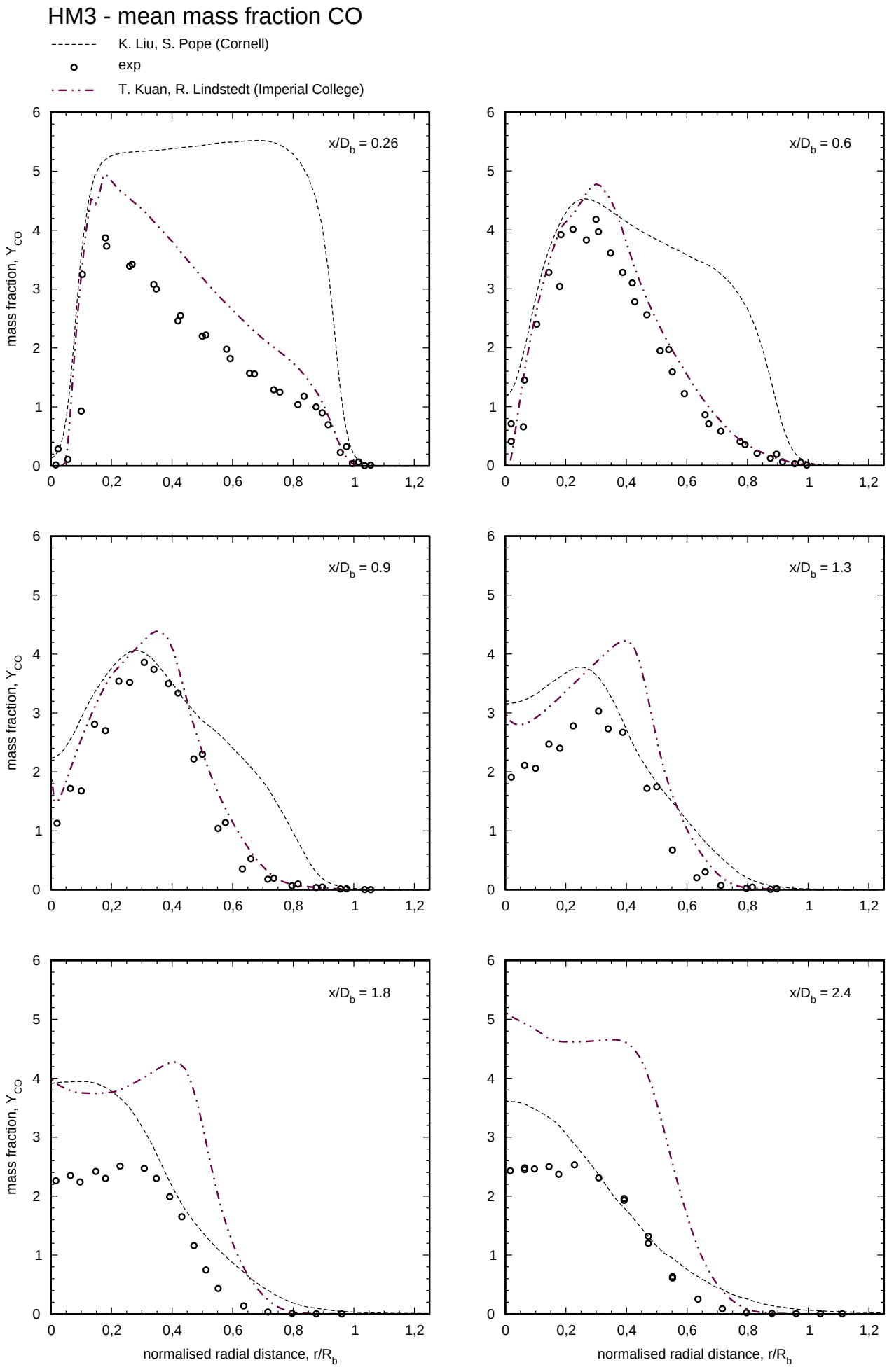
HM3 - mean mass fraction CO
K. Liu, S. Pope (Cornell)
exp
T. Kuan, R. Lindstedt (Imperial College)
x/D_b = 0.26
x/D_b = 0.6
x/D_b = 0.9
x/D_b = 1.3
x/D_b = 1.8
x/D_b = 2.4
mass fraction, Y_CO
normalised radial distance, r/R_b

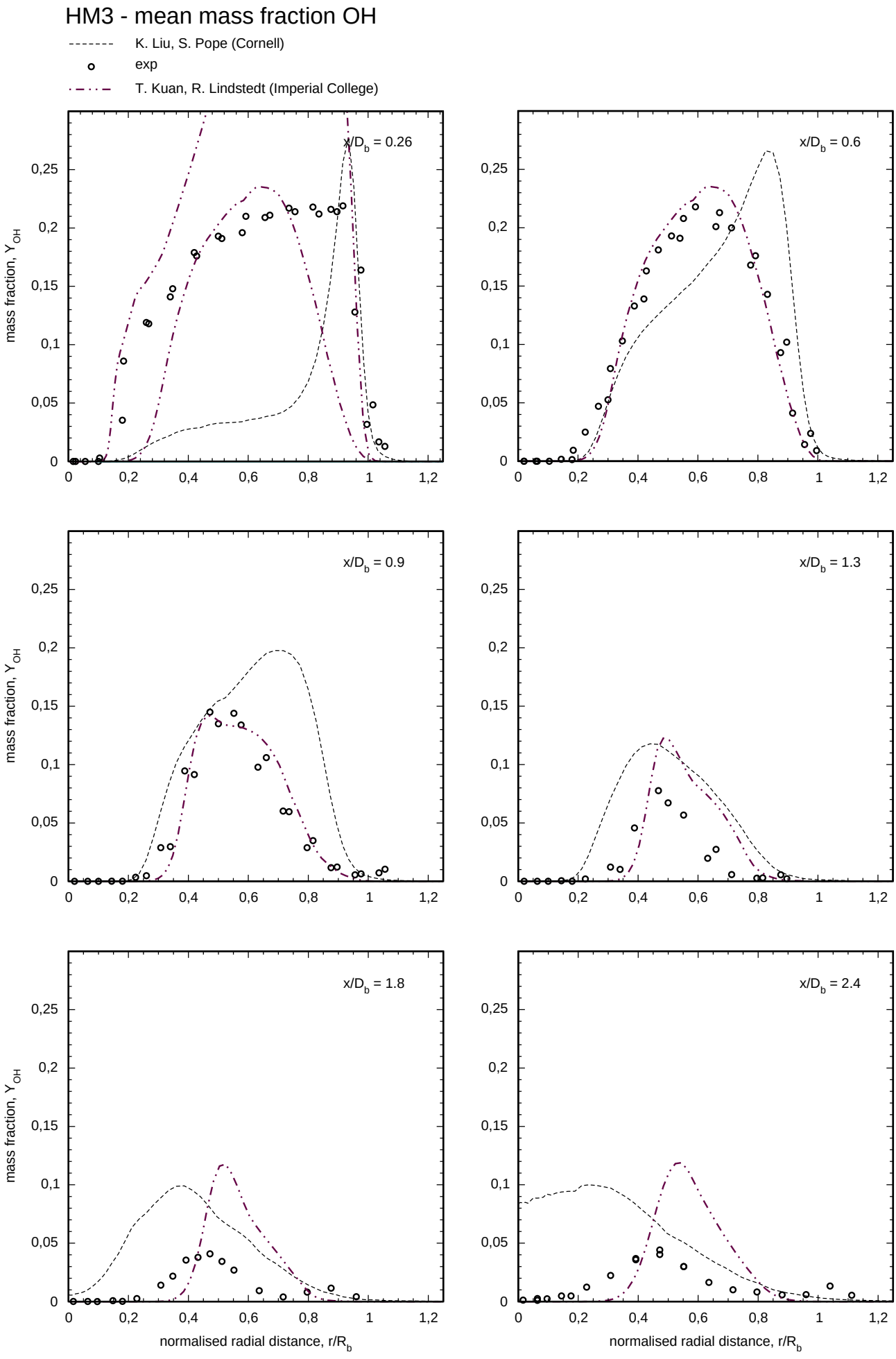
HM3 - mean mass fraction OH
K. Liu, S. Pope (Cornell)
exp
T. Kuan, R. Lindstedt (Imperial College)
x/D_b = 0.26
x/D_b = 0.6
x/D_b = 0.9
x/D_b = 1.3
x/D_b = 1.8
x/D_b = 2.4
mass fraction, Y_OH
normalised radial distance, r/R_b
0
0,05
0,1
0,15
0,2
0,25
0,2
0,4
0,6
0,8
1
1,2

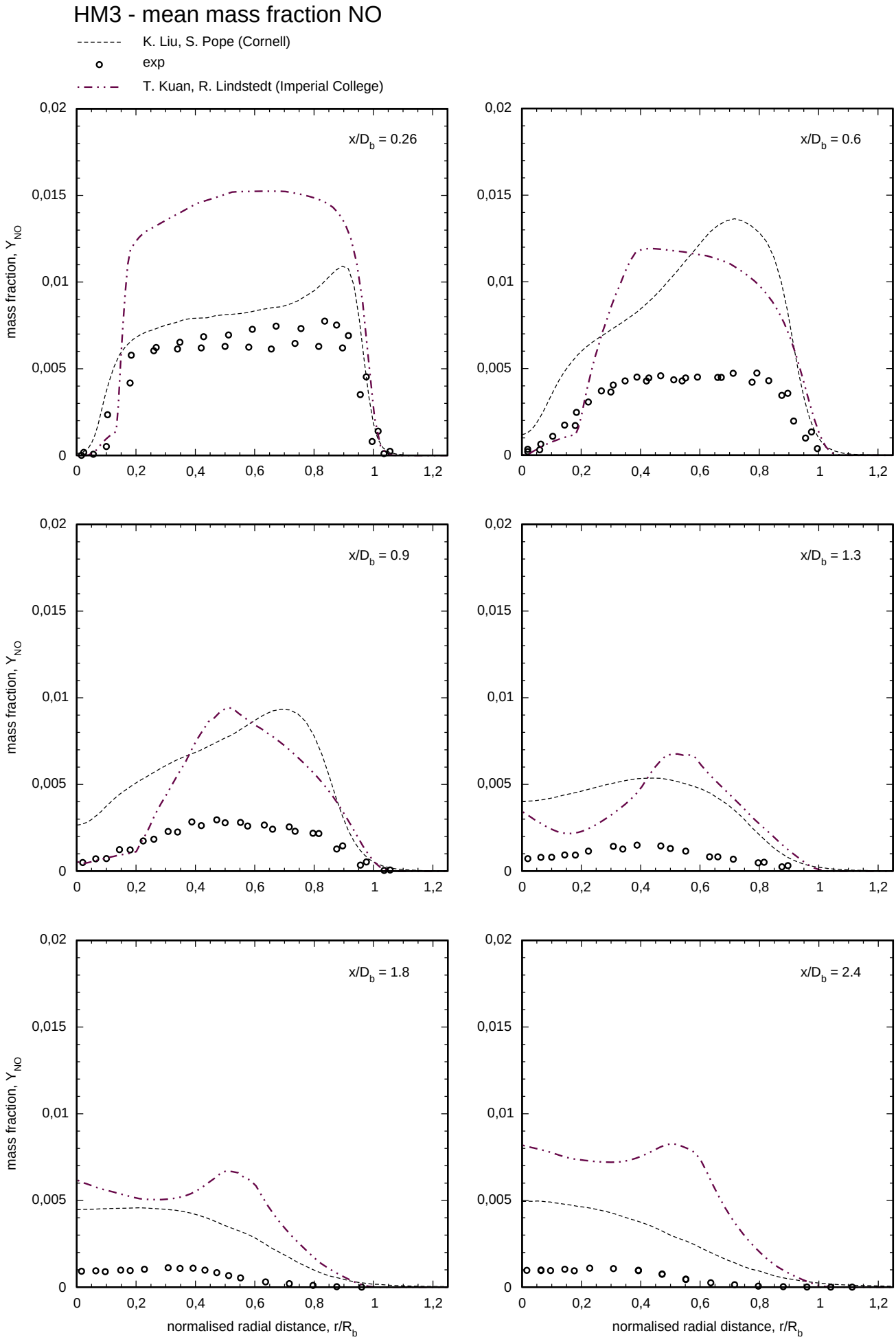
HM3 - mean mass fraction NO
K. Liu, S. Pope (Cornell)
exp
T. Kuan, R. Lindstedt (Imperial College)
x/D_b = 0.26
x/D_b = 0.6
x/D_b = 0.9
x/D_b = 1.3
x/D_b = 1.8
x/D_b = 2.4
mass fraction, Y_NO
normalised radial distance, r/R_b
0
0,005
0,01
0,015
0,02
0,2
0,4
0,6
0,8
1
1,2

Discussion on: Statistical Modeling of Extinction and Reignition

Stephen B. Pope

Cornell University

with contributions from:

Sandia, DLR, Ghent/Delft, Purdue, Washington, Imperial College, Cornell, Queensland

TNF7, Chicago

July 24, 2004

Discussion Outline

- Local extinction and re-ignition
- Conclusions from TNF6
- Review of mixing models in PDF methods
- Calculations comparing the performance of different mixing models
  - PaSR; DNS; Delft; Barlow & Frank D,E,F; Bluff body flames
- Dimensionality and conditioning
- New modeling directions
- Conclusions, Questions, Suggestions

Flame Luminosity Images – Lifted Methane Flame

Lifted CH_4 jet flame, Re=7100

Images of flame luminosity show multiple holes (local extinction) in the flame sheet.

3D impression is of eddies pushing outward and punching through the flame.

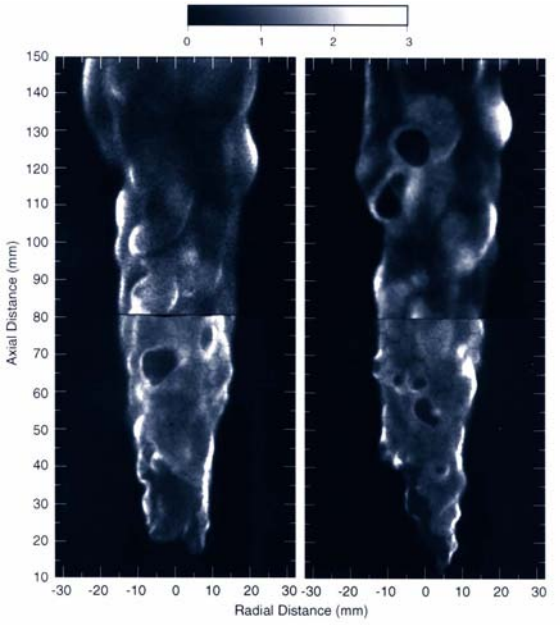

Schefer C&F (1997)

Simultaneous PIV and Multi-Frame OH PLIF Imaging

DLR $CH_4/H_2/N_2$ flame. Higher jet velocity leads to localized extinction and re-ignition.

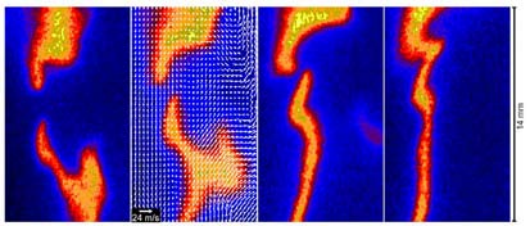

Flame reconnection in low-strain region

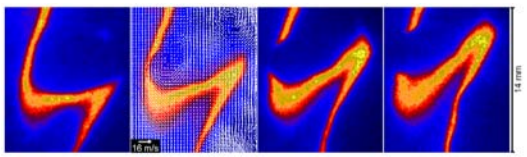

Local extinction – vortex interacts with flame

Hult, Josefsson, Alden, & Kaminski (2000)

Flame F: Scatter Plots of CO vs. ξ at x/D = 15, Expt. and PDF Calc.

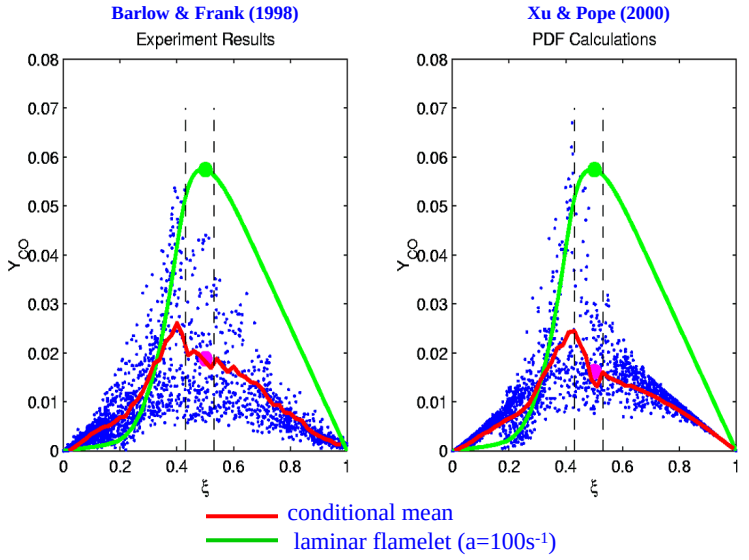

Mixing Models in PDF Methods

- Following a fluid particle, species mass fractions change due to:
  - Reaction
  - Mixing (molecular diffusion)
- Relevant mixing models
  - IEM/LMSE (Villermaux & Devillon 1972, Dopazo & O'Brien 1974)
  - Modified Curl (MC, Janicka et al. 1977)
  - Euclidean minimum spanning tree (EMST, Subramaniam & Pope 1998)
- Does it make a difference?

Qualitatively Different Behavior of Mixing Models: PaSR Test

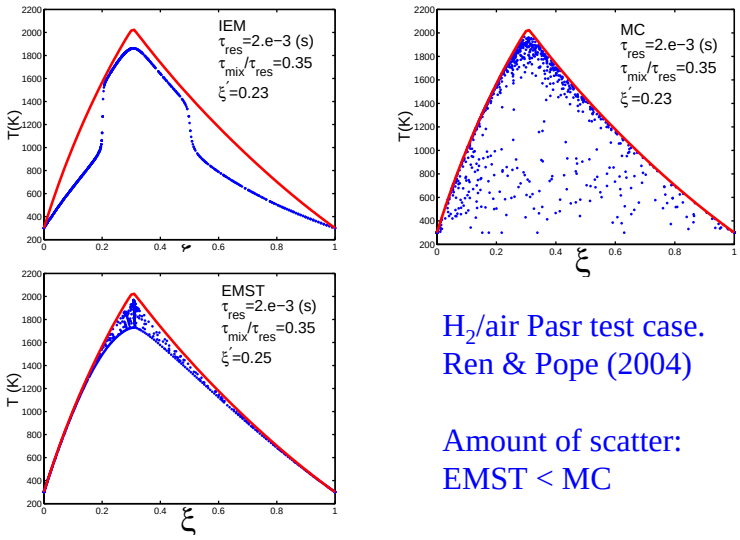

H_2/air Pasr test case.
Ren & Pope (2004)

Amount of scatter:
EMST < MC

Mixing Models: PaSR Test

Ren & Pope (2004): Conditional mean temperature against residence time, showing blow-off

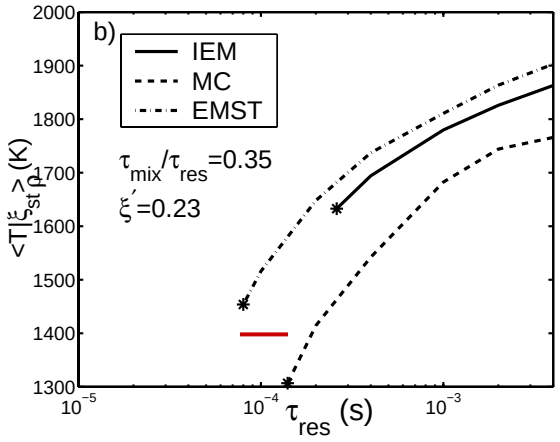

Resilience to extinction:
EMST > MC > IEM

Residence time in flame F is half that in flame D

Preliminary Conclusions on Mixing Model Performance

- Resilience to extinction:
  - EMST > MC > IEM
- Amount of scatter
  - EMST < data < MC
- Effect of increasing C_ϕ is to reduce scatter and to inhibit extinction

Mixing Model Performance: DNS Study

(Mitarai, Riley, Kosaly, Univ. of Washington
Accepted for publication by Physics of Fluids)

- Motivation:

  Good predictions are related to *ad hoc* choice

  of mixing frequency constant (Pope, TNF6)
- Objective:

  To test mixing models (IEM, MC, EMST) using DNS

  where exact values of mixing frequency can be obtained
  - Tests are designed for RANS & LES

Test Configuration

(Mitarai, Riley, Kosaly, Univ. of Washington
Accepted for publication by Physics of Fluids)

- Non-filtered test (RANS):
  particle mixing interactions
  take place in entire DNS box
- Filtered test (LES):
  particles mixing interactions
  locally within subvolumes

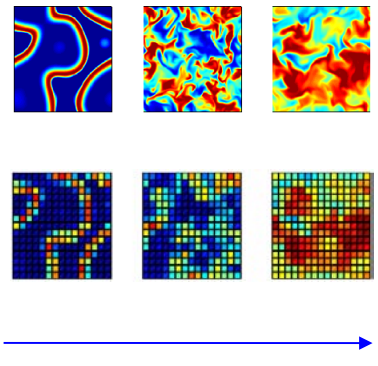

Time

Results: Non-filtered Test (RANS)

(Mitarai, Riley, Kosaly, Univ. of Washington
Accepted for publication by Physics of Fluids)

- EMST reasonably predicts mean quantities
  while IEM & MC underestimate
- All models fail to predict scatter plot

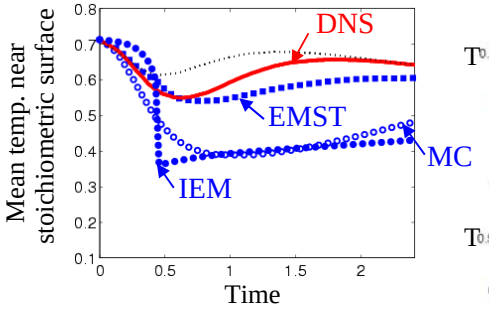

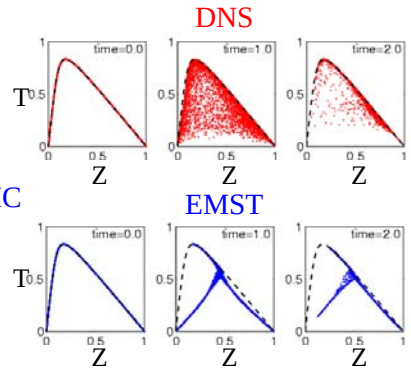

FLUENT's PDF Calculations of Turbulent Piloted Methane/Air Jet Flames D, E and F

- Turbulence Model: Standard k-ε, RSM
- Chemistry: 9-species, 5-step mechanism
- Mixing Models: IEM, MC and EMST
  - EMST predicts the best and MC shows the largest discrepancy.
  - Good comparison with experiments for flames D and E, but large overpredictions for flame F.
  - EMST predicts largest extinction; Very little extinction predicted for flame F.

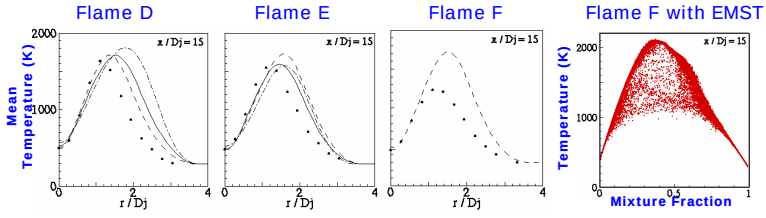

Symbols: experiment; lines: Computations with IEM (solid), EMST (dashed) and MC (dash-dotted).

Scatter plots of flame E:

CO mass fraction against mixture fraction

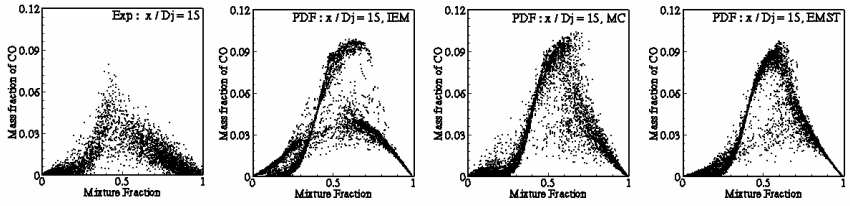

- Computations of three mixing models compared with experimental data.
- Mesh: 14000, 2D axisymmetric
- Turbulence Model: k-e
- 20 particles/cell for IEM and EMST calculations and 40 particles/cell for MC calculations
- x/Dj = 15 (shown) : location of highest extinction
- Extinction predicted by computations lower compared to experiments.

Experimental data: Barlow, R.S., and Frank, J.H., 1988.

Results: Filtered Test (LES)

(Mitarai, Riley, Kosaly, Univ. of Washington
Accepted for publication by Physics of Fluids)

- IEM & MC describe extinction/reignition to some extent, but ignite slowly
- EMST reasonably predicts extinction/reignition

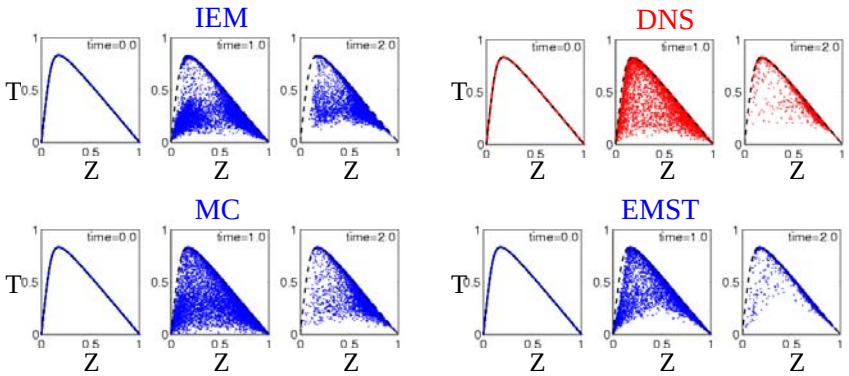

IEM, modified Curl's (CD) and EMST mixing models in transported Scalar PDF simulations for Delft Flame III

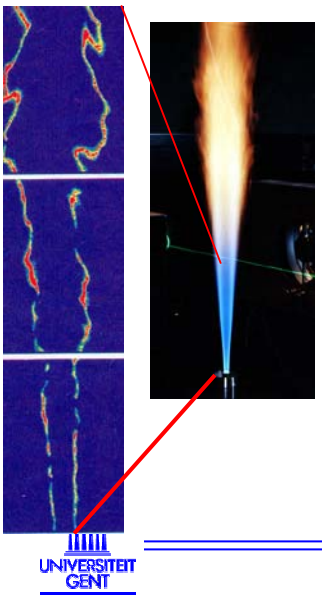

- **Bart Merci[1], Bertrand Naud[2] and Dirk Roekaerts[3,4]**

- [1] Ghent University, Dept. of Flow, Heat and Combustion Mechanics
- [2]LITEC – CSIC, Zaragoza
- [3]Delft University of Technology, Faculty of Applied Sciences
- [4]Shell Global Solutions International BV, Amsterdam

UNIVERSITEIT GENT

TNF7, July 2004

Joint PDF of temperature and mixture fraction

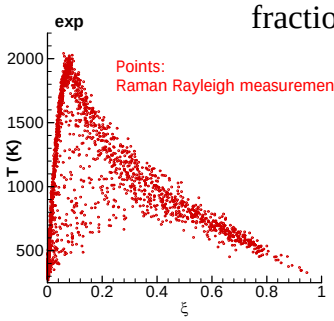

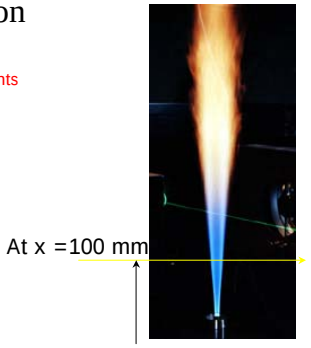

Results P.A. Nooren

Global flame shape (experimental pilot flame thermal power)

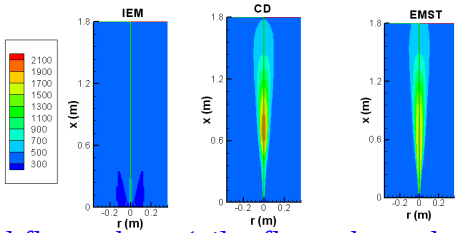

IEM: no flame
CD: flame lift-off
EMST: attached
Exp: attached

Global flame shape (pilot flame thermal power increased by 50%)

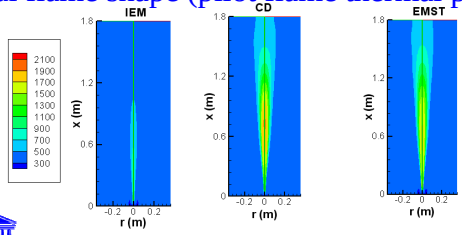

IEM: no flame
CD: attached
EMST: attached

Scatter plots (experimental pilot flame thermal power)

Exp EMST CD

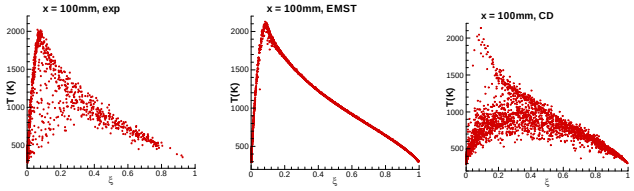

Scatter plots (increased pilot flame thermal power)

EMST CD

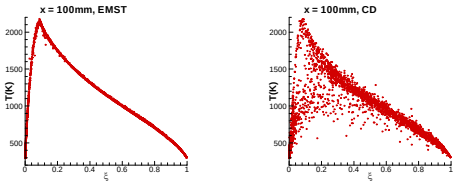

UNIVERSITEIT GENT

Scatter plots (experimental pilot flame thermal power)

Exp EMST CD

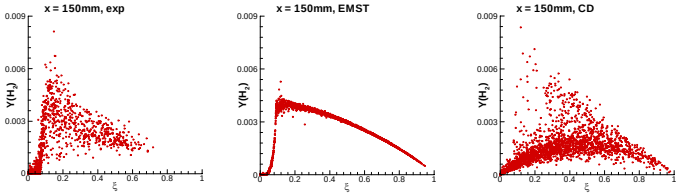

Scatter plots (increased pilot flame thermal power)

EMST CD

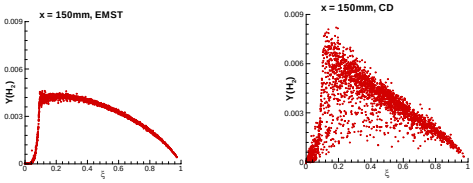

UNIVERSITEIT GENT

Conclusions
• Only EMST yields a qualitatively correct flame shape with the experimental pilot flame thermal power.
• CD yields attached flame when pilot flame power is increased.
• There is too much (unphysical) scatter with CD.
• There is too little scatter with EMST (due to chemistry model?).

PDF Calculations of the Bluff Body Flame HM1

- Imperial College
  - Kuan & Lindstedt (2004)
  - RSM/Composition PDF
  - 20 species ARM
  - Modified Curl, C_ϕ=2.3
- Cornell
  - Liu, Pope & Caughey (2004)
  - Velocity-Composition PDF
  - 19 species ARM/ISAT
  - EMST, C_ϕ=1.5

Scatter Plots of T in HM1 at x/D=0.26

Kuan & Lindstedt

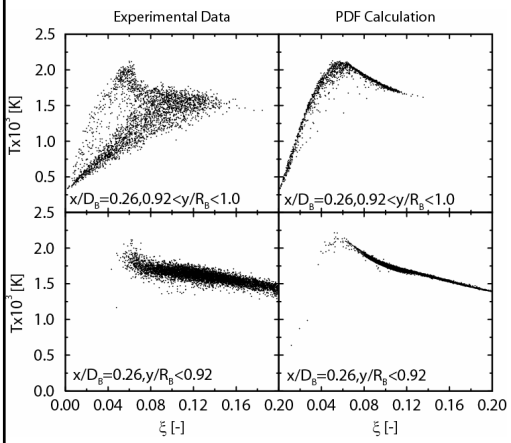

Liu, Pope & Caughey

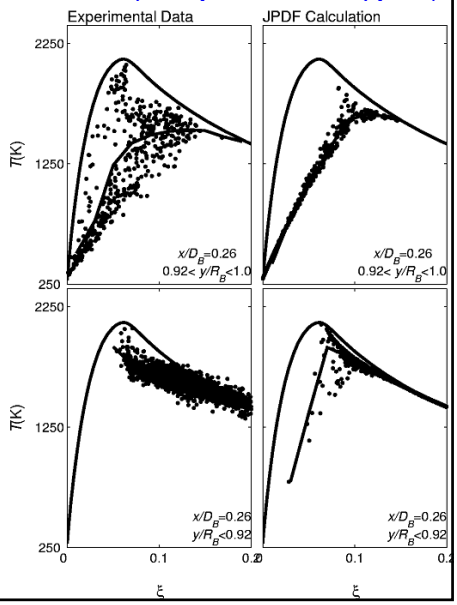

Scatter Plots of T in HM1

Kuan & Lindstedt

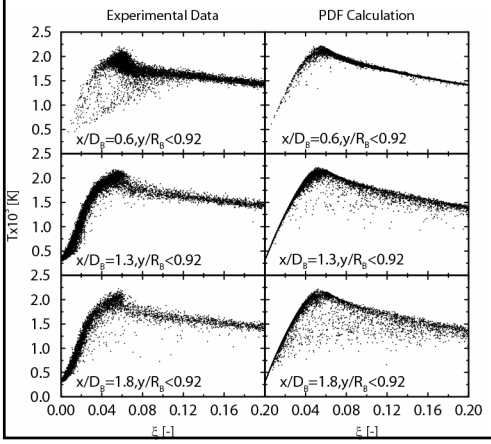

Liu, Pope & Caughey

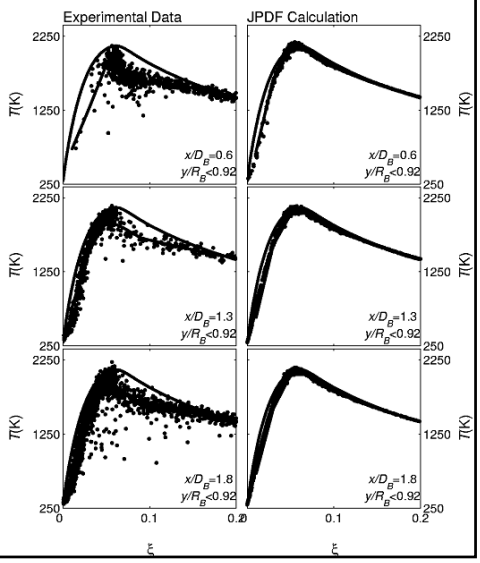

Dimensionality and Conditioning

- In the simplest cases (far from local extinction), the instantaneous composition is determined by one (ξ) or two (ξ,χ) variables (e.g., CMC, SFM)
  - 1D or 2D manifold in composition space
- With local extinction, what is the dimensionality of the accessed region in composition space?
  - 2D, 3D, 4D? Appropriate conditioning variables?
  - PDF methods n_s-D
  - CMC – in between
- (See, Pope (2004), Flow, Turbulence & Combustion)

DNS of Spatially-Evolving CO/H2/N2-Air Jets with Extinction

James C. Sutherland, Jacqueline H. Chen & Philip J. Smith

- Composition
  - Fuel: 45% CO, 5% H2, 50% N2
  - Oxidizer: Air at 300 K
  - fst = 0.4735
- Full chemical kinetics
  - 12 species, 33 reactions
- Mixture-averaged transport
- High order numerics
  - 8th order spatial accuracy
  - 4th order temporal accuracy
    - fully coupled integration scheme
- Spatially-evolving configuration yields statistically stationary results

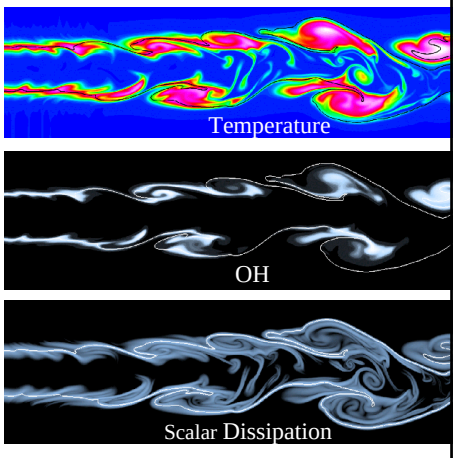

Selection of Progress Variables is Crucial!

Temperature conditioned on (f_{st} , χ)

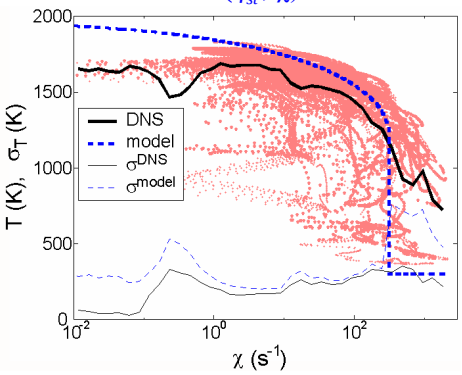

Temperature conditioned on (f_{st} , Y_{CO2})

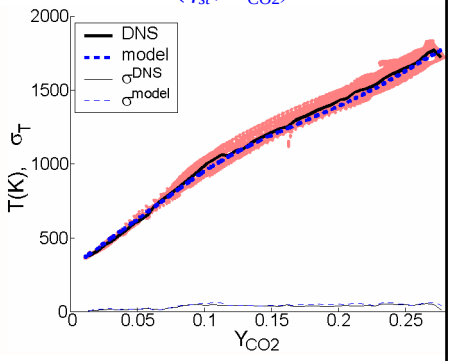

Blue line: Flamelet solution (including unsteady extinction)
Red points: DNS data
Black line: conditional mean DNS data

Parameterization of the Progress Variable Source Term

The source term for the progress variable must also be accurately parameterized

Blue line: Flamelet solution (including unsteady extinction)
Red points: DNS data
Black line: conditional mean DNS data

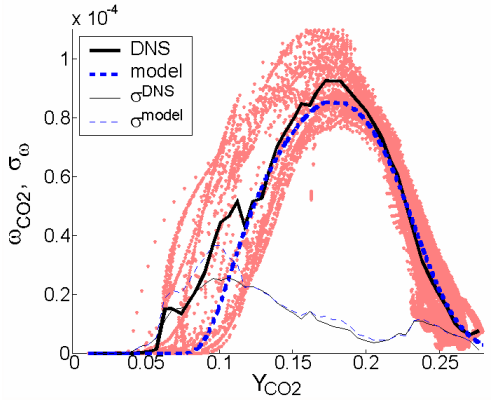

Conclusions

- Progress-variable approaches provide natural ways to efficiently parameterize extinction.
- Choice of progress variables is important
- Results from CO/H_2 jets with extinction show:
  - All scalars can be parameterized well by *TWO PARAMETERS*: mixture fraction and CO_2 mass fraction
    - This includes reaction rate of CO2…
- Parameterization for hydrocarbons may require more complicated progress variables such as $CO+CO_2+H_2O+C_2H_2$
  - CH_4/H_2 DNS corroborates this statement.
  - May also require more than 2 parameters…

New Modeling Directions

- Modified flamelet model
- Multiple Mapping Conditioning

New Lagrangian Flamelet model

(Mitarai, Kosaly, Riley, Univ. of Washington
Combust. Flame **137** (2004) 306-319)

Fluid particle tracking in DNS.

$\chi_{st,i}(t)$ can be determined from the DNS

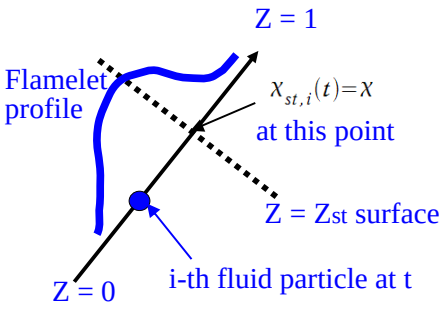

Equation of the i-th flamelet:

$$\frac{\partial T_i}{\partial t} = \frac{\chi_{st,i}(t)}{2} F(Z,t) \frac{\partial^2 T}{\partial Z^2} + S(Z,T_i)$$

Boundary condition:

$$T(Z,t) = 0 \quad Z \to 0,1$$

The flamelet model accounts for extinction

but not for reignition

Modification of Flamelet Model

(Mitarai, Kosaly, Riley, Univ. of Washington
Combust. Flame **137** (2004) 306-319)

Extinguished flamelet

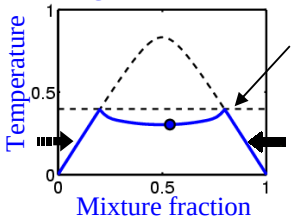

Average temperature at time t

Heat

Burning flamelet

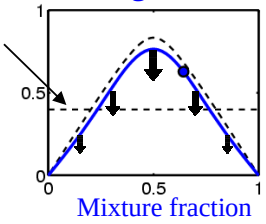

Equation used:

Same as in original model

Boundary condition used:

$$T_i(Z,t) = T_{eq}(Z) \quad for$$
$$Z \; values \; T_{eq}(Z) \leqslant \langle T \rangle$$

Equation used:

$$\frac{\partial T_i}{\partial t} = \frac{\chi_{st,i}(t)}{2} F(Z,t) \frac{\partial^2 T}{\partial Z^2} + S - c(t) T_i$$

Boundary condition used:

Same as in original model

Results and Discussion

(Mitarai, Kosaly, Riley, Univ. of Washington
Combust. Flame **137** (2004) 306-319)

Comparison to the DNS data

Mean temperature

Mean temperature near stoichiometric surface

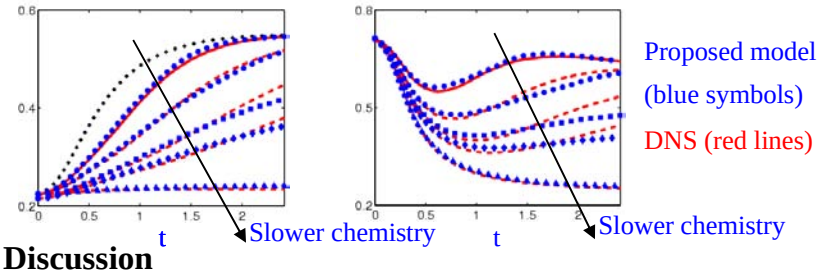

Proposed model (blue symbols)

DNS (red lines)

Discussion

- Comparison to DNS data is encouraging
- In future application to combustion shear flows $\chi_{st,i}(t)$ can be determined from known stochastic differential eq.

Multiple Mapping Conditioning (MMC) (Klimenko & Pope, 2003)

- Generalization of Mapping Closure: inhomogeneous and independent scalars
- Divide fluctuations in accessed composition space (Pope, 2003) of scalars into major and minor by mapping into reference space of smaller dimension
- Pdf consistent
- Has deterministic and stochastic forms

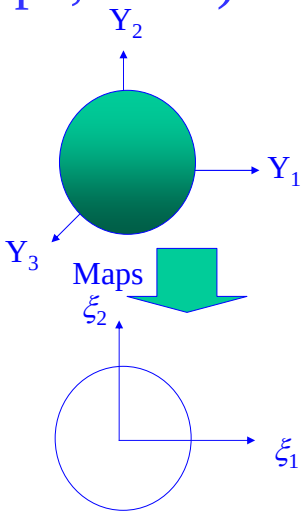

Klimenko & Wandel

Comparison of Models

	IEM	MC	EMST	MMC
Conservation of means	Yes	Yes	Yes	Yes
Decay of variances	Yes	Yes	Yes	Yes
Boundedness	Yes	Yes	Yes	Yes
Linearity and indep.	Yes	Yes	No	Yes
Relaxation to Gaussian	No	No	No	Yes
Numerical convergence	Yes	Yes/No	No	Yes
Localness	No	No	Yes	Yes
Fast Chemistry Limit	No	No	Yes	Yes

Compiled by S.B. Pope

Model Hierarchy

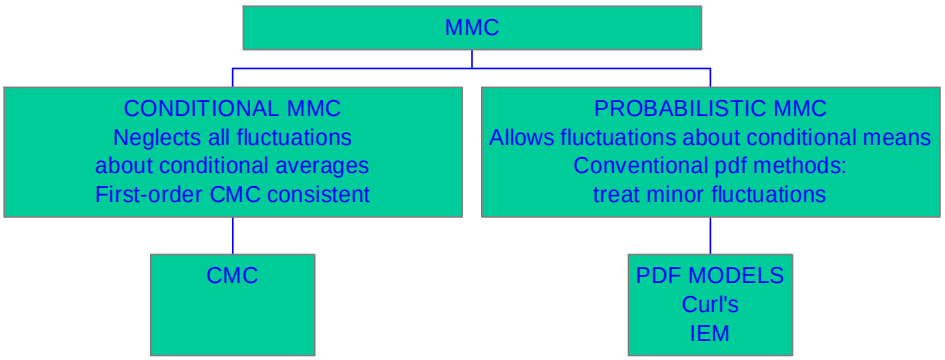

Klimenko & Wandel

Probabilistic MMC

Klimenko & Wandel

Minor dissipation via Curl's, IEM

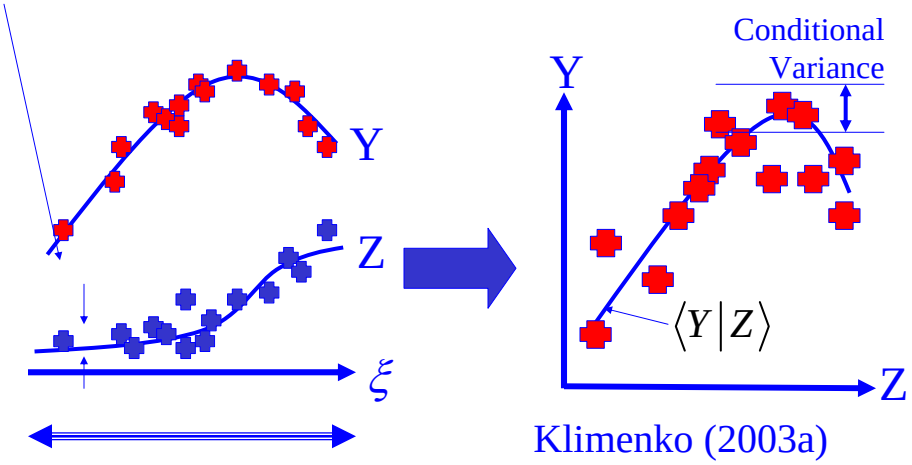

Generalized Mapping Closure

Klimenko (2003a)

Minor dissipation timescale selected so that conditional variance is matched

Multiple Reference Variables

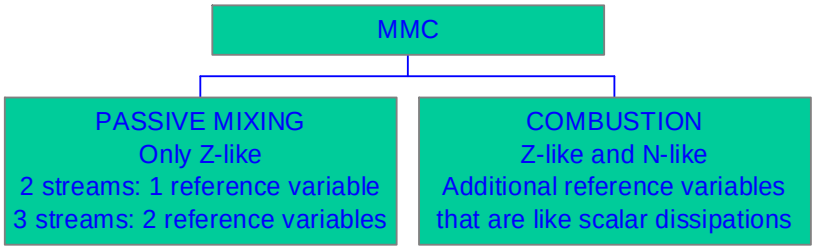

- First ξ_0 is Z-like; $\xi_1,\ldots,\xi_n$ are dissipation-like

Klimenko & Wandel

Conclusions (1/2)

- Improving understanding of mixing model performance
  - Resilience to extinction: EMST > MC > IEM, increases with increasing C_ϕ
  - Amount of scatter: EMST < data < MC, decreases with increasing C_ϕ
  - Better performance in LES
- Little progress in understanding performance of different mechanisms
  - Availability of mechanisms
  - Controlled studies

Conclusions (2/2)

- Ignition in H_2 flame in vitiated co-flow:
  - Dominated by chemistry
  - MC and EMST yield good agreement
- Bluff body flames
  - Non-reactive mixing captured by EMST in HM1
  - Joint PDF calculations fail to predict local extinction in HM3
- Dimensionality and conditioning
  - Explored by theory and DNS

Update on radiation

By D. Roekaerts, Delft University of Technology, The Netherlands

Introduction and summary of slides

TNF target flames typically have a low radiative heat loss. Consequently, the predictions of computational models for flow field, temperature and chemical composition do not depend strongly on the radiation model and a simple model, the optically thin model can be used. To predict features strongly depending on accuracy of temperature, notably NO formation, accurately more sophisticated radiation modeling is useful, at least when flow and combustion models already give good agreement for main species and mean temperature. The answer corresponding to a detailed radiation model should be somewhere between the limits of the adiabatic calculation and the optically thin model, provided turbulence radiation interaction is properly taken into account.

In the contribution at the workshop an outline is given of what is involved in a detailed radiation model. Reference is made to recent works concerning spectral radiative effects, turbulence/radiation interaction and measurements and calculations of spectral radiation intensities.

It is shown that using the Planck mean absorption coefficient one finds little difference between the optically thin approximation and a full solution of the radiative transfer equation using discrete ordinates method (DOM). This is explained by the fact that the emission term is at least one order of magnitude larger than the absorption term in the RTE when the Planck mean absorption coefficient is used. However, the Planck mean absorption coefficient yields a poor estimation of the absorption term. Using a spectral model (SLW) in combination with the DOM the absorption is found to be higher and the radiative heat loss is in better agreement with the experimental data at least for Flame D. To address other flames of different power or size the analysis of Li and Modest on scale up is of interest. (See references on slides)

Conclusion of the presentation

Because different authors in the literature used a different mix of models and put emphasis on different aspects, the answer on the question which model is recommended for the TNF flames as next step beyond the optically thin model, is not yet fully clear. But the following statements may set the some restrictions on how to proceed:

- It is important to take into account turbulence-radiation interaction, most importantly the effect of temperature fluctuations on the mean emission.
- The effect of correlation between fluctuations in temperature and absorption coefficient is relatively small, but not negligible.
- Spectral effects seem important in the evaluation of absorption term.
- Explicit confirmation that the ‘thin eddy approximation’ is valid is needed. This could be tested in line calculations.

In the discussion suggestions were made to construct a simple model extending the optically thin model with a optically thick treatment of the 4.3 μm band of CO2 (Bilger) and to treat the absorption term using the modified Planck mean absorption coefficient, depending on both local temperature and temperature of the surroundings (Gore).

Update on radiation

D. Roekaerts

TNF website:

"Radiation mainly affects the NO predictions in the TNF target flames.

In general, one can expect an adiabatic flame calculation to over predict NO levels (if all other submodels are correct), while an optically thin model is expected to under predict NO levels.

The answer corresponding to a detailed radiation model should be somewhere between these limits.

At present, the majority of modelers in the TNF Workshop are satisfied with this limitation of the present radiation model."

What is involved in "detailed radiation model" and what is the benefit ?

Other keywords used in literature ...

- **P.J. Coelho, O.J. Teerling and D. Roekaerts**, **Spectral radiative effects and turbulence/radiation interaction** in a non-luminous turbulent jet diffusion flame, Combustion and Flame, 133: 75-91, 2003
- P.J. Coelho, O.J. Teerling and D. Roekaerts, Spectral radiative effects and turbulence-radiation-interaction in a turbulent piloted jet diffusion flame, in Computational Thermal Radiation in Participating Media, Proceedings of the Eurotherm Seminar 73, April 15-17, 2003, Mons, Belgium, P. Lybaert, V. Feldheim, D. Lemonnier and N. Selçuk, editors, Elsevier, 2003
- P.J. Coelho, Detailed numerical calculation of radiative transfer in a nonluminous turbulent jet diffusion flame, Combustion and Flame, 136:481-492, 2004
- **Yuan Zheng, R.S. Barlow, Jay P. Gore**, **Measurements and calculations of spectral radiation intensities** for turbulent non-premixed and partially premixed flames, J. Heat Transfer, 125: 678-686, 2003
- **Genong Li and Michael F. Modest**, Application of composition PDF methods in the investigation of **turbulence-radiation interactions**, J. Quant. Spect. and Rad. Transfer, 73:2-5:461-472, 2002
- Genong Li and Michael F. Modest, Importance of turbulence-radiation interactions in turbulent diffusion jet flames, J. Heat Transfer 125: 831-838, 2003

- **Radiative transfer equation (no scattering)**

$$\frac{dI_\eta}{ds} = -\kappa_\eta I_\eta + \kappa_\eta I_{b\eta}$$

$$\eta = \frac{1}{\lambda}$$

Wave number

The radiative flux follows from I
Divergence of radiative flux is source term in energy equation
(Integration over directions and over wave number needed)

Problems:
-Spectral averaging difficult due to strong dependence on η
-RANS-averaging or LES-filtering difficult due to nonlinearities (TRI)

TNF optically thin model: neglects absorption term and uses
a Planck mean absorption coefficient for the emission term

TRI in emission term easily taken into account by PDF averaging ...

TU Delft
Delft University of Technology

Definition of Planck mean absorption coefficient

$$\int_0^\infty I_{b\eta}\kappa_\eta d\eta \equiv \kappa_P \int_0^\infty I_{b\eta} d\eta = \kappa_P \frac{\sigma T^4}{\pi}$$

Planck mean
absorption coefficient is
obtained using a spectral
model, e.g. narrow band model

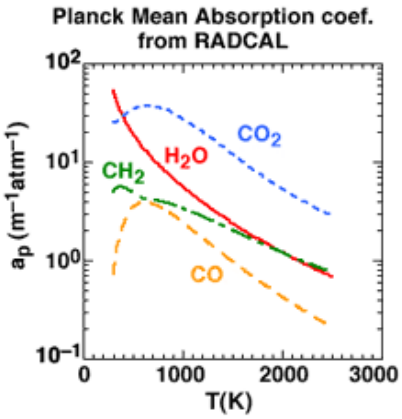

TU Delft

Spectral radiative effects and turbulence-radiation interaction
P.J. Coelho, O.J. Teerling, D. Roekaerts

- **Comparison of radiation modelling approaches:**
  - **Optically thin approx. / Planck mean absorption coeff.**
  - **Discrete Ordinates Method / Planck mean absorption coefficient**
  - **Discrete Ordinates Method / advanced spectral model (SLW)**
- **Comparison of closures of the mean radiative source terms (TRI)**

DOM: discrete ordinates method
SLW: spectral line based weighted sum of gray gases

TU Delft
Delft University of Technology

Input data from experiment for radiative calculations of Sandia Flame D

1. **Mean temperature and species concentration fields:**
   Interpolated / extrapolated from measured profiles
2. **Mean and variance of mixture fraction**
   (define pdf of mixture fraction - clipped Gaussian pdf):
   interpolated / extrapolated from measured profiles
3. **Flamelet relationships T(Z), $\rho(Z)$, $y_i(Z)$:**
   Interpolated / extrapolated from instantaneous experimental data

This approach using experimental input on composition and temperature is expected to introduce lower uncertainty in the radiative transfer calculations than that introduced by a coupled reactive fluid flow/heat transfer simulation

TU Delft
Delft University of Technology

spectral line based weighted sum of gray gases model

A different look at the spectrum: ordering by absorption coefficient rather than wave number: distribution function F

For two species: statistical independence approximation is used

PROBLEM: the distribution function depends on T and p

Way out: assumption of ideal spectrum

See: Denison and Webb, Trans. ASME 117:359-365 (1995)

7

TU Delft

Spectral line based weighted sum of gray gases model

Take together all pieces of the spectrum where water has absorption in a range (labeled by j) and CO2 has absorption in a range (labeled k)

The absorption cross section domain is divided in subintervals indexed with j (for H2O) and k (for CO2).

The absorbing medium is considered as a mixture of gray gases, associated with each of the subintervals.

The weight factors are

$$a_{jk} = \left[F_w\left(\tilde{C}_{w,j+1}\right) - F_w\left(\tilde{C}_{w,j}\right)\right]\left[F_c\left(\tilde{C}_{c,k+1}\right) - F_c\left(\tilde{C}_{c,k}\right)\right]$$

The spectral parameter η is replaced by indices j and k !

8

TU Delft

- **Discrete ordinates method (DOM) combined with SLW**
  Overbar denotes RANS averaging

$$\frac{d\bar{I}^{m}_{jk}}{ds} = -\bar{\kappa}_{jk}\,\bar{I}^{m}_{jk} + \overline{a_{jk}\kappa_{jk}\,I_b}$$

The label m belongs to DOM
The labels j and k belong to SLW

In a non spectral model the labels j and k are absent because only total intensity (integral over the spectrum) is calculated

Correlation between absorption coefficient and intensity neglected in absorption term (thin eddy approximation)

TU Delft
Delft University of Technology

- **Radiative heat source appearing in the energy equation**

$$\overline{\nabla\cdot\mathbf{q}} = \sum_{k=0}^{N_g}\sum_{j=0}^{N_g}\left(4\pi\,\overline{a_{jk}\,\kappa_{jk}\,I_b} - \bar{\kappa}_{jk}\sum_{m=1}^{M} w_m\,\overline{I^{m}_{jk}}\right)$$

- **Closure of the mean emission term:**
  Full TRI

$$\overline{a_{jk}\,\kappa_{jk}\,I_b} = \bar{\rho}\int_0^1 \frac{a_{jk}(Z,X_R)\,\kappa_{jk}(Z,X_R)\,I_b(Z,X_R)}{\rho(Z,X_R)}\,\tilde{P}(Z)\,dZ$$

Note that experimental input is used here, but also an assumed shape of the PDF...

- **Partial TRI**

$$\overline{a_{jk}\kappa_{jk}\,I_b} = \overline{a_{jk}\kappa_{jk}}\quad\overline{I_b}$$

Z is mixture fraction, P(Z) is the PDF of mixture fraction
X is a heat loss parameter

TU Delft
Delft University of Technology

- **Sandia Flame D: Non-dimensional radiant power versus height x/Lst**

- **DOM calculations**
  - 1 - Planck mean, partial TRI
  - 2 - Planck mean, full TRI
  - 3 - SLW, partial TRI
  - 4 - SLW, full TRI

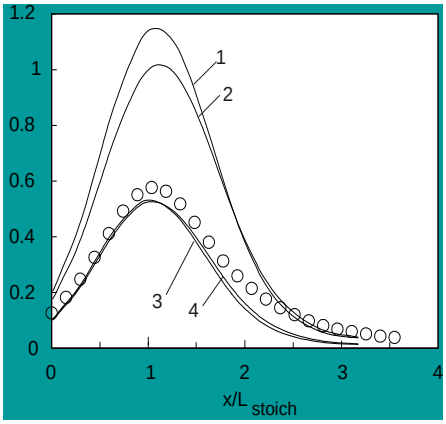

DOM includes absorption in contrast with optically thin model)

SLW is spectral model, Planck mean is gray model

In the partial TRI model the correlation between absorption coefficient and black body emissivity is neglected

11

Lstoich = 47 d

TU Delft
Delft University of Technology

- **Predicted and measured fraction of radiative heat loss:**

1. Measured - 5.1% (887 W)
2. Optically thin approximation - 9.5%
3. DOM, Planck mean, partial TRI - 8.7%
4. DOM, Planck mean, full TRI - 8.0%
5. DOM, SLW, partial TRI - 3.8%
6. DOM, SLW, full TRI - 3.9%

Further refinements in Coelho, 2004

Other model results on in TRI in
Zheng, Barlow, Gore, 2003 and Li and Modest, 2003

12

TU Delft
Delft University of Technology

- **Optically thin approximation and DOM / Planck mean absorption coefficient predictions are close ...**

  ... because the emission term is at least one order of magnitude larger than the absorption term in the RTE when the Planck mean absorption coefficient is used

- **The DOM / SLW heat loss is much lower (and in better agreement with the experimental data) than the DOM / Planck mean ...**

  ... because the Planck mean absorption coefficient yields a poor estimation of the absorption term

- **The difference between predictions with the considered full and partial TRI model is relatively small compared the effects of radiation model**

TU Delft
Delft University of Technology

Recall the definition of
Planck mean absorption coefficient

$$\int_0^\infty \kappa_\eta I_{b\eta} d\eta \equiv \kappa_P \int_0^\infty I_{b\eta} d\eta$$

- **The use of the Planck mean absorption coefficient in the absorption term in the DOM uses the following approximation**

$$\int_0^\infty \kappa_\eta \int_{4\pi} I_\eta \, d\Omega d\eta \approx \kappa_P \int_0^\infty \int_{4\pi} I_\eta \, d\Omega d\eta$$

  - Calculation of both terms using the DOM/SLW shows that the 1st term is much larger than the 2nd one
  - The absorption term is strongly underestimated if the Planck mean absorption coefficient is employed
  - In this way, the radiative heat loss is overestimated

TU Delft
Delft University of Technology

Recommendations

- Because different authors used different mix of models and put emphasis on different aspects, situation is not fully clear yet, but
- TRI is relatively important (=> include fluctuations)
- Spectral effects seem important in evaluation of absorption term (=> go beyond Planck mean)
- Explicit confirmation that thin eddy approximation is valid is needed (=> can be tested in line calculations)
- But sophisticated radiation modeling only useful when species and temperature predictions are OK

TU Delft

Modelling Scalar Dissipation

R W Bilger
School of Aerospace,Mechanical and Mechatronic Engineering
The University of Sydney

TNF7 Chicago
July 2004

Outline

- Motivation
- Some commonly used models
  - Descriptions
  - Advantages and disadvantages
- Consistency with pdf transport equation
- $<N|\eta>$ as a source of error
- Modelling scalar dissipation fluctuations
- Relationship to mixing models
- Relationship to dissipation of reactive scalars

Motivation

- Definitions: $\chi \equiv 2D \nabla\xi . \nabla\xi$; $N \equiv \chi/2$;
  ξ is mixture fraction and η its sample space value
- Flamelet codes employ $N(\xi)$ and its fluctuations
- CMC requires $<N|\eta>$ for first order closure and info on $<N''^2|\eta>$ for second order closure
- Flamelet and CMC results for Flames D E and F appear to be sensitive to scalar dissipation modelling
- What is relationship to mixing models used in pdf calculations?

Some Commonly Used Models for $<N|\eta>$, $N(\xi)$

- Counterflow laminar flamelet
  - $N(\xi) = \frac{2a}{\pi} \exp\left(-2\left[\text{erfc}^{-1}(2\xi)\right]^2\right)$ (1)
- Amplitude Mapping Closure
  - $<N|\eta> = <N> \exp\left(-2\left[\text{erfc}^{-1}(2\eta)\right]^2\right) / I_P$ (2)
- Advantages:
  - Some physical basis; literature pedigree
- Disadvantages:
  - Physically unrealistic; cumbersome to use

Some Commonly Used Models for <N|η>, N(ξ)

- Girimaji's model
  - $<N|\eta> = 2\frac{\varepsilon}{k}\frac{<\xi>(1-<\xi>)}{<\xi''^2>}\frac{I(\eta)}{P(\eta)}$ (3)
  - Homogeneous turbulence
  - Beta function pdf – integrate pdf transport eq
- Advantages:
  - Some physical basis; literature pedigree; robust
- Disadvantages:
  - Physically unrealistic in inhomogeneous flows
  - Cumbersome to use

Pdf Transport Eqn

$$\frac{\partial \rho_\eta P(\eta)}{\partial t} + \nabla \cdot \left(\rho_\eta P(\eta) < \mathbf{v} \mid \eta >\right) = -. \frac{\partial^2 \rho_\eta P(\eta) < N \mid \eta >}{\partial \eta^2} \quad (4)$$

- Model for conditional velocity

Linear $$< \mathbf{v} \mid \eta > = < v > + \frac{< v'\xi' >}{< \xi'^2 >}(\eta - < \xi >) \quad (5)$$

Gradient $$< \mathbf{v} \mid \eta > = < v > - D_T \nabla \ln(P) \quad (6)$$

- Presumed form of pdf
- Integrate pdf transport eqn by parts

Pdf Transport Eqn

- Devaud *et al.* (2004) use

Linear $$<\mathbf{v}\,|\,\eta>=<v>+\frac{<v'\xi'>}{<\xi'^2>}(\eta-<\xi>)$$ (5)

  – Problems, as not fully consistent with $<\xi^2>$ eqn

- Mortensen (2004) uses

Gradient $$<\mathbf{v}\,|\,\eta>=<v>-D_T\nabla\ln(P)$$ (6)

  – Fully consistent

- Presumed form of pdf $P(\eta;\mu)$
- Result: $$P(\eta)N(\eta)=-\frac{\partial\Pi(\eta)}{\partial\mu_j}S_j+D_T\frac{\partial^2\Pi(\eta)}{\partial\mu_j\partial\mu_k}\frac{\partial\mu_j}{\partial x_i}\frac{\partial\mu_k}{\partial x_i}$$ (7)

Mortensen: Position 1

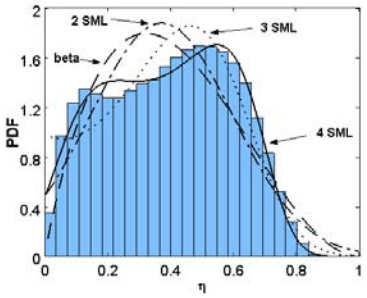

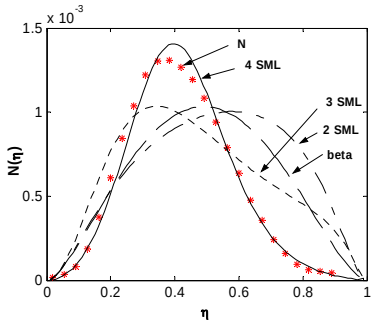

Mortensen: Position 2

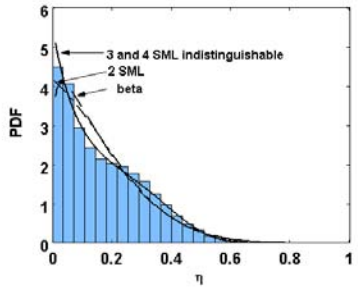

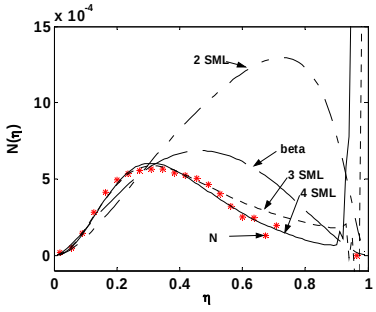

Piloted Jet Flames

- $\langle N|\eta \rangle$ has bimodal shape in near field
- Need to solve for higher moments?
- MC-PDF modellers should report results for higher moments?

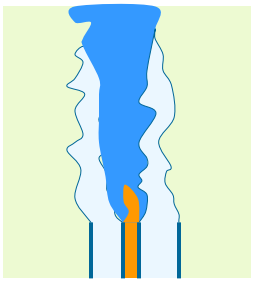

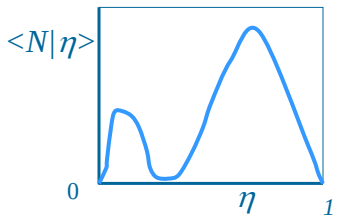

Other Models

- **Smith, et al (1992):** 24th Symposium:
  - $<\chi|\eta> = <\chi(r^*)>$ where $<\xi(r^*)> = \eta$
  - Roomina PhD thesis shows good agreement with Girimaji method
- **Kempf in RANS**

$$\chi(r) = 2\frac{\xi''^2(r)}{k(r)/\varepsilon(r)} \qquad \langle\chi|\eta\rangle = \frac{\int \bar{\rho}\chi(r)\tilde{P}(\eta,r)dr}{\int \bar{\rho}\tilde{P}(\eta,r)dr}$$

-

CSD in LES

- **Kronenburg in LES**

$$\chi_{sgs} = \nu_t / Sc_t \cdot \frac{\partial\tilde{\xi}}{\partial x_i}\frac{\partial\tilde{\xi}}{\partial x_i} \qquad \nu_t = C\Delta^2\left\|\tilde{S}_{ij}\right\|$$

- **Kempf in LES**

  The filtered scalar dissipation rate is determined from a model by Girmaji&Zhou simplified by de Bruyn Kops et al. [1,2]. This model relies on the definition of the scalar dissipation rate in filtered quantities and tries to compensate for filtering by considering a turbulent diffusivity Dt..

$$\tilde{\chi} = (\tilde{D} + D_t)(\nabla\tilde{\xi})^2$$

  x~ is the filtered scalar rate of dissipation, D~ the filtered molecular diffusivity, Dt the turbulent diffusivity, f~ the filtered mixture fraction (which is actually transported)

Large Eddy Simulation of Flame D - Darmstadt

Grid:

Cylindrical

1,968,000=1025x32x60 nodes

0.28 mm axial

0.45 radial (equidistant at axis; exponential from inner shear layer outwards)

2*π /32 circumferential

Scalar dissipation model:

Girimaji, Zhou, modified by: de Bruyn Kops, Riley, Kosaly

$$\tilde{\chi} = 2(\widetilde{D}+D_t)(\partial\tilde{f}/\partial x_i)^2$$

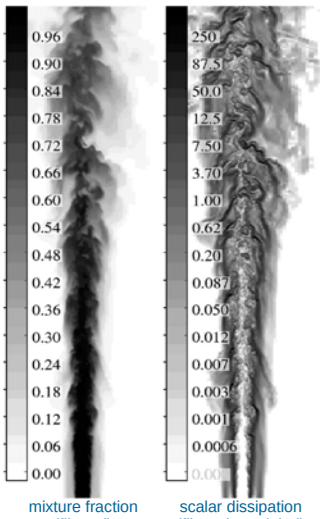

mixture fraction (filtered)

scalar dissipation (filtered, modeled)

<N/η> As a Source of Error

- Klimenko and Bilger (1999) show error to be equivalent to a false chemical reaction rate of

$$\rho_\eta \left(N_\eta^{\text{model}} - N_\eta^{\text{true}}\right)\frac{\partial^2 Q_i}{\partial \eta^2}$$

- Error depends on relative size of advectn/diffusn/reactn terms
- Mortensen (2004) has more detail

Modelling Scalar Dissipation Fluctuations

- Log-normal distribution?
- $N'/\langle N\rangle$ increases with Re due to intermittency of dissipation
- Sreenivasan (2004) gives

  $N'/\langle N\rangle = 0.85 R_\lambda^{0.26}$
- Flow dependent?

Relationship to MC-PDF Mixing Models

- Pdf methods use various mixing models
- What do these models imply for $\langle N|\eta\rangle$?
  - $\langle N|\eta\rangle$ can be obtained from Mortensen's Eq (7) assuming Eq (6) is fully consistent
  - Higher moments needed => large number of particles?
  - Convergence for large number of particles?
- What do these models imply for $N'/\langle N\rangle$ and distribution of N ?
  - Can Re dependence be included?

Dissipation of Reactive Scalars

- Second-Order Closure:
  - Swaminathan & Bilger (1999)
  - Flamelet closure shows good agreement with DNS
- Doubly-Conditional CMC
  - Kronenburg (2004)

$$\langle D\nabla\xi.\nabla\xi \,|\, \xi=\eta, C=\zeta\rangle; \langle D\nabla\xi.\nabla C \,|\, \xi=\eta, C=\zeta\rangle; \langle D\nabla C.\nabla C \,|\, \xi=\eta, C=\zeta\rangle$$

- Implications for experiments
  - Difficuties near $dT/d\eta$ = 0
- More work is needed

Comparison of Measured and Modeled Scalar Dissipation: Progress and Challenges

Rob Barlow,
Sandia National Laboratories

TNF7 Workshop, 22-24 July 2004, Chicago

- Recent progress in scalar dissipation experiments
- Measured and modeled results from piloted jet flames
- Key areas for current and future work
  - 1D, 2D & 3D measurements
  - Spatial resolution requirements and spatial averaging effects
  - Small-scale structure of turbulent reacting flows
  - Noise contribution to scalar dissipation and its variance
  - Using simulations to understand experiments
  - How best to compare measured and modeled results

Sandia National Laboratories

Recent Progress in Scalar Dissipation Experiments

- Sandia: Line-imaged Raman/Rayleigh/LIF + crossed PLIF
  - Karpetis et al., Opt. Lett. (2004); PCI 30 (2004)
  - Barlow & Karpetis, Flow Turb. Combust. (2004); PCI 30 (2004)
- TU Darmstadt: Line-imaged Raman/Rayleigh
  - Geyer, Kempf, Dreizler, Janicka, PCI 30 (2004)
- Sandia: Rayleigh (polarized/depolarized) imaging + CO PLIF
  - Frank, Kaiser, Long, PCI 29 (2002)
- UT Austin: Rayleigh 2-point time traces for 2D thermal dissipation
  - Wang & Clemens, PCI 30 (2004)
- Related experimental work in nonreacting flows
  - Mi & Nathan, Exp. Fluids (2003)
  - Wang & Tong, PCI 30, (2004)

Sandia National Laboratories

Measured and Modeled Results for Piloted CH_4/Air Flames

- Line-imaging (1D) results from flames C,D,E
- Several contributed calculations (some descriptions in the handout)
  - Chandy et al. – RANS/PDF D,E,F
  - Chen – RANS/PDF D,E,F
  - Goldin – RANS/PDF D,E,F
  - Huh et al. – RANS/CMC D,E,F
  - Kronenberg – RANS D
  - Ihme & Pitsch – LES/SFPV D
  - Kempf – LES D
  - Kronenberg – LES D
- Radial profiles and conditional means of χ at x/d=7.5, 15, 30
- Avoid contents of Symposium papers (mostly)

Sandia National Laboratories

Line Imaging of Raman/Rayleigh Scattering and CO LIF

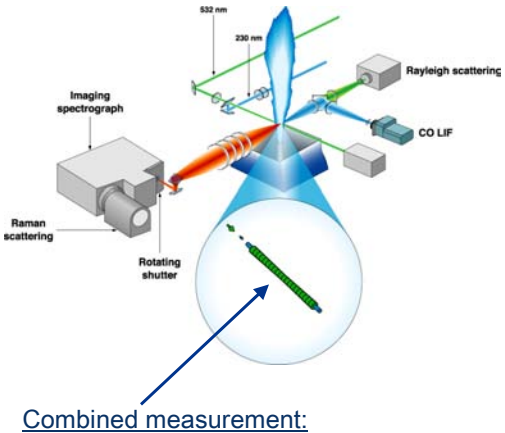

Two data sets

Flame	Re_j
C	13,400
D	22,400
E	33,600
F	44,800

Sydney burner

Combined measurement:

- T, N_2, O_2, CH_4, CO_2, H_2O, H_2, CO
- 200-μm spacing, ~7-mm segment
- mixture fraction
- scalar dissipation (1D - radial)

Sandia National Laboratories

Same Flames? (1997 vs. 2003)

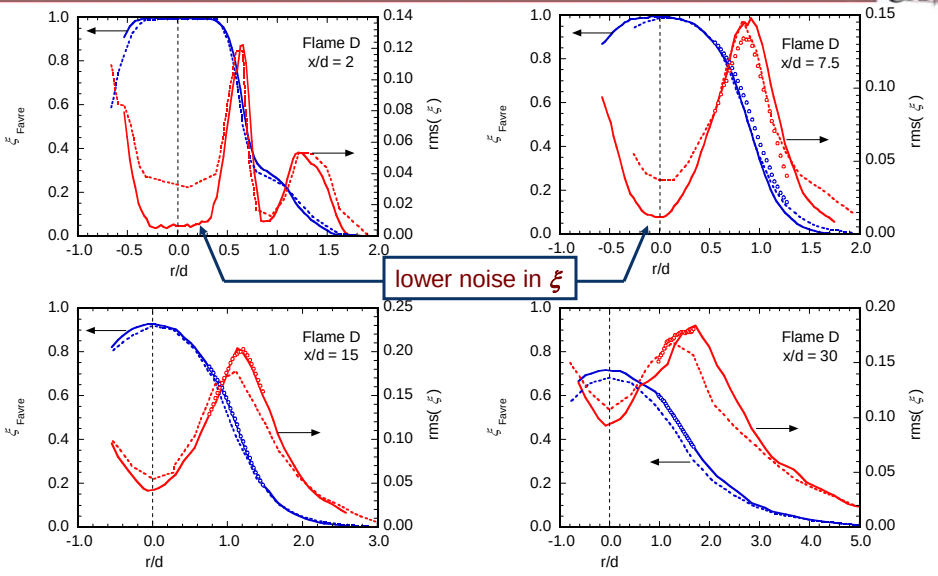

dashed – Barlow&Frank, PCI (1998) solid – Barlow&Karpetis, FTC (2004) symbols – present, PCI 30

Sandia National Laboratories

Comparison Plots: Radial profiles (pp 151)

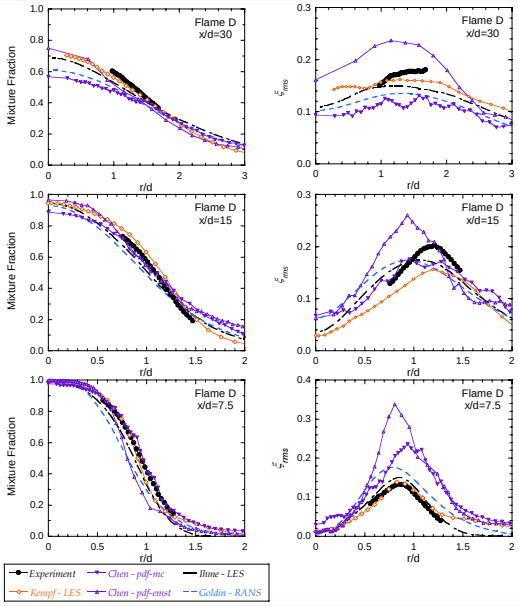

- Favre average ξ and ξ'' in flame D
- Significant spread in modeled ξ''. Why?
- Factor of ~2 in ξ'' means factor of ~4 in $(\xi'')^2$
- Does this translate to factor of ~4 in modeled χ?

$$\tilde{\chi} = C_\phi \frac{\varepsilon}{k} \widetilde{\xi''^2}$$

Sandia National Laboratories

Comparison Plots: Radial profiles (pp 153)

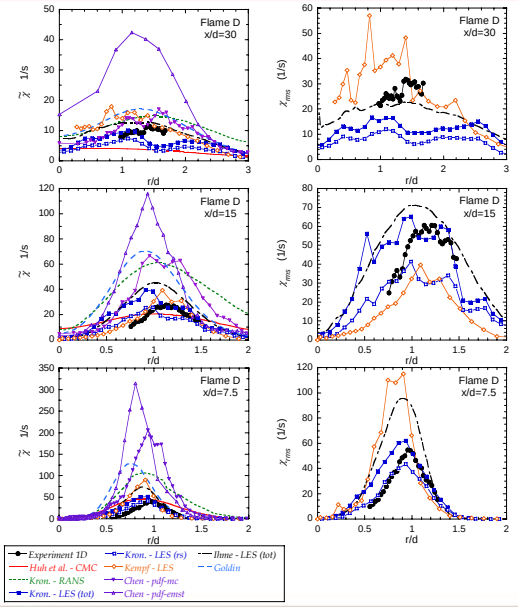

- Favre average χ and χ'' in flame D
- Significant spread in modeled χ, even for RANS calculations with same (??) model.

$$\tilde{\chi} = C_\phi \frac{\varepsilon}{k} \widetilde{\xi''^2}$$

Comparison Plots: Radial profiles (pp 153)

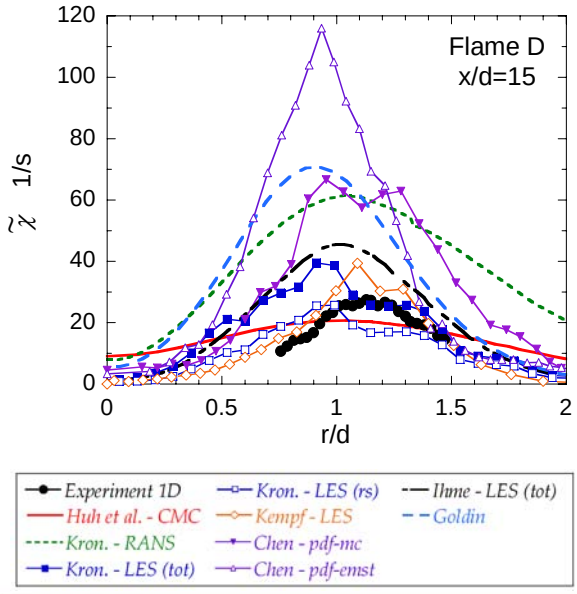

Other contributions:

- Chandy et al. – Fluent with composition PDF (see pp. 158-161)
  χ_{max} ~ 120/s
- Pope & Goldin (TNF6) Fluent with comp. PDF (see pp. 162-163)
  χ_{max} ~ 75/s
- Why such wide variation in predictions?

Comparison Plots: Conditional mean and rms (pp 152)

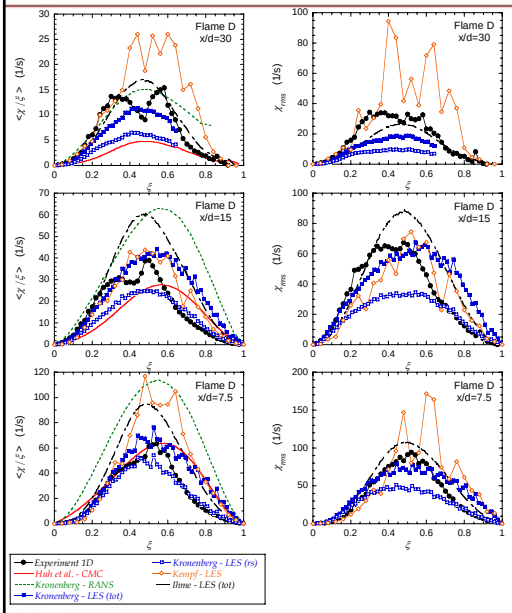

- Experimental results are not density weighted (may not be important for flame D)
- LES – How well resolved?
- Echekki et al. – ODT much higher χ and χ_{rms}

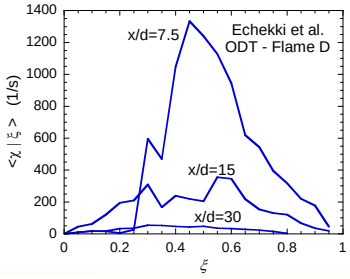

Sandia National Laboratories

Lots of Questions

- Questions on the experiment
  - 1D measurements are shown, what more do we know from 2D, 3D results?
  - Is spatial resolution adequate? What are the effects of spatial averaging?
  - How important is noise in measurements of ξ, $(\xi'')^2$, χ, $(\chi'')^2$?
  - Can these effects be quantified and separated?
  - What more must be done before we can use measurements to "validate" scalar dissipation models?
- Questions on the models
  - Why such a wide variation among the RANS results for $(\xi'')^2$ and χ ?
  - How far are we from fully resolved simulations of attached jet flames?
  - Can we get the 3D/1D ratio and understand noise effects from LES?
- Questions for both
  - What level of measurement uncertainty is still useful for model validation?
  - What about thermal dissipation? (easier to measure)

Sandia National Laboratories

Experimental Issues (Are we ready to compare?)

- Angle bias (1D measurements in 3D field)
  - How to compare 1D or 2D measurements with modeled χ_{3D}
  - 3D "measurements" (Karpetis & Barlow Symposium paper)
  - Can we use LES? (see Geyer et al. and Kempf et al. Symposium papers)
- Spatial averaging
- How important is the noise contribution to $(\xi'')^2$, χ, and $(\chi'')^2$?

Sandia National Laboratories

Instantaneous 2-D Measurements of Reaction Rate, Temperature, Mixture Fraction, and Scalar Dissipation in Turbulent Jet Flames

- Instantaneous 2-D measurements reveal detailed structure of turbulent nonpremixed flames
- Simultaneous imaging:
  - Reaction rate of CO + OH → CO_2 + H
  - Mixture fraction (ξ) and temperature
  - Scalar dissipation rate $\chi = 2D \nabla\xi \cdot \nabla\xi$
- Conditional mean scalar dissipation in flame D, x/d=15

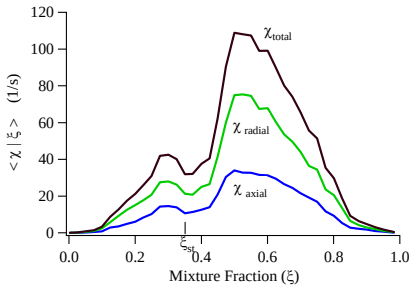

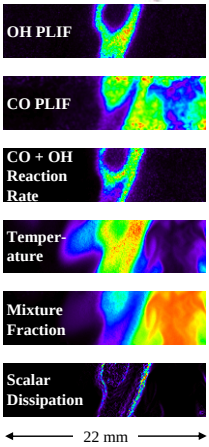

Frank, Kaiser, and Long, *Proc. Combust. Inst.*, 29:2687 (2002)

Fielding, Frank, Kaiser, Smooke, and Long, *Proc. Combust. Inst.*, 29:2703 (2002)

Angle Bias: Ratio of 3D to 1D Scalar Dissipation

- Add crossed OH PLIF to determine flame orientation (Karpetis et al., Opt. Lett., 2004)
- Details on Monday morning (Karpetis & Barlow, PCI 30, 2004)

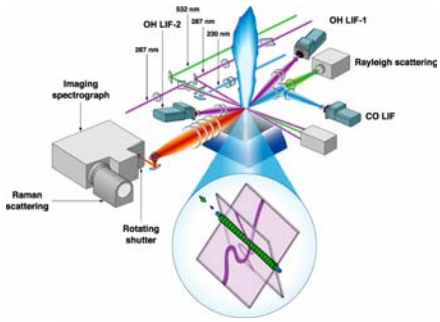

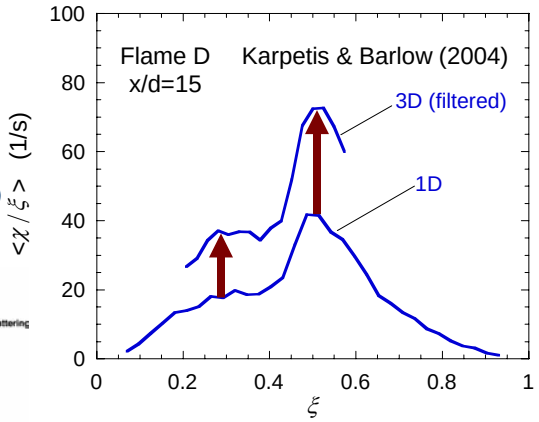

- Factor between ~1.6 and ~2 at x/d=15 in flame D
- Isotropic → 3, but interesting regions in flames are usually not isotropic

Sandia National Laboratories

Comparison of Imaging and Multiscalar Line Measurements in Flame D (x/d = 15)

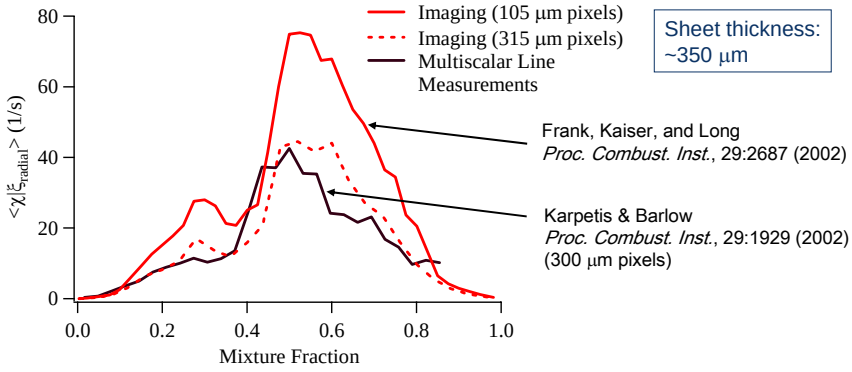

- Line and planar imaging measurements show good agreement when 2D images are binned to give a comparable pixel size
- How much of this effect is noise filtering vs. spatial averaging?

Experimental Issues (Are we ready to compare?)

- Angle bias (1D measurements in 3D field)

- Spatial averaging
  - Physical limitations (laser thickness, optics, signal strength)
  - Are we resolving the smallest scales?
  - How can we quantify spatial averaging effects?

- How important is the noise contribution to $(\xi'')^2$, χ, and $(\chi'')^2$?

Spatial Resolution Requirements: Nonreacting Flows

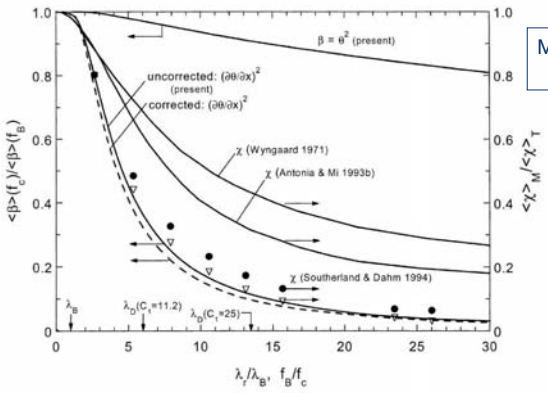

Mi & Nathan, Exp. Fluids, 2003 (see also Pitts et al., 1999)

Fig. 2. Effect of probe spatial resolution on measurements of several scalar properties in the far field of a turbulent circular jet. Variances of the measured scalar fluctuation θ and its streamwise derivative $\partial\theta/\partial x$ for the present investigation (Re_j=180) were obtained from spectra ($\Phi_{\theta\theta}$, $\Phi_{\partial\theta/\partial x}$) of θ low-pass-filtered at different cutoff frequencies f_c. The mean scalar dissipation rates (●, Re_j=52; ∇, Re_j=45) were measured at different spatial resolution scales λ_f by Southerland and Dahm (1994). The symbol λ_B denotes the Batchelor length scale

- Need resolution at Batchelor scale (or close to it) to measure dissipation

- Problem to evaluate λ_B in flames (low Re, big temp range, nonisotropic, developing region)

Spatial Averaging Effect in LES and Experiment

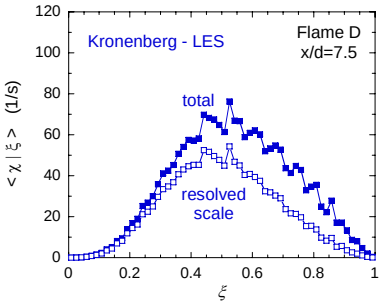

LES grid…

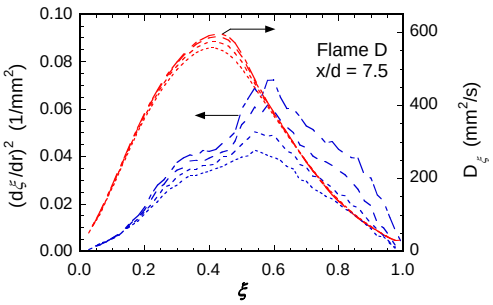

Successive spatial filtering of line data
Filters widths: ~0.3, 0.7, 1.1, 1.5 mm

- LES and experiment both indicate better resolution in lean samples, smaller length scales in rich part of the flame at x/d=7.5
- Not very turbulent on the lean side at these conditions

Sandia National Laboratories

Experimental Issues (Are we ready to compare?)

- Angle bias (1D measurements in 3D field)
- Spatial averaging

- How important is the noise contribution to $(\xi'')^2$, χ, and $(\chi'')^2$?
  - Appears to be no problem for $(\xi'')^2$
  - Recent analysis by D. Geyer (TU Darmstadt)

Sandia National Laboratories

Noise in Laminar Flame Measurement

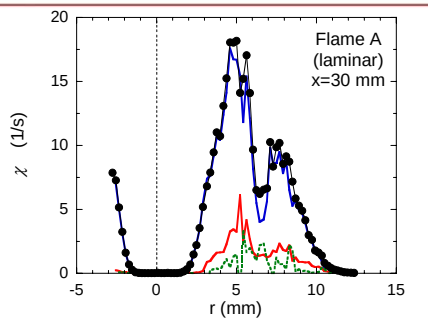

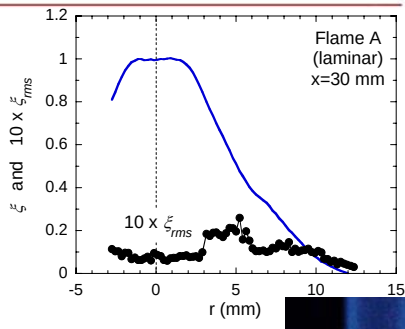

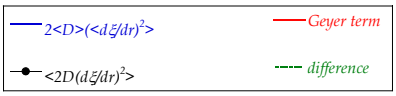

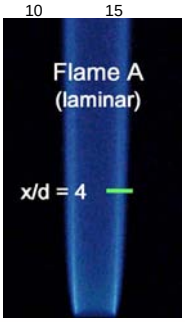

- Scalar dissipation two ways:
  - calculate χ from the average profiles of D_ξ and ξ
  - single-shot D_ξ and (dξ/dr), then average
- Compare to noise analysis by D. Geyer

Sandia National Laboratories

Scaling of χ with Reynolds Number

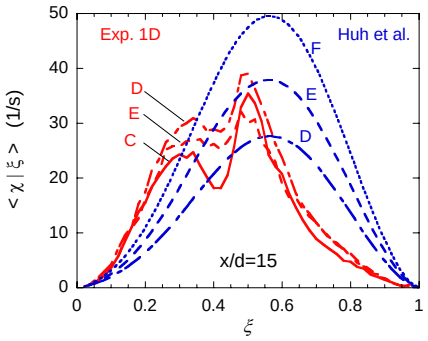

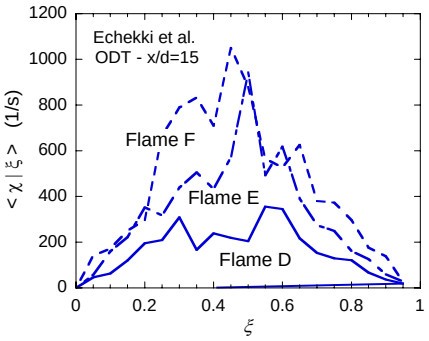

- Chandy et al. show radial profiles of χ increasing ~linearly with Re
- Measurements show less than linear (flames C,D,E) and slight decrease from D to E at x/d=15.

Sandia National Laboratories

Effect of Local Extinction on χ

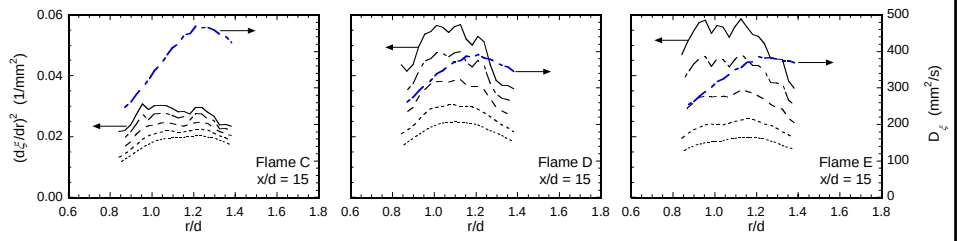

- Successive spatial filtering of line data
  - Look at $(d\xi/dr)^2$ and D(T) separately
  - Extrapolate to estimate fully resolved result (solid line) for $(d\xi/dr)^2$
- Gradients comparable in flames D & E, while diffusivity decreases due to finite-rate chemistry and local extinction. See also Starner et al., CST 129:141, 1997 (Fig. 19).
- Models do not seem to show this effect

Sandia National Laboratories

Lots of Questions

- Questions on the experiment
  - 1D measurements are shown, what more do we know from 2D, 3D results?
  - Is spatial resolution adequate? What are the effects of spatial averaging?
  - How important is noise in measurements of ξ, $(\xi'')^2$, χ, $(\chi'')^2$?
  - Can these effects be quantified and separated?
  - What more must be done before we can use measurements to "validate" scalar dissipation models?
- Questions on the models
  - Why such a wide variation among the RANS results for $(\xi'')^2$ and χ ?
  - How far are we from fully resolved simulations of attached jet flames?
  - Can we get the 3D/1D ratio and understand noise effects from LES?
- Questions for both
  - What level of measurement uncertainty is still useful for model validation?
  - What about thermal dissipation (easier to measure)

Sandia National Laboratories

Scalar dissipation in Flames D, E, F – Contributions from J-Y Chen

Flow Model: Reynolds stress model parabolic code
Turbulence-Chemistry Interaction Model: Joint Scalar PDF
Chemistry Model: Reduced Chemistry 12-step developed from gri1.2 with ISAT
Grid Size: 70 cells across half of the jet: 400 Particles/cell
Radiation Model: included with H2O, CO, CO2, CH4 recommended by workshop web information (prior to updated on CO2)
Mixing Model: **EMST with time scale ratio=1.5**

Flow Model: Reynolds stress model parabolic code
Turbulence-Chemistry Interaction Model: Joint Scalar PDF
Chemistry Model: Reduced Chemistry 12-step developed from gri1.2 with ISAT
from x/D=0-7 flamelet model is used otherwise, flame blow out occurs.
Grid Size: 70 cells across half of the jet: 400 Particles/cell
Radiation Model: included with H2O, CO, CO2, CH4 recommended by workshop web information (prior to updated on CO2)
Mixing Model: **Modified Curl with time scale ratio=2.0**

Favre average scalar dissipation rate estimated from
Xf= C_phi * f"f" * epsilon/k

Scalar dissipation in Flames D, E, F – Contributions from G. Goldin

The plots were generated from RANS simulations on an axi-symmetric mesh. I use the standard k-e turbulence model with c_eps_1 changed from the default value of 1.44 to 1.56. I use a turbulent Schmidt number of 1 for the fmean and fvar equation, and the standard model for the mean scalar dissipation...

<X> = C_phi * fvar * eps/k where C_phi=2.

This simulation differs from others in that I am using the Constructed PDF model to get the scalar field, as opposed to Steady Laminar Flamelets plus assumed shape PDFs. However, since for low speed flows the combustion only couples to the flow through density, and the density of the Constructed PDF and Laminar Flamelets should be very similar, I suspect that my results will be the same as the "standard RANS approach".

Scalar dissipation in Flames D, E, F – Contribution from Huh et al.

The scalar dissipation results here are obtained by the Favre averaged k-e-g turbulence model [1,2] and the beta pdf assumption based on the mean and variance of mixture fraction. These are used in the CMC predictions of the first and the second order CMC for Flame D, E and F to be presented at the TNF Workshop, July 2004.

References

1. Roomina, M. R. and Bilber, R. W., Combustion and Flame Vol. 125 (3) 2001, p1176-1195.
2. Launder, B. E., Morse, A., Rodi, W. and Spalding, D. B., NASA Free Shear Flows Conference, Virginia, NASA Report Number SP-311, 1972.

Scalar dissipation in Flames D – Contribution from Andreas Kempf

The scalar dissipation is the modeled scalar dissipation rate, i.e. the one that we assume to be the filtered scalar rate of dissipation. The data is taken from the simulation for the Symposium paper by F. Flemming, A. Kempf, J. Janicka.

Scalar dissipation in Flame D – RANS Contribution from Andreas Kronenberg

Favre means as function of r/D. Scalar dissipation is obtained from

$$\chi(r) = 2\,\xi''^2(r)k(r)/\,\varepsilon(r).$$

Conditional means as function of mixture fraction, ξ. The conditional means are obtained from the unconditional values via

$$\langle \chi \,|\, \eta \rangle = \frac{\int \bar{\rho}\chi(r)\,\tilde{P}(\eta, r)dr}{\int \bar{\rho}\,\tilde{P}(\eta, r)dr}.$$

Scalar dissipation in Flame D – LES Contribution from A. Kronenberg

We modelled the filtered scalar dissipation as

$$\tilde{\chi} = \chi_m + \chi_{sgs}$$

The mean scalar dissipation can be computed from the resolved scales as

$$\chi_m = \nu / Sc \cdot \frac{\partial \tilde{\xi}}{\partial x_i}\frac{\partial \tilde{\xi}}{\partial x_i}$$

with Sc=0.7. The sgs contributions are modelled using

$$\chi_{sgs} = \nu_t / Sc_t \cdot \frac{\partial \tilde{\xi}}{\partial x_i}\frac{\partial \tilde{\xi}}{\partial x_i}$$

The turbulent Schmidt number is 0.4 and the turbulent viscosity is determined by

$$\nu_t = C\Delta^2 \left\| \tilde{S}_{ij} \right\|$$

with Δ being the mesh width and S_{ij} being the strain tensor. The constant C is obtained from the dynamic procedure as described in Piomelli and Liu (Phys. Fluids 7(4), 1995), viz

$$C\,(\mathbf{x}, t) = \frac{(\widehat{C^* \alpha_{ij}^a} - L_{ij}^a)\hat{\bar{S}}_{ij}^a}{2\hat{\bar{\rho}}\Delta_T^2 |\hat{\bar{S}}| \hat{\bar{S}}_{kl}^a \hat{\bar{S}}_{kl}^a},$$

with

$$\alpha_{ij} = 2\bar{\rho}\Delta_G^2 |\bar{S}| \bar{S}_{ij}.$$

The test filter width is 3Δ. The constant C is then test filtered using a test filter width of 3Δ. Our computational grid is 92x92x200 grid nodes (Cartesian co-ordinates) and covers a physical domain of 12D*12D*50D. The mesh is slightly stretched with

Δmin=0.0714 D = 0.514 mm in cross flow direction

Δmin=0.16 D = 1.152 mm in axial direction

at the nozzle exit. The mesh is nearly uniform (with Δmin) in the region x,y < 2D and z<10D. The cell aspect ratios range from = 0.57-2.86. There are more than 2500 LES cells in every CMC cell. Taking the conditional mean of χ, we obtain <χ|η> for each CMC cell.

LES of Sandia Flame D Using a Steady Flamelet/Progress Variable Model

Matthias Ihme and Heinz Pitsch
Stanford University

July 9, 2004

Modeling Procedure

- Low Mach-number LES code in cylindrical coordinates
- Determination of all sub-filter quantities by dynamic procedure:

$$\widetilde{Z''^2}_{\rm SGS} = C_Z \Delta^2 |\nabla \widetilde{Z}|^2 \,,$$
$$\widetilde{\chi}_{\rm SGS} = 2 C_\chi \Delta^2 |\widetilde{S}| |\nabla \widetilde{Z}|^2 \,,$$

  where C_Z and C_χ are obtained from a dynamic model [1]

Combustion Model

- Steady flamelet/progress variable model expresses all chemical species as function of mixture fraction Z and flamelet parameter λ, $\boldsymbol{Y} = \boldsymbol{Y}(Z, \lambda)$ (this corresponds to horizontal projection of all transitional flame states onto the S-shaped curve)

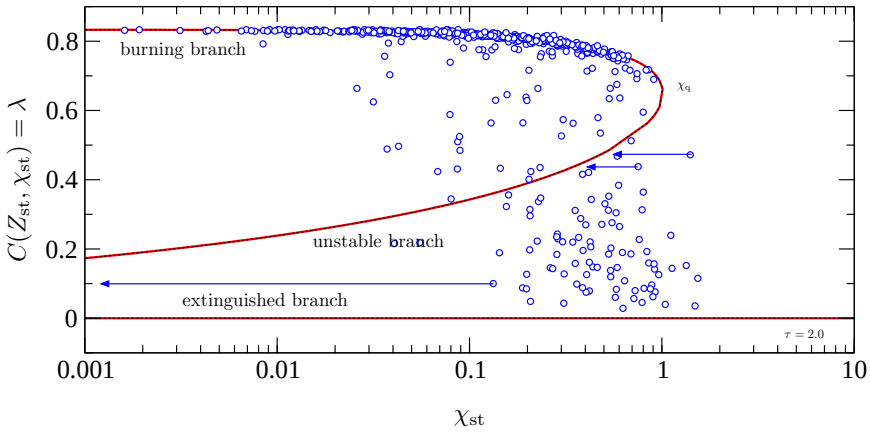

- Determination of mean quantities by presumed PDF-approach
- Express flamelet parameter λ in terms of progress variable C ($C := Y_{\rm CO_2} + Y_{\rm CO} + Y_{\rm H_2O} + Y_{\rm H_2}$)
- Solve transport equations for $\widetilde{Z}$ and $\widetilde{C}$
- Steady flamelet library
- GRI.Mech. 2.11 (49 species, 279 reactions)

Solution Domain

- Grid: $256 \times 152 \times 64$ $(80 \times 23.50 \times 2\pi)$
  - $\Delta x_{\min} = 0.0625$ (nozzle), $\Delta x_{\max} = 0.977$
  - $\Delta r_{\min} = 0.0325$ (centerline), $\Delta r_{\max} = 0.616$

Boundary and Inlet Conditions

- Inlet condition from periodic turbulent pipe, by matching $\widetilde{U}$ and $\sqrt{\widetilde{u''^2}}$ from experiments by A. Dreizler
- Convective outflow boundary conditions

Radiation and Flamelet-Library

- No radiation-model
- Pre-computed flamelet-library using `FlameMaster` (counter-diffusion flame configuration), parameterization of all chemical species as $\widetilde{\boldsymbol{Y}} = \widetilde{\boldsymbol{Y}}(\widetilde{Z}, \widetilde{Z''^2}, \widetilde{C})$.

Results

- Reasonable agreement with experimental data for $\widetilde{Z}$, $\sqrt{\widetilde{Z''^2}}$, $\widetilde{T}$, $\sqrt{\widetilde{T''^2}}$, $\widetilde{U}$ and $\sqrt{\widetilde{u''^2}}$
- Good agreement with experimental data of radial profiles for $x/D = \{30, 45\}$ for $\sqrt{\widetilde{u''^2}}$ and $\widetilde{u''v''}$ (TNF4: most numerical results under-predicted turbulent fluctuations)
- Under-prediction of jet-spreading rate $\widetilde{u''v''}$ at $x/D \sim 45$
- Broader radial profile of $\widetilde{Z}$ than experimentally measured
- Over-prediction of $\widetilde{Z}$ for $x/D \geq 45$ (lean part)

  $\Rightarrow$ Over-prediction of temperature (in lean part)
- Excellent agreement of CO_2 for all 3 downstream locations
- Present simulation over-predicts conditional mean values compared to experiments
- Over-prediction of conditional mean chemical species results in shift of conditional PDF's towards higher sample space values
- Predicted width ($\equiv$ variance) of PDF is comparable with results obtained from measurements

References

[1] C. D. Pierce and P. Moin. Progress-variable approach for large eddy simulation of turbuent combustion. Report No. TF-80, Stanford University, 2001.

Predictions of Mean Scalar Dissipation Rate in the Barlow and Frank flames D, E and F

A. J. Chandy[1], G. M. Goldin[2], and S. H. Frankel[1]
[1]Purdue University, West Lafayette, IN – 47906
[2]FLUENT Inc., Lebanon, NH - 03766

In this paper we present calculations of the mean scalar dissipation rate $\tilde{c}$ for the Barlow and Frank [1] flames D, E and F. The calculations are performed using the composition PDF method incorporated in the FLUENT CFD code. The details of the calculation are as follows.

1. The flow is calculated using the standard k-e turbulence model with the standard values of the constants.
2. The standard modeled composition PDF Transport equation is solved by the Lagrangian particle method.
3. The EMST mixing model is used with the standard value of mixing constant ($C_?$) = 2.0.
4. A 9-species, 5-step Computer Assisted Reduced Mechanism (CARM) for methane oxidation is used, implemented via ISAT.

Since the mean scalar dissipation rate cannot be estimated directly from FLUENT, a User Defined Function (UDF) was formulated to estimate the mixture fraction variance and thereby calculate the mean scalar dissipation rate which is given by

$$\tilde{c} = C_f \frac{e}{k} \widetilde{x''^2} \tag{1}$$

where e is the turbulent dissipation rate

k is the turbulent kinetic energy

$\widetilde{x''^2}$ is the mixture fraction variance

For reference figures 1 (a), (b), 2 (a), (b) and 3 (a), (b) show radial profiles of mean mixture fraction (fmean) and mixture fraction variance (frms) for flames D, E and F estimated by the UDF at 3 axial measurement locations, i.e., x/Dj = 7.5, 15 and 30 and compared to experimental data. The mean mixture fraction profiles match almost exactly with experiments, however there are overpredictions in the mixture fraction variance profiles. Figures 1 (c), 2 (c) and 3 (c) show the radial profiles of mean scalar dissipation (chi) at the first 6 axial measurement locations, i.e., x/Dj = 1, 2, 3, 7.5, 15 and 30.

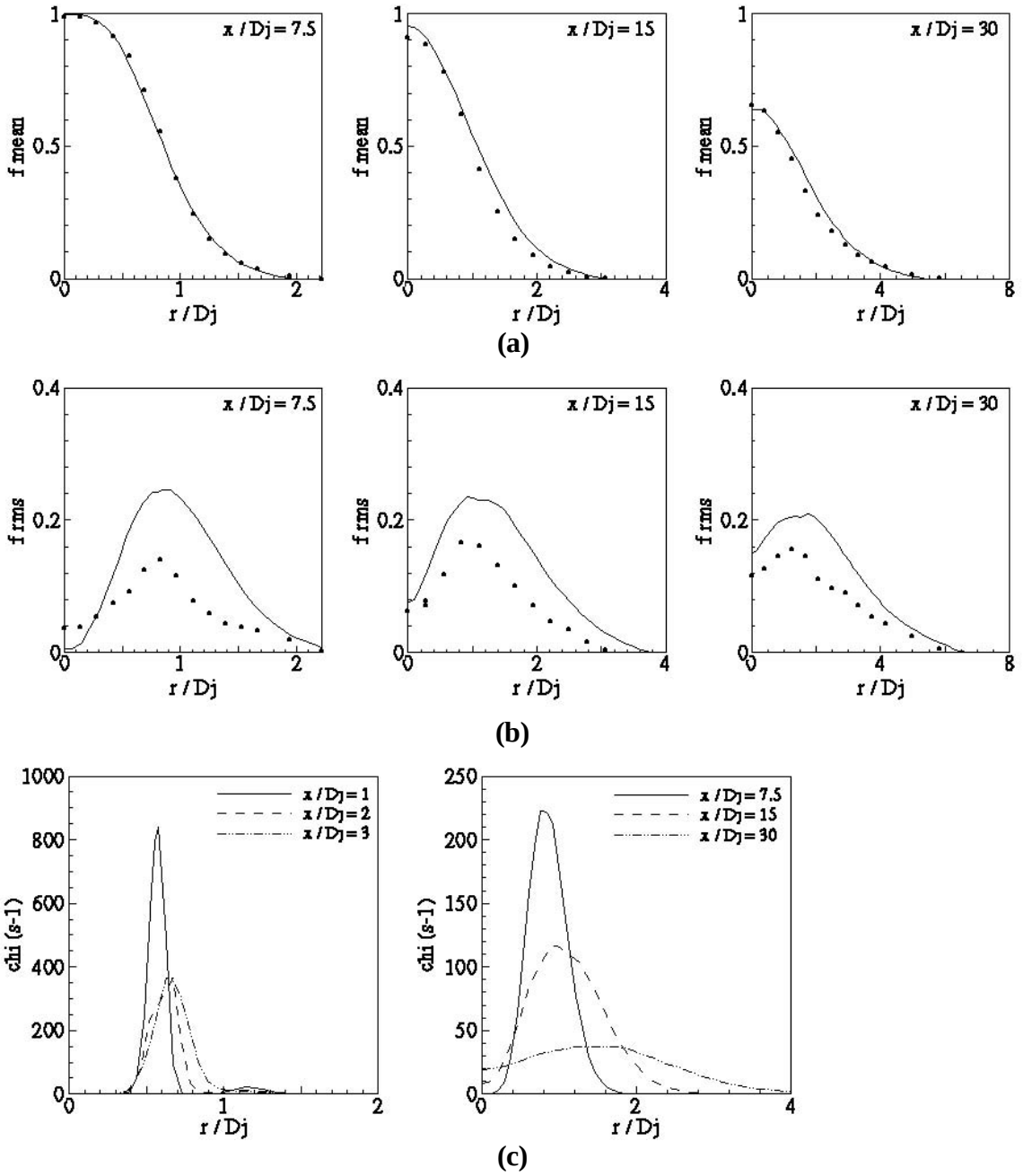

Figure 1. Radial Profiles of (a) Mean mixture fraction (fmean) (b) RMS of mixture fraction (frms) (c) Mean scalar dissipation (chi) for flame D; Symbols: Experimental, Lines: Computational

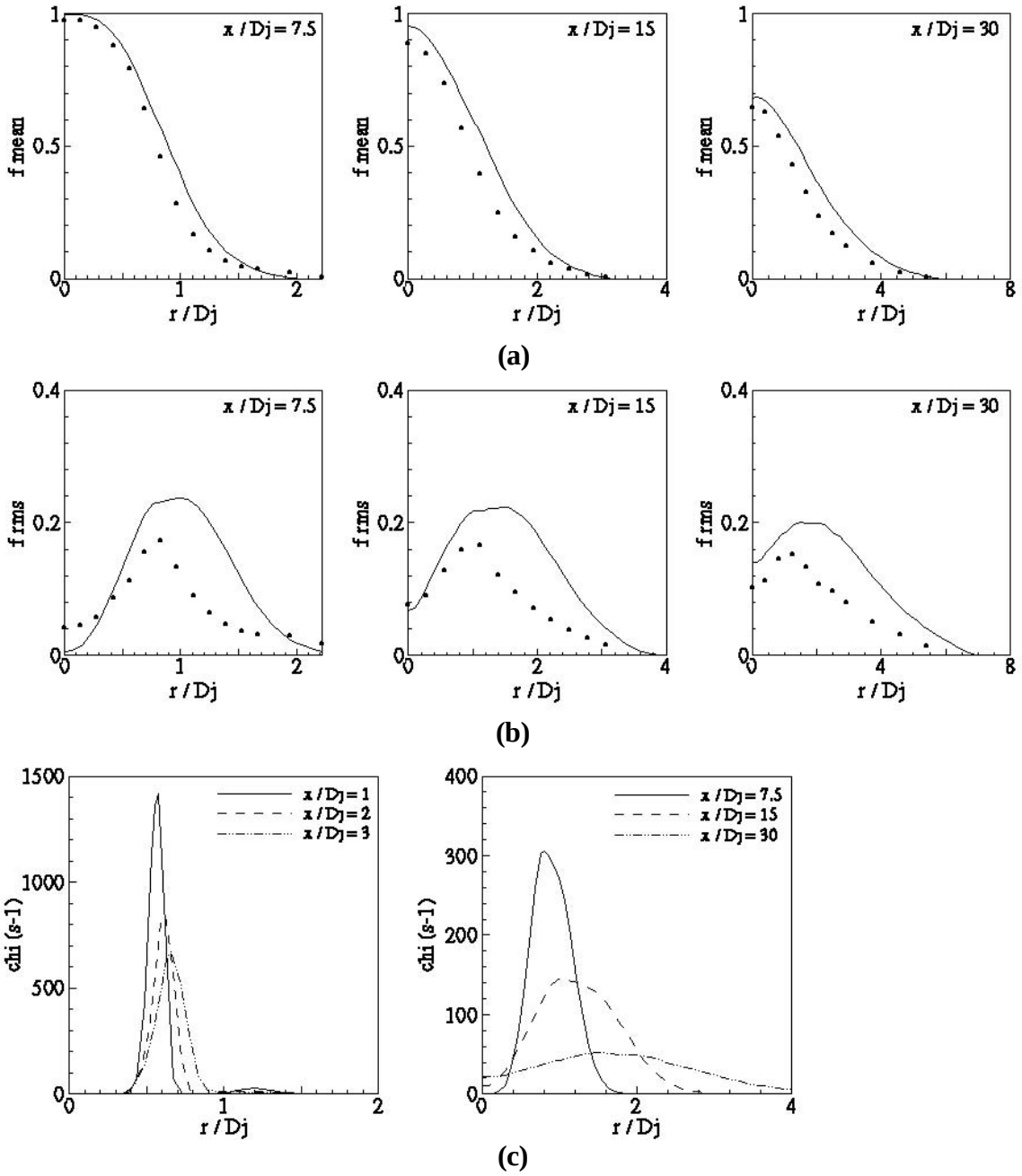

Figure 2. Radial Profiles of (a) Mean mixture fraction (fmean) (b) RMS of mixture fraction (frms) (c) Mean scalar dissipation (chi) for flame E; Symbols: Experimental, Lines: Computational

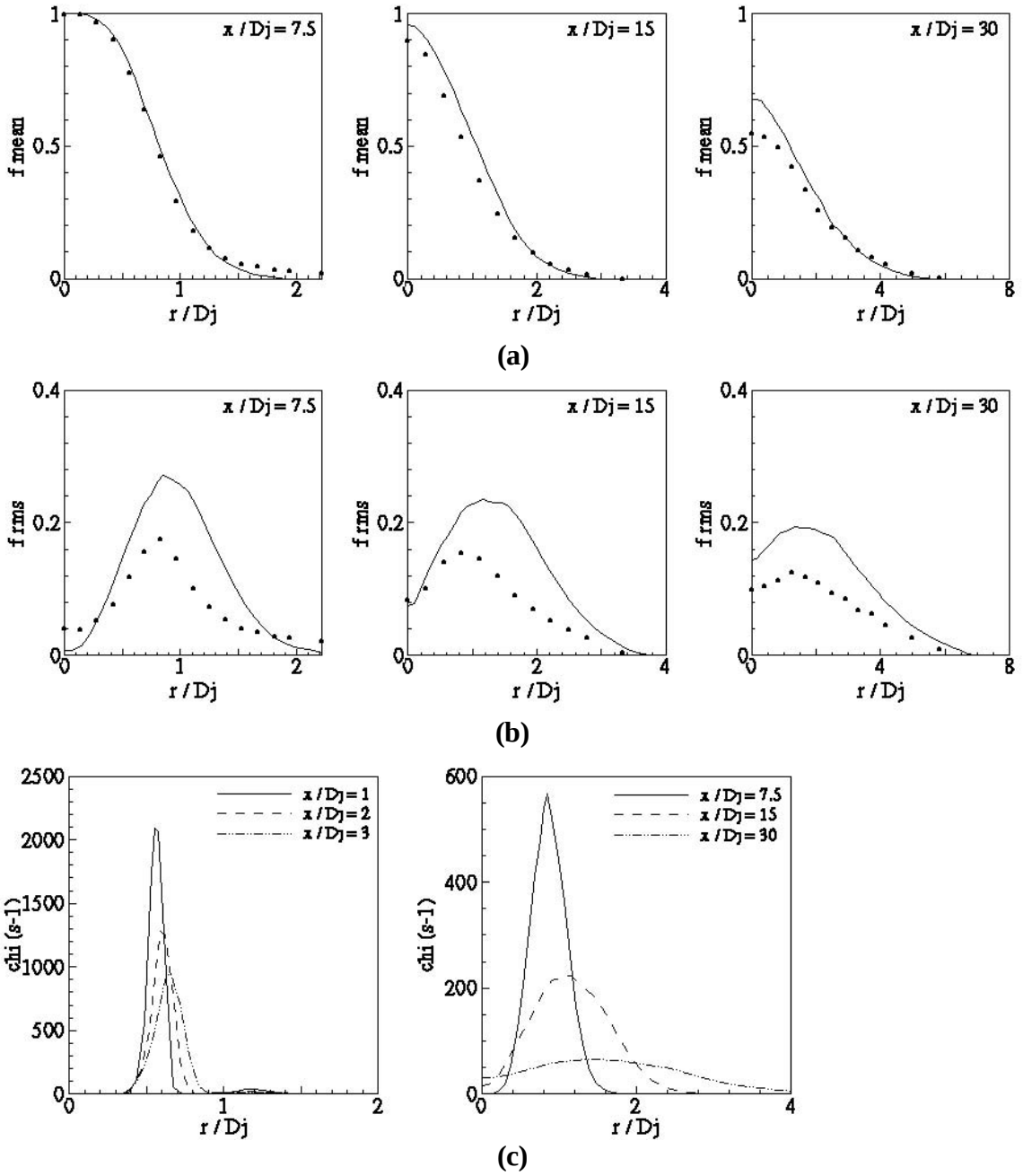

Figure 3. Radial Profiles of (a) Mean mixture fraction (fmean) (b) RMS of mixture fraction (frms) (c) Mean scalar dissipation (chi) for flame F; Symbols: Experimental, Lines: Computational

REFERENCES

[1] Barlow, R. S., and Frank, J.H., 1998, "Effect of turbulence on species mass fractions in methane/air jet flames," *Proceedings of Combustion Institute,* 27, pp. 1087.

Predictions of the Mean Scalar Dissipation Rate in the Barlow & Frank Flame D

by

Stephen B. Pope

Cornell University
Ithaca NY 14853

Graham M. Goldin

Fluent Inc.
Lebanon, NH

July 2002

In this note we present calculations of the mean scalar dissipation rate $\tilde{\chi}$ for the Barlow & Frank (1998) Flame D. The calculations are performed using the composition PDF method incorporated in the Fluent CFD code. The details of the calculations are as follows.

1. The flow is calculated using the standard k-ε turbulence model with the standard values of the constants, except for $C_{\varepsilon 1} = 1.52$.
2. The standard modelled composition PDF transport equation is solved by the distributed-particle method.
3. PDF transport is modelled by gradient diffusion, with $\sigma_\phi = 1.0$.
4. The IEM mixing model is used with the standard value $C_\phi = 2.0$.
5. A 16-species C_1 mechanism for methane is used, implemented via ISAT.
6. To ensure numerical accuracy, convergence tests were performed with respect to grid size, number of particles, and the ISAT error tolerance.

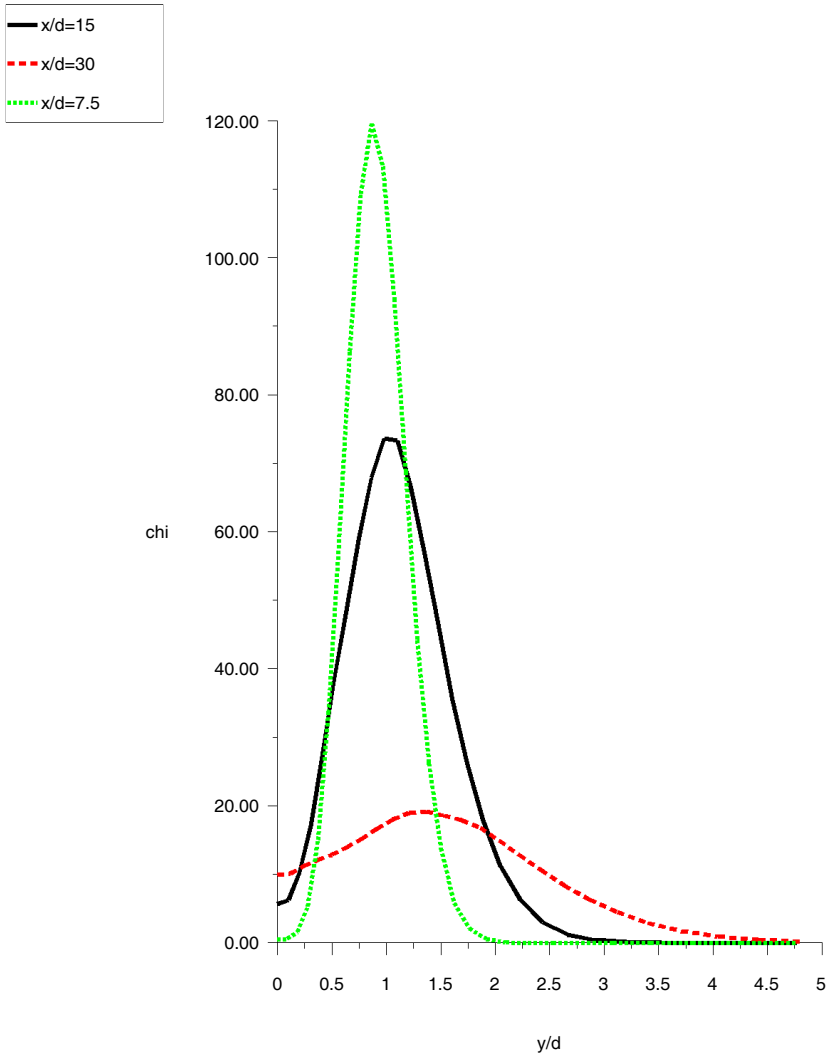

Figure 4: Favre mean scalar dissipation (s^{-1}) against radial distance at different (downstream) axial locations.

Calculated scalar dissipation rate for the Sandia/ETH H_2 jet flame and the flame of Cabra et al.

Renfeng Cao and Stephen B. Pope
Mechanical and Aerospace Engineering, Cornell University,

Five plots are included in this file. Figs. 1-3 are for the Sandia/ETH H_2 jet flame [1-3] and Figs. 4-5 are for the turbulent lifted flame in a vitiated coflow, which is developed by Cabra et al. [4,5].

The flamelet model in the commercial CFD software, FLUENT, is used for calculations of the Sandia/ETH H_2 jet flame. For these calculations, 30 flamelets are used and the maximum value of scalar dissipation for burning flamelet is about 135 (s^{-1}).

Joint velocity-turbulent frequency-composition PDF are used for the H_2/N_2 turbulent lifted flame calculations [6,7]. A detailed chemistry mechanism, the Li mechanism [8] (10 species and 21 reactions), is implemented using ISAT [9]. The EMST mixing model is used in the joint PDF calculations. The liftoff height of this flame is found to be very sensitive to the coflow temperature. The coflow temperature is adjusted to 1033 K for these calculations in order to yield the same liftoff height as the reported measurements [5].

Reference:

1. *R.S. Barlow, Sandia H_2/He Flame Data – Release 2.0, http://www.ca.sandia.gov/TNF , Sandia National Laboratories (2003)*
2. *Barlow, R.S. and Carter, C.D., Combust. Flame 97:261-280 (1994)*
3. *Barlow, R.S. and Carter, C.D., Combust. Flame 104:288-299(1996)*
4. *Cabra R, and Dibble R.W., http://www.me.berkeley.edu/cal/VCB/ , 2002*
5. *Cabra, R., T. Myhrvold, J.Y. Chen, R.W. Dibble, A.N. Karpetis and R.S. Barlow, Proc. Combust. Inst, 29 1881-1888 (2002)*
6. *Masri, A..R.., Cao, R.., Pope, S.B., and Goldin, G.M,, Combust. Theory Model. 8:1-22, 2004*
7. *Cao, R, Pope, S.B., and Masri, A.R,. "Turbulent lifted flame in a vitiated coflow investigated using joint PDF calculations", Combust. Flame (submitted)*
8. *Li, J., Zhao, Z., Kazakov, A., and Dryer, F.L., Fall Technical Meeting of the Eastern States Section of the Combustion Institute, Penn State University, University Park, PA, October 26-29, 2003.*
9. *Pope,S.B., Combust. Theory and Model., 1, 41-63, 1997*

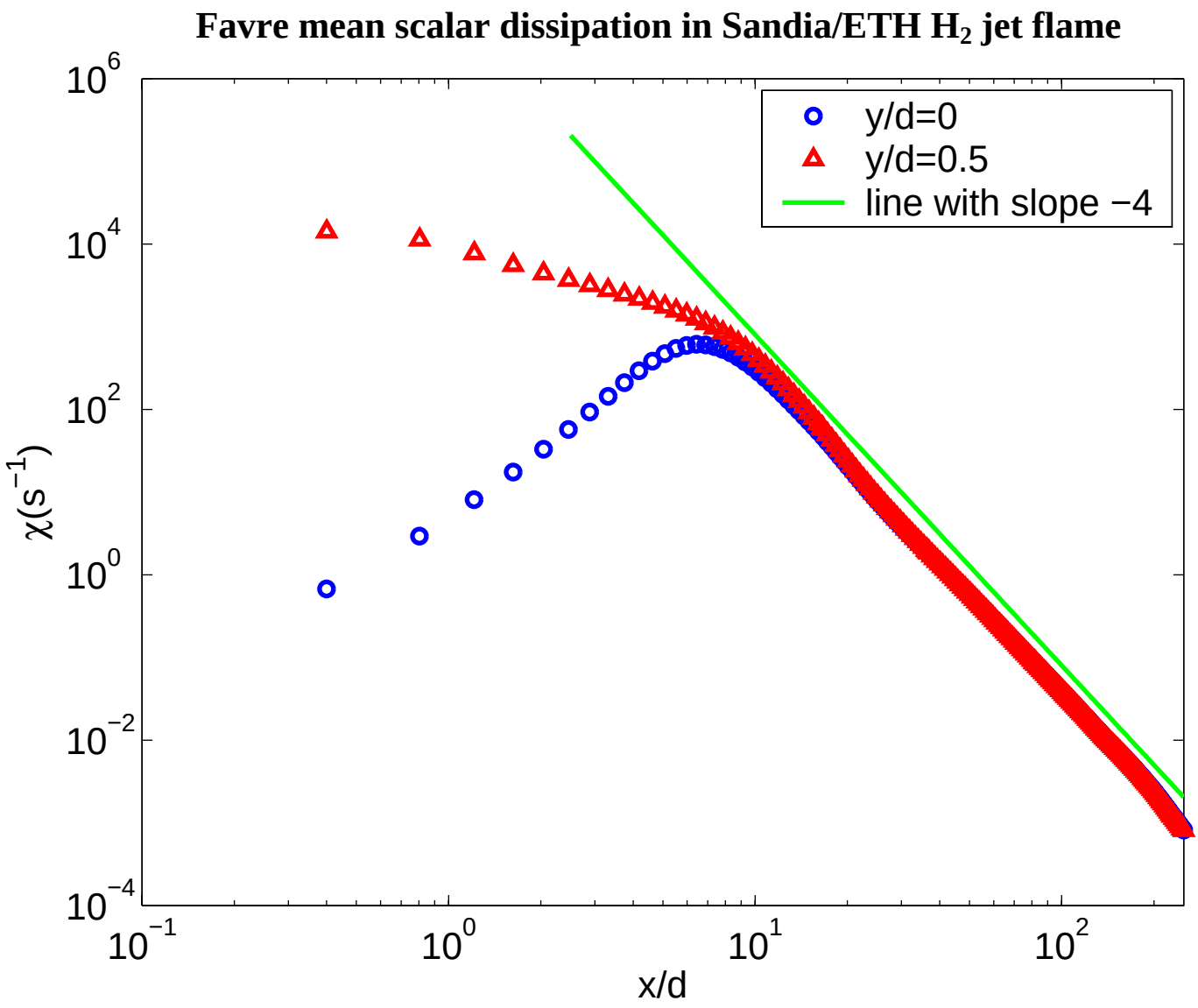

Figure 1: Axial profiles of the Favre mean scalar dissipation rate (s^{-1}) at radial locations y/d=0 and y/d=1/2

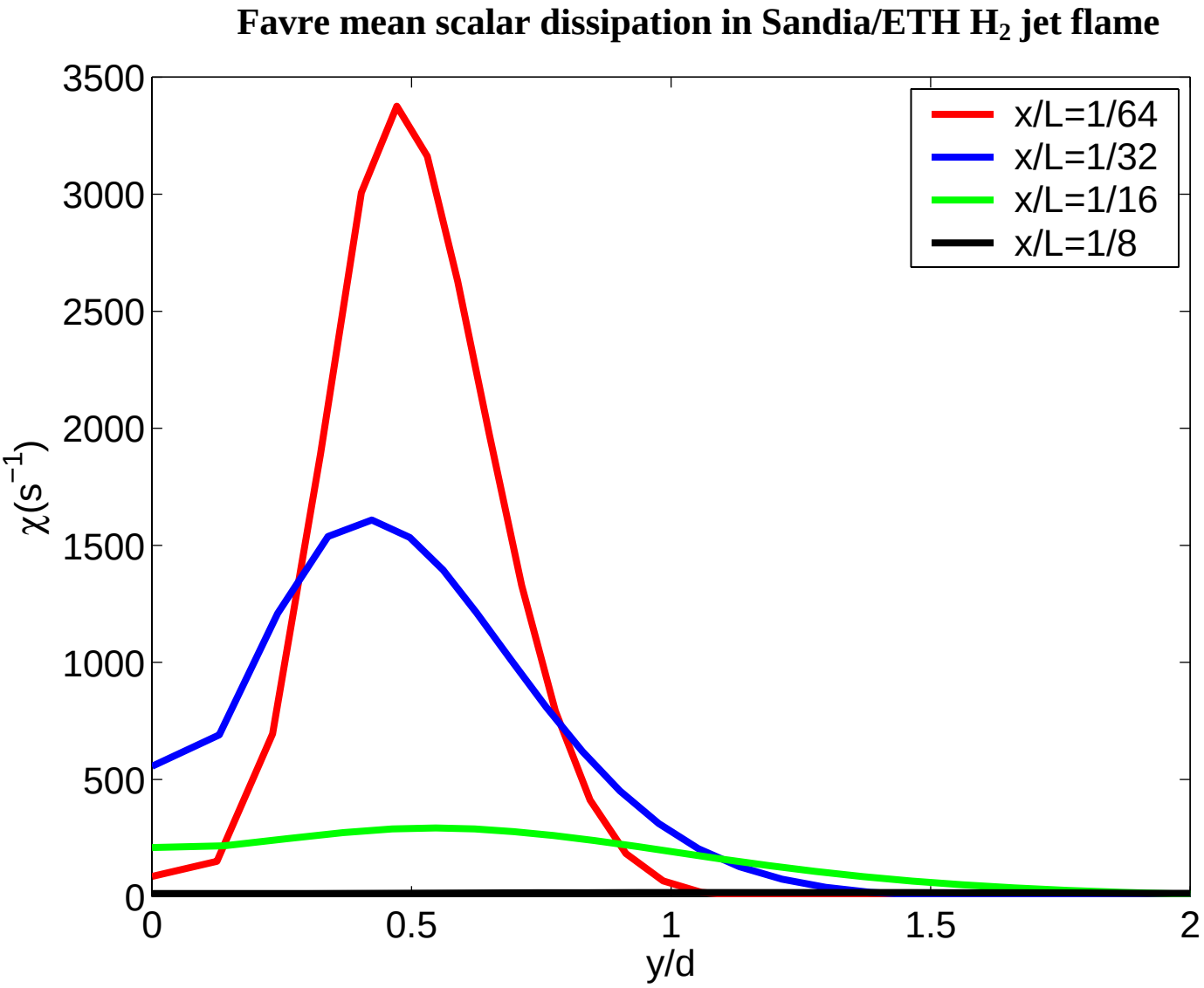

Figure 2: Favre mean scalar dissipation (s^{-1}) against radial distance at different (upstream) axial locations

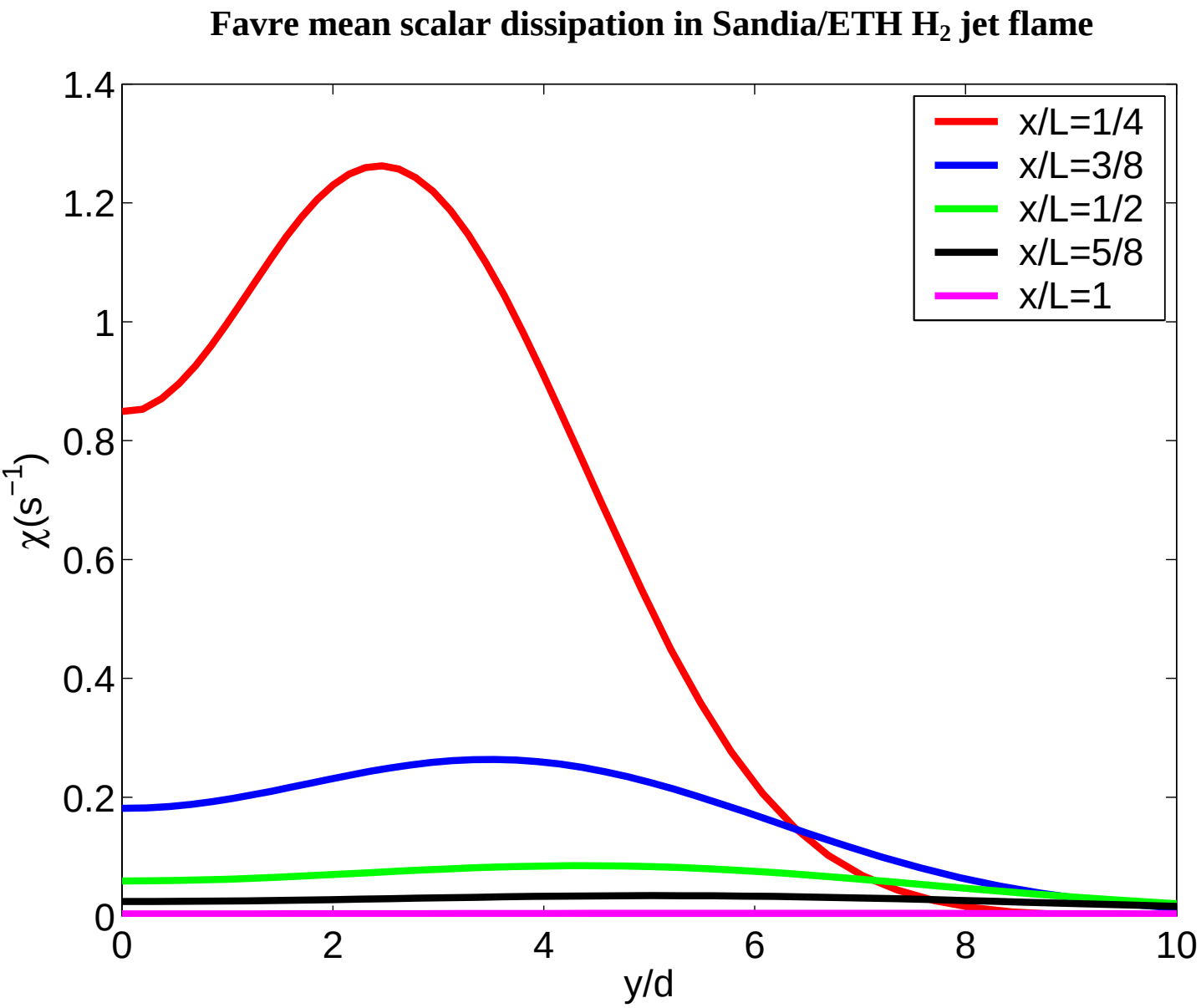

Figure 3: Favre mean scalar dissipation (s^{-1}) against radial distance at different (downstream) axial locations

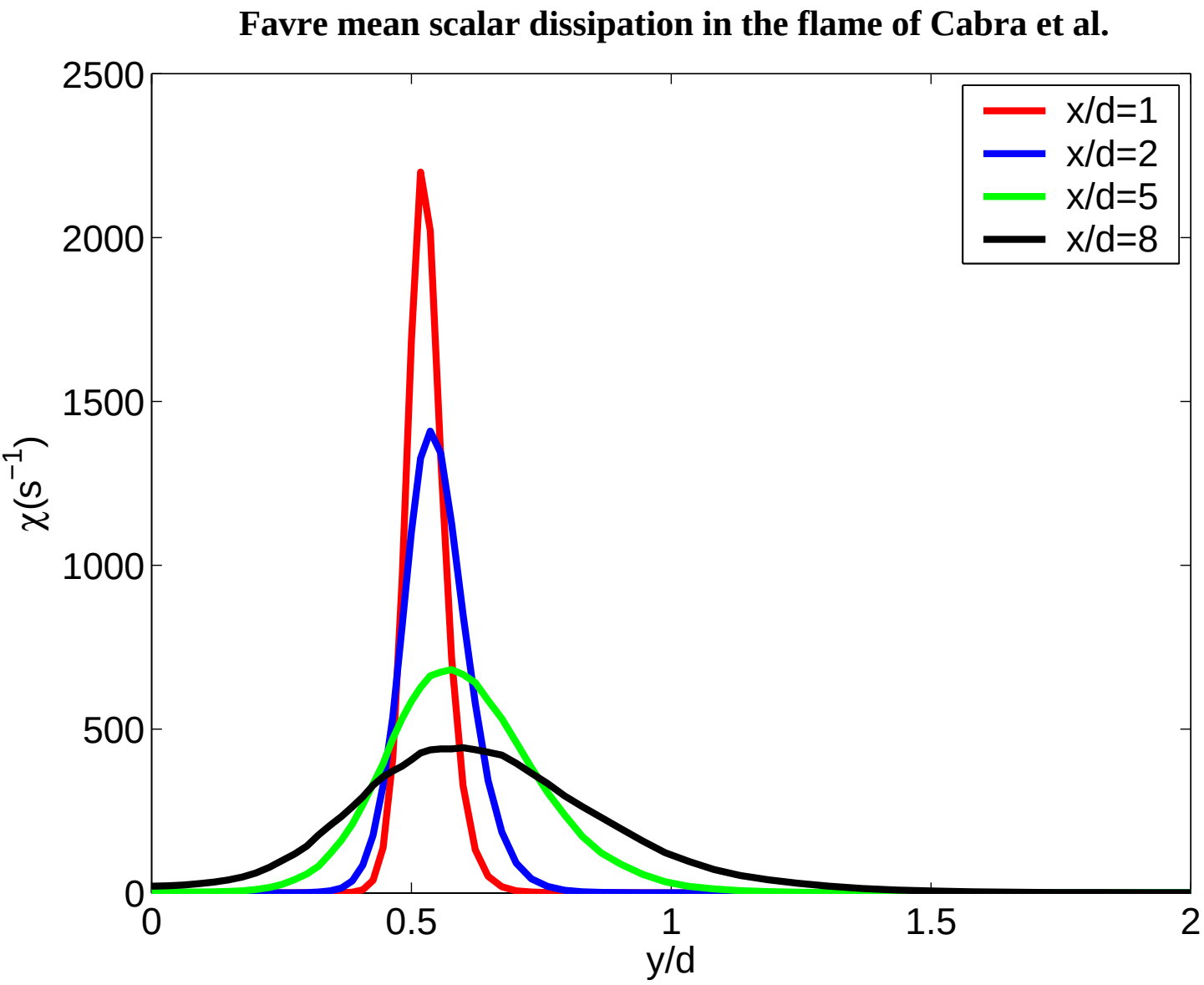

Figure 4 Favre mean scalar dissipation (s^{-1}) against radial distance at different (upstream) axial locations

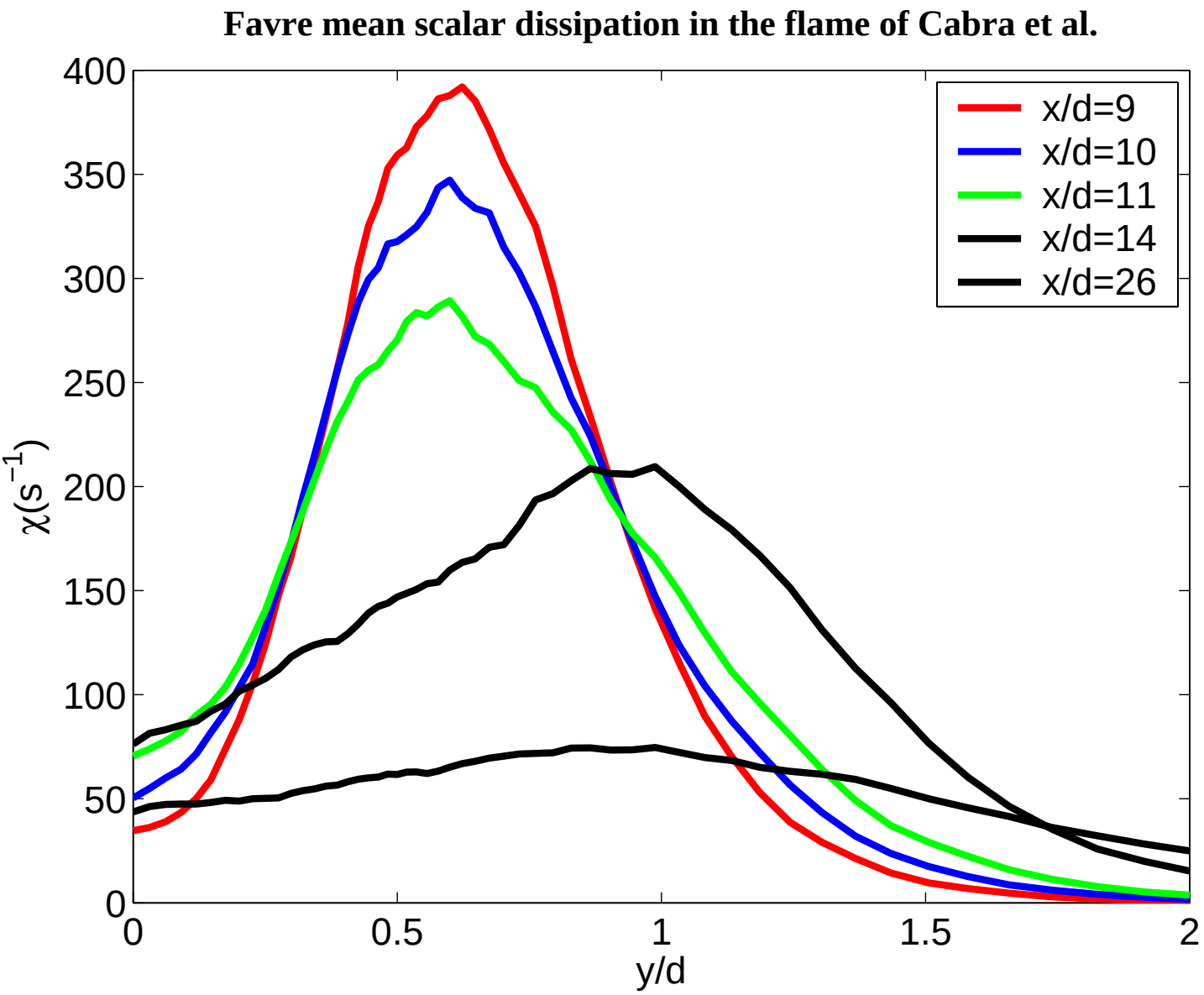

Figure 5: Favre mean scalar dissipation (s^{-1}) against radial distance at different (downstream) axial locations

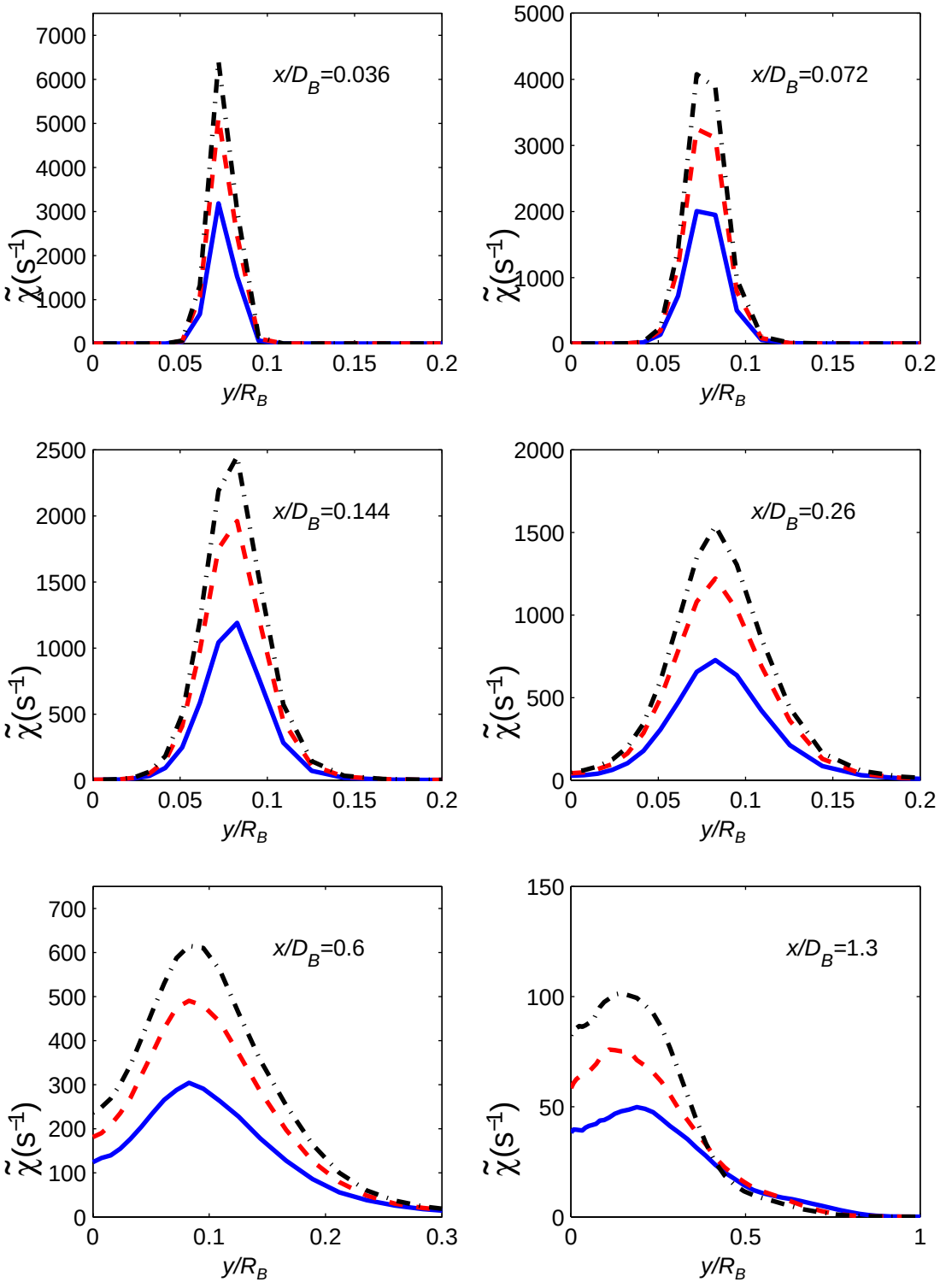

Liu and Pope: Scalar dissipation in bluff-body flames HM1 (solid), HM2 (dash), and HM3 (chain-dash).

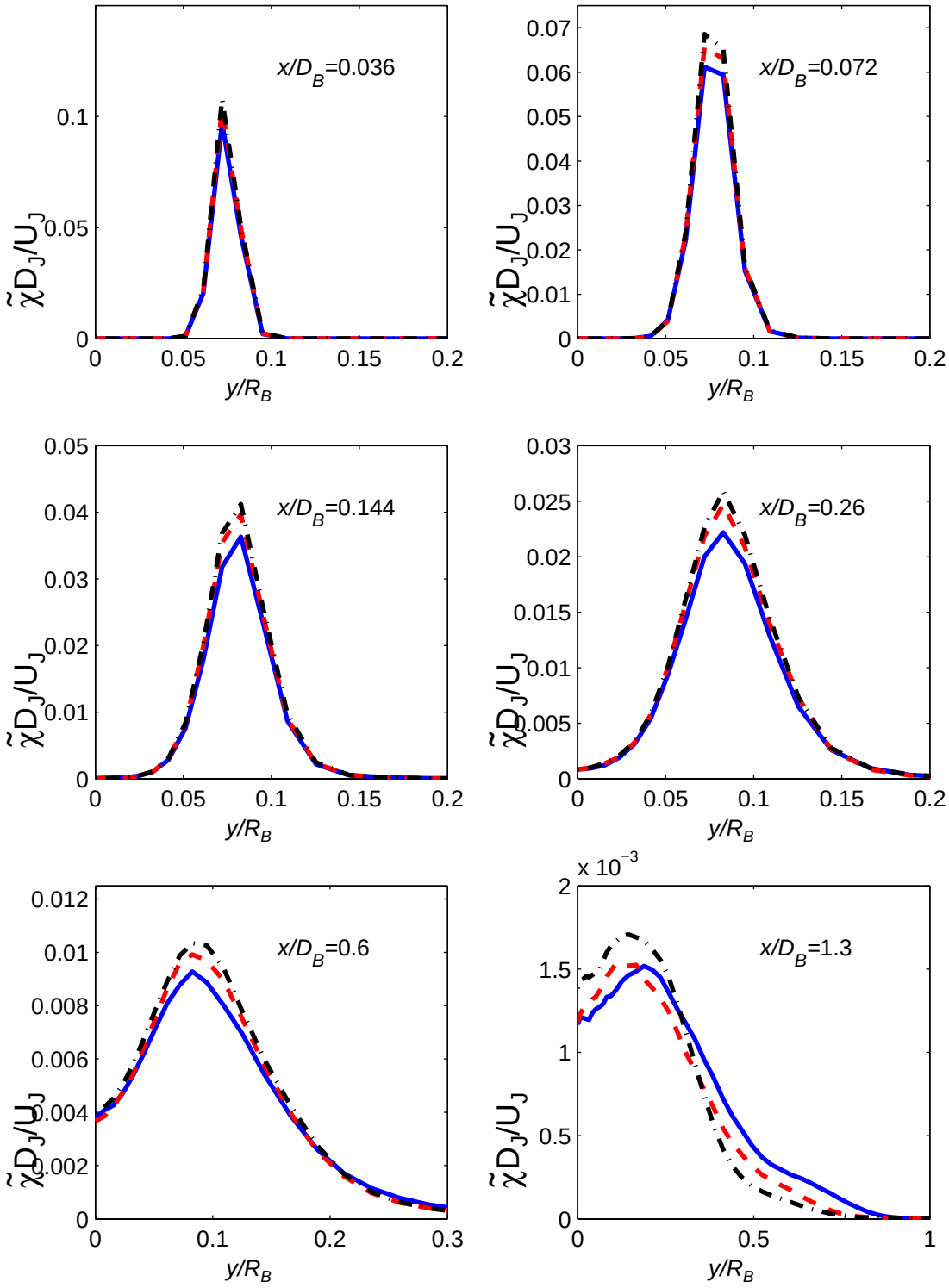

Liu and Pope: Normalized scalar dissipation in bluff-body flames HM1 (solid), HM2 (dash), and HM3 (chain-dash).

TNF7

LES of Combustion

Coordinator
Johannes Janicka

TNF 7, 2004

Structure of the Section

- **Status of Combustion LES**
  - **Progress in the last 2 years**
  - **Non premixed flames, TNF-flames, (premixed flames)**
- **Modelling of finite chemistry effects with LES**
  - **Ability of classical models**
  - **New models, limits, research topics**
- **Quality assessment and V&V of LES**
  - **Assessment of numerical and modelling errors**
  - **Rules for "good"LES**
- **Validation experiments for LES**
  - **Additional experiments**
  - **SGS-model validation**
- **Emerging new LES topics**
  - **Combustion noise**
  - **High resolved LES**

TNF 7, 2004

Status of Combustion LES

- Growing field of research
  - No. of paper
    - → Combustion Symp.
    - → TSFP
- Wide range of application
  - Reacting mixing layer
  - TNF-flames (Flame D is the favourite candidate)
  - Generic GT-combustion (with growing complexity)
  - 2-Phase flow
- Applied models (non premixed)
  - A-B-chemistry
  - Steady flamelets *(deMare & Jones, Kempf & Janicka)*
  - Unsteady flamelets *(Pitsch)*
  - CMC *(Kronenburg)*
  - PDF (FDF) *(Frankel, Pitsch)*

TNF 7, 2004

Status of Combustion LES (cont.)

- Applied models (premixed)
  - Subgrid BML-(Bray-Moss-Libby)-model *(Cant)*
  - Thickened flame front model *(Poinsot)*
  - Linear-Eddy-Model *(Menon, Kerstein)*
  - Level set approach (G-equation) *(Pitsch, Düsing & Janicka)*
  - Partially premixed *(Vervisch)*
- Increasing No. of grid points of CV´s
  - Example EKT
    - → 1996 (TNF 1: Naples): 80.000
    - → 2000 (TNF 5:Boulder): 400.000
    - → 2004 (TNF 7: Chicago): 2000.000

Moors law !

TNF 7, 2004

Predicted Flames EKT

Fuel	Configuration	Re	LES-Reference	Remarks
H_2/N_2	Jet Flame (Tacke, EKT)	10000	Comb, Flow, Turb., 2000	TNF-target-flame
H_2/N_2 (diluted)	Jet Flame (Tacke, EKT)	16000	29th Proc. Comb. Inst., 2002	TNF-target-flame
CH_4/Air (Flame D)	Jet Flame (Barlow, Schneider, EKT)	22400	30th Proc. Comb. Inst., 2004, Comb. & Flame, 2003	TNF-target-flame
CH_4-H_2-N_2	Jet Flame (DLR, Schneider, EKT)	15200	TSFP-2, 2001	TNF-target-flame
CH_4	Bluff Body (Masri, US)	12100 70400	Sub. Comb. & Flame, 2004	TNF-target-flame
CH_4	Opp. Jet (Imperial Coll. group, Geyer, EKT)	7200 5500	28th Proc. Comb. Inst., 2000, 30th Proc. Comb. Inst., 2004	TNF-target-flame
Natural Gas	Premixed swirl burner	40000	TSFP-3, 2003	complex configuration
Natural Gas	Premixed slot burner ORACLES-Burner	25000	Sub. Comb. & Flame, 2004	thin reaction regime
Natural Gas	Turbomeca Swirler in pressurized rig	46000	Work in progress	technical configuration
-NR-	Jet in a Crossflow (Rodi)	21000 10500	TSFP-2, 2001	complex configuration

Predicted Flames EKT

Fuel	Configuration	Re	LES-Reference	Remarks
H_2/N_2	Jet Flame (Tacke, EKT)	10000	Comb, Flow, Turb., 2000	TNF-target-flame
H_2/N_2 (diluted)	Jet Flame (Tacke, EKT)	16000	29th Proc. Comb. Inst., 2002	TNF-target-flame
CH_4/Air (Flame D)	Jet Flame (Barlow, Schneider, EKT)	22400	30th Proc. Comb. Inst., 2004, Comb. & Flame, 2003	TNF-target-flame
CH_4-H_2-N_2	Jet Flame (DLR, Schneider, EKT)	15200	TSFP-2, 2001	TNF-target-flame
CH_4	Bluff Body (Masri, US)	12100 70400	Sub. Comb. & Flame, 2004	TNF-target-flame
CH_4	Opp. Jet (Imperial Coll. group, Geyer, EKT)	7200 5500	28th Proc. Comb. Inst., 2000, 30th Proc. Comb. Inst., 2004	TNF-target-flame
Natural Gas	Premixed swirl burner	40000	TSFP-3, 2003	complex configuration
Natural Gas	Premixed slot burner ORACLES-Burner	25000	Sub. Comb. & Flame, 2004	thin reaction regime
Natural Gas	Turbomeca Swirler in pressurized rig	46000	Work in progress	technical configuration
-NR-	Jet in a Crossflow (Rodi)	21000 10500	TSFP-2, 2001	complex configuration

TNF 7, 2004

Steady LES-Flamelet-Model: D-Flame

Mixture fraction

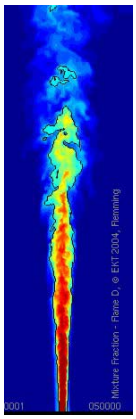

Temperature

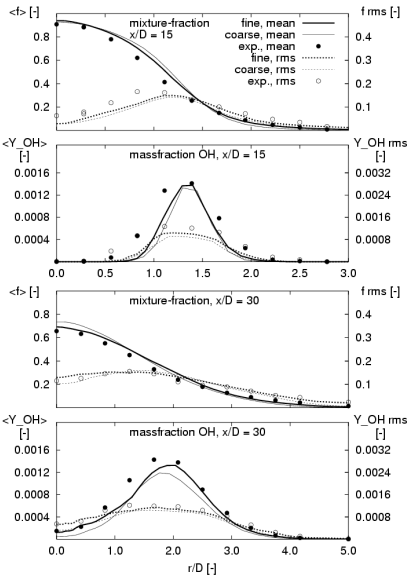

Kempf et. al. (2004)

TNF 7, 2004

Steady LES-Flamelet-Model: D-Flame

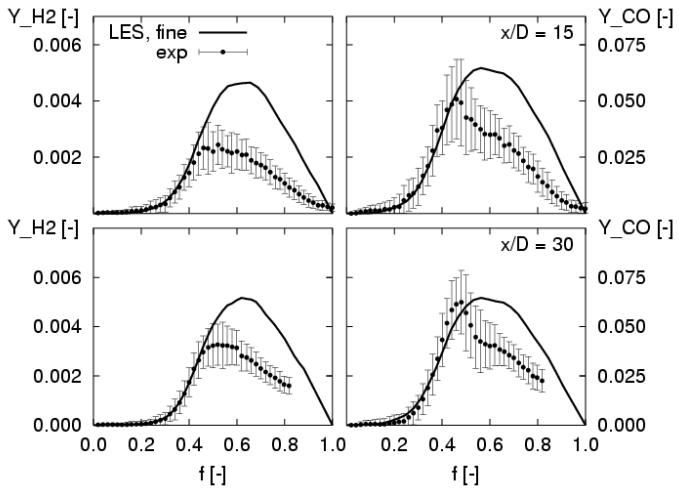

TNF 7, 2004

Turbomeca Swirler: LES-Results

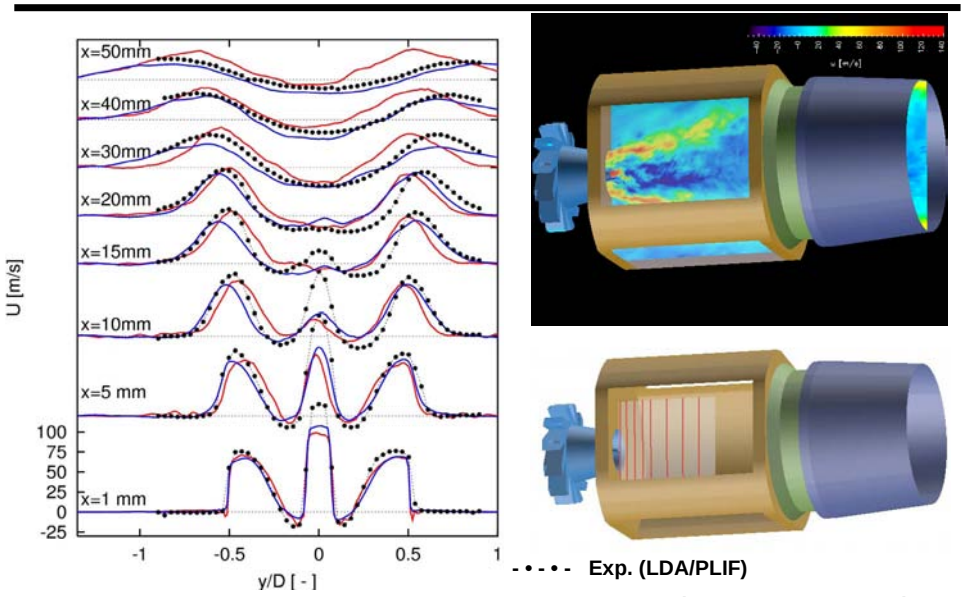

TNF 7, 2004

Turbomeca Swirler: LES-Results

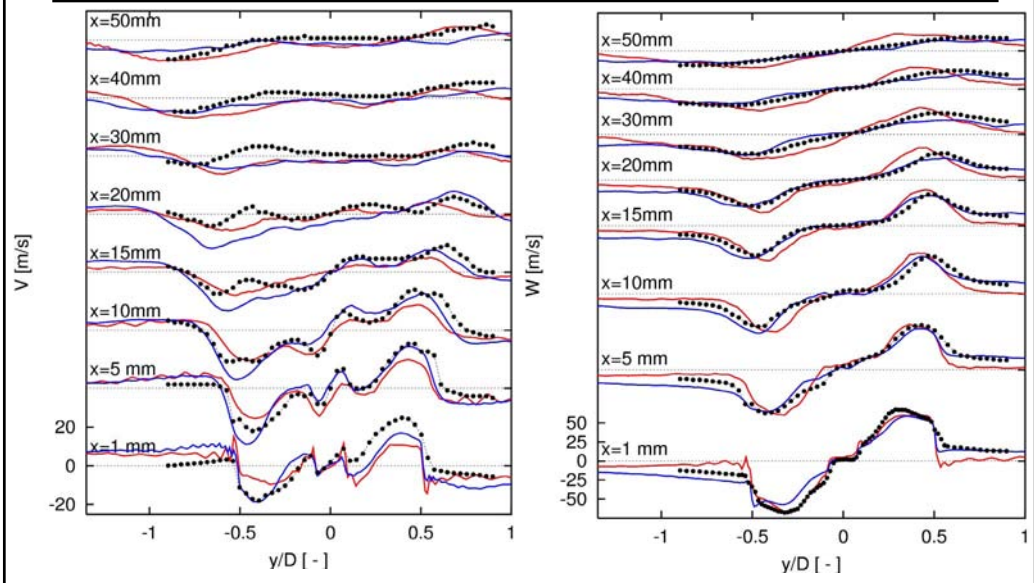

TNF 7, 2004

Turbomeca Swirler: LES-Results

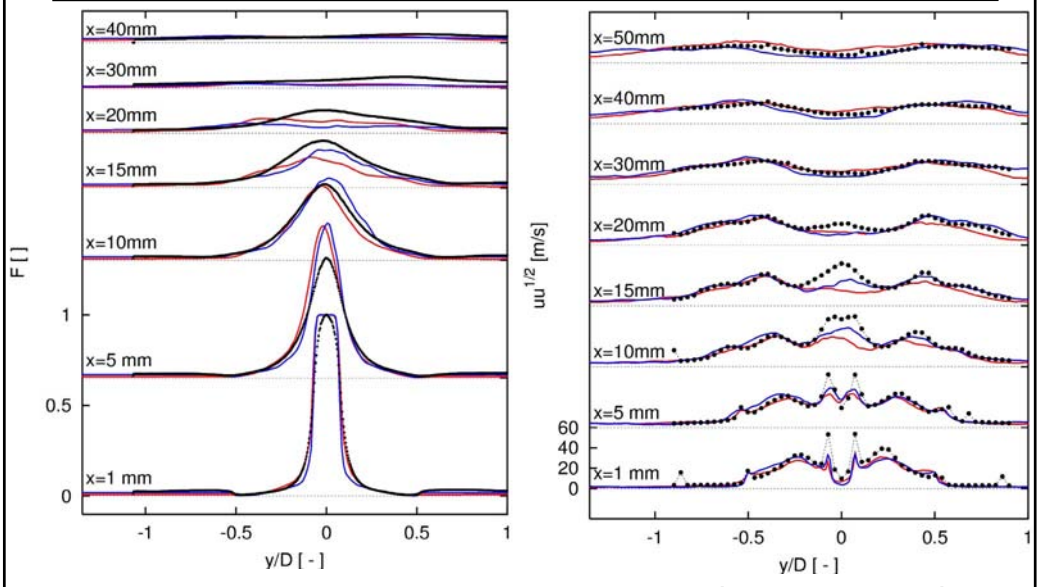

Turbomeca Swirler: LES-Results

Prerequisite for swirling flows

- Precessing vortex core →recirculation zone in the inflow nozzle
- Swirler must be resolved
- Unsteady method
- Flows with week swirl have different characteristics

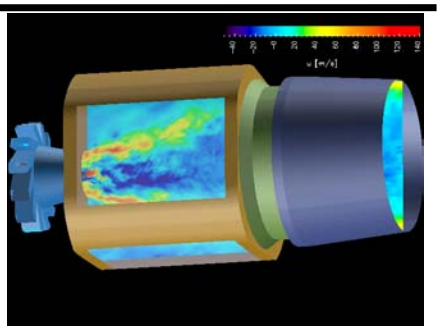

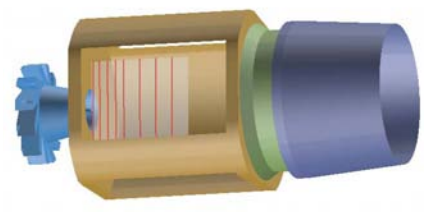

FLUENT's LES/PDF Calculations of Piloted Methane/Air Jet Flame D (Results from Steve Frankel, Purdue)

- **Combustion Model: Partially premixed.**
- **Chemistry: Equilibrium; assumed PDF with 11 species.**
  - **Discrepancies in LES predictions of scalars; attributed to equilibrium chemistry.**
  - **Good flow predictions.**

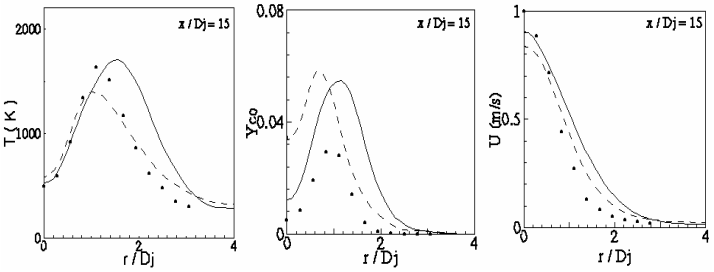

Symbols: experiment; lines: Computations; RANS/PDF (solid), LES/Partially Premixed (dashed).

- **Current Work:**
  - **Combustion Model: Composition Joint PDF**
  - **Chemistry: 9-species, 5-step mechanism**

Structure of the Section

- Status of Combustion LES
  - Progress in the last 2 years
  - Non premixed flames, TNF-flames, (premixed flames)
- **Modelling of finite chemistry effects with LES**
  - **Ability of classical models**
  - **New models, limits, research topics**
- Quality assessment and V&V of LES
  - Assessment of numerical and modelling errors
  - Rules for "good"LES
- Validation experiments for LES
  - Additional experiments
  - SGS-model validation
- Emerging new LES topics
  - Combustion noise
  - High resolved LES

Finite Chemitry Effects: Introduction

- **Prediction quantities**
  - **Minor species**
    - **→OH**
    - **→CO, H2 in rich regime**
  - **Extinction**
  - **Reignition**
  - **Ignition, ignition delay**
  - **(not lifted flames)**
- **Challenge**
  - **Steady flamelet model not sufficient to predict these effects**
  - **Laminar flame analysis suggests a „large“ number (10-20) of reactive species necessary to predict these phenomena**
  - **Classical finite chemisty models (PDF (FDF), CMC, LEM, unsteady flamelets) can be applied in the LES framework (prove of principles)**
  - **These methods are extreme expensive (few mill. Grid points with 50-100 particles in a cell)**

TNF 7, 2004

Finite Chemitry Effects: Perspective

- **(Any finite chemistry effect needs different consideration !)**
- **Relax and wait for faster computers (we know the principle solution!)**
  - **Every two years a new paper with the same model (but more reaction, particles, CV,……)**
- **Adaptivity of detailed chemistry**
  - **Idea: Flames are 2-D: only in same 10000 cells (of a few mill.) detailed chemistry is necessary**
  - **In CMC environment easy to implement: take a crude grid for the chemistry → next**
- **More physics (asymptotics)**
  - **Idea: In LES framework more (time dependent, spatially resolved) information are available**
  - **Use of these information for predicting phenomena**

TNF 7, 2004

Andreas Kronenburg

TNF 7, 2004

Conditionally Filtered Transport Equations

The conditionally filtered species transport equations can be written as

$$\frac{\partial \overline{Y|\eta}}{\partial t} + \overline{\underline{u}|\eta}\,\nabla \overline{Y|\eta} + \frac{\nabla \cdot \left(\rho_\eta \overline{\underline{u}"Y"|\eta} P\right)}{\overline{\rho|\eta}\ P} - \overline{N|\eta}\,\frac{\partial^2 \overline{Y|\eta}}{\partial \eta^2} = \overline{W|\eta} \qquad \text{Eq. 1}$$

which is identical in form to the CMC transport equations for conditionally averaged quantities. η denotes the sample space of mixture fraction and the conditional filter for scalar ϕ is defined by

$$\overline{\phi|\eta} = \frac{\int \phi\psi\left(\xi(x',t)-\eta\right)G\left(x-x',\Delta\right)dV}{P(\eta)} \qquad \text{Eq. 2}$$

Page no./ref

TNF 7, 2004

Closures

The assumptions employed in Eq. (1) are

1) Analogy between particle diffusion in conserved scalar space and Markov process

2) Diffusive term in pdf transport equation has been neglected

Further closures for conditionally averaged reaction rate, velocity and scalar dissipation are

1. 1st order closure for the reaction rate $\overline{W|\eta} = W\left(\overline{Y_i|\eta}\right)$

2. The spatial variation of the conditional moments is much smaller than the spatial variation of unconditionally filtered quantities, hence LES cells are much smaller than CMC cells. Homogeneity and smoothness of the conditional moments within one CMC cell are assumed and the conditional scalar dissipation and the conditional velocity can be obtained from the unconditional values.

3. Conditional fluctuations are negligible.

Computations of Sandia Flame D

2nd order explicit solver for compressible flow (BOFFIN) in Cartesian co-ordinates

LES sgs-models:	Smagorinsky model for the turbulent viscosity, where the proportionality constant is determined dynamically. The turbulent Schmidt number is 0.4
LES grid:	92x92x200
CMC grid:	4x4x40
Chemical Mechanism:	reduced CH_4-mechanism with 21 species based on detailed 48 species, 300 reactions CH_4-mechanism

Computational requirements: approx. 650 CPU hrs for 10 ms

approx. ¼ LES, ¾ CMC

Results for Sandia Flame D (CO)

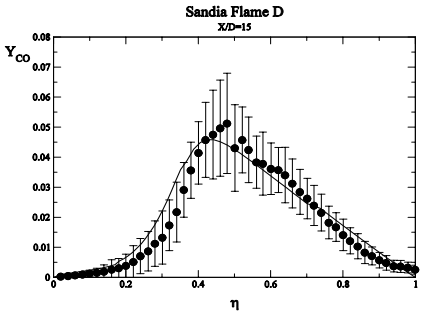

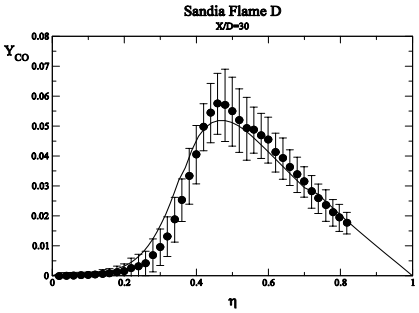

Results for Sandia Flame D (H_2)

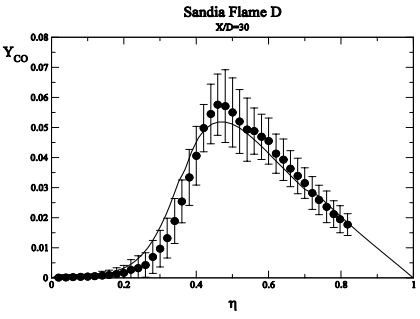

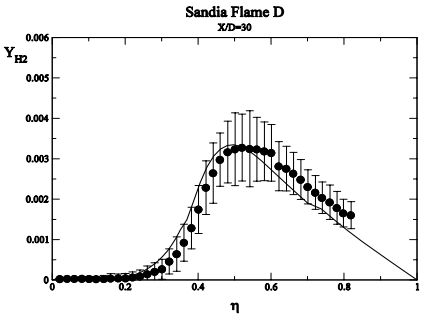

Structure of the Section

- Status of Combustion LES
  - Progress in the last 2 years
  - Non premixed flames, TNF-flames, (premixed flames)
- Modelling of finite chemistry effects with LES
  - Ability of classical models
  - New models, limits, research topics
- Quality assessment and V&V of LES
  - Assessment of numerical and modelling errors
  - Rules for “good”LES
- Validation experiments for LES
  - Additional experiments
  - SGS-model validation
- Emerging new LES topics
  - Combustion noise
  - High resolved LES

TNF 7, 2004

Quality assessment (V&V)

- Classical V&V
  - Provides information about numerical and modeling errors
  - 3 Different solution on different grids
  - Richardson extrapolation (4th solution free of charge, error order)
  - → Estimation of numerical errors (verification)
  - Comparison with experiments (or DNS)
  - Include error bars
  - → Estimation of modelling errors (validation)
  - → Deduce an index of quality

TNF 7, 2004

Quality assessment (V&V)

- Classical V&V not feasible for LES (?)
  - Implicit filtering is the preferred description
    - → Smallest sum of numerical and modelling error (hopefully)
    - → No distinction between both errors
    - → Go to explicit filtering ?
  - Reduction of grid size by a factor of 2 extents computation time by a factor of 16 (the phd student is gone)
  - Stronger interaction between model and numeric e.g.
    - → Numerical accuracy of scalar equation
    - → Density treatment of schemes based on low Mach-No formulation
    - → Averaging and clipping of coefficients in dynamic procedures
- Compared to RANS-Models the status of CLES is less complete *(Pope (2003))*
  - Ratio of resolved to total kinetic energy is not constant in the computational domain
  - Turbulence resolution length scale varies
- Objective: Quality assessment of LES directly during the computation run or with additional reasonable additional effort

TNF 7, 2004

Analysis of Resolved Part of turbulent Kinetic Energy

- Calculation of ratio $RES_K = K_{RES}/(K_{RES}+K_{SGS})$
- K_{SGS} e.g. by Lilly
  - $K_{SGS} = C_1 * \nu_t^2 / (\Delta)^2$
  - ν_t by dynamic procedure

→ RES_k values of 0.8 -0.85 suggest a reasonable resolved LES

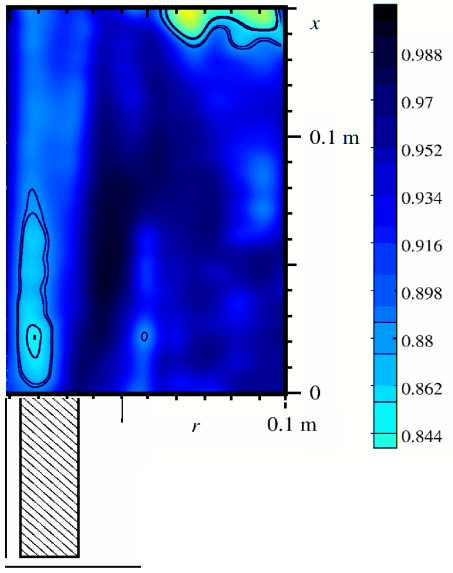

TNF 7, 2004

Structure of the Section

- Status of Combustion LES
  - Progress in the last 2 years
  - Non premixed flames, TNF-flames, (premixed flames)
- Modelling of finite chemistry effects with LES
  - Ability of classical models
  - New models, limits, research topics
- Quality assessment and V&V of LES
  - Assessment of numerical and modelling errors
  - Rules for "good"LES
- Validation experiments for LES
  - Additional experiments
  - SGS-model validation
- Emerging new LES topics
  - Combustion noise
  - High resolved LES

TNF 7, 2004

Validation experiments for LES

- **Scientific question**

  What typ of validation experiments do we need for combustion LES ?
- **Classical one-point information *(Barlow)***
  - **One-point velocity and scalar moments**
  - **Pdf´s**
  - **boundary conditions (very often not the available)**

    →Desirable: measurements in nozzle or swirler
- **LES offers spatial and temporary information → should be utilized for validation**
  - **Spatial and/or temporary correlations *(Dreizler)***

TNF 7, 2004

Validation experiments for LES

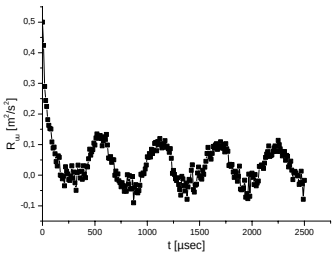

Autocorrelation function

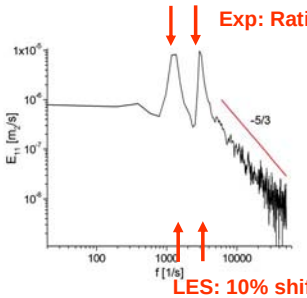

LES: 10% shift in frequency
Ratio 2.1

TNF 7, 2004

Validation experiments for LES

- Scientific question

  What typ of validation experiments do we need for combustion LES ?
- Classical one-point information *(Barlow)*
  - One-point velocity and scalar moments
  - Pdf´s
  - boundary conditions (very often not the available)
    - → Desirable: measurements in nozzle or swirler
- LES offers spatial and temporary information → should be utilized for validation
  - Spatial and/or temporary correlations *(Dreizler)*
  - **Gradients of velocity and scalars**
  - **Scalar-dissipation rate**
- **Future challenge**
  - **Experimental methods for combustion SGS-validation**
    - → **Structural information (correlation factor, anisotropy level)**

TNF 7, 2004

Structure of the Section

- Status of Combustion LES
  - Progress in the last 2 years
  - Non premixed flames, TNF-flames, (premixed flames)
- Modelling of finite chemistry effects with LES
  - Ability of classical models
  - New models, limits, research topics
- Quality assessment and V&V of LES
  - Assessment of numerical and modelling errors
  - Rules for “good”LES
- Validation experiments for LES
  - Additional experiments
  - SGS-model validation
- Emerging new LES topics
  - Combustion noise
  - High resolved LES

TNF 7, 2004

Emerging new LES topics

- **Combustion noise**
  - Prediction of noise emissions of combustion sytems is a future challange
    - → Thermo- acoustic instabilities is a subset of noise emission prediction
  - Interesting from a funding perspective
    - → Funding for combustion research may be reduced in future
    - → Noise emission is field of growing importance for all industrialized countries
  - LES is suitable method to resolve the important part of noise emissions
- **Combustion noise prediction**
  - Compressible formulation
    - → Expensive
  - Incompressible formulation and combination with CAA-methods
    - → Taking sources for combustion noise from incompressible LES
    - → Feeding this information in CAA framework (Lighthill formulation, LEE)
    - → Advantage: Inexpensive, fulfil different numerical requirements

TNF 7, 2004

LES of DLR-A flame sound
(Re=15,200, Ma=0.12)

Steve Frankel

- Equations: **Favre-filtered compressible NSE, Z**
- Numerics: **4th RK time, optimized 6th-order compact finite-difference for axial/radial direction with Fourier pseudospectral for azimuthal direction**
- Boundary conditions: **random forcing; non-reflecting characteristic BCs with exit buffer zone**
- SGS Models:
  - **Dynamic Smagorinsky model for stresses/scalar flux**
  - **Steady laminar flamelet model with state relationships from experimental mean flame statistics for combustion**
- Computation domain: **120R X 80R (w/ 70R exit zone)**
- Grid: **480 X 192 X 32; radial stretching**

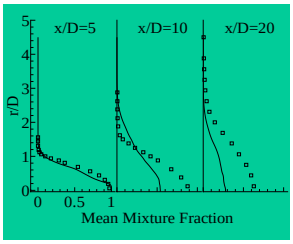

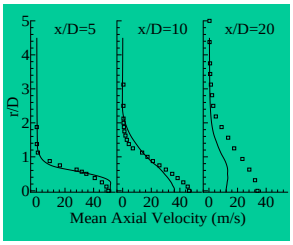

CO_2 with Z_{st} contour

Experimental data from Sandia TNF website: http://www.ca.sandia.gov/TNF/DataArch/DLRflames.html

Sound prediction for DLR-A flame

Steve Frankel

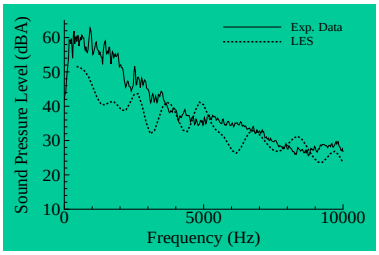

Far-field sound spectra with comparison to data

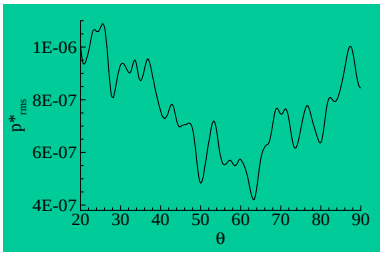

Far-field sound directivity(source location x/R=6; receiver location x/R=39; angle measured from the positive x-axis)

High resolved Combustion LES

- Approaches were published in recent years, which have features of both DNS and LES, e.g. *(Oefelein(2003), Kempf et. al. (2003,2004))*
  - DNS of flow field ($\Delta \sim \eta$), modelling of combustion, or
  - LES with small SGS-viscosity (ν_{SGS} < (<) ν)
- Possible application
  - Provide better models for χ, *P(f),* $\tilde{f}''^2$ in nonpremixed combustion
  - Effects of flame front wrinkling in premixed combustion
    - → $\Delta \sim \eta$, $\Delta > l_f$, $\Delta < l_G$
  - Estimation of effect of spatial averaging of experiments
  - Interesting approach for future research: Embedded DNS
    - → DNS of a small domain of a technical combustion system
    - → Boundary condition from LES of complete system
    - → Closing the gap between DNS and experiments

TNF 7, 2004

Turbulent Opposed Flames

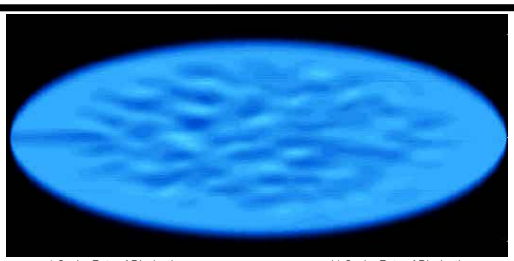

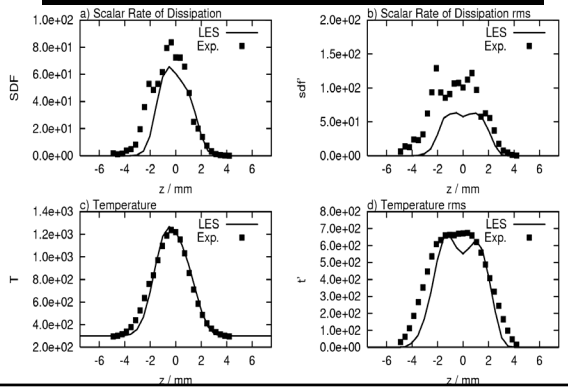

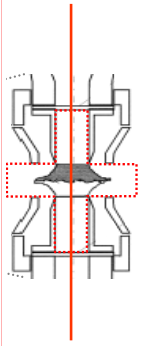

TNF 7, 2004

Smart Reduction of Computation Domain

- Reduction of computational domain by a factor of e.g. 2 in every direction
- Feasible for jet flame prediction
- Flame D
- 2.0 mill. CV for both simulations

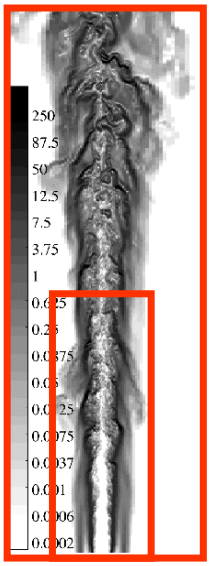

Standard domain

Reduced domain

TNF 7, 2004

Smart Reduction of Computation Domain

- Reduction of computational domain by a factor of e.g. 2 in every direction
- Feasible for jet flame prediction
- Flame D
- 2.0 mill. CV for both simulations

→ Expectation: Both predictions should show small deviations

→ Conclusion: Sum of modelling and numerical errors is small

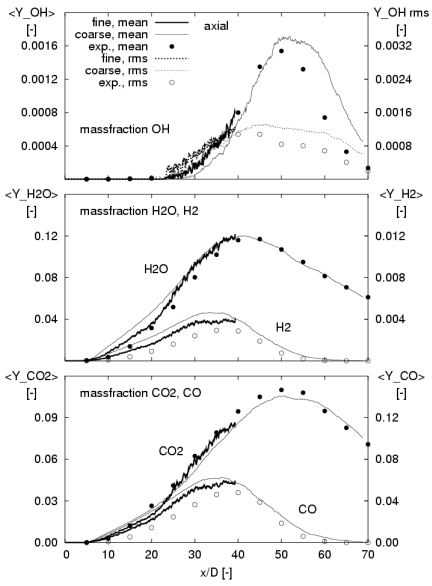

TNF 7, 2004

Linking DNS, LES, RANS and Experiments

Coordinator: Luc Vervisch

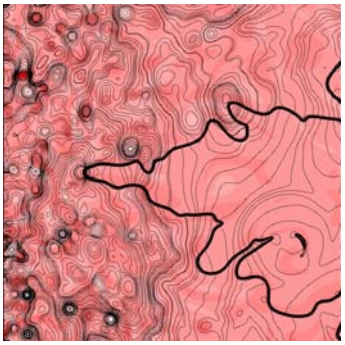

- **Resolution for "real" DNS**
- **TNF structure**
- **DNS and experiments (spray)**
- **LES and experiments**
- **Premixed turbulent combustion**
- **Scalar dissipation rate a possible perspective…**

Contribution from: J.H. Chen, E.R. Hawkes, C.A. Kennedy, S.D. Mason, J.C. Sutherland, Y. Mizobuchi, N.Chakraborty, S. Cant, Andreas Kempf, Dirk Geyer, Andreas Dreizler, Johannes Janicka, Pascale Domingo, Julien Réveillon.

Resolution needed for real combustion DNS:

- **Flow resolution:**

$$\eta_k \approx \frac{l_t}{Re_\lambda^{3/2}}$$

$$10^{-6}\,\mathrm{m} < \eta_k < 10^{-4}\,\mathrm{m}$$

For a 1 cm^3 simulation:

$$10^6 < N < 10^{12}$$

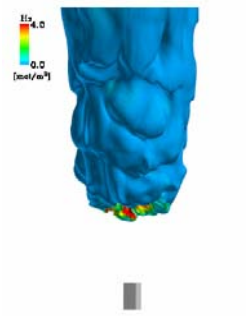

Mizobuchi et al, Proc. Combust. Inst. 2002

Re_λ	Memory	Speed	Year
70	50 Gbytes	50 Gflops	1993
300	50 Tbytes	50 Tflops	2002
1500	50 Pbytes	50 Pflops	2015?

J. Jiménez, Eng. Turbulence Modelling and Experiments-5, 2002

Resolution needed for real combustion DNS:

- **Flame resolution:**

  Reference freely propagating methane-air stoichiometric premixed flame with PREMIX, GRI and complex transport properties:

$$h \approx 5.10^{-6}\mathrm{m} \qquad \Delta t \approx 1.10^{-6}\mathrm{s}$$

Even with simplified chemistry, with 'real' viscosity the mesh size stays very small…

For a 1 cm^3 simulation depending on the fuel:

$$10^8 < N < 10^{12}$$

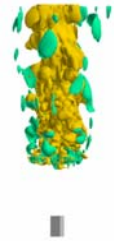

Jet-flame DNS: 3 cm^3 by Mizobuchi et al. (200 Millions nodes)

So far, three types of DNS:

- **DNS of synthetic model problem (freely decaying turbulence).**
- **DNS of laboratory flame, but at much lower Re.**
- **DNS of laboratory flame.**

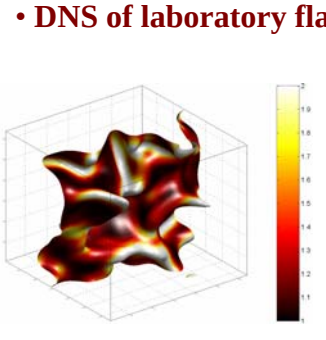

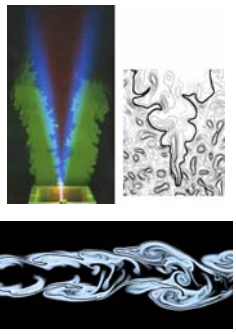

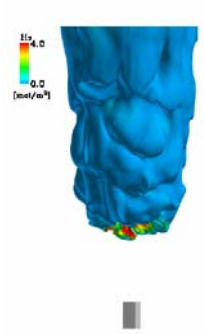

Synthetic problem **Laboratory flame at lower Re** **Real jet-flame**

Chemistry:
- **Single-step**
- **Reduced**
- **Tabulated**
- **Detailed**

Transport:
- **Fixed Lewis and Schmidt**
- **Variable Lewis & Schmidt**
- **Complex**

FLAME MODELING ANALYSIS FROM DNS:

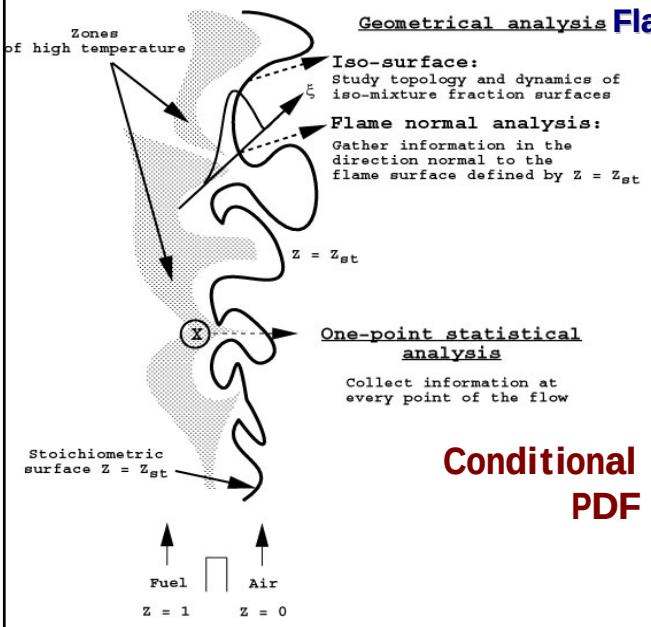

Flame surface density
G-Eq or c-Eq

Flamelet modeling

Conditional Moment Closure
PDF modeling

Nonpremixed DNS Datasets

James C. Sutherland & Jacqueline H. Chen

- **Spatially-evolving nonpremixed jets:**
  - Provide *statistically stationary* results
- **Datasets (500K – 2.5 Million nodes):**
  - CO/H2 Jets
    - Detailed chemical kinetics
    - With & without extinction
  - CH4/H2 Jets
    - Reduced kinetic mechanism (17 species, 13 reactions)
- **Questions addressable:**
  - Differential Diffusion effects
  - Chemistry/flow field interaction
  - Effects of curvature on flame structure, diff-diff, etc.
  - Finite-rate chemistry effects & model evaluation

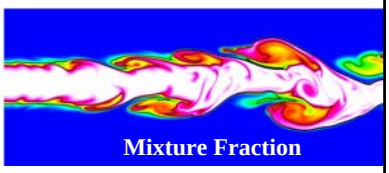

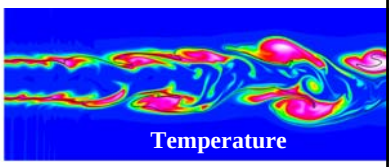

Is the "finite rate chemistry" concept enough to get the meaning of life?

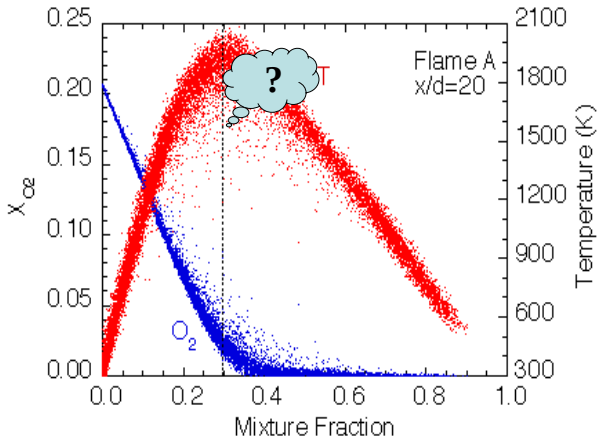

Pickett and Ghandhi, Combust. Flame 132 (2003) 138-156

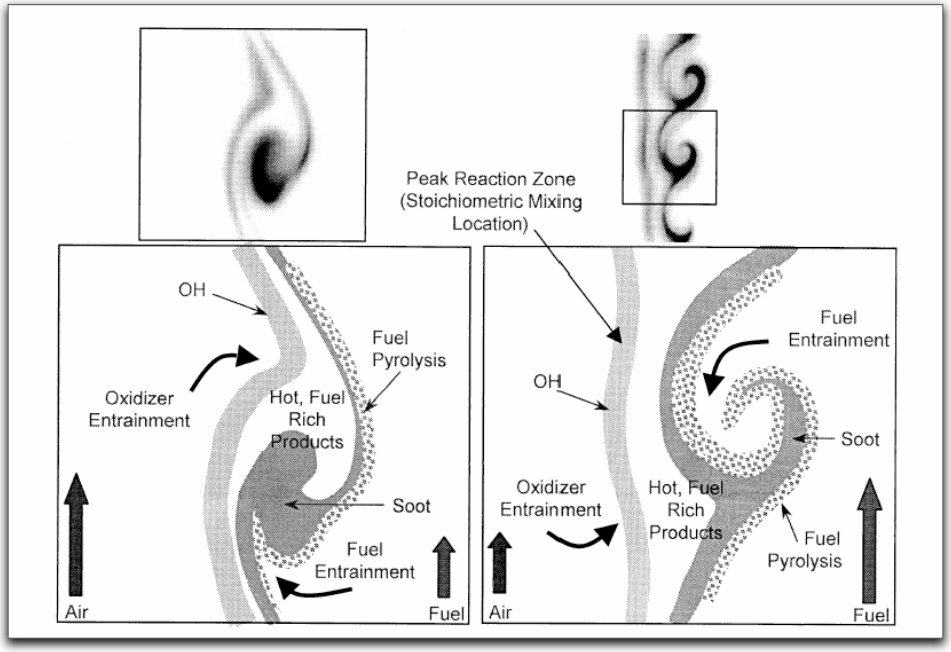

Dilution by burnt gases:

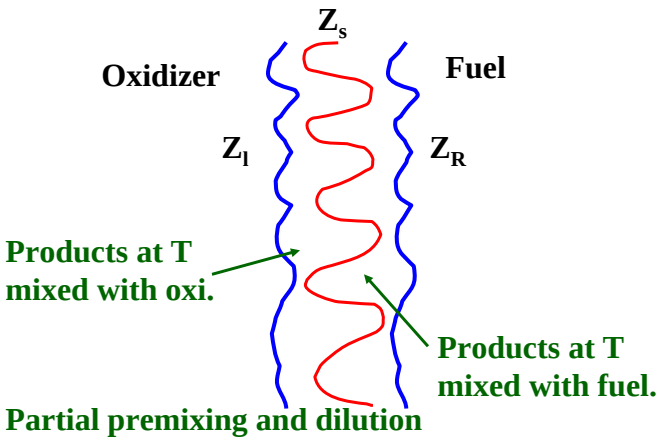

Dilution by brunt gases:

G. Fereira, 1996, Zurich & S. Pope's talk

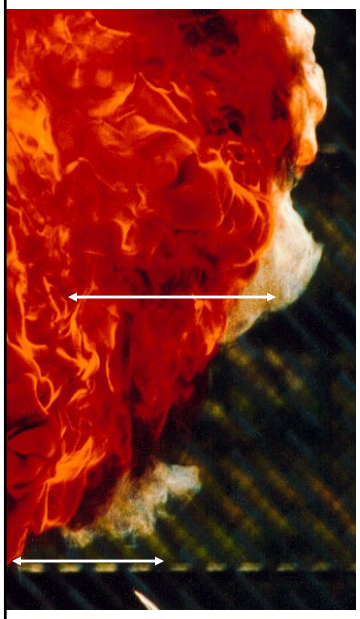

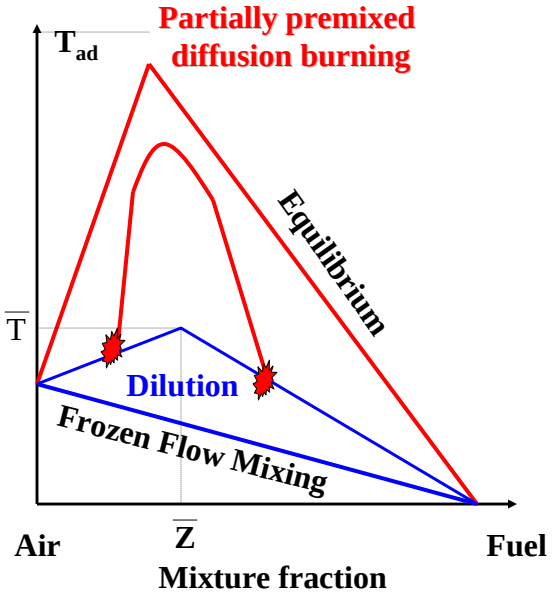

Summary of TNF-DNS observations:

(1) Cold flow partial premixing:

Pure Fuel and pure Oxidizer are mixed before burning.

(2) Dilution of reactants by burnt gases:

Turbulent diffusion mixes Fuel with products and Oxidizer with products before they meet within reaction zones.

Cold flow partial premixing:

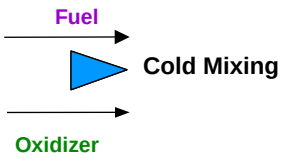

Turbulent

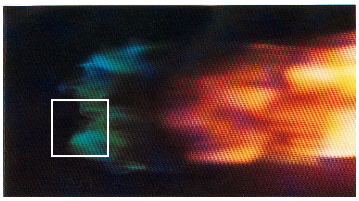

Muniz & Mungal, Combust. Flame 111(1/2), 1997

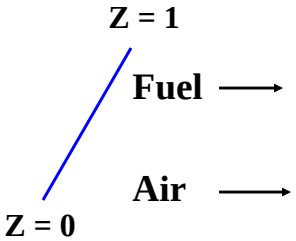

Laminar

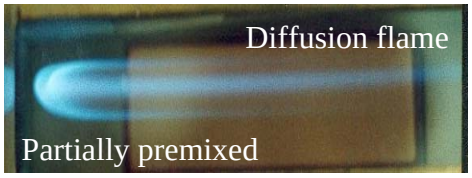

Kioni et al. Combust. Flame, 954, 276, 1993

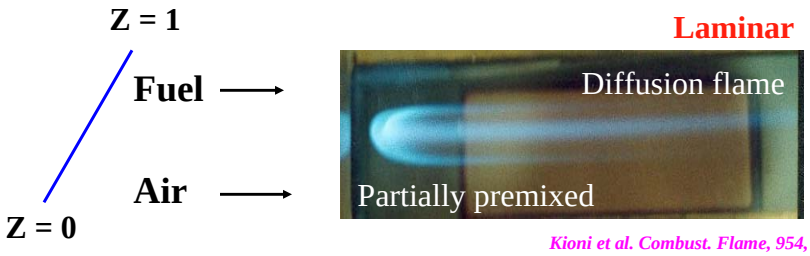

Kioni et al. Combust. Flame, 954, 276, 1993

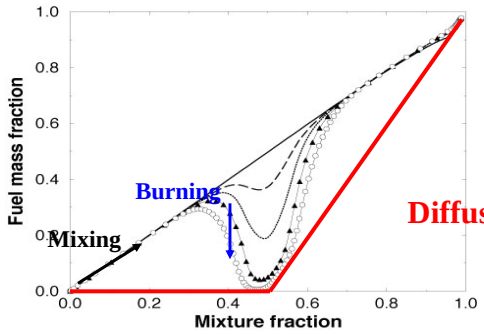

Favier & Vervisch, Combust. Flame, 125(1/2),788-803, 2001

- **Propagation and stability :**
  - Dold, Combust. Flame, 76:71-88, 1989.
  - Hartley & Dold, Combust. Sci. and Tech. 80:23-46, 1991.
  - Buckmaster, Combust. Sci. Tech., 115:41-68, 1996.
  - Buckmaster, Hegab & Jackson, Phys. Fluids, 12(12):1592-1600, 2000.
  - Nayagam, Balasubramaniam & Ronney, Combust. theory and modelling, 3(4):727-742, 1999.
  - Ghosal & Vervisch, JFM, 415, 227-260, 2000.
  - Ghosal & Vervisch, Combust. Flame, 124(4), 646-655, 2001.
  - Azzoni, Ratti, Puri, & Aggarwal, Combust. Flame, 119(1/2):23--40, 1999.
  - Daou & Linan, Combust. Theory Modelling, 2(4):449-477, 1998.
  - Mahalingam, Thévenin, Candel & Veynante Combust. Flame, 118(1/2):221--232, 1999.

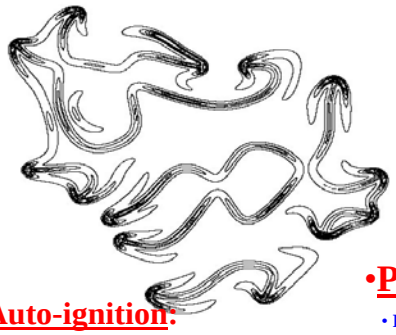

- **Quenching:**
  - Shay & Ronney, Combust. Flame, 112(1/2):112-171, 1998.
  - Nayagam, Balasubramaniam & Ronney, Combust. theory and modelling, 3(4):727-742, 1999.
  - Favier & Vervisch, Combust. Flame, 125(1/2), 788-803, 2001
  - Boulanger & Vervisch, Combust. Flame, 130(1/2), 1-14, 2002

- **Auto-ignition:**
  - Domingo & Vervisch, Proc. Combust. Inst., 26:233-240,1996

- **Pollution:**
  - Plessing et al., Combust. Flame, 115(3) 335-353, 1998.
  - Echekki & Chen, Combust. Flame, 114(1/2) 231-245, 1998.

DNS of weakly turbulent flame bases (Domingo et al, submitted)

Gaseous **Spray**

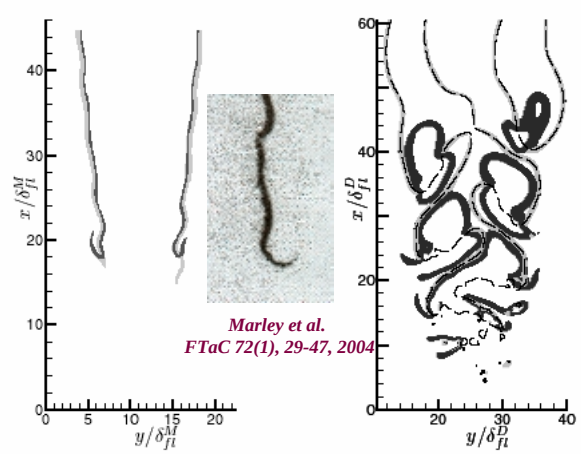

Marley et al.
FTaC 72(1), 29-47, 2004

Turbulent flame base structure (gaseous case)(Domingo et al, submitted) :

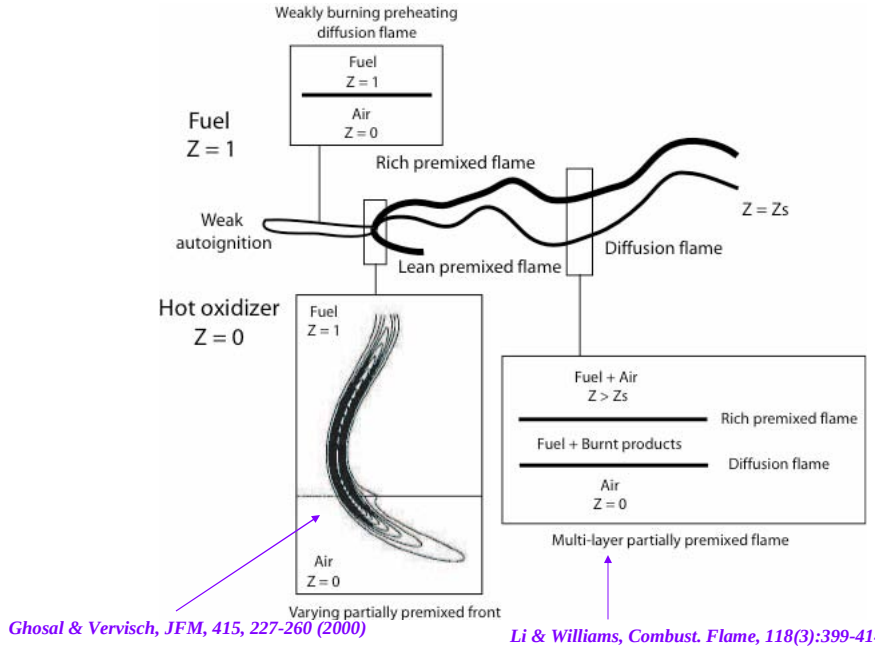

Ghosal & Vervisch, JFM, 415, 227-260 (2000)

Li & Williams, Combust. Flame, 118(3):399-414, (1999)

DNS of nonpremixed jet-flames (Y. Mizobuchi):

Experiment by Cheng et al. 1992
Nozzle diameter : 2mm
Jet velocity : 680m/sec

Chemistry
9-species, 17-reactions (Westbrook,1982)
Rigorous transport properties

Scheme
Finite-volume
Upwind-flux (3rd order)
Explicit time-integration (2nd order)

Simulation size and Cost
200million nodes
291 CPUs (Fujitsu PRIMEPOWER)
160 hours /CPU for 0.1msec simulation

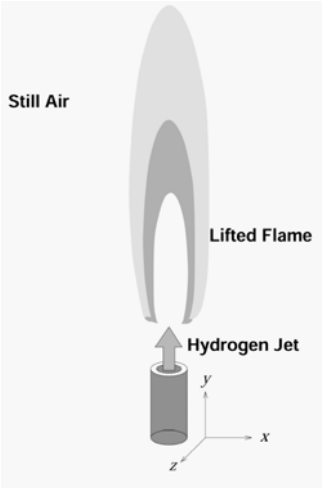

Computational domain ≈ $3cm^3$

- **Main grid: Rectangular, 72 blocks with 2.9 million nodes/block**
- **Sub grid: Cylindrical (around nozzle), 3 blocks, with 0.13 million nodes/block**

Grid spacing ≈ 0.05 mm **Total nodes** ≈ 200 million

10 nodes in H_2 consumption layer of H_2/air stoichiometric laminar premixed flame

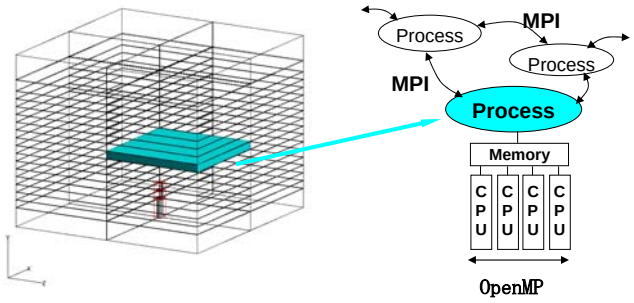

Parallelization: MPI (inter-process) + **OpenMP** (intra-process)

Structure of the lifted flame:

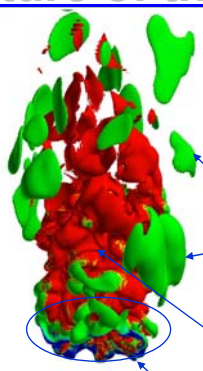

Rich premixed
Diffusive
Lean premixed

Iso-surface of
H_2 consumption rate
at 10^4mol/sec/m^3

Analysis based on flame index (F.I.)
F.I. = $\nabla Y_{H2} \cdot \nabla Y_{O2}$.
F.I > 0:premixed, F.I. < 0:diffusive

The flame consists of three elements.

Diffusion flame islands:
- Island-like form
- Combustion controlled by molecular diffusion of O_2

Turbulent rich premixed flame:
- Complex structure which is largely different from the laminar flamelet

Leading edge flame:
- Triple flame like structure at stable locations
- 3-D and unsteady with large time scale
- Stabilization mechanism

Deviation of heat release layer from H2 consumption layer:

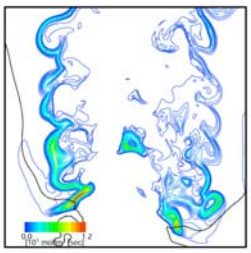

H_2 consumption rate

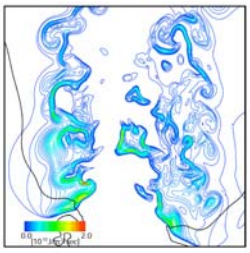

Heat release rate

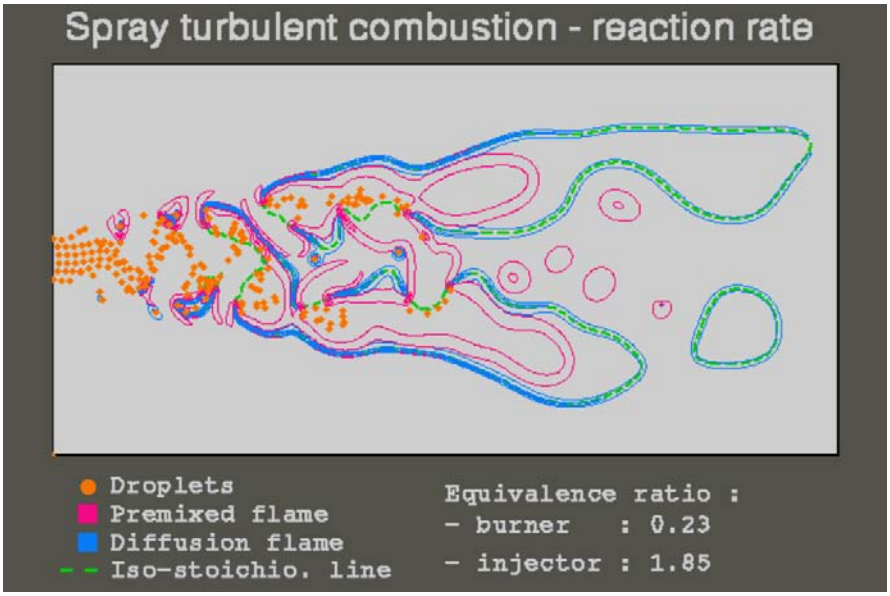

Réveillon & Vervisch, submitted, 2004

Volume of the injected droplets:

$$v_d = \frac{1}{d^I} \frac{\dot{m}_F/\rho_d}{\dot{m}_F/\rho_d + \dot{m}_O/\rho}$$

Number of droplets per unit volume

$\dot{m}_O >> \dot{m}_F$

$$v_d \approx \frac{1}{d^I} \frac{\rho}{\rho_d} \frac{\dot{m}_F}{\dot{m}_O} = \frac{1}{d^I} \frac{\rho}{\rho_d} \frac{\Phi^I_{LO}}{s_r}$$

Surface of the droplets:

$$s_0 = \left(6\sqrt{\pi} v_d\right)^{2/3} \approx \left(6\sqrt{\pi} \frac{1}{d^I} \frac{\rho}{\rho_d} \frac{\Phi^I_{LO}}{s_r}\right)^{2/3}$$

Premixed

Diffusion

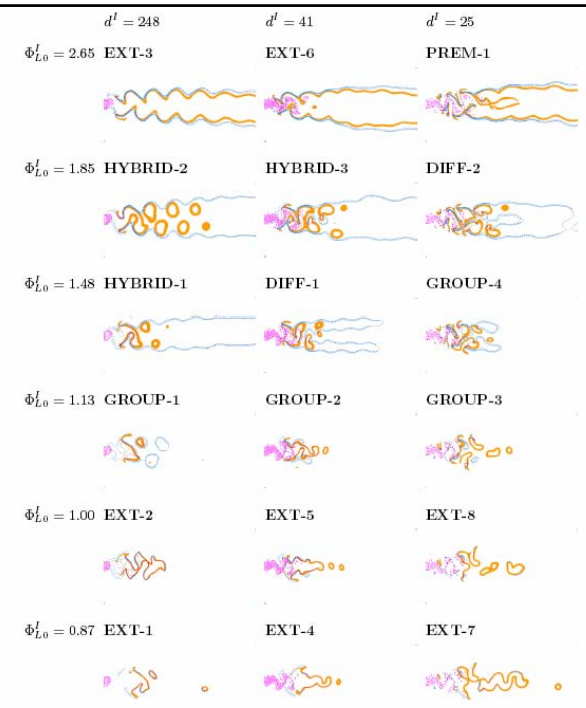

Φ = 0.28

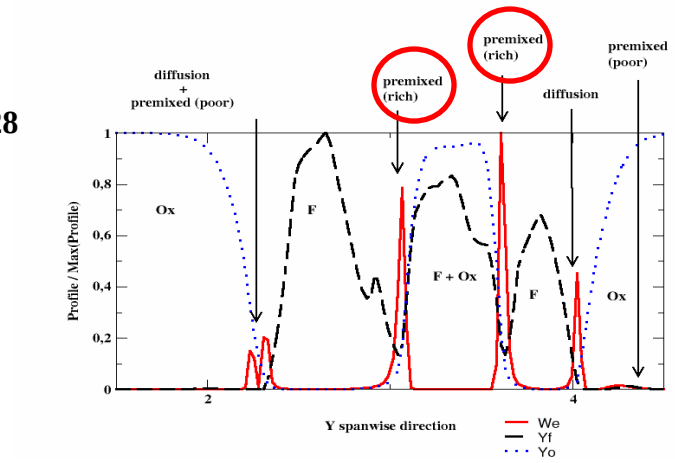

All combustion regimes are observed!

DNS to help understand experiments:

Ethanol spray turbulent flame bases

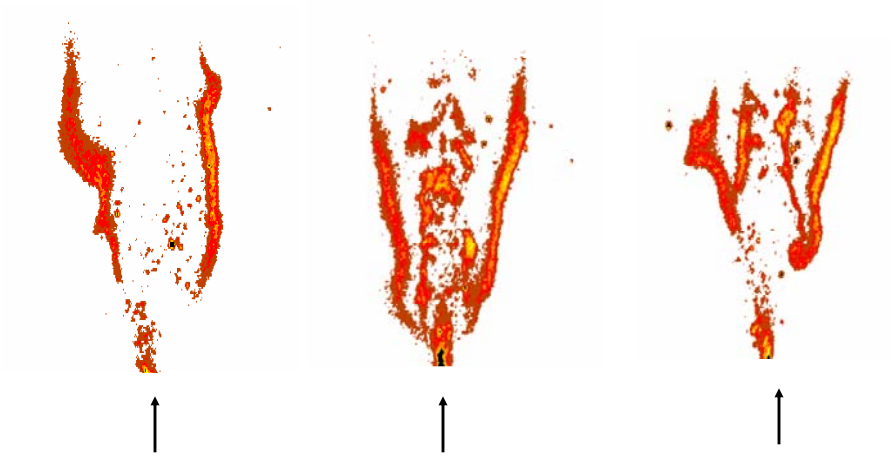

Cessou & Stepowski Combust. Sci and Tech. 118, 361-381, 1996

• **Open double-flame:**

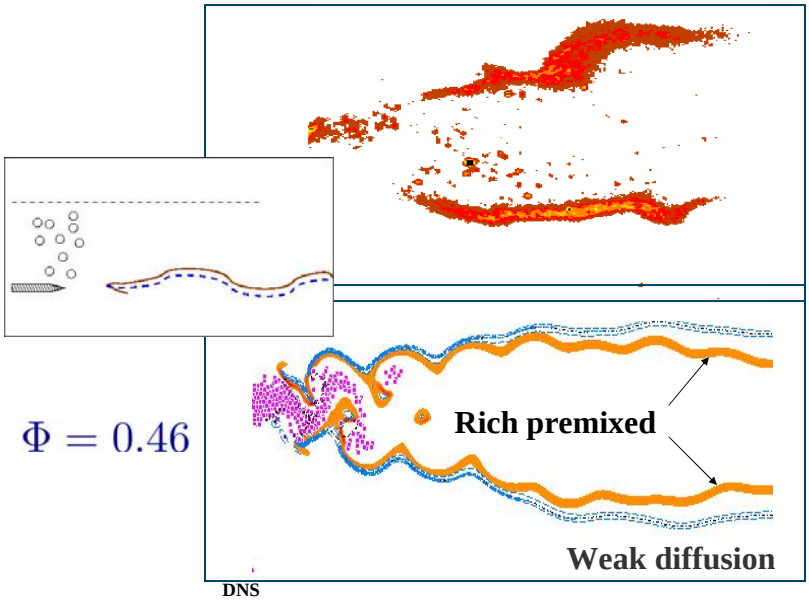

• **Hybrid regime**:

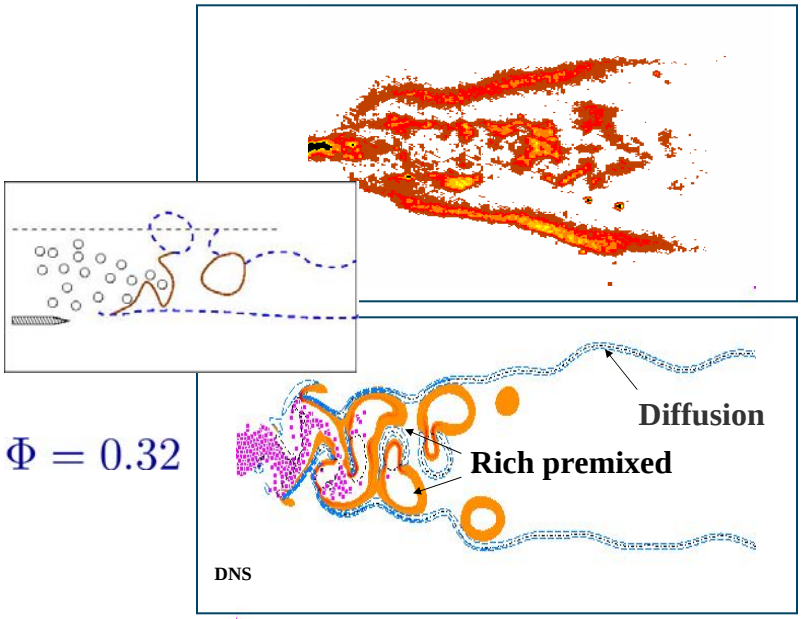

• **Group combustion**:

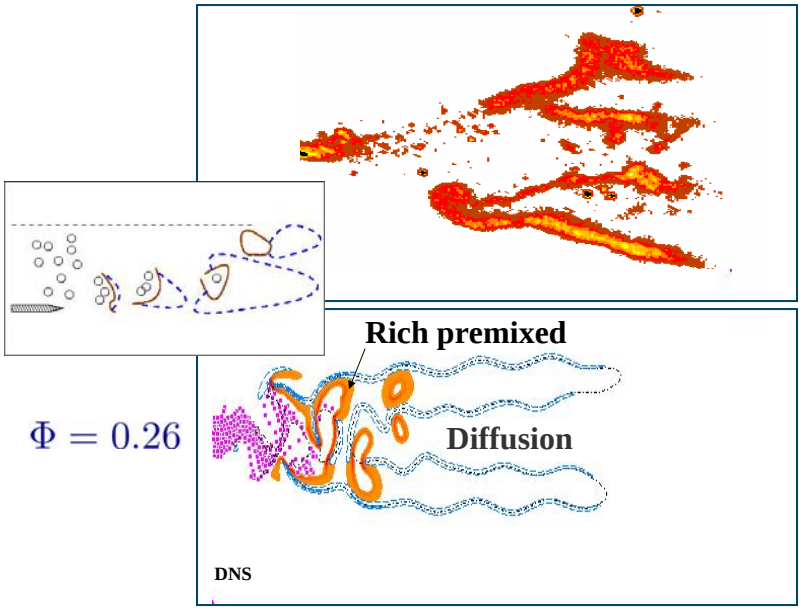

Highly resolved LES for physical analysis of combustion:

Re = 6,650 (0.92 blow-off) Fuel: CH_4/air (17/83 vol.)
Turbulence generators Oxidizer: Air

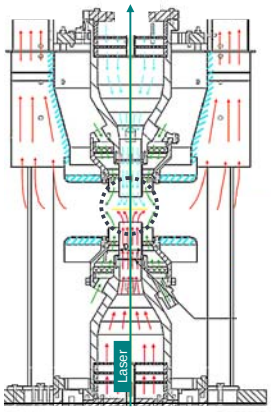

Darmstadt Opposed Jet
Line-Raman, Rayleigh, LIF, PIV, LDA

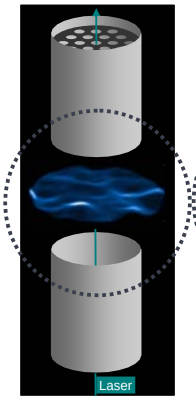

Light emission
Based on OH from LES

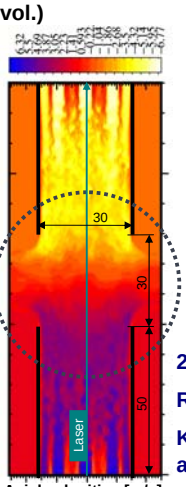

Axial velocities [m/s]
Snapshot from LES

Axial velocity fluctuation (rms)

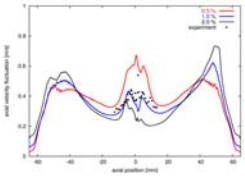

2,856,384 nodes

Resolution: 0.25 mm axial

Kolmogorov length: 0.13 mm at nozzle exit

Steady flamelets

Andreas Kempf, Dirk Geyer, Andreas Dreizler, Johannes Janicka

Pdfs of displacement speed S_d and its components (S_r, S_n & S_t)

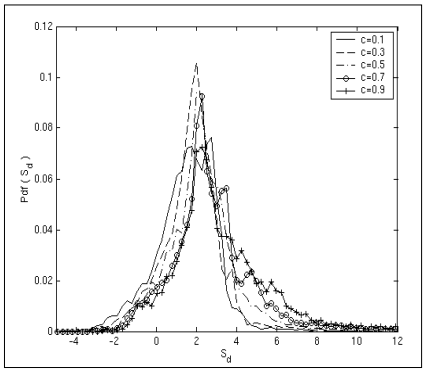

Pdf of S_d at different c isosurfaces across the flame brush

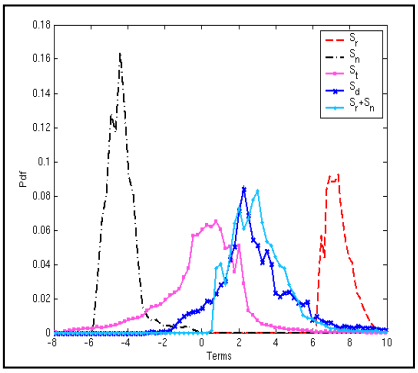

Pdf of S_r, S_n, S_t, S_d and (S_r+S_n) at c = 0.8 close to the location of maximum reaction rate

N.Chakraborty & R.S.Cant

UNIVERSITY OF CAMBRIDGE

Pdfs of displacement speed S_d in spherical and planar flames

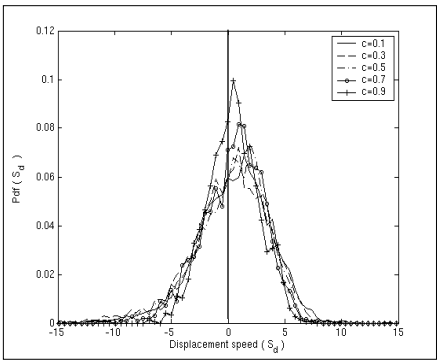

Spherical kernel case

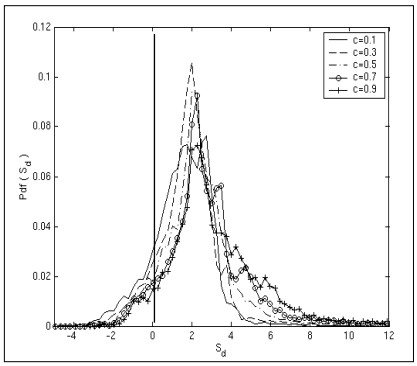

Planar flame case

Cranfield UNIVERSITY

UNIVERSITY OF CAMBRIDGE

N.Chakraborty, K.W.Jenkins & R.S.Cant

Curvature effects on displacement speed S_d and its components (S_r, S_n & S_t): Slide 1

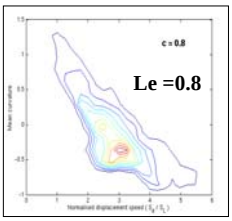

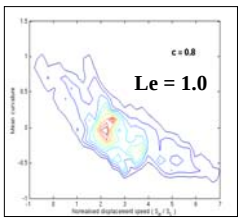

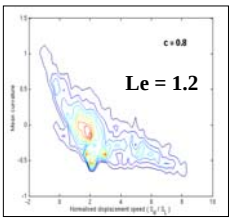

Joint pdf contours of S_d and mean curvature

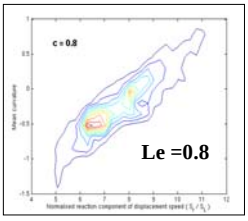

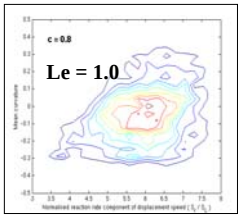

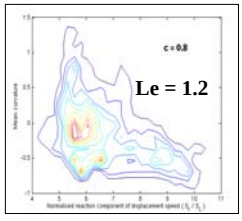

Joint pdf contours of S_r and mean curvature

UNIVERSITY OF CAMBRIDGE

N.Chakraborty & R.S.Cant

Curvature effects on displacement speed S_d and its components (S_r , S_n & S_t): Slide 2

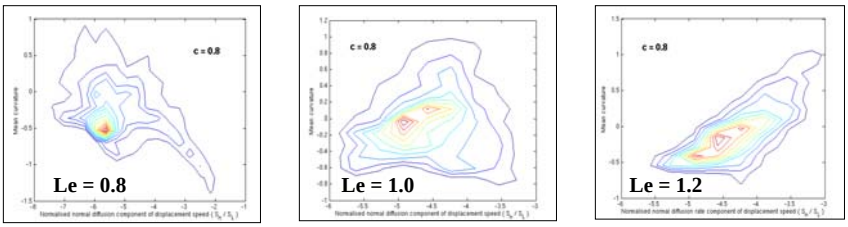

Joint pdf contours of S_n and mean curvature

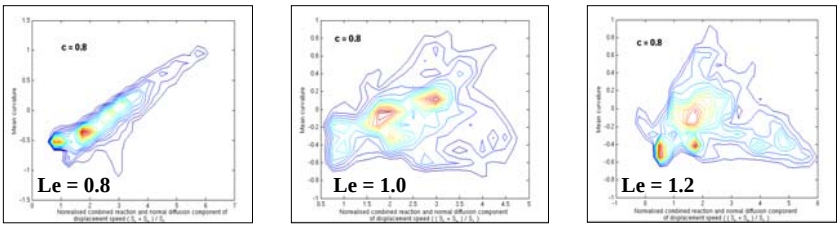

Joint pdf contours of S_r+S_n and mean curvature

UNIVERSITY OF CAMBRIDGE

N.Chakraborty & R.S.Cant

Effect of curvature dependence of S_d on SDF $|\nabla c|$ transport shown through the SDF propagation source term $-\nabla.(S_d \vec{N}|\nabla c|)$

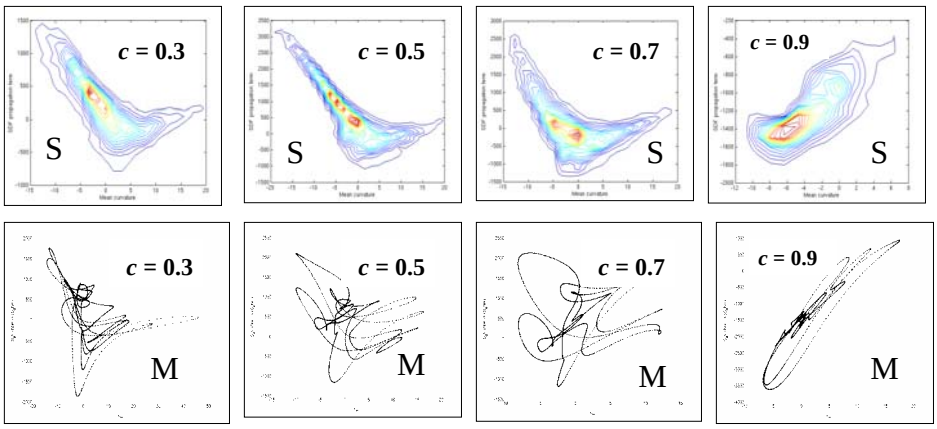

Contours of joint pdf between SDF propagation term and mean curvature

S = 3D DNS with simplified chemistry
M = 2D DNS with CH_4 chemistry

Sandia National Laboratories

UNIVERSITY OF CAMBRIDGE

N.Chakraborty & R.S.Cant
E.R. Hawkes & J.H.Chen

Flame normal statistics:

Joint pdfs of flame normal components

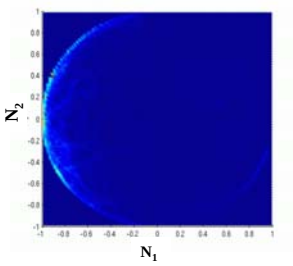

$N_1^2 + N_2^2 = 1$

Flame locally has a predominantly cylindrical structure

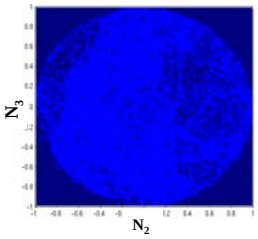

$N_2^2 + N_3^2 = \varepsilon^2$

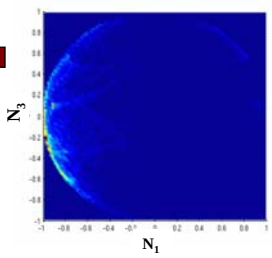

$N_1^2 + N_3^2 = 1$

N.Chakraborty & R.S.Cant

UNIVERSITY OF CAMBRIDGE

Behaviour of flame normal correlations (orientation factors):

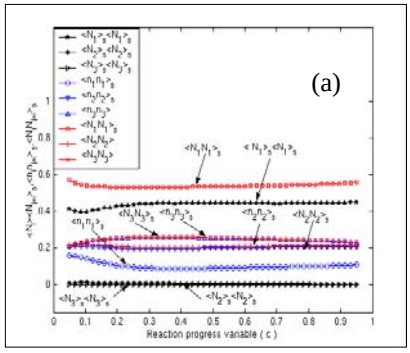

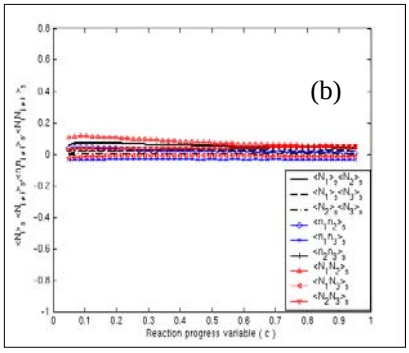

Variation with reaction progress variable across the flame brush of the RANS orientation factor $\langle N_i N_j \rangle_s$ and its contributing terms: (a) Diagonal terms $\langle N_i N_{j=i} \rangle_s$, $\langle N_i \rangle_s \langle N_{j=i} \rangle_s$ and $\langle n_i n_{j=i} \rangle_s$; (b) Off-diagonal terms $\langle N_i N_{j\neq i} \rangle_s$, $\langle N_i \rangle_s \langle N_{j\neq i} \rangle_s$ and $\langle n_i n_{j\neq i} \rangle_s$.

N.Chakraborty & R.S.Cant

UNIVERSITY OF CAMBRIDGE

The frequency of mixing is in fact composed of two fundamental physical quantities: "Speed of mixing" and local thickness of the reactive layer:

$$\chi_c = V_d / l_d = D|\nabla c|^2$$

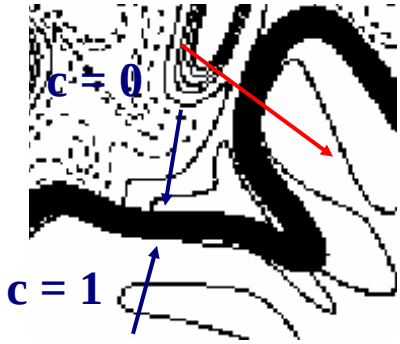

Speed of mixing:

$$V_d = D|\nabla c|$$

Layer thickness:

$$l_d = |\nabla c|^{-1}$$

Vervisch et al. 2004, J. of Turbulence, 5(4), pp. 1-36.

Flame length scale in turbulent micro-mixing modeling…

$$\overline{\chi}_c = \left(\overline{V_d / l_d}\right)$$

$$\overline{\chi}_c = \left(\overline{V_d / l_d}\right)$$

$$\overline{\chi}_c \stackrel{?}{=} \overline{\mathcal{F}}\left(V_d = D|\nabla c|, l_d = |\nabla c|^{-1}\right)$$

Use surface average:

Flame surface during DNS of autoignition

$$\langle \overline{a} \rangle_s = \frac{\overline{a|\nabla c|}}{\overline{|\nabla c|}}$$

$$a = V_d = D\,|\nabla c|$$

Mixing speed

Scalar dissipation rate

$$\left\langle \overline{D\,|\nabla c|} \right\rangle_s \overline{|\nabla c|} = \overline{\chi}_c$$

Length scale

Veynante & Vervisch, Prog In Energ Sci, 28:193-266 2002

SGS modeling for the scalar dissipation rate in premixed turbulent combustion (LES-Closure) (Domingo et al.):

$$\overline{\rho\chi} = \langle \rho D |\nabla c| \rangle_s \overline{|\nabla c|}$$

One-dimensional unstrained premixed flamelet (mixing speed)

SGS flame surface density

$$\overline{|\nabla c|} = \Xi\,|\nabla \overline{c}| \approx C_{SGS} \frac{\overline{c}(1-\overline{c})}{\Delta}$$

Or use a correlation: $\Xi \approx \frac{U_T}{S_L}$

Vervisch et al. 2004, J. of Turbulence, 5(4), pp. 1-36.

From DNS to LES of premixed turbulent combustion using presumed PDF

- **Tabulate chemistry using FPI or FGM (Similar to Bradley's RANS flamelet approach).**

FPI (Flame Prolongation of ILDM): Gicquel et al Proc. Combust. Inst.Vol. 28, 1901-1908, 2000.
Fiorina et al Combust. Theory and Modeling, 7(3):449-470, 2003.
FGM (Flamelet Generated Manifod): Oijen et al Combust. Flame, 127(3):2124-2134, 2001.

- **Use Beta PDF for the progress variable, which is the control parameter of the chemistry tabulation.**

- **Solve balance equations for filtered mean and SGS variance of progress variable.**

$$\overline{\rho c} \qquad \widetilde{\chi}_c$$

$$\overline{\rho}\widetilde{c}_{var} = \overline{\rho c c} - \overline{\rho}\widetilde{c}\,\widetilde{c}$$

$$\Rightarrow \quad \widetilde{P}(c^*)$$

$$\widetilde{Y}_i = \int_0^1 Y_i^{FPI}(c^*)\widetilde{P}(c^*)dc^* \qquad \widetilde{\omega}_c = \int_0^1 \dot{\omega}_c^{FPI}(c^*)\widetilde{P}(c^*)dc^*$$

ORACLES: Combusting flow LES (Domingo et al.)

$$\frac{\Delta}{\delta_{fl}} \approx 25$$

$\Phi = 0.75$

LES accurately reproduces flame flickering when forced with measured inlet spectrum

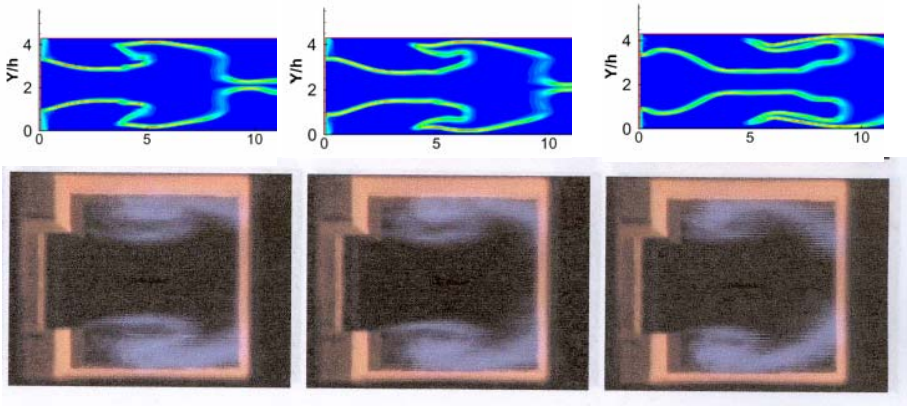

ORACLES: Combusting flow LES

$\Phi = 0.75$ **FPI-FGM (GRI) Presumed PDF & SGS** $\overline{\rho \chi_c}$

Mean centerline velocity

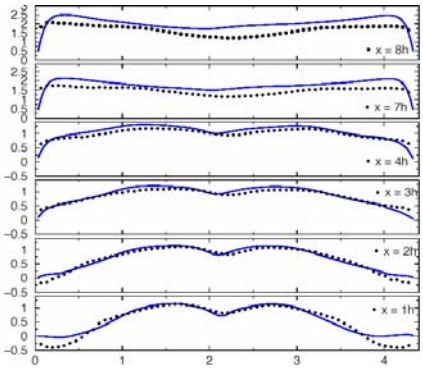

Mean spanwise velocity

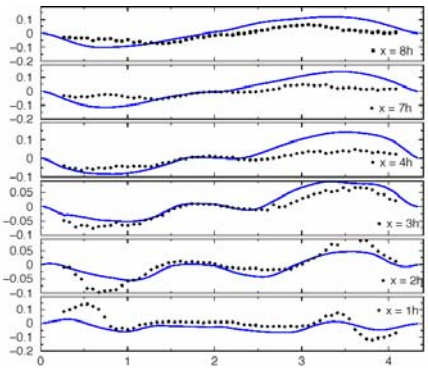

LES basic tests (discussion…):

$\langle a \rangle$ **Reynolds average**

$\overline{a}$ **Spatially Filtered**

Δ **Filter size**

h **Mesh size**

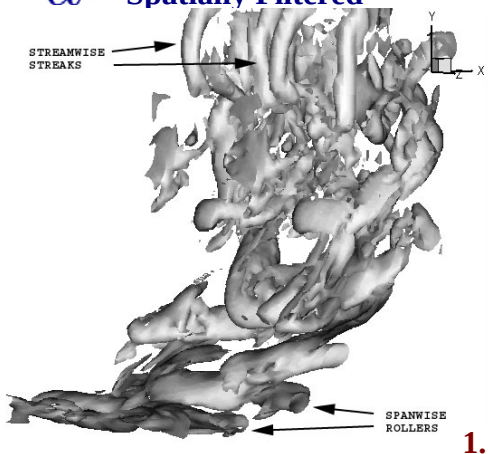

Curved mixing layer

Blin, Hadjadj & Vervisch, J. of Turbulence, 246-258, 2003

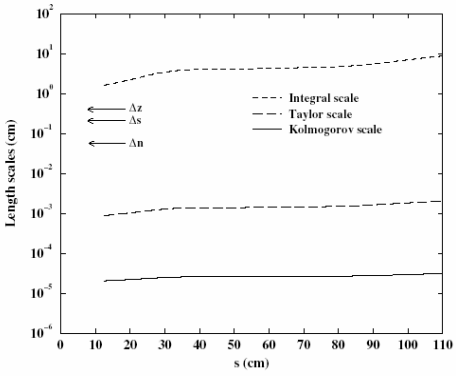

1. Provide a relevant estimate of the filter size used in the simulation.

2. Vary the filter size and check if basic flame properties are preserved.

Among various options, an easy one: check the SGS modeling by increasing the filter size.

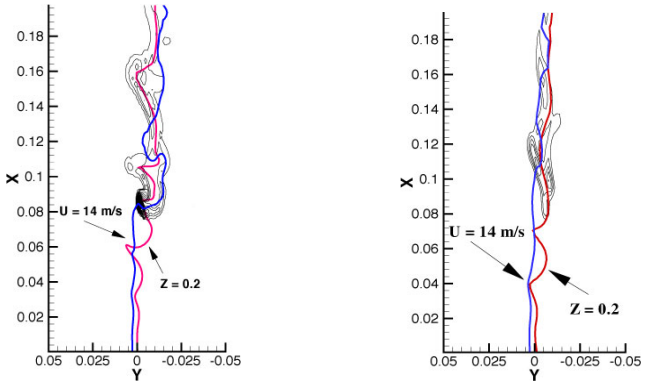

Fine mesh **Coarse mesh**

Domingo et al., "Partially premixed flamelets in LES of nonpremixed combustion" Combust. Theory and Modelling, 6(4), pp. 529-551(2002).

LES basic tests

1. Provide relevant estimate of the filter size used in the simulation.

2. Vary the filter size and check if basic flame properties are preserved.

The statistical properties of the total signal (resolved + SGS) should not depend on the filter size. Error bar can be provided.

3. When there is no subgrid turbulence, the SGS closure should reproduce a filtered laminar flame.

See S. Pope J. of Turbulence 2003 for refined analysis

Update on Lifted Flames

TNF7
Chicago, 22-24 July 2004

How broad is the scope?

- Lifted jet flames in cold co-flow
  - Blow-off and Lift-off heights (Kalghatgi, Peters, Sonju, Takahashi)
  - Effects of co-flow (Dibble and Dahm)
  - Effects of cross-flow (Kalghatgi, Mungal,…)
  - Stabilization theories (Vanquickenborne, Broadwell, Peters, Bilger)
  - Computations (Oran, Peters, Devaud and Bilger)
  - Imaging (Schefer, Lyons, Mungal, Pitz, Kohse, Hassel, Kelman,…)
  - Reviews (Pitts)
- Focus here on selected efforts and cover some recent configurations for auto-ignition and lifted flames in vitiated co-flow.

Some Lifted and Auto-igniting flames

- Lifted flames in cold co-flow
  Experiments by Lyons et al.
- Lifted flames in cold co-flow
  A different burner, experiments by Mansour
- Auto-ignition in turbulent duct flow burner
  Experiments and calculations (Markides and Mastorakos)
- Counter-flow burner, auto-ignition
  Experiments (Kortschik and Peters, 30 Symp. Paper)
- Lifted flames in vitiated co-flow
  Experiments and calculations by Chen et al.
- Lifted flames in vitiated co-flow
  Experiments and calculations by Pope et al.

TNF7
Chicago, 22-24 July 2004

Aerospace, Mechanical & Mechatronic Engineering
University of Sydney

Analysis of Local Flame Extinction in Lifted Non-premixed Flames:PIV and Sequential CH-PLIF

Kevin M. Lyons
North Carolina State University
Raleigh, NC

Kyle A. Watson
University of the Pacific
Stockton, CA

Campbell D. Carter and Jeffrey M. Donbar
Air Force Research Laboratory, AFRL/PRA
Wright Patterson AFB, OH

Highlight of continued research in lifted flames: rendering the formation of local extinction shown with sequential CH-PLIF with velocity field (PIV) showing fluid motion toward the reaction zone.

Experimental Details

Test Conditions

$Re_d = 6400$

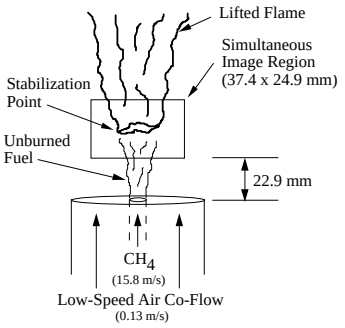

2-Shot CH-PLIF & PIV Arrangement

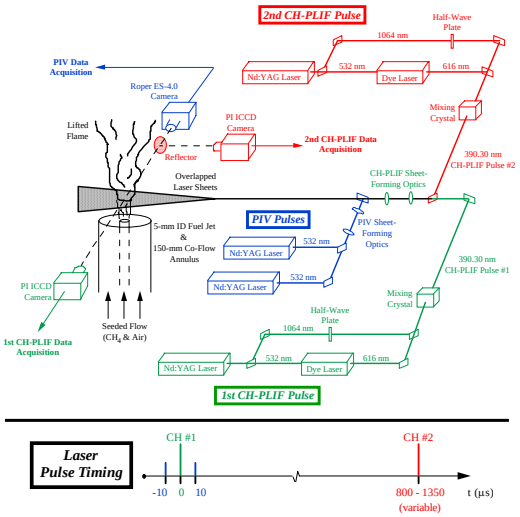

1st CH-PLIF Image (t = 0) **2nd CH-PLIF Image** (t = 1.25 ms)

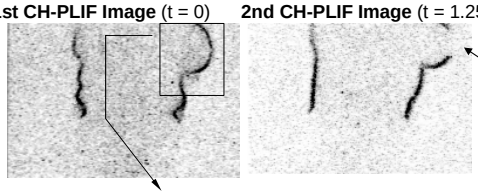

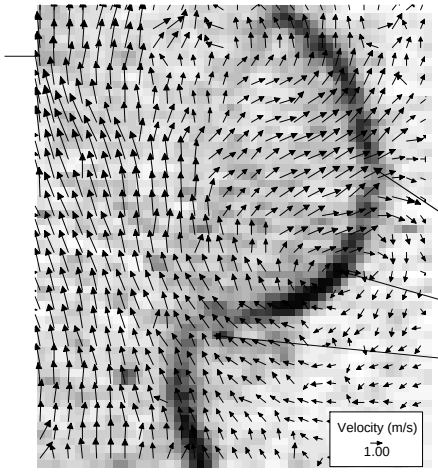

"Is the region extinguished due to strain, or is it related to the lean conditions and the large radial position?"

Outflow Preceding Extinction

Center of Vortex

Strong Entrainment

Lyons, Watson, Carter and Donbar

Information from Lyons et al. on their lifted flame data

- Co-flow velocities range from 0 to 10m/s
- Flames are well isolated from room currents
- Velocity measurements at selected axial locations
- Reynolds numbers about 4300, 5400 and 8300
- Fuels: methane, some ethylene and propane data
- Images of CH, OH, 2-shot CH, and Rayleigh
- Quantitative PIV images (See Watson et al. CST 2003)

The Flow Field Structure at the Base of Lifted Turbulent Partially Premixed Jet Flames

Mohy S. Mansour
Mechanical Engineering Department
The American University in Cairo
Mansourm@aucegypt.edu

Partially Premixed Lifted Flame

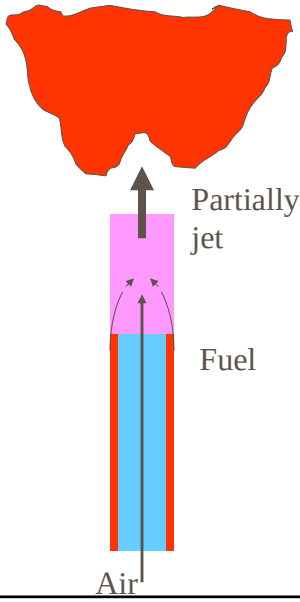

Stability Curves and Flames

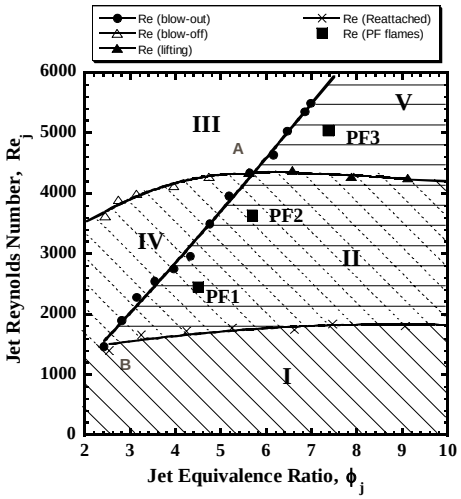

Heat release in kW

PF1	2.39
PF2	4.39
PF3	7.57

Instantaneous Shots: PF1

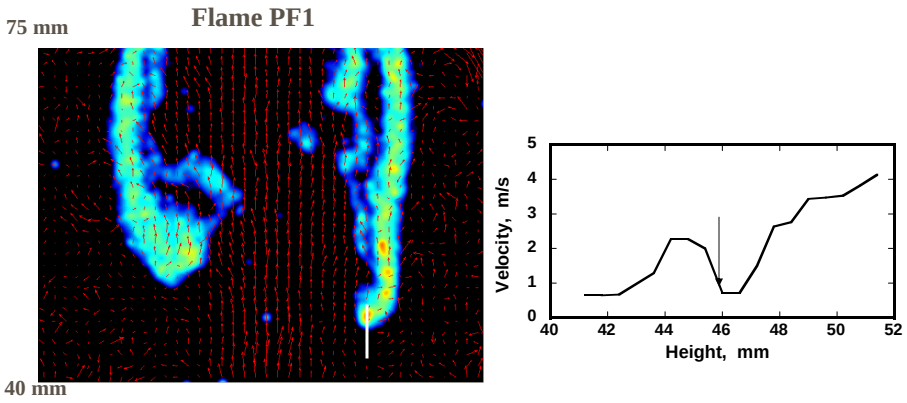

Vertical profiles of mean and rms of velocity

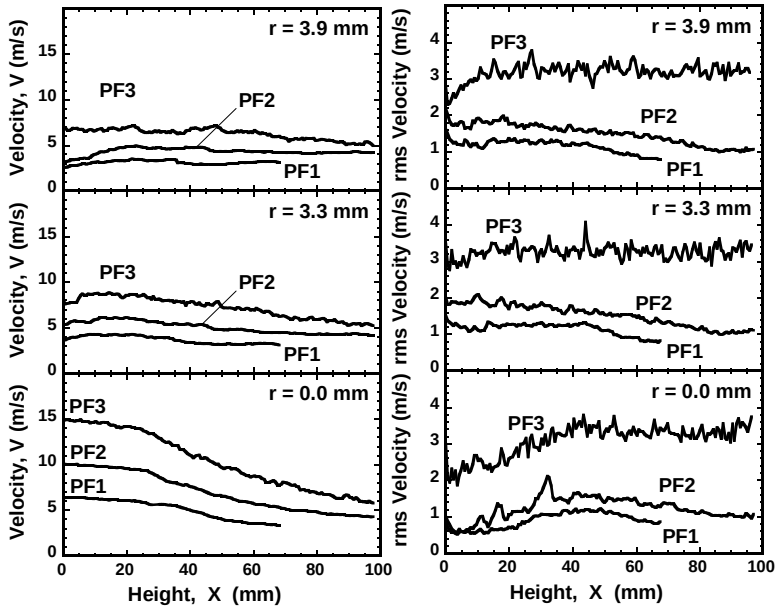

Modelling and experiments relevant to lifted flames

E. Mastorakos (em257@eng.cam.ac.uk)
C. Markides, I.S. Kim

http://www.eng.cam.ac.uk/~em257/

Engineering Department **University of Cambridge**

Burner: Autoignition in turbulent duct flow

1. Apparatus

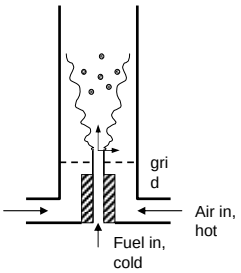

Atmospheric pressure,
Air T up to 1100K
Bulk velocities up to 40m/s

Fuels: Diluted H2, C2H2, C2H4, C7H16

Turbulence intensity boosted by grids.

Continuous injection, mixing like "diffusion from point source".

(Markides & Mastorakos, 2004, To appear in 30th Symp. on Combustion)

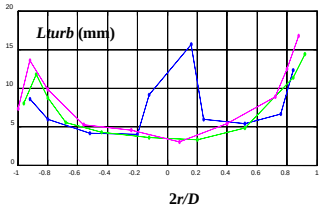

Engineering Department **University of Cambridge**

Calculations with CMC

2. CMC for jet flames

2D-CMC code interfaced with FLUENT (but inert flowfield neglects expansion)

- Lift-off height OK ➔ CMC spatial diffusion term probably not very wrong.
- Scalar diss. rate lower than extinction value at lift-off

(Kim & Mastorakos, 2004, To appear in 30th Symp.)

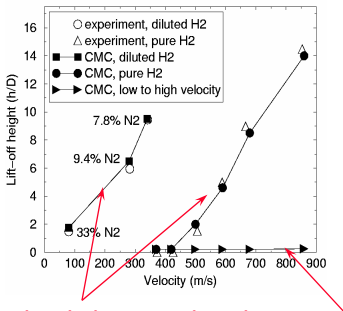

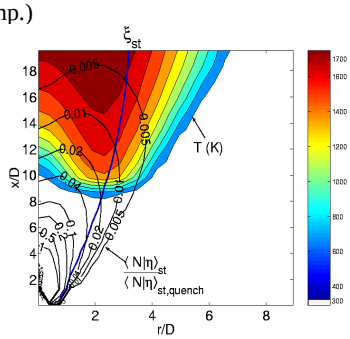

Put "hot kernel" close to experimental lift-off height and wait for steady solution

Start from attached flame and increase Ujet: Flame stays attached, consistent with experiment

Experiments: Autoignition in turbulent duct flow

2. Visualization

Ignition spot appears and then disappears.

Location of ignition spot is random.

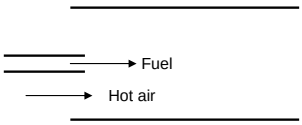

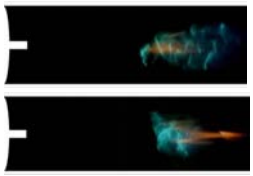

C2H2 ignition, natural light (1/125s exp.)

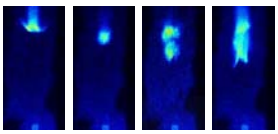

OH chemiluminescence (0.2 ms exp.): Individual spots, not connected flame

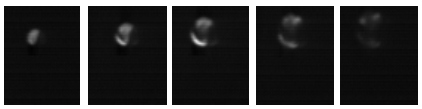

Ignition spot development at 20kHz: nothing, spot, spherical flame, nothing (consistent with DNS!)

Experiments: Autoignition in turbulent duct flow

2. Visualization

Qualitative regimes of operation (for all Ujet/Uair tested between 1 and 5):

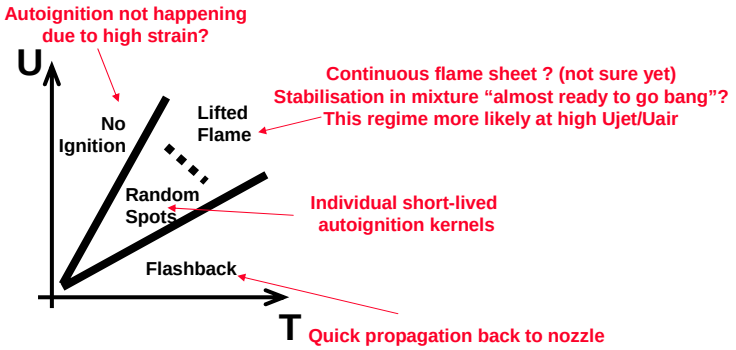

Experiments: Autoignition in turbulent duct flow

3. Analysis of "random spots" regime

Define ***ignition time*** as ***residence time*** calculated from

$$t = \frac{\langle L \rangle}{U^*} = \int_0^{\langle L \rangle} \frac{dx}{U(x)}$$

<L> : mean distance of spots from injector

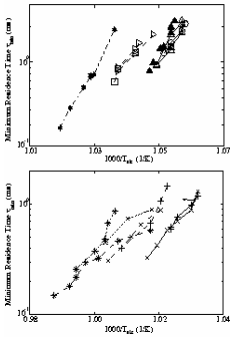

Ignition time depends on T (expected) and also on U_{air}.

Ignition <u>time</u> delayed at high velocities.

EXPERIMENTAL & NUMERICAL INVESTIGATION OF A SERIES OF LIFTED CH4 TURBULENT JET FLAMES INTO A VITIATED COFLOW

R. Cabra, J.Y. Chen, and R.W. Dibble
Department of Mechanical Engineering
University of California at Berkeley

A.N. Karpetis and R.S. Barlow
Combustion Research Facility
Sandia National Laboratories

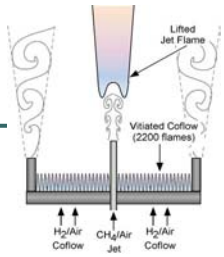

CH_4/Air Jet

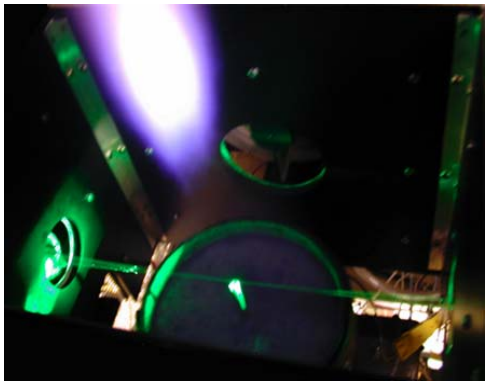

Mean Properties at Jet Centerline

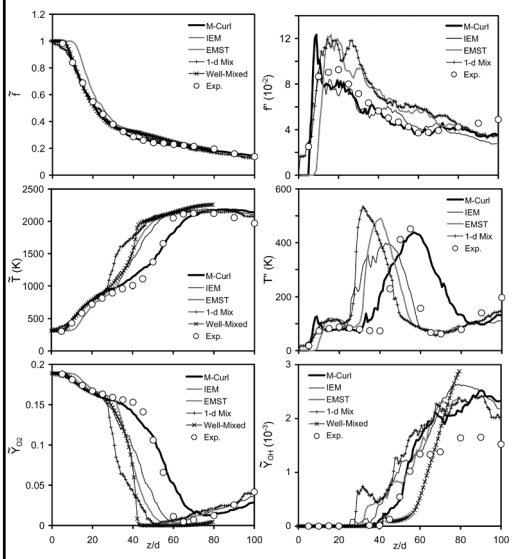

Temperature Scatter Plots M. Curl Mixing Model

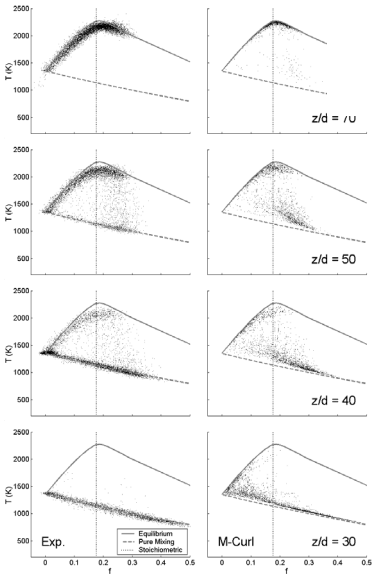

Sensitivity of Flame Base Location (H) to Jet Velocity (V_{jet}) & Coflow Velocity (V_{coflow})

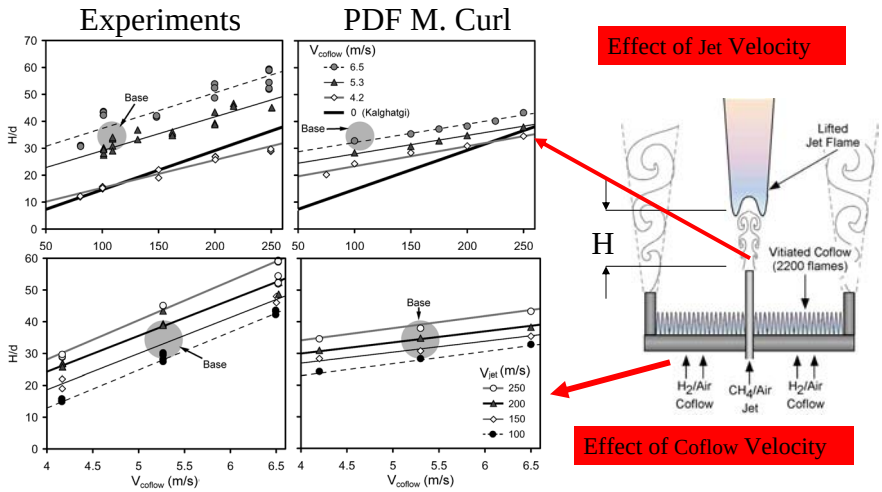

Sensitivity of Flame Base Location (H) to Coflow Properties by Changing Stoichiometry

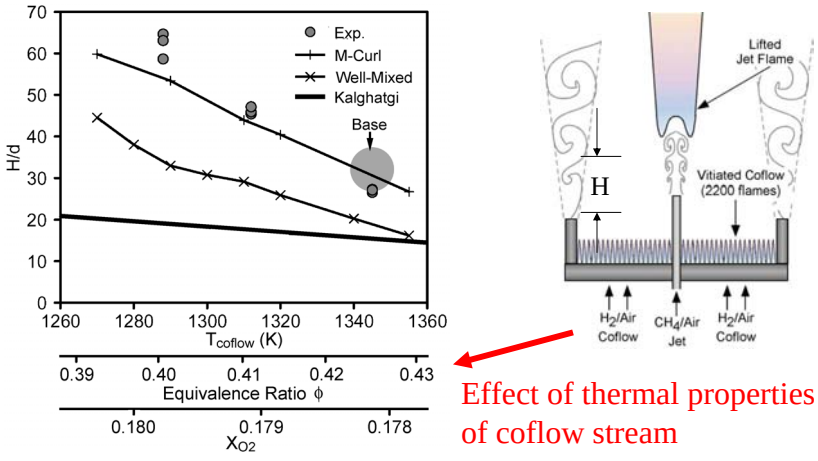

Effect of thermal properties of coflow stream

Observations

- Well-mixed, EMST, 1-D, and IEM mixing models predict early ignition vs. M. Curl predicting a slightly late ignition
- Sensitivity of lift off height to jet & coflow velocities is under-predicted by modified Curl mixing Model
- Sensitivity of lift off height to thermal properties is predicted correctly independent of mixing Model

Hydrogen Jet Flame in a Vitiated Co-Flow
Cao, R., Pope, S.B. and Masri, A.R.

Joint PDF Calculations

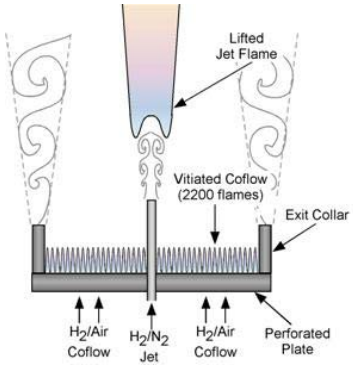

d = 4.57 mm

U_J = 107 m/s

U_c = 3.5 m/s

T_c = 1045 K

H_2/N_2 (1:3)

Cabra et al. (2002)
Kent (2003)

Effect of Mixing Models and Chemical Mechanism

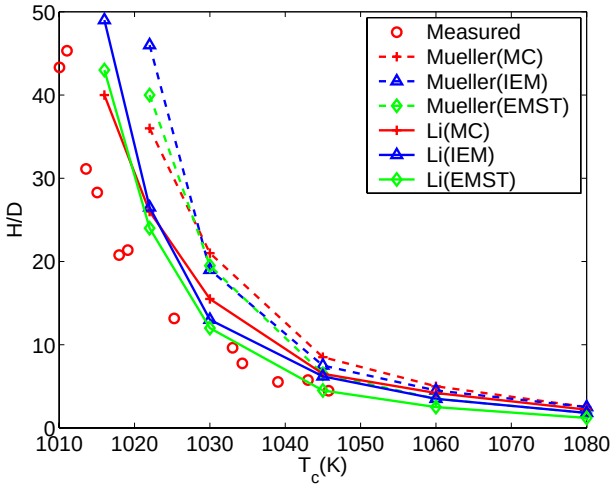

Expt.: Kent (2003)
Calc: Cao et al. (2004)

Scatter Plots of T vs. ξ at z/d = 8 and 26

Mueller Mechanism

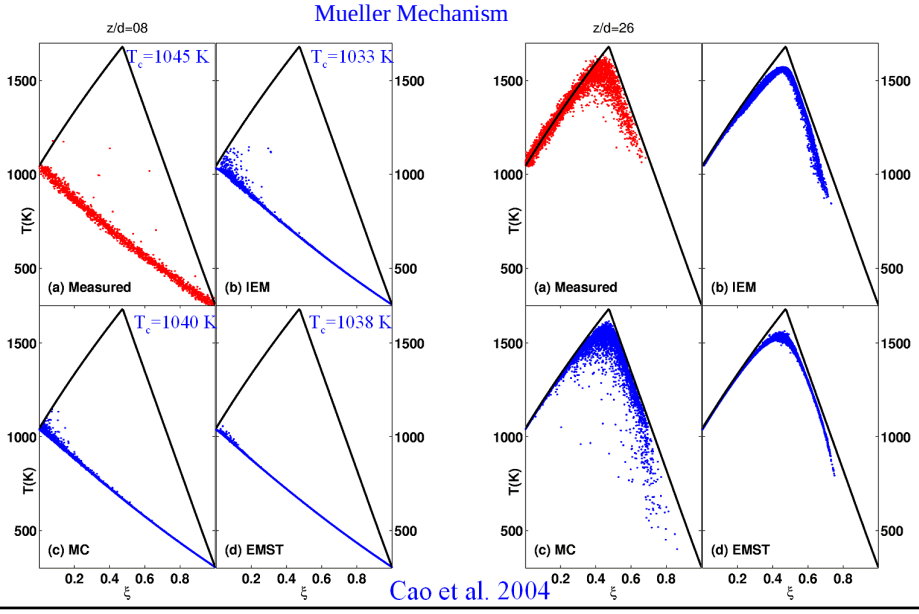

Cao et al. 2004

Scatter Plots of T vs. ξ at z/d = 11 and 14

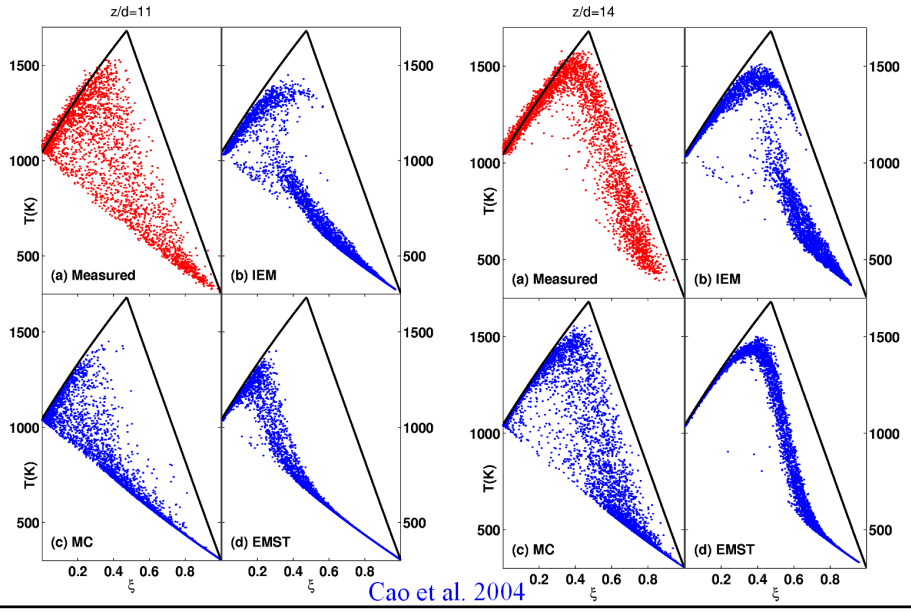

Cao et al. 2004

Hydrogen Jet Flame in a Vitiated Co-Flow

Gordon, R., Masri, A.R., Pope, S.B. and Goldin, G.M.

Used numerical experiments to develop criteria for identifying auto-ignition

Three possible criteria

- Budgets of convection, diffusion, reaction
- Local Damkholer number based on H radical (DNS studies of Echekki and Chen (C&F 134:169-191, 2003))
- History of selected radicals such as HO_2 (also based DNS of Echekki and Chen which show that with auto-ignition HO_2 build up to a critical threshold prior to thermal runaway.

TNF7
Chicago, 22-24 July 2004

Aerospace, Mechanical & Mechatronic Engineering
University of Sydney

Species Transport Budgets for the flame cases

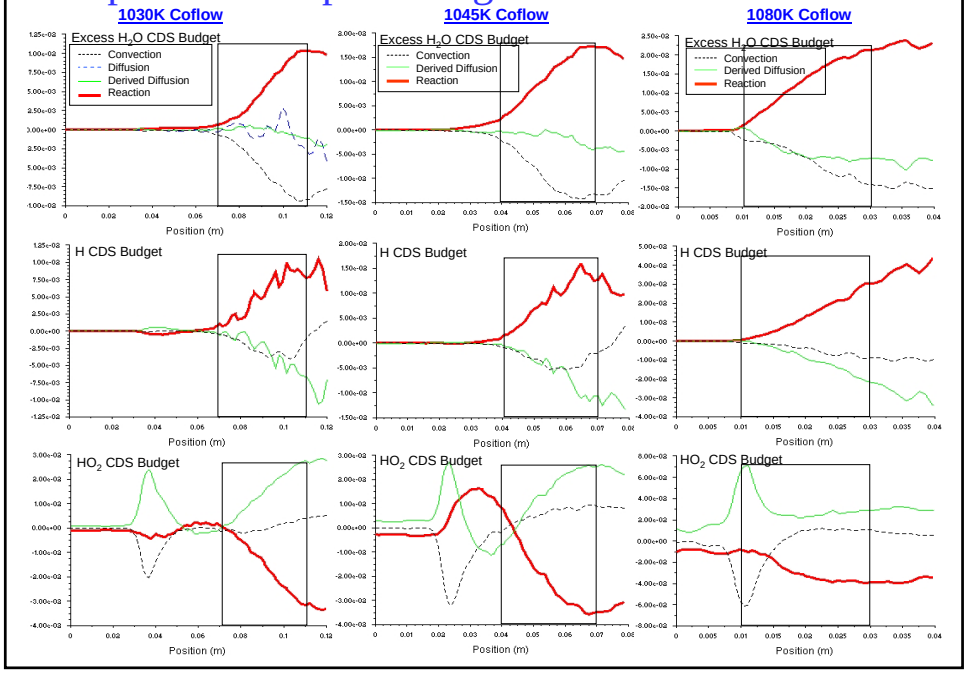

Local H Radical Damköhler number

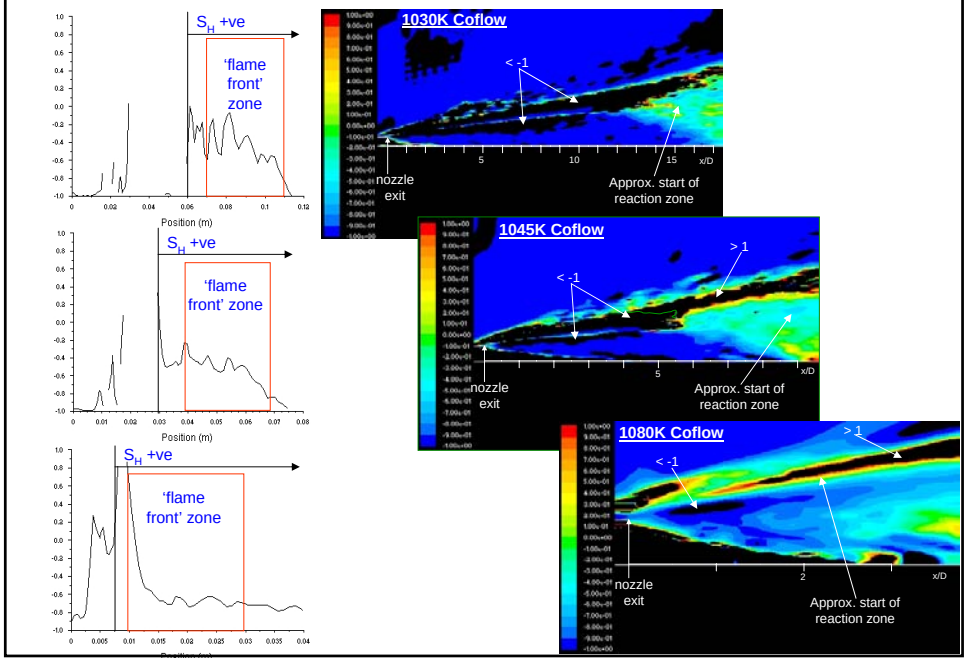

Radical Profiles

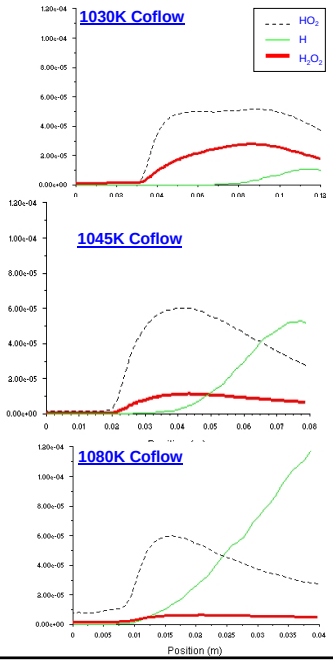

Conclusions

- The criteria for testing autoignition behaviour were validated in the 1-d cases
- The first two flame cases exhibit distinctive autoignition stabilisation behaviour
- The hottest coflow flame case (T_{coflow} = 1080K) exhibits more complex behaviour:
  - The early stages of the CDS budgets, the Da_H profile and contour map, and the high radical concentrations show that the flame could be autoigniting
  - The high diffusive contribution in the H radical CDS budget, the reactive consumption of the HO_2 radical, and the early onset of the H radical production all indicate possible lifted flame behaviour
- It is likely that this flame is being stabilised by a combination of competing, complex combustion mechanisms

END

Hydrogen Jet Flame in a Vitiated Co-Flow

Gordon, R., Masri, A.R., Pope, S.B. and Goldin, G.M.

Composition PDF calculations (FLUENT+ISAT)

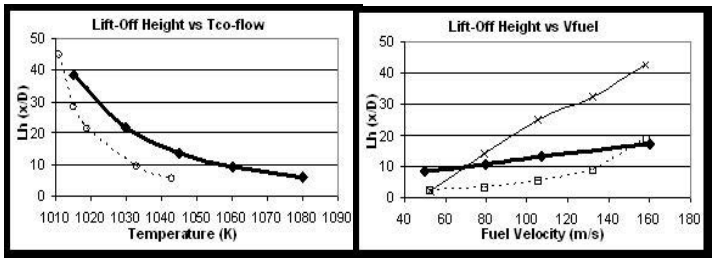

Lift-off Height variation with $T_{Co\text{-}flow}$ and Jet velocity)

Aerospace, Mechanical & Mechatronic Engineering
University of Sydney

1-d Autoignition and Premixed test case: Criterion 1: CDS Budgets

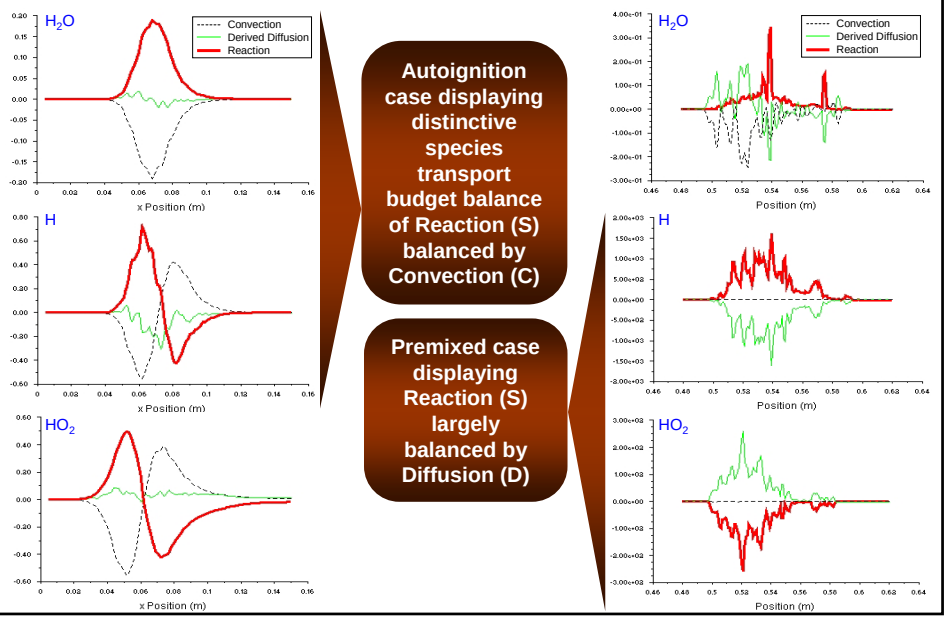

1-d Autoignition and Premixed test case: Criteria 2 & 3: Da_H and radical mass fractions

Da_H for the autoignition case lies between -1 and 1, whereas for the premixed case it is almost always equal to -1

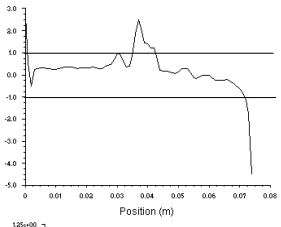

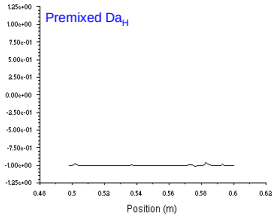

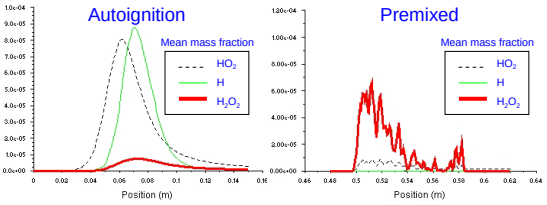

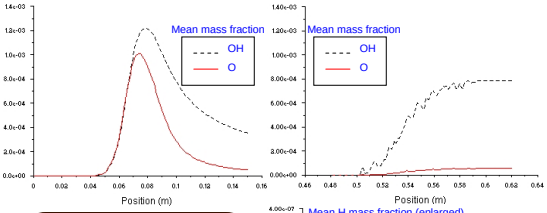

H production appears to be delayed with respect to the onset of HO_2 in the autoignition case

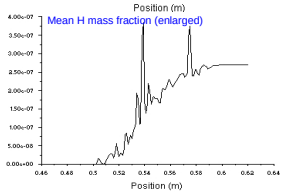

Local H Radical Damköhler number

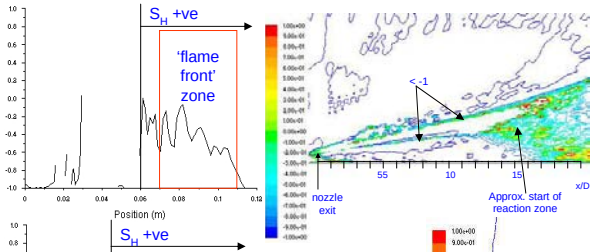

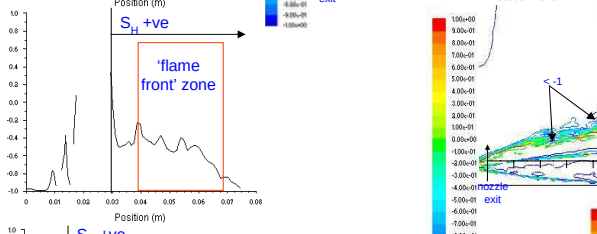

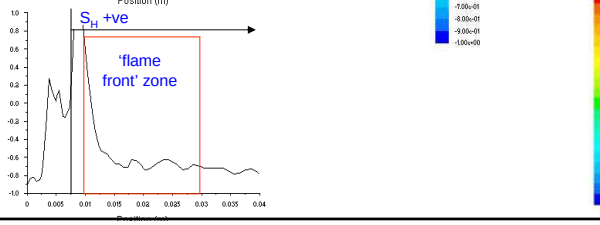

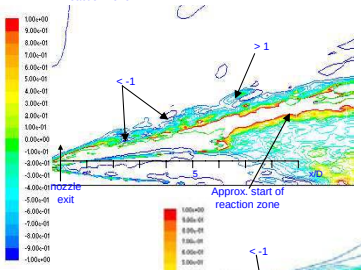

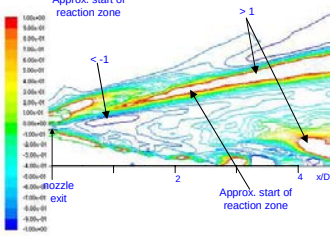

Turbulent premixed combustion – status quo of experimental studies **Andreas Dreizler, TU Darmstadt**

Preamble

Similar to the different flame series available for non- or partially premixed flames in the framework of the international TNF workshop, it seems to be desirable to accordingly generate data bases on series of turbulent premixed flames. For this purpose modellers and experimentalists need to agree on common topics to focus at and on target flames to be detailed investigated in terms of flow and scalar field (of course this is an old question but it is maybe different from the specific view of the TNF-community!?).

Tackling turbulent premixed flames, the following targets may be distinguished:

- Turbulent burning velocity
  - Parameterisation on experimental data
  - Flame stabilisation
  - Dependency on geometry
- Flame front structure and flame topology
  - Dependency on stretch and curvature
  - Dependency on **local** flow field properties; for corrugated flames, role of Gibson length
  - Le-number effects
  - Extinction
  - Dependency on geometry
- Turbulence – chemistry interaction
  - Flame front → conditional data, scalar gradients, flame-vortex interaction
  - Post-flame region → compositional structure, pollutants, residence times
- Unmixedness and secondary air entrainment/stratification, influence of pilot
  - Triple/edge flames/lifted flames
  - Stratified flames
- Others?

With respect to experimental characterisation the following issues might be important:

- Do we still need (line) Raman or are planar techniques such as LIF or Rayleigh sufficient? → reaction progress, reaction rate ~ *grad T*
- Spatial resolution – other requirements than for nonpremixed flames?

- Demand for conditioned data sets which would require simultaneous scalar-flow-measurements? → flame-vortex interaction, scalar turbulent flux [9, 14, 17], relative velocities [27] local flow properties (maybe conditioned on reaction progress) for parameterisation of burning velocity/flame structure
- In terms of modelling, is scalar turbulent flux of high importance? ($\overline{\rho u'' c''}$, countergradient diffusion)
- Is unsteady stretching an issue? → PIV-sequences

As a first step, the following table presents an overview on some **experimental studies** performed on different types of burners. Notice, that this table is far from complete. You are encouraged to notify me to include other important work which I have missed. For each burner, experimental investigations are partitioned into various flow and scalar field properties important for numerical modelling purposes. Not included to this list are investigations regarding fan stirred combustion vessels. Some studies on flame front structure/topology, and on burning rates are included but especially with this regard the list is far off from being complete as a vast variety of investigations has been published.

Following general statements can be made:
Bunsen-type flames

- In general, multi-scalar measurements to get a view on the compositional structure, are rare; Raman/Rayleigh/LIF measurements have been performed only in piloted Bunsen-type flames [7,15,16], for [15,16] flow field data are missing
- Flame series studies have been performed by varying either equivalence ratio [15] or Reynolds number [7]. Influence of equivalence ratio on quantities such as NO formation are reported in [15], Reynolds number effects on flame structure are reported in [7].
- Influence of pilot/secondary air entrainment on compositional structure and finite rate chemistry effects might be a general problem?

Opposed jet/stagnation point flames

- Relatively easy flow field characterised by bulk strain rate, length scales can be easily changed by different sized turbulent generating plates, mean flame orientation perpendicular to mean flow direction
- Focus often was on extinction limits [4-6]
- Information on detailed compositional structure is not available
- Configuration very well suited to measure burning rates [12, 27]
- Flow patterns sensitive to changes in initial conditions [27]

Low swirl burner

- Sufficient information on flow field is available
- In terms of scalar field temperature and reaction progress are documented, secondary air entrainment seems to be no issue [1-3]

Aerodynamically stabilized flames (V-, bluff body, swirl stabilized flames)

- V-flames:

    - relatively well documented sets of experiments
    - More detailed information on compositional structure required
- Bluff-body, swirl stabilized flames
    - More detailed information on compositional structure, reaction progress, location of heat release zones,… required
    - Some ongoing research
- …

To be discussed:

- Priority list of topics from viewpoint of TNF-modelling-community
- Which flame is best suited for selected topic(s) and which information is missing?

→ Hints for experimentalists

	Quantity	Bunsen, piloted	Opp Jet, impinging flow	Low swirl	V-flames	Bluff-body	swirl
Flow field	Statistical moments	7,11,13,14, 16 (HWA, cold), 27	4 (cold & hot case), 12, 17, 27, 29	1,2,3	8 (axial), 20, 27		10 (cold & hot), 19
	Length scales	7	4, 17	1,2	8		10 (cold & hot)
	PSD		4	1,3			10 (cold & hot)
	Vorticity field						19
	Local strain rate				21		
	Conditioned velocities		27, 29		21		24
Scalar field	T	7 (2D), 11 (2D), 15, 16		3 (2D)	8	22, 23	24
	grad T				8 (3D)	23	24
	Concentrations main species	7 (including OH), 15, 16				22, 23	24
	Concentrations CO, NO (finite rate chemistry)	7 (CO), 15, 16				22	18, 24
	Progress variable	7,14, 27	12, 17, 27, 28, 29	1,2,3	27		24
	PDF of progress variable			1 (PDFs of Rayleigh signal)			
	curvature	13	28				
	Secondary air entrainment	16					24
	Extinction limits		Exemplary: 4,5,6 (6: forced extinct.), 28				18
	Flamelet orientation		28		20		
Burning velocity, turbulent flame speed			12	3			
Turbulent scalar flux		14	17		9	9	
In preparation	25						26

References

1 B. Bédat, R.K. Cheng: Experimental study of premixed flames in intense isotropic turbulence, Comb. Flame 100: 485 – 494 (1995)

2 R. K. Cheng: velocity and scalar characteristics of premixed turbulent flames stabilized by weak swirl, Comb. Flame 101: 1 – 14 (1995)

3 T. Plessing, C Kortschik, N. Peters, M.S. Mansour, R.K. Cheng: Measurements of the turbulent burning velocity and the structure of premixed flames on a low-swirl burner, Proc. Comb. Inst. 28: 359 -366 (2000)

4 L.W. Kostiuk, K.N.C. Bray, R.K. Cheng: Experimental study of premixed turbulent combustion in opposed streams. Part I – nonreacting flow field, Comb. Flame 92: 377 – 395 (1993)

5 E. Korusoy, J.H. Whitelaw: Extinction and relight in opposed flames, Exp. in Fluids 33: 75 – 89 (2002)

6 K. Sardi, A.M.K.P. Taylor, J.H. Whitelaw: Extinction of turbulent counterflow flames under periodic strain, Combust. Flame 120: 265 – 284 (2000)

7 Y.-C- Chen, N. Peters, G. A. Schneemann, N. Wruck, U. Renz, M.S. Mansour: The detailed structure of highly stretched turbulent premixed methane-air flames, Combust. Flame 107: 223 – 244 (1996)

8 A. Soika, F. Dinkelacker, A. Leipertz: Measurement of the resolved flame structure of turbulent premixed flames with constant Reynolds number and varied stoichiometry, Proc. Comb. Inst. 27: 785 – 792 (1998)

9 D. Most, F. Dinkelacker, A. Leipertz: Direct determination of the turbulent flux by simultaneous application of filtered Rayleigh scattering thermometry and particle imaging velocimetry, Proc. Comb. Inst. 29: 2669 – 2677 (2002)

10 C. Schneider, A. Dreizler, J. Janicka: Fluid dynamical structure of atmospheric reacting and isothermal swirling flows, in preparation, C. Schneider, A. Dreizler, J. Janicka: Turbulence structure of non-reacting and combusting premixed swirled flows, Proceedings of the European Combustion Meeting 2003, Orleans

11 A. Buschmann, F. Dinkelacker, T. Schäfer, M. Schäfer, J. Wolfrum: Measurement of the instantaneous detailed flame structure in turbulent premixed combustion, Proc. Comb. Inst. 26: 437 – 445 (1996)

12 E. Bourguignon, L.W. Kostiuk, Y. Michou, I. Gökalp: Experimentally measured burning rates of premixed turbulent flames, Proc. Comb. Inst. 26: 447 – 453 (1996)

13 T.-W. Lee, A. Mitrovic: Highly turbulent premixed flames stabilized in a co-axial jet flame burner, Proc. Comb. Inst. 26: 455 – 460 (1996)

14 J.H. Frank, P.A.M. Kalt, R.W. Bilger: Measurement of conditional velocities in turbulent premixed flames by simultaneous OH PLIF and PIV, Comb. Flame 116: 220 – 232 (1999); 14a: P.A.M. Kalt, J.H. Frank, R.W. Bilger: Laser imaging of conditional velocities in premixed propane-air flames by simultaneous OH PLIF and PIV, Proc. Comb. Inst. 27: 751 – 758 (1998)

15 Q.V. Nguyen, R.W. Dibble, C.D. Carter, G.J. Fiechtner, R.S. Barlow: Raman-LIF measurements of temperature, major species, OH, and NO in a methane-air Bunsen flame, Combust. Flame 105: 499 – 510 (1996);

16 J.H. Frank, R.S. Barlow: Simultaneous Rayleigh, Raman, and LIF measurements in turbulent premixed methane-air flames, Proc. Comb. Inst. 27: 759 – 766 (1998)

17 E.J. Stevens, K.N.C. Bray, B. Lecordier: Velocity and scalar statistics for premixed turbulent stagnation flames using PIV, Proc. Comb. Inst. 27: 949 – 955 (1998)
18 R.W. Schefer, D.M. Wicksall, A.K. Agrawal: Combustion of hydrogen-enriched methane in a lean premixed swirl-stabilized burner, Proc. Comb. Inst. 29: 843 – 851 (2002)
19 J. Ji, J.P. Gore: Flow structure in lean premixed swirling combustion, Proc. Comb. Inst. 29: 861 – 867 (2002)
20 S. Sattler, D.A. Knaus, F.C. Gouldin: Determination of three-dimensional flamelet orientation in turbulent V-flames from two-dimensional image data, Proc. Comb. Inst. 29: 1785 – 1792 (2002)
21 D. Most, M. Raisch, F. Dinkelacker, A. Leipertz: Simultaneous measurements of the planar velocity and temperature structure for the characterisation of flames, In: Proceedings of the 10th International Symposium of Applications of Laser techniques to Fluid Mechanics, paper 33.2, Instituto Superior Tecnico, Lisbon, Portugal, 2000
22 S.P. Nandula, R.W. Pitz, R.W. Barlow, G.J. Fiechtner, AIAA 96-0937, 1996
23 R. Schießl, A. Hoffmann, D. Malcherek, D. Schmidt, T. Dreier, J. Wolfrum, C. Schulz, and U. Maas, "Experimental and numerical study of mixing processes in a turbulent premixed flame," Combust. Flame, in review (2004).
24 M. Gregor, A. Nauert, A. Dreizler: work in progress at EKT, TU Darmstadt
25 VCB-piloted premixed jet, http://www.aeromech.usyd.edu.au/thermofluids/Autoignition/VCB...
26 Confined ultra-lean swirl burner: http://www.ca.sandia.gov/CGT/cgtBurner.html
27 R.K. Cheng, I.G. Sheperd: The influence of burner geometry on premixed flame propagation, Comb. Flame 85: 7-26 (1991).
28 L.W. Kostiuk, I.G. Shepherd, K.N.C. Bray: Experimental study of premixed turbulent combustion in opposed streams. PartIII – Spatial structure of flames, Comb. Flame 118: 129 – 139 (1999).
29 S.C. Li, P.A. Libby, F.A. Williams: Experimental investigation of a premixed flame in an impinging turbulent stream, Proc. Combust. Inst. 25: 1207 – 1214 (1994).

Premixed Combustion

Contributors:
Robert Cheng,
Joe Oefelein, Rob Barlow, Stewart Cant, Luc Vervisch,
Friedrich Dinkelacker, Assaad Masri

Coordinator:
Andreas Dreizler

Outline

Issues
Burners
Current work
Discussion

Outline

- Important issues of premixed combustion
- Burners
  - Classification
  - What has been measured
  - ➔ What experimental information is lacking?
- Current work/new burners designs
- Discussion
  - → identify topics the TNF community can contribute (avoid competition with Premixed Workshop)
  - → Some inputs from Robert Cheng to parameterize reaction rates and some thoughts on regime diagrams (available)

Important issues of premixed combustion

Issues | Burners | Current work | Discussion

- Turbulent burning velocity
  - Definition? (Local versus global definition)
  - How to be measured best? Which geometry? Parameterization?
  - → Summary of discussion within the "Premixed Workshop" by Robert Cheng available
- Flame front structure and topology
  - Agreement on regime diagram?
  - Classification by **local** properties?
  - More measurements to resolve flame front structure?
  - Some statements to this topic by Robert Cheng available
  - …
- Compositional structure, finite rate chemistry effects
  - At the flame front → prompt NO
  - Post flame region → CO oxidization, thermal NO, pollutants
  - Extinction/re-ignition
- Deviation from perfect premix
  - Secondary air entrainment
  - Stratification

Experimental investigations - Premixed burners

Issues | Burners | Current work | Discussion

- Vast variety of investigations → very limited selection summarized
- Classification of stationary flames
  - Piloted Bunsen } **envelope**
  - Opposed jet/stagnation point } **unattached**
  - Low swirl
  - V-flame } **oblique**
  - Bluff-body
  - Swirl
- Instationary flames
  - Fan stirred bombs → excluded here due to low repetition rate in typical experiments → bad statistics

Three General Categories of Stationary Premixed Turbulent Flames

Oblique Flames **Envelope Flames** **Unattached Flames**

- Common features of stationary flame experiments:

  Flow uniformity – plug flow with flat mean and rms velocity distributions across burner opening
  Isotropic turbulence - controlled by turbulence generator (grid or perforated plate) with relative low or no shear
  Homogeneous mixture - thoroughly mixed upstream with emphasis on stoichiometric to lean conditions

Envelope Flame

- Generated by anchoring the flames at the rim of the burner
- Turbulent flame brushes burn towards the center and merge to form an envelope over the premixture
- Under moderate flow and turbulence levels where open flame tip and local extinction (or quenching) are not likely to occur, the premixture cannot escape without burning
- Most studies use pilot flames to extend the test matrix because the burner rim is not a very effective flame stabilizer

Waiting for picture from Driscoll

Plane-Symmetric Envelope Flame
Generated in a rectangular shaped burner (or slot burner) with flame brushes originating at two opposite edges. To preserve the "envelope" features, the two remaining sides of the burner need to be confined.

Axi-symmetric Envelope Flame
Also known as conical flames.

Envelope Flames

- *Relevant properties for validating theories and simulations:*
  - mean flame height (defined by intersection point of mean scalar contour at apex)
  - global turbulent burning velocity (defined by inferred mean flame surface area and premixture flow rate)
- *Properties not recommended for analysis*
  - local displacement flame speed (local flow velocity normal to flame brush, large variations & uncertainties, ambiguity at the flame tip)

Waiting for picture from Driscoll

Plane-Symmetric Envelope Flame
Generated in a rectangular shaped burner (or slot burner) with flame brushes originating at two opposite edges. To preserve the "envelope" features, the two remaining sides of the burner need to be confined.

Axi-symmetric Envelope Flame
Also known as conical flames.

Piloted Bunsen (envelope) flames

Issues
Burners
Current work
Discussion

- Principal setup
- Differences in design
  - Turbulence grid in central jet
  - Size of pilot → should be large for defined boundary conditions
- Quantities measured
  - Statistical moments of velocities
  - Length scales
  - Compositional structure
  - Temperature, progress vaiable
  - Curvature
  - Secondary air entrainment
  - Turbulent scalar flux
  - → Comprehensive data set

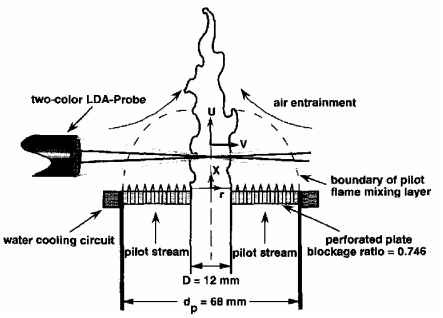

Chen et al. C&F 107

Boundary conditions
- Exit plane velocities
- Exit plane length scales
- Lowest scalar profile at x/D=2.5

Unattached Flames

- Unattached flames do not need flame stabilizers
- Sustain in divergent flows by virtue of the propagating nature of premixed flames
- Flame brushes are locally normal to the approach flow and free to respond to incident turbulence without being constrained or "pinned down" at the flame attachment point.

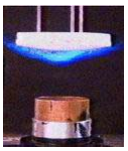

Unattached flames in impinging flows
The divergent flow generated by impingment on a stagnation plate or against each other allows the flame to position itself at a short distrance upstream of the stagnation plane.

Unattached flames in swirl-generated diverging Flow
Low swirl produces a divergent flow with the swirling motion confined to the flow periphery. In the center region, the turbulent flame brush is swirl free.

Unattached Flames

- ***Fundamental properties for validating theories and simulations:***
  - **displacement flame speed (defined at a mean scalar value)**
  - **flame brush thickness (defined by scalar contours)**

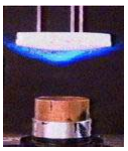

Unattached flames in impinging flows
The divergent flow generated by impingment on a stagnation plate or against each other allows the flame to position itself at a short distrance upstream of the stagnation plane.

Unattached flames in swirl-generated diverging Flow
Low swirl produces a divergent flow with the swirling motion confined to the flow periphery. In the center region, the turbulent flame brush is swirl free.

LAWRENCE BERKELEY NATIONAL LABORATORY
Prepared by R. K. Cheng for presentation at TNF7

Opposed jets/stagnation point (unattached) flames

- Principal setup
- Quantities measured
  - Statistical moments of velocities
  - Length scales and PSD
  - Combined velocity-density measurements, turbulent scalar flux
  - Progress variable
  - Extinction limits
  - Flamelet orientations

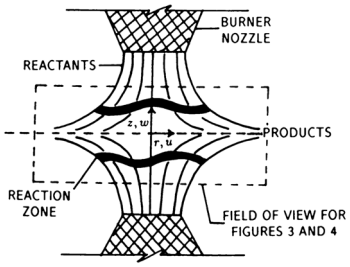

Source: Libby et al.

- Missing:
  - Local flow properties (strain, vorticity,…)
  - Compositional structure
  - Scalar gradients

Boundary conditions (Kostiuk et al. C&F 92)
- Exit plane PSD, time and length scales

Low swirl (unattached) flames

- Principal setup

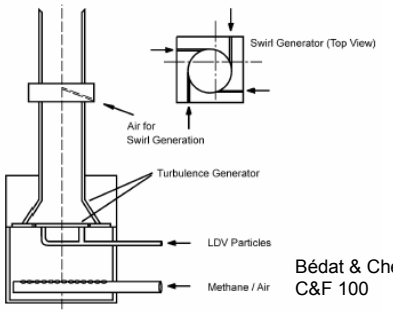

Bédat & Cheng C&F 100

- Quantities measured
  - Statistical moments of velocities
  - Length scales and PSD
  - Temperature and progress variable
  - Missing:
    - Local flow properties (strain, vorticity,…)
    - Compositional structure
    - Scalar gradients

Boundary conditions (Bédat & Cheng C&F 100)
- Measurement planes start at 5 – 10 mm above nozzle

Oblique Flames

- Generated by a flame holder at the center of the burner
- Turbulent flame brushes interact with incident turbulence and grow thicker downstream of the stabilizer
- The sizes of the flame holder kept to a minimum so to reduce its influences on the developing turbulent flame brush
- Larger stabilizers for investigating the contributions of the stabilizer wake (i.e. shear turbulence) to flame characteristics and blow-off

Plane-Symmetric Oblique Flame
A V-flame stabilized by a small rod is the most common rendition of a plane-symmetric laboratory oblique flame. Over 40 publications on this configuration

Axi-symmetric Oblique Flame
A small bluff body or pilot flame generate an axi-symmetric oblique flame that shapes like an inverted cone.

Oblique Flames

- ***Relevant Properties for Validating Theories and Simulations:***
  - **flame brush orientation (define by a mean scalar contour)**
  - **brush thickness and growth rate (define by scalar contours)**
- ***Properties not recommended for analysis***
  - **displacement flame speed (large variations & uncertainties)**

Plane-Symmetric Oblique Flame
A V-flame stabilized by a small rod is the most common rendition of a plane-symmetric laboratory oblique flame. Over 40 publications on this configuration

Axi-symmetric Oblique Flame
A small bluff body or pilot flame generate an axi-symmetric oblique flame that shapes like an inverted cone.

LAWRENCE BERKELEY NATIONAL LABORATORY
Prepared by R. K. Cheng for presentation at TNF7

V- (oblique) flames

Issues | Burners | Current work | Discussion

- Principal setup

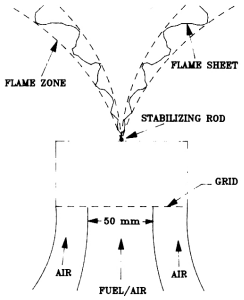

- Quantities measured
  - Statistical moments of velocities, conditioned velocities
  - Length scales
  - Local strain
  - Temperature and progress variable
  - Temperature gradients
  - Turbulent scalar flux
  - Missing:
    - Compositional structure

Boundary conditions
- Nothing reported

Bluff body flames

Issues | Burners | Current work | Discussion

- Principal setup

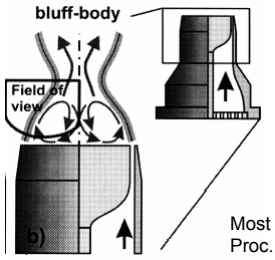

Most et al.
Proc. Comb. Symp. 29

- Quantities measured
  - Most: turbulent scalar flux
  - Nandula: T, compositional structure
  - Schiessl (to appear): T, grad T, compositional structure
  - Missing:
    - Any flow field data

Boundary conditions
- Nothing reported

Swirl flames

Issues
Burners
Current work
Discussion

→ work in progress, shown subsequently

Lack of experimental information

Issues
Burners
Current work
Discussion

- Flame series are rare
- “Complete” validation sequences are rare
- Agreement on turbulent burning velocity (definition, data,…) missing
- Lack of measurements on:
  - Local flow properties
  - Local turbulent burning velocity
  - Compositional structure
  - Scalar gradients, especially with higher resolution
  - Boundary conditions not sufficiently well characterized
  - Lean stratified flames → project planned at Darmstadt

Boundary conditions

Issues
Burners
Current work
Discussion

- High priority: more detailed boundary/inlet conditions
- Measurements at nozzle exit
- Measurements inside the nozzle
- Make use of DNS to predict in-nozzle flow field → example premixed swirled flames (Darmstadt)

Current work on premixed combustion within TNF

Issues
Burners
Current work
Discussion

- Sandia → Joe Oefelein
- Erlangen → Friedrich Dinkelacker
- Sydney → Assaad Masri
- Darmstadt

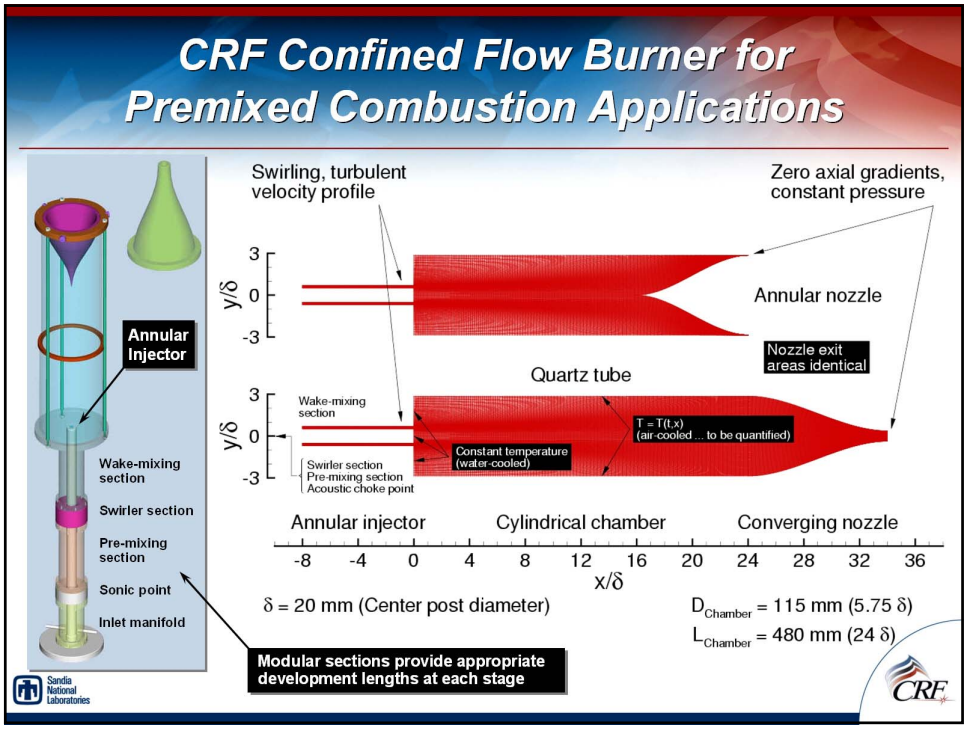
CRF Confined Flow Burner for Premixed Combustion Applications
Swirling, turbulent velocity profile
Zero axial gradients, constant pressure
Annular Injector
Wake-mixing section
Swirler section
Pre-mixing section
Sonic point
Inlet manifold
Annular nozzle
Nozzle exit areas identical
Quartz tube
Wake-mixing section
Constant temperature (water-cooled)
T = T(t,x) (air-cooled ... to be quantified)
Swirler section
Pre-mixing section
Acoustic choke point
y/δ
Annular injector
Cylindrical chamber
Converging nozzle
x/δ
δ = 20 mm (Center post diameter)
D_Chamber = 115 mm (5.75 δ)
L_Chamber = 480 mm (24 δ)
Modular sections provide appropriate development lengths at each stage
Sandia National Laboratories
CRF

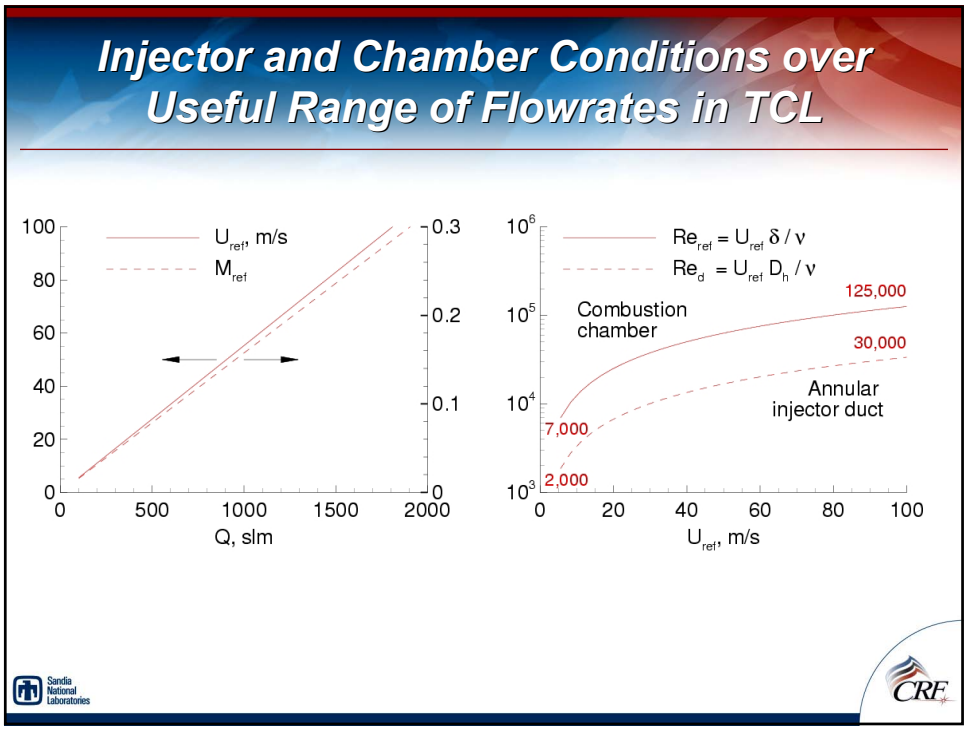
Injector and Chamber Conditions over Useful Range of Flowrates in TCL
U_ref, m/s
M_ref
Q, slm
Re_ref = U_ref δ / ν
Re_d = U_ref D_h / ν
Combustion chamber
Annular injector duct
125,000
30,000
7,000
2,000
U_ref, m/s
Sandia National Laboratories
CRF

Baseline Target Flame and Validation Sequence (Preliminary)

CH_4–Air:
U_{ref} = 28 m/s, ϕ = 0.62, S = 0.82
Re_d = 9410, Re_{ref} = 35220

- Cold-flow PIV, LDV
  - Burner inlet conditions
  - Instantaneous, time-averaged velocity
  - Mean, rms, cross-stress terms
- Reacting PIV, LDV, PLIF
  - Duplicate cold-flow measurements
  - Instantaneous, time-averaged minor species
  - Instantaneous, time-averaged flame structure
  - Velocity-scalar correlations
- Raman-Rayleigh-LIF point, line
  - Instantaneous, time-averaged temperature
  - Instantaneous, time-averaged major species

- Experimental burner designed, operational
- Well-defined non-ambiguous flow conditions
- Injector walls and faceplate BC's characterized
- Heat transfer characteristics of quartz tube pending

Sandia National Laboratories

CRF

Premixed Flame Data at LTT - University of Erlangen

Dr. Friedrich Dinkelacker
University of Erlangen, Germany

- V-Flame Data
- Bunsen Flame Data (Ring stabilized)
- Bluff-Body Flame Data
- Double-Flow-Burner (future)
- High-Pressure-Flames (Data not yet suitable for validation of calculation)

TNF 7 - Chicago, 22. - 24. 7. 2004

TNF7 2004 (1)

V-Flame Data

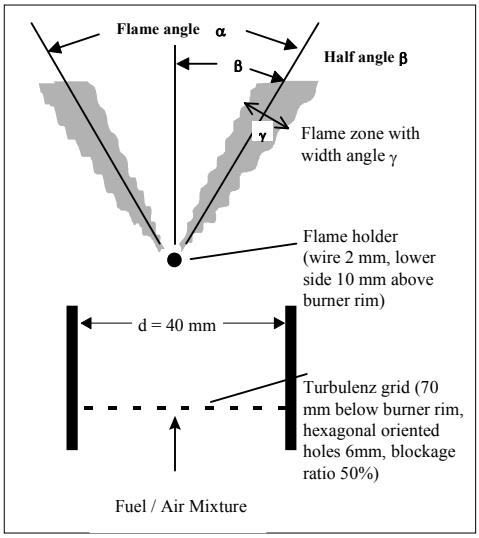

Characteristics:
- V-Flame, 2mm wire
- Grid turbulence
- Inlet d = 40 mm
- Re_t = 45 or 87
- Methane/Air
- 6 Flames measured:
  U = 1.85; 3.04 m/s
  Φ = 0.53; 0.61; 0.74

Measured Quantities:
- Axial Inflow Velocity
- Axial Inflow Turbulence Intensity
- Integral scale at Inflow (one value on axis)
- Mean Reaction Progress Field (resp., Flame Angle α and Flame Brush Width β)

Publication:
- (Diploma Thesis A. Soika, Erlangen 1996)
- Data available from fdi@ltt.uni-erlangen.de

Ring-Stabilized Bunsen Flame Data

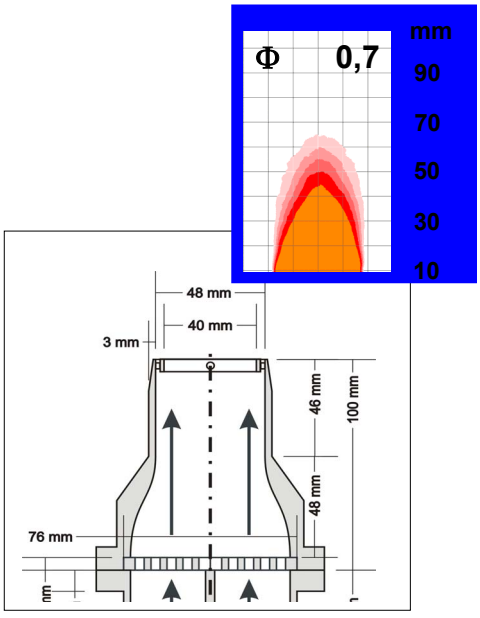

Characteristics:
- Bunsen Flame
- Grid turbulence
- d_i = 40 mm d_a = 48 mm
- Ring stabilization (*foll. Johnson et al. CF 1998*)
- Methane/Air
- 8 Flames measured:
  3 Flow rates
  Φ = 0.62; 0.7; 0.8; 1.0
- Disadvantage: Flow not fully symmetric

Measured Quantities:
- Inflow Velocity *U, V* (Profiles)
- Inflow Turbulence Intensity *u', v'* (Profiles)
- Integral scale near Inflow
- Mean Reaction Progress Field
- Conditioned Flow in Flame (in progress)
- Turbulent Flux (in progress)

Publication:
- (2 Diploma Thesis Erlangen 2003, 2004)
- Data available in future via fdi@ltt.uni-erlangen.de

Bluff-Body Stabilized Flames

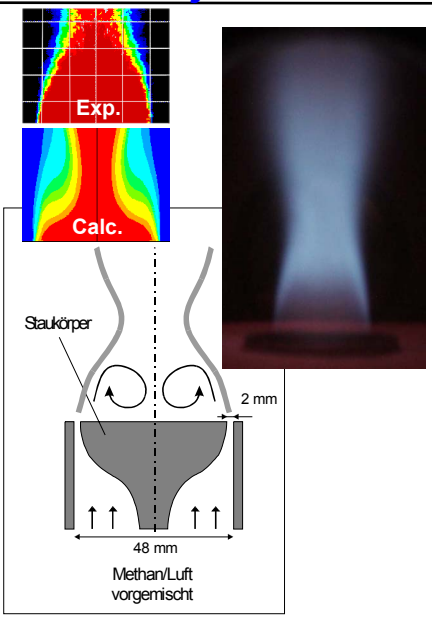

Characteristics:

- Flame stabilized by Recirculation behind Bluff-Body
- D_i = 44 mm, D_a = 48 mm
- Methane/Air
- Flow is complex
- Range of stability is large
- Re_t = 450 - 2850
- > 13 Flames measured:
  U = 4.9; 13.8; 21.3; 28.7 m/s
  Φ = 0.55; 0.65; 0.70; 0.80; 1.00

Measured Quantities:

- Axial Inflow Velocity
- Turbulence Intensity (some point)
- Integral scale (some points)
- Mean Reaction Progress Field
- Flame Lift-Off Height *(29. Comb. Symp, 1801, 2002)*

Publication:

- (2 Diploma Thesis, Erlangen 1997, 1998)
- Data not sorted, maybe available via fdi@ltt.uni-erlangen.de

TNF7 2004 **(4)**

Double-Flow-Burner *(in preparation)*

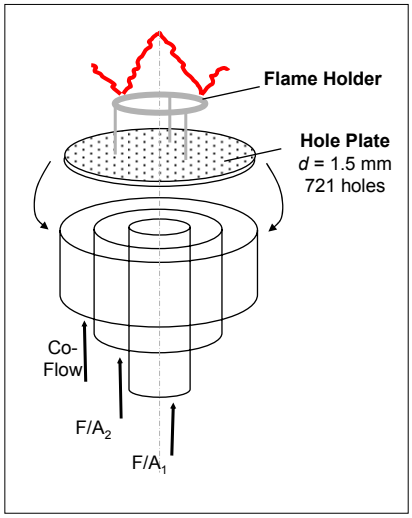

Characteristics:

- Concentric Double Flow Burner
- 721 small holes
  - to prevent wall mixing effect
  - for homogeneous turbulence production
- D_i = 35 mm, D_a = 70 mm, D_{Coflow} = 125 mm
- U = 2 - 4 m/s
- u'/U = 40 % (expected)

Measured Quantities (planned):

- Flow, Turbulence
- Reaction Progress Field
- Conditioned Turbulence
- Turbulent Flux

Later:

- Mixing
- Rich-Lean Staging
- Lean-Lean Staging
- Local Extinction

TNF7 2004 **(5)**

Double-Flow-Burner (in preparation)

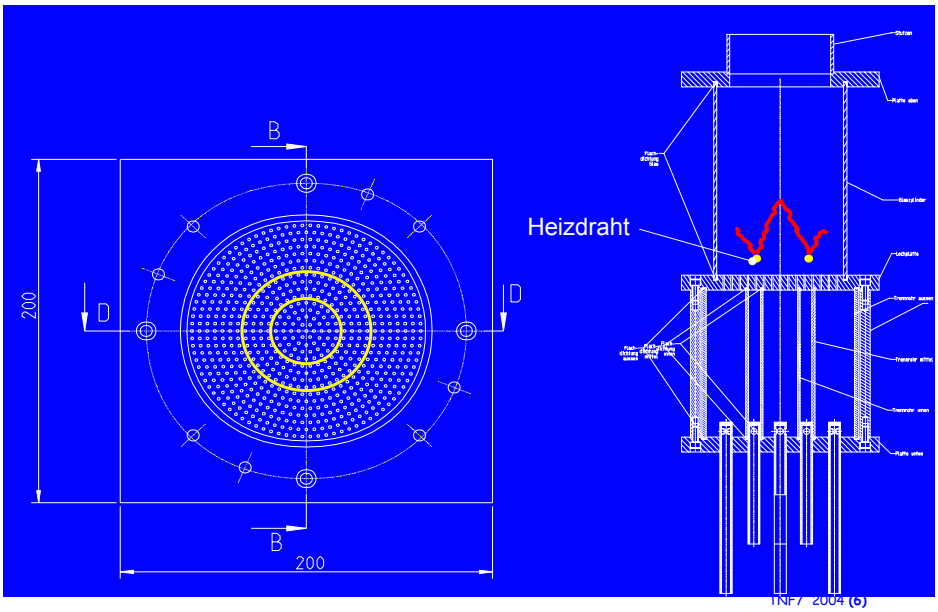

TNF7 2004 **(6)**

Comment to Data Collection for Premixed Flames

My Priority List to be Measured in Premixed Flames for Validation Data:

1. **Data Series**, with at least Pos. 2 and 3
2. **Inlet Conditions** (Flow, Turbulence, Fuel/Air Ratio)
3. **Averaged Flame Position** (Reynolds Averaged Reaction Progress (2D-Field or along Profiles), or at least simplified geometrical description, e.g., flame angle from , average flame brush thickness)
4. **Heat Release** (but this is difficult, maybe instead measurement of **Flame-Surface-to-Volume-Ratio**)
5. **Flow Field in Flame Zone** (But: comparison with calculation is difficult, since calculation with Favre averaged flow, while experiment (often) with Reynolds averaged flow. Transformation needs conditioned flow measurement).
6. **Turbulence in Flame Zone** (unconditioned and if possible also conditioned).
7. **Temperature and Species Measurement** (unconditioned and if possible also conditioned to reaction progress). (Generally no high priority, only some tests of "Thin-Flame-Assumption" with high accuracy necessary)
8. **Pollutants**, measured in flame.
9. **Other quantities** (e.g., turbulent flux. Important for special modelling questions, but less important for validation data collection)

TNF7 2004 **(7)**

A New Piloted Premixed Burner in Vitiated Co-flow

Dunn, M., Bilger, R.W., and Masri, A.R.

TNF7

Chicago, 22-24 July 2004

Burner Configuration

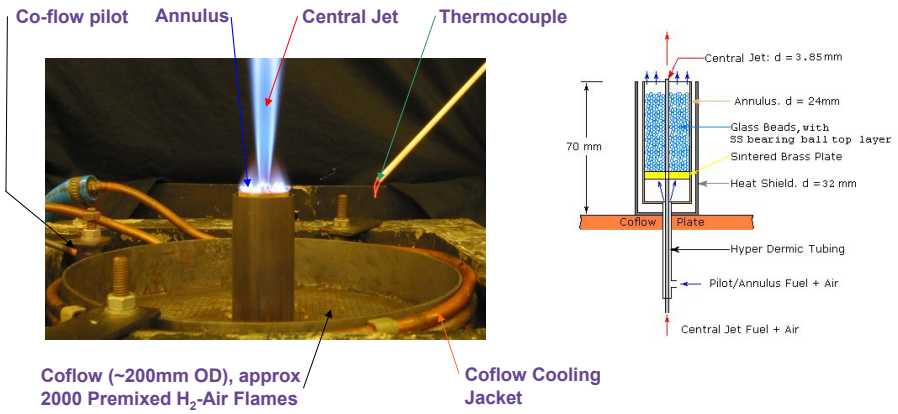

TNF7
Chicago, 22-24 July 2004
Aerospace, Mechanical & Mechatronic Engineering
University of Sydney

Burner Characteristics

- Extension of Cabra's vitiated co-flow burner
- New pilot annulus stabilizes central premixed flame to the nozzle
- High shear rates between jet and co-flow may lead to local extinction further downstream of pilot annulus
- Co-flow temperatures may be high enough and equal to adiabatic temperatures of fuel mixtures
- Local extinction may then be due to shear only.

Co-flow

Over exposed photo showing the Co-flow potential core for a typical flame (approx height 2D 400mm).

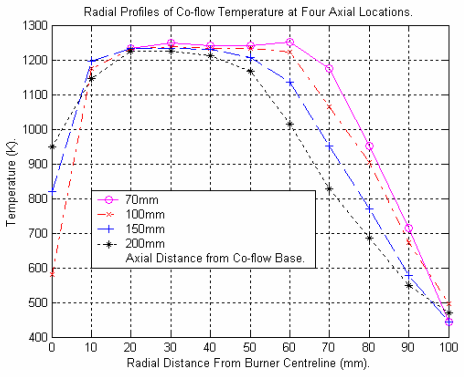

Thermocouple profiling results for a 1250K Co-flow with no annulus or central jet flame.

Results - 1

Investigation of extinction driven by a combination of straining and quenching mechanisms, where $T_{Co\text{-}flow} < T_{adiabatic}$ central jet.

160 m/s – Flame Fully Attached, beginning to thin

180 m/s – Flame undergoing extinction re-ignition

220 m/s – Flame undergoing extinction without re-ignition

Results - 2

Investigation of extinction driven by pure straining mechanisms, where $T_{Co\text{-}flow} = T_{adiabatic}$ central jet.

100 m/s – Flame completely attached

200 m/s - two flame zones beginning to emerge

300 m/s - two flame zones completely separated

Darmstadt premixed swirl burner

- Design

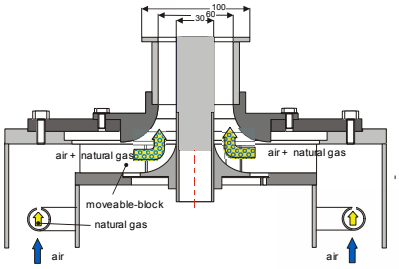

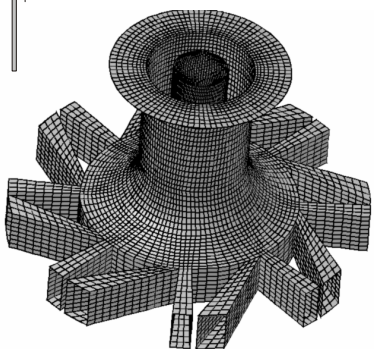

Darmstadt premixed swirl burner

- Operating conditions

		PSF-30	PSF-30D	PSF-90	PSF-150
$S_{0,th}$	[-]	0.75	0.75	0.75	0.75
P	[kW]	30	30	90	150
λ	[-]	1.2	1.2	1.2	1.0
Q_{gas}	[m_n^3/h]	3.02	3.02	9.06	15.1
Q_{air}	[m_n^3/h]	34.91	34.91	104.33	145.45
Q_{N2}	[m_n^3/h]	-	6.98	-	-
$Re_{ge.}$	[-]	10000	11950	29900	42300

Darmstadt premixed swirl burner

Issues
Burners
Current work
Discussion

- Validation sequence
  - Flow field (done)
    - ✓ Statistical moments of 3 vel. comp., 2 Re-stress comp.
    - ✓ Integral times and length scales
    - ✓ PSD of axial velocity component (E_{11})
    - ✓ Velocities conditioned on OH boundary within the flame brush
  - Scalar field
    - ✓ Flame brush (done)
    - ✓ Fractal dimension of OH boundary (done)
  - In preparation:
    - Compositional structure, secondary air entrainment, scalar gradients →1D Raman/Rayleigh
    - Flame vortex interaction, local extinction → PIV/PLIF (in collaboration with Mark Linne)

Darmstadt premixed swirl burner

Issues
Burners
Current work
Discussion

- Selected results (1)
- Isothermal case → precessing vortex core
  - Constant Strouhal number of 0.25
  - Characteristic frequency scales with Re-number

Experiment - PSD

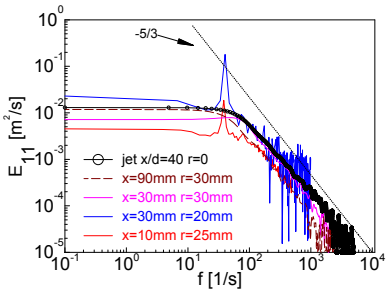

DNS – iso-pressure surfaces

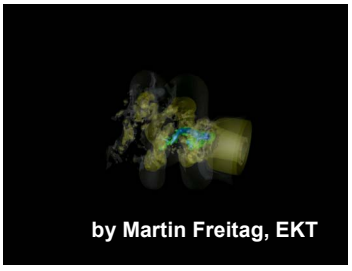

Darmstadt premixed swirl burner

Issues
Burners
Current work
Discussion

- Selected results (2) – flow field inside the nozzle
- Comparison DNS – experiment, isothermal case

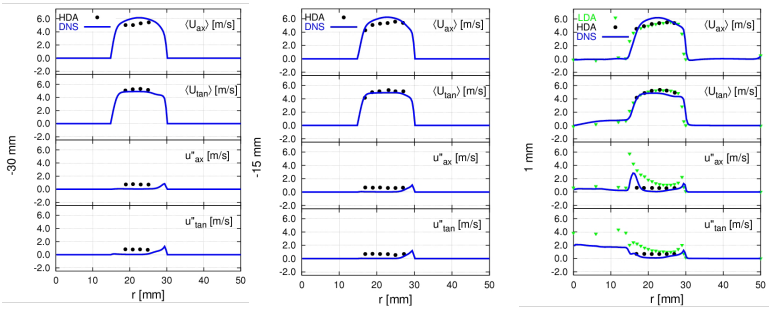

→ Make use of DNS to generate high-fidelity boundary conditions for TNF target flames

Darmstadt premixed swirl burner

Issues
Burners
Current work
Discussion

- Selected results (2) – downstream the nozzle
- Comparison DNS – LES – experiment, isothermal case

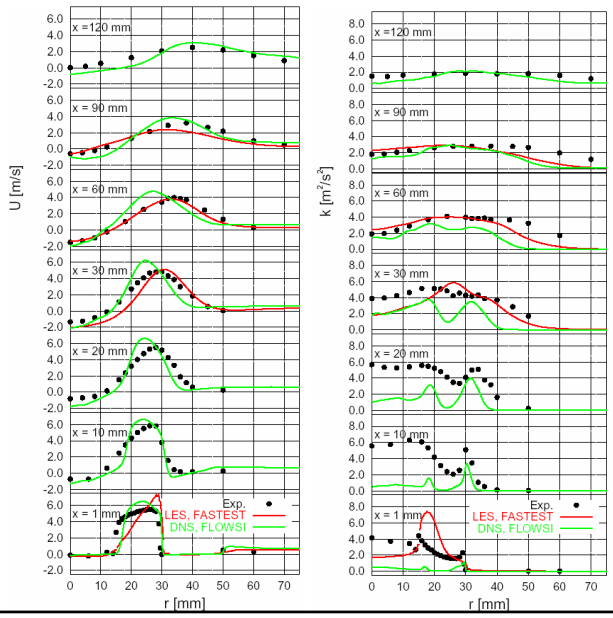

Darmstadt premixed swirl burner

- Selected results (3)
- Comparison isothermal – combusting case

Issues
Burners
Current work
Discussion

Experiment – auto correlation

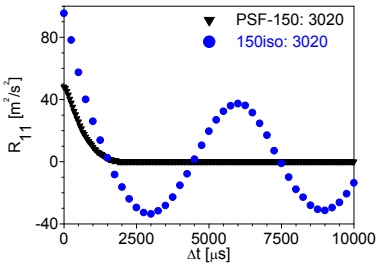

Experiment - PSD

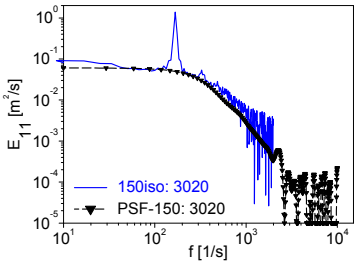

Darmstadt premixed swirl burner

- Selected results (4)
- Preliminary: LDV measurements conditioned on distance from burned/unburned boundary (OH PLIF)

Issues
Burners
Current work
Discussion

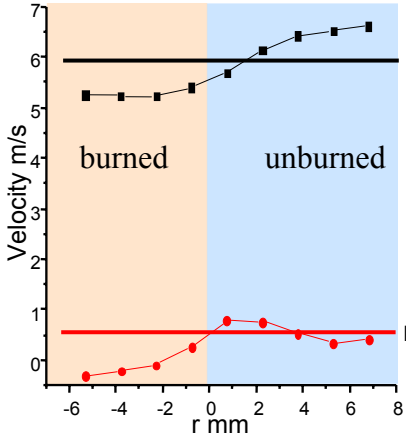

Mean unconditioned LDV 5.90 m/s

u mean
v mean

x = 20 mm
r = 24 mm

Mean unconditioned LDV 0.56 m/s

Darmstadt premixed stratified flame

- Burner setup and measurements scheduled for 2005 - ?
- Current design proposal

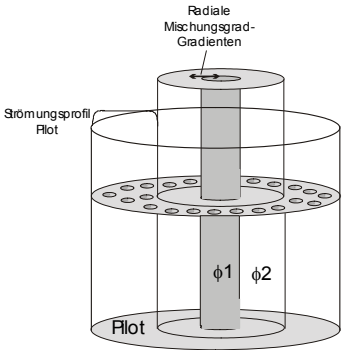

→ Lean CH_4-air mixture

→ Mixture fraction gradients

→ Validation sequence: Velocity and scalar field, gradients, high spatial resolution

Discussion

- TNF to be extended to premixed flames and comparisons of different models already at TNF 8?
- Discussion /agreement on
  - Target flame
  - Topic to focus at
- Supplementary experimental information
  - Boundary conditions
  - Compositional structure
  - Pollutants
  - Combined velocity – scalar measurements
  - Flame – vortex interaction
  - …
  - Who is doing these additional measurements?
- Collaboration with Premixed Workshop, avoid any competition!?

RKC's Answers to the Questions on Regime Diagram

- What are the regimes of premixed turbulent combustion?
  - For all practical purposes, wrinkle thin flame remains most significant especially under gas turbine conditions
- What are the characteristics of individual regimes?
  - Much is known about wrinkled thin flames but less about the others
- What parameters are needed to distinguish and characterize the different regimes?
  - 3D spatial scalar information and measured (not inferred) velocity statistics and scales
- Has our focus on the regime diagram and especially the Klimov-Williams criterion limited our thinking?
  - Definitely, as we were too focused on looking for statistically rare flame broadening events
- Can the different regimes be located adequately on a 2-D parameter plane?
  - No, we recognized this limitation back in 1988 but have yet to come up with an adequate solution
- What experiments and experimental capabilities are need to investigate regime space and its boundaries?
  - Stable flames propagating in turbulence at least an order of magnitude higher than most current experiments

Quantifying Turbulent Burning Rate

- Possible measures are
  - local heat release rate
  - local flame front propagation
  - Local displacement flame speed (turbulent burning speed)
  - Global flame speed
  - flame surface density
  - burning rate integral
  - consumption speed.
  - others?
- How are these quantities defined, measured, related?
  - Some answers in next slide
- On what do they depend?
  - burner/flame configuration
  - hydrodynamic/thermal instabilities
  - turbulence properties
  - other?
- What are governing parameters?
- How useful are these different measures? Why? Are some more useful than others?

Definitions and Measurements of Burning Rate Parameters

- Local heat release rate
  - Quantitative imaging of scalar of the flame fronts. Which one to use is debatable
- Local flame front propagation, S_L
  - Flow velocity locally normal to the surface of a wrinkled flame.
  - Measured by combined PIV with scalar imaging, error can be large due to extraction of small quantity (< 0.5 m/s) from much faster flow (> 3 m/s)
- Local displacement flame speed (turbulent burning speed), S_d
  - Flow velocity locally normal to the turbulent flame brush
  - Unambiguous for unattached flames only
  - Relatively easy to measure by using PIV or LDV.
- Global flame speed, S_b
  - Flow velocity obtained from a mean flame surface and the premixed flow rate
  - Meaningful only for envelope flames
- Flame surface density, Σ
  - Scalar imaging to obtain wrinkling factor and statistics of flame front orientations
  - Difficult to measure when flame is highly contorted
- Burning rate integral, B_t
  - Integration of Σ through the flame brush
  - Integration paths differ at different regions of the flame brush
- **Consumption speed, S_c**
  - Deduced by applying a correction factor to S_T to account for the effect due to divergence
  - S_c and B_t Should be consistent

LAWRENCE BERKELEY NATIONAL LABORATORY

Prepared by R. K. Cheng for presentation at TNF7